Physiol Rev 92: 1393–1478, 2012
doi:10.1152/physrev.00036.2011

hERG K^+ CHANNELS: STRUCTURE, FUNCTION, AND CLINICAL SIGNIFICANCE

Jamie I. Vandenberg, Matthew D. Perry, Mark J. Perrin, Stefan A. Mann, Ying Ke, and Adam P. Hill

Mark Cowley Lidwill Research Programme in Cardiac Electrophysiology, Victor Chang Cardiac Research Institute, Sydney, New South Wales, Australia; St Vincent's Clinical School, University of New South Wales, New South Wales, Australia; and University of Ottawa Heart Institute, Ottawa, Canada

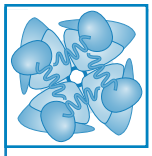

Vandenberg JI, Perry MD, Perrin MJ, Mann SA, Ke Y, Hill AP. hERG K^+ Channels: Structure, Function, and Clinical Significance. *Physiol Rev* 92: 1393–1478, 2012; doi: 10.1152/physrev.00036.2011.—The *human ether-a-go-go related gene* (hERG) encodes the pore-forming subunit of the rapid component of the delayed rectifier K^+ channel, Kv11.1, which are expressed in the heart, various brain regions, smooth muscle cells, endocrine cells, and a wide range of tumor cell lines. However, it is the role that Kv11.1 channels play in the heart that has been best characterized, for two main reasons. First, it is the gene product involved in chromosome 7-associated long QT syndrome (LQTS), an inherited disorder associated with a markedly increased risk of ventricular arrhythmias and sudden cardiac death. Second, blockade of Kv11.1, by a wide range of prescription medications, causes drug-induced QT prolongation with an increase in risk of sudden cardiac arrest. In the first part of this review, the properties of Kv11.1 channels, including biogenesis, trafficking, gating, and pharmacology are discussed, while the second part focuses on the pathophysiology of Kv11.1 channels.

I. INTRODUCTION

A. The Kv11.1 Channel

The *human ether-a-go-go related gene* (hERG) encodes the pore-forming subunit of a delayed rectifier voltage gated K^+ (VGK) channel.[1] These channels are variously referred to as I_{Kr}, hERG, or Kv11.1 (233). In this review, *KCNH2*, the official name for the *human ether-a-go-go related gene,* is used when referring to the gene, KCNH2 when referring to the mRNA, hERG when referring to the channel protein, Kv11.1 when referring to the fully assembled channels studied in heterologous expression systems, and I_{Kr} when discussing the native channel. HERG is a member of one of the three subfamilies of the ether-a-go-go family of VGK channels (ether-a-go-go, Kv10.x; ether-a-go-go related, Kv11.x; and ether-a-go-go like, Kv12.x). Within the family of Kv11.x, there are three members, Kv11.1 (hERG), Kv11.2 (hERG2), and Kv11.3 (hERG3), but only K_V11.1 is discussed in this review.

The family name "ether-á-go-go" was coined by Kaplan and Trout in 1969 (314) and was intended as a humorous reference to how the legs of mutant flies shake under ether anesthesia like the go-go dancers of the 1960s (Ganetzky, personal communication). It should be pointed out though, that hERG itself is the human ortholog of a different protein, which is encoded by the sei (seizure) locus (636, 673). *KCNH2* was first cloned in 1994, by Warmke and Ganetzky, by screening a human hippocampal cDNA library with a mouse homolog of the *Drosophila* "*ether-à-go-go*" (EAG) K^+ channel gene (678). *KCNH2* was shown to be located on chromosome 7, and analysis of the sequence revealed that it shared features with both VGK channels as well as cyclic nucleotide-gated (CNG) channels. Shortly thereafter, the Keating laboratory identified mutations in *KCNH2* as the basis of chromosome 7-associated long QT syndrome (now referred to as LQTS type 2) (132). Later in that year, Trudeau et al. (643) and Sanguinetti et al. (547) showed that Kv11.1 channels pass the rapid compo-

[1]Rectification refers to a conductance that changes with voltage. An inwardly rectifying channel is one that passes more inward current than outward current for comparable electrochemical driving forces, whereas an outwardly rectifying channel passes more outward current than inward current. Delayed refers to the fact that the changes in conductance occur over time (this may vary from milliseconds to many seconds).

nent of the delayed rectified K^+ current I_{Kr}, and that these channels were the molecular target for class III antiarrhythmic drugs.

B. Historical Overview

Just over 40 years ago, in back-to-back papers in the *Journal of Physiology*, Tsien and Noble (448, 449) demonstrated that there were two kinetically distinct components of the delayed rectifier K^+ current in cardiac myocytes, which they termed I_{x1} (now referred to as the rapid delayed rectifier, I_{Kr}) and I_{x2} (now referred to as the slow delayed rectifier, I_{Ks}). In the original description, the currents I_{x1} and I_{x2} were shown to be carried largely by K^+, but as the reversal potentials were more positive than E_K, the authors concluded that they may also have a small conductance for other ions and hence used the term *x*, rather than K. This work was controversial at the time (442) and was not fully accepted until identification of the genes encoding these separate conductances were discovered in the mid 1990s (51, 546, 547, 643, 678). It is salient to review the key features of I_{Kr} as identified by Tsien and Noble over 40 years ago. The two components of I_K were separated on the basis of kinetic properties using an envelope of tails protocol (448), which is still a key protocol used for measuring rates of activation of I_{Kr}/Kv11.1 channels (see sect. IV*D*). Second, they showed that the rapid component exhibited inward rectification (discussed in detail in sect. IV). Third, they suggested that these two current components were sufficient to account for cardiac repolarization (449).

In the subsequent two decades, numerous groups confirmed the presence of the rapid component of the delayed rectifier K^+ conductance in a range of cardiac preparations (145, 271, 450, 460, 572). The most notable finding among these studies was that of Shibasaki (572) who observed an initial "hook" during deactivation current recordings of the I_K component in rabbit sinoatrial node cells (see **FIGURE 1**). He correctly surmised that "a fraction of I_K is partially inactivated during the depolarization, and on hyperpolarization this inactivation is removed with a fast time course, which gives rise to a 'hook'." This hook current is one of the most characteristic features of I_{Kr} and Kv11.1 channels and was subsequently shown to be due to a rapid voltage-dependent inactivation process (see sect. IV*C*).

In the early 1990s, Sanguinetti and Jurkiewiecz (548) showed that the two delayed rectifier K^+ currents could be separated pharmacologically. In particular, they noted that class III antiarrhythmic drugs (which were being vigorously pursued in the pharmaceutical industry at the time) acted on the rapid component, which they termed I_{Kr}. Subsequently, a wide range of drugs, from every therapeutic class, have been shown to inhibit I_{Kr} channels (see sect. V). Sanguinetti and Jurkiewiecz also showed that whereas the slow component, I_{Ks} was highly sensitive to activation by β-adrenergic

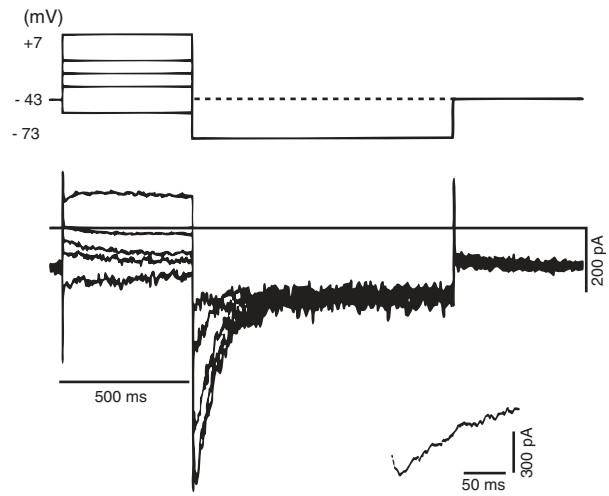

FIGURE 1. First recording of hooked tail currents recorded from rabbit sinoatrial nodal cell. *Top panel*: voltage protocol. *Bottom panel*: current traces. An expanded version of the tail current recorded at −73 mV (in presence of symmetrical 150 mM K^+) is shown in the *inset* at the bottom and clearly illustrates the "hooked" appearance characteristic of I_{Kr}/Kv11.1 currents. [From Shibasaki (572), copyright John Wiley and Sons Ltd.]

stimulation, the I_{Kr} component appeared to be insensitive to β-adrenergic stimulation (549). This has profound implications for the differences in arrhythmogenic triggers in patients with defects in I_{Kr} versus I_{Ks} (see sect. VII).

The cloning of *KCNH2* in 1994 (678), and demonstration that it underlies chromosome 7-associated long QT syndrome (LQTS type 2) (132) and that its gene product, the Kv11.1 channel, is the molecular target for the vast majority of drugs that cause drug-induced arrhythmias (547), led to a huge increase in interest in Kv11.1 channels. In the last 16 years, a plethora of studies investigating the biogenesis (see sect. III), molecular and structural basis of gating (see sect. IV), pharmacology (see sect. V), and regulation (see sect. VI) have contributed to a better understanding of the clinical importance of inherited mutations in KCNH2 (see sects. VII and IX) as well as the molecular basis of drug-induced QT prolongation (sect. VIII). Whilst the role of Kv11.1 channels has been most extensively investigated in the heart, they are also expressed in numerous other tissues (see sect. X) and recently have been implicated in the pathogenesis of schizophrenia (279).

II. GENOMIC AND PROTEIN STRUCTURE

A. *KCNH2* gene

The human *KCNH2* gene spans ~33 kb of region q36.1 on chromosome 7 (accession no. NG_008916). It is read in the reverse strand, and the major transcript KCNH2–1a (accession no. NM_000238.3) contains 15 exons (see **FIGURE 2**) (285). The gene contains two additional transcription start

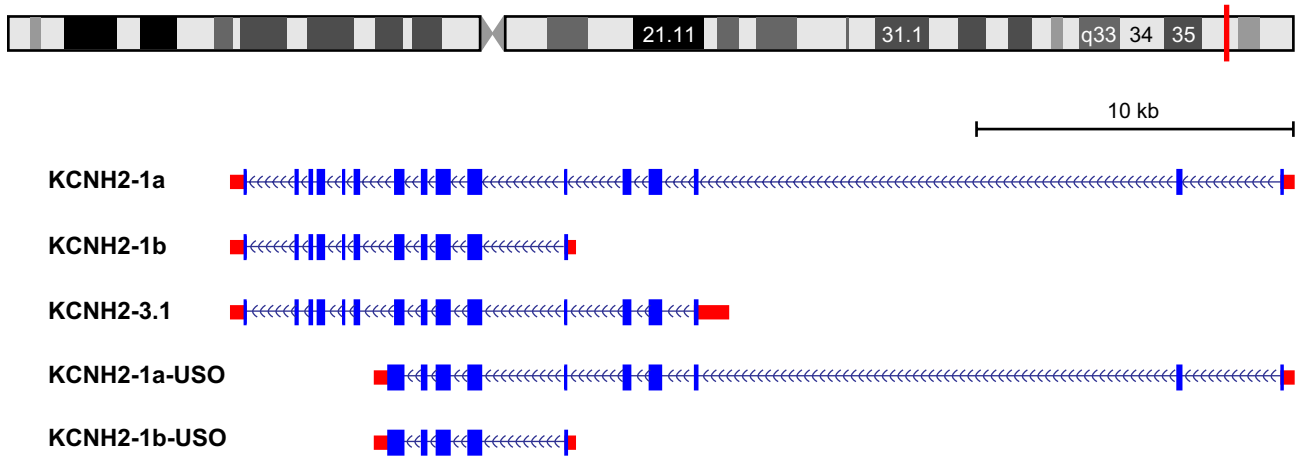

FIGURE 2. Genomic structure of KCNH2. Genome browser view of chromosome 7 q36.1. KCNH2 is transcribed in the reverse direction. Three alternative transcription start sites and two alternative termination sites give rise to five transcripts. 5′ UTR and 3′ UTR are shown in cyan and coding regions in blue.

sites. KCNH2–1b (accession no. NM_172057) has a transcription start site in intron 5, resulting in a transcript missing the first five exons of KCNH2–1a and containing an alternative exon 5b (358, 383). KCNH2–1b is identical to KCNH2–1a from exon 6 onwards. KCNH2–1c (accession no. FJ938021; sometimes referred to as KCNH2–3.1) has a transcription start site in intron 2 of KCNH2–1a. It is missing the first two exons of KCNH2–1a and has an additional six amino acids at the 5′ end of exon 3 but thereafter is identical to KCNH2–1a (279). In addition to the stop codon in exon 15 of KCNH2–1a, exon 9 may be translated for an additional 88 unique amino acids followed by a 3′ UTR within intron 9 of the KCNH2–1a transcript. Transcripts with this premature COOH-terminal truncation are sometimes referred to as $hERG_{USO}$ (338).

The dbSNP build 132 of the human genome on the UCSC genome browser (http://genome.ucsc.edu) lists 251 single nucleotide polymorphisms (SNPs; where the minor allele frequency is ≥1%). This includes 32 SNPs in coding regions (15 synonymous and 17 nonsynonymous), 9 SNPs in untranslated regions, and the remainder in introns. The two SNPs that appear to have the strongest connection to (patho)physiological phenotypes are rs1805123 in exon 11 and rs1036145 in intron 2. The minor allele in rs1805123 results in residue 897 changing from lysine to threonine (K897T) and has been identified in genome-wide association studies as a significant determinant of QT interval duration (126, 374, 397, 444, 496). The minor allele in SNP rs1036145 is significantly correlated with expression of the KCNH2–1c isoform, which is correlated with development of schizophrenia (279).

B. hERG Protein

The KCNH2–1a transcript gives rise to a 1,159-amino acid protein (hERG) that is a member of the superfamily of VGK channels (678). It contains six transmembrane segments (S1-S6) with S1-S4 contributing to the voltage sensor domain (VSD) and S5-S6 along with the intervening pore loop contributing to the pore domain (see **FIGURE 3**). The functional channel is a tetramer with the pore domain from each of the four subunits lining the central ion conduction pathway. In addition to the membrane-spanning region, the hERG protein contains large cytoplasmic NH_2-terminal and COOH-terminal domains. The NH_2 terminus contains a Per-Arnt-Sim (PAS) domain (425) that defines the *ether-a-go-go* subfamily of VGK channels (678). The COOH terminus contains a cyclic nucleotide binding domain (cNBD), which shares homology with the cNBD of CNG channels and hyperpolarization activated channels (HCN). Overall, hERG channels share a greater degree of homology with CNG and HCN channels than with other VGK channels (even when just the pore regions are considered; see **FIGURE 4**) (678).

In vertebrate genomes there is a significant correlation between exon boundaries and protein domains (379). Within the *KCNH2* gene, exon 1 encodes the 5′ UTR and first 26 residues, which play a significant role in regulating deactivation kinetics of the channel (see sect. IV*F*). Exons 2 and 3 encompass the PAS domain. Exon 6 encodes the last portion of the cytoplasmic NH_2 terminus and first three TM segments. Exon 7 encodes the fourth TM segment, i.e., the segment containing the positive charges that are thought to act as the principal voltage-sensing region within the VSD (see sect. IV*E*), along with the majority of the pore domain. It is notable that the exon 7/8 boundary occurs at a glycine residue (Gly648 in hERG) that is one of the most highly conserved residues in all K^+ channels (296) and defines the boundary between the upper and lower halves of the pore cavity. Exons 8–10 encode the c-linker and cNBD domains, while the remaining five exons encode the distal COOH-terminal domain.

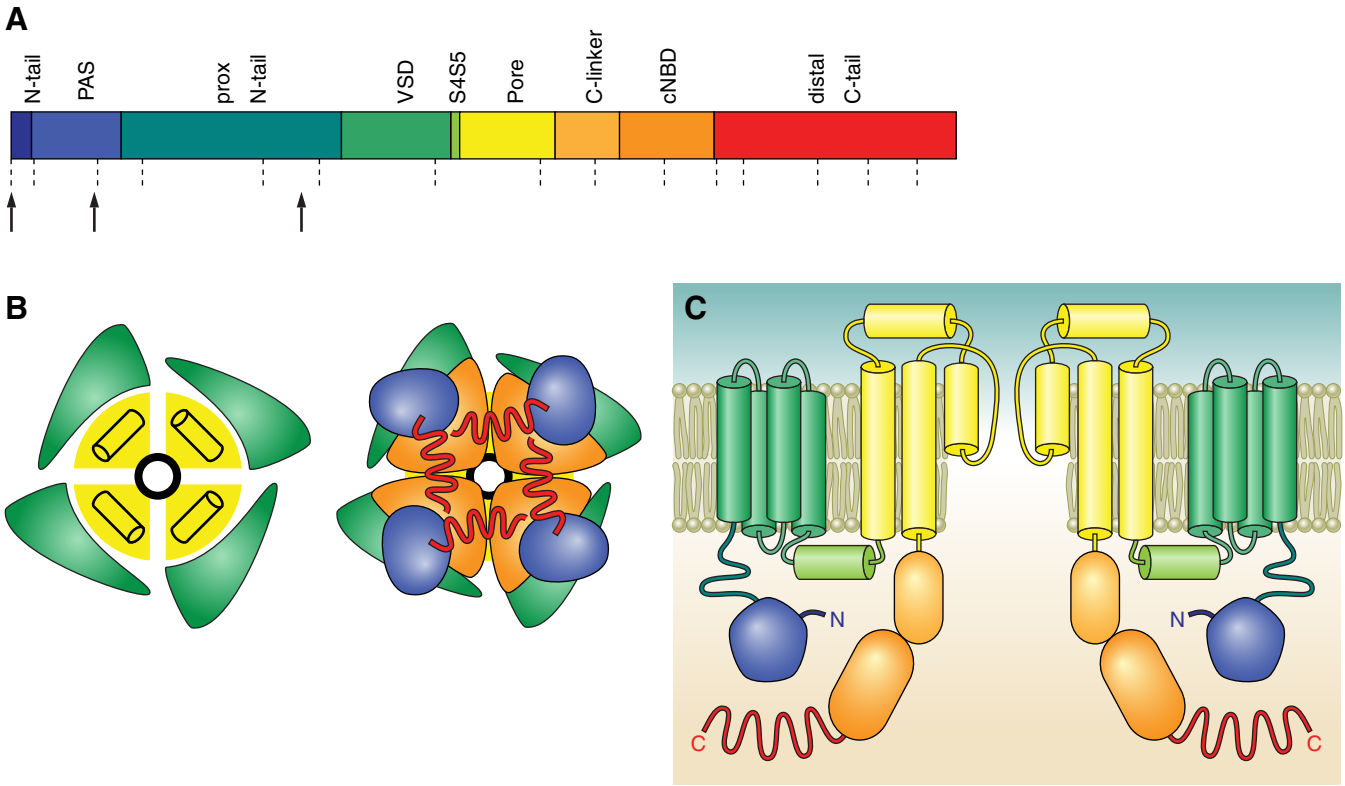

FIGURE 3. Topology and structure of Kv11.1 channels. *A*: linear sequence of hERG-1a with domains color coded. Arrows indicate the transcription start sites, and dashed lines show the sites of exon-exon boundaries. *B*: representations of the extracellular view (*left*) and intracellular view (*right*) of the tetrameric structure of Kv11.1 channels. *C*: topology of two opposing hERG1a subunits color-coded as in *A* and *B*.

Based on sequence homology to potassium and cyclic nucleotide-gated channels with known structures, numerous homology models of the Kv11.1 channel have been constructed (304, 343, 591, 603, 628, 646, 705). The homology models have usually included only the pore domain regions, with the focus being on structural basis of ion permeation or drug binding. Invariably, these models have left out the extracellular S5P linker, as this linker is considerably longer in Kv11.1 channels (~40 amino acids) than it is in other K^+ channels (typically 12–15 amino acids; Refs. 378, 641), so there is no good template to use for constructing homology models in this region. In addition, some models have not included the outer helix, S5 (591), as the homology between Kv11.1 and other VGK channels is so low in this domain (304). Of course, the other major omission from published homology models are the cytoplasmic domains. There are atomic resolution structures available for the cytoplasmic NH_2-terminal PAS domain of Kv11.1 channels (residues 1–135; Refs. 367, 425, 431, 445). In addition, there is sufficient sequence homology between Kv11.1 and the murine HCN2 channel (707) and the zebrafish ELK channel (75) in the c-linker and cNBD domains for us to be confident that Kv11.1 will have a similar structure to that for mHCN2 and zELK in this region (11, 431). It should be noted though that the functional roles of the domains are likely to be very different between Kv11.1 and HCN channels (see sect. VI*B*). As with the pore domain models, it is very likely that the central core of the cytoplasmic assembly will resemble that of the HCN2 channel, but the precise relationship between the PAS domain and C-linker/cNBD remains to be determined. Furthermore, there is no information available with regard to the structure of the proximal NH_2-terminal and distal COOH-terminal domains of Kv11.1 channels. While it is very likely that the structure of Kv11.1 will be broadly similar to that of other VGK and CNG channels, it is the subtle differences that distinguish Kv11.1 from other VGK channel structures that will be most illuminating with respect to understanding the unique properties of Kv11.1, and in this regard, there is very little known.

C. Kv11.1 Channels

KCNH2 encodes the pore-forming subunit of a K^+-selective voltage-gated ion channel, Kv11.1, which passes the rapid component of the delayed rectifier K^+ current, I_{Kr} (547, 643). Within the critical five central residues of the selectivity filter region, Kv11.1 channels are highly homologous to canonical K^+ channels, and Kv11.1 channels have high selectivity for K^+ over Na^+ (p_K: p_{Na} > 100:1) (547, 643), comparable to that observed in a range of other K^+ channels (257). In contrast, CNG and HCN channels do not contain the consensus sequence for K^+-selective channels (T/S-V/I/L-G-F/Y-G) and so are not K^+ selective, making them functionally quite different from Kv11.1 channels.

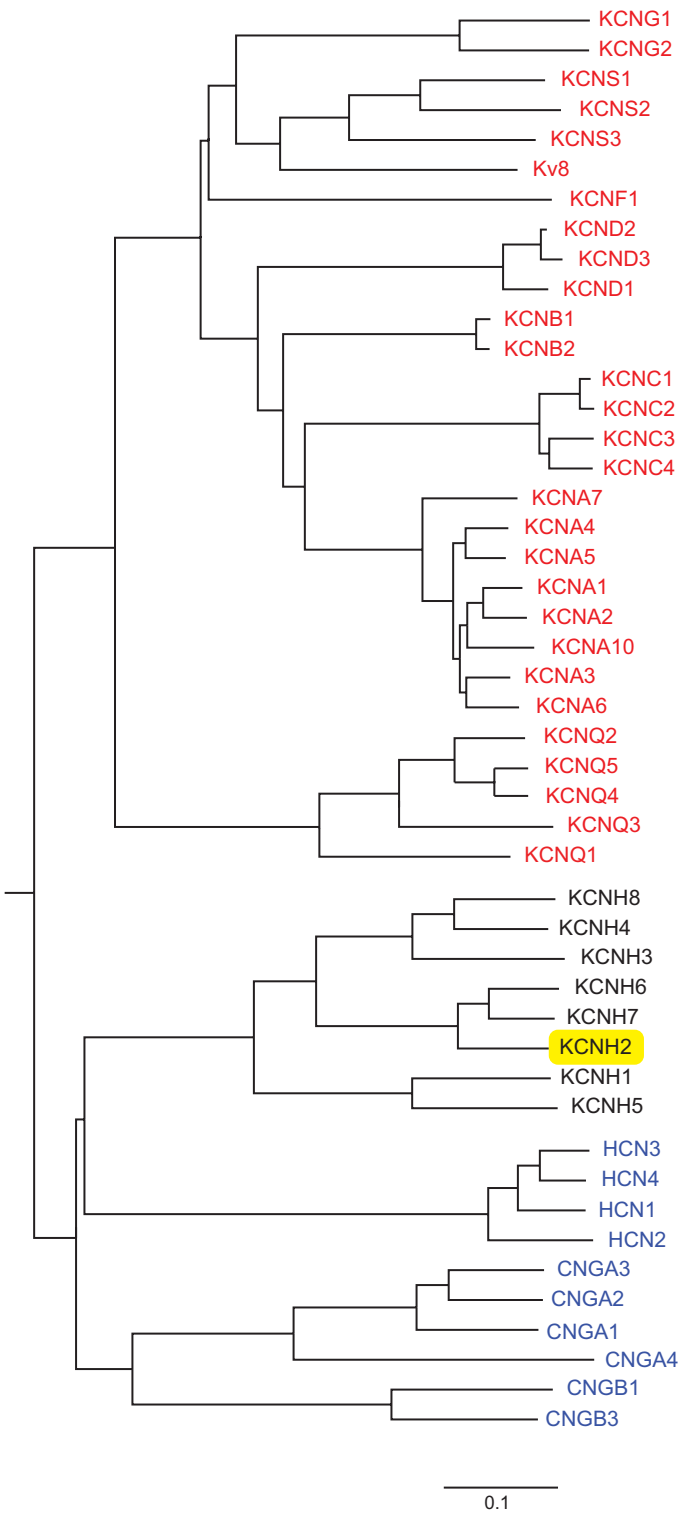

FIGURE 4. Cladogram of voltage-gated K^+ channel superfamily. Sequences were aligned on the pore domain region, using ClustalW. Canonical voltage-gated K^+ channels are shown in red, EAG family in black, and CNG/HCN family in blue.

Kv11.1 channels can exist in closed, open, or inactivated states (see **FIGURE 5**). Like other voltage-gated K^+ channels, they contain multiple positive charges in the S4 domain and this acts as the primary voltage sensor for channel opening (500, 601, 720). The inactivation process of Kv11.1 channels, however, exhibits a number of unusual features. Most notably, the kinetics of inactivation are much more rapid than the kinetics of activation (558, 583, 588), and second, the inactivation process is voltage-dependent (547, 583, 643), although whether inactivation is intrinsically voltage-dependent or derives its voltage-dependence from coupling to activation is unresolved (see sect. IV*G*). This unique combination of properties underlies the physiological role I_{Kr} plays in cardiac repolarization (see below). The molecular and structural bases of the unusual gating kinetics of Kv11.1 channels are discussed in detail in section IV.

D. Physiological Role of I_{Kr}

I_{Kr} channels are expressed in a wide range of tissues, but their physiological function is best characterized in cardiac cells. The slow activation and deactivation kinetics, coupled to rapid voltage-dependent inactivation and recovery from inactivation (see sect. IV for more detail of gating), makes the current passed through I_{Kr} channels ideally suited for determining the duration of the plateau phase of the action potential (AP) in atrial and ventricular myocytes (550, 583). Maintenance of this plateau is crucial for ensuring there is sufficient time for calcium release from the sarcoplasmic reticulum to enable cardiac contraction. As repolarization begins, I_{Kr} channels recover from inactivation, thereby passing more current and hastening repolarization, leading to greater recovery from inactivation (see **FIGURE 5*C***). This positive feedback loop ensures that repolarization is relatively rapid and robust. During terminal repolarization, I_{Kr} channels close slowly and so remain open for a substantial period after the membrane potential has returned to the resting (diastolic) level. As the resting membrane potential is close to the potassium reversal potential, there is little current flow through Kv11.1 channels in the early diastolic period, but they still contribute to the relative refractoriness of cardiac cells immediately following completion of repolarization. If a premature beat occurs during the early diastolic interval, there will be a large increase in I_{Kr} that will antagonize the depolarization of the cell (390, 583) (see **FIGURE 5*C***). Conversely, in clinical scenarios where I_{Kr} is reduced, due to loss-of-function mutations (sect. VII) or drug block (sect. VIII), patients are more prone to arrhythmias initiated by premature beats (58) (see **FIGURE 6**).

I_{Kr} also contributes to pacemaking activity in sinoatrial (SA) and atriventricular node cells (109, 191, 421, 652, 692). In SA node cells, I_{Kr} reaches maximum levels approximately midway through the repolarization phase (421). The slow deactivation and decay of I_{Kr} after the AP also contributes to diastolic depolarization. Thus inhibition of I_{Kr} leads to slowing of SA node cell firing. This has been demonstrated in isolated cells (109, 361, 462), intact nodes (652), and whole hearts (191). Whilst, I_{Kr} is not classically considered a "pacemaker" current, Kurata et al. (341) have aptly described it as an oscillation amplifier and frequency stabilizer.

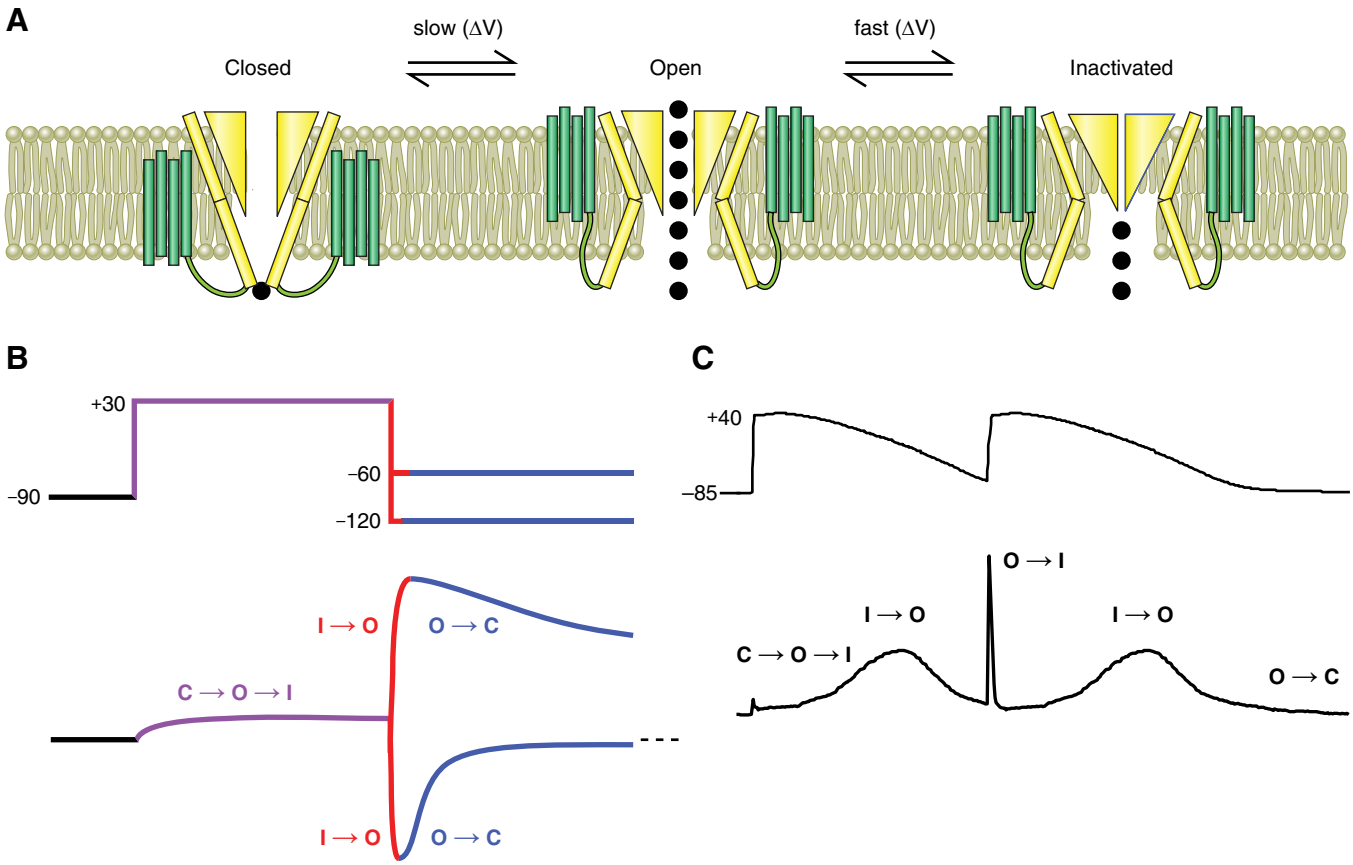

FIGURE 5. Gating of Kv11.1 channels. *A*: Kv11.1 channels can exist in closed, open, or inactivated states. Transitions between them are voltage dependent, with the transition between the closed and open states being slower than transitions between open and inactivated states. *B*: redrawn current traces during the two-step voltage protocol shown at top of panel. Transitions between different states are color coded. *C*: Kv11.1 current recorded from transfected CHO cell in response to an AP voltage waveform. During repolarization of the first AP waveform, the current increases due to recovery from inactivation and then decreases as the electrochemical gradient for K^+ efflux decreases. At the end of the first AP, almost all channels are still in the open state; hence, a premature stimulus gives rise to a very large current, but the channels then rapidly inactivate.

Extra-cardiac roles for I_{Kr} include spike-frequency adaptation and regulation of burst duration in neurons (see sect. XB) as well as regulation of resting membrane potential and AP firing frequency in smooth muscle (sect. XC) and endocrine cells (see sect. X*D*). I_{Kr} channels are also upregulated in a number of tumor cell lines where they are postulated to contribute to cell proliferation (sect. X*E*).

III. BIOGENESIS AND TRAFFICKING OF Kv11.1 CHANNELS

As with other polytopic membrane proteins, the vast majority of mutations in *KCNH2* result in defects in biogenesis (544). Consequently, there has been considerable interest in understanding the biogenesis of Kv11.1 channels. Defects in biogenesis may occur at the level of mRNA processing (716), mRNA stability (218), or protein folding and trafficking (19, 176, 733). Indeed, only a small proportion of the over 459 putative mutants identified to date result in channels that have normal biogenesis but then have abnormal function. There has been a particular focus on understanding channel trafficking with the hope that in some cases at least the defective trafficking properties of mutant channels can be rescued by pharmacological chaperones (522).

Like other proteins destined for the plasma membrane, KCNH2 mRNA is processed in the nucleus and the channel subunits then synthesized in the endoplasmic reticulum (ER). The nascent polypeptide chains fold and assemble into a tetramer within the ER before being exported to the Golgi apparatus where the channels undergo complex glycosylation before being trafficked to the plasma membrane. Mature channels are transported to the plasma membrane in COPII coated vesicles (140) and remain at the plasma membrane with a half-life of ~10 h (176, 216, 656) (see **FIGURE 7**). Whilst there is less known about the degradation of hERG, mature tetrameric channels are likely internalized in endocytic vesicles, tagged with ubiquitin and then degraded in lysosomes (227). In addition to degradation of the mature protein, any protein subunits that do not fold prop-

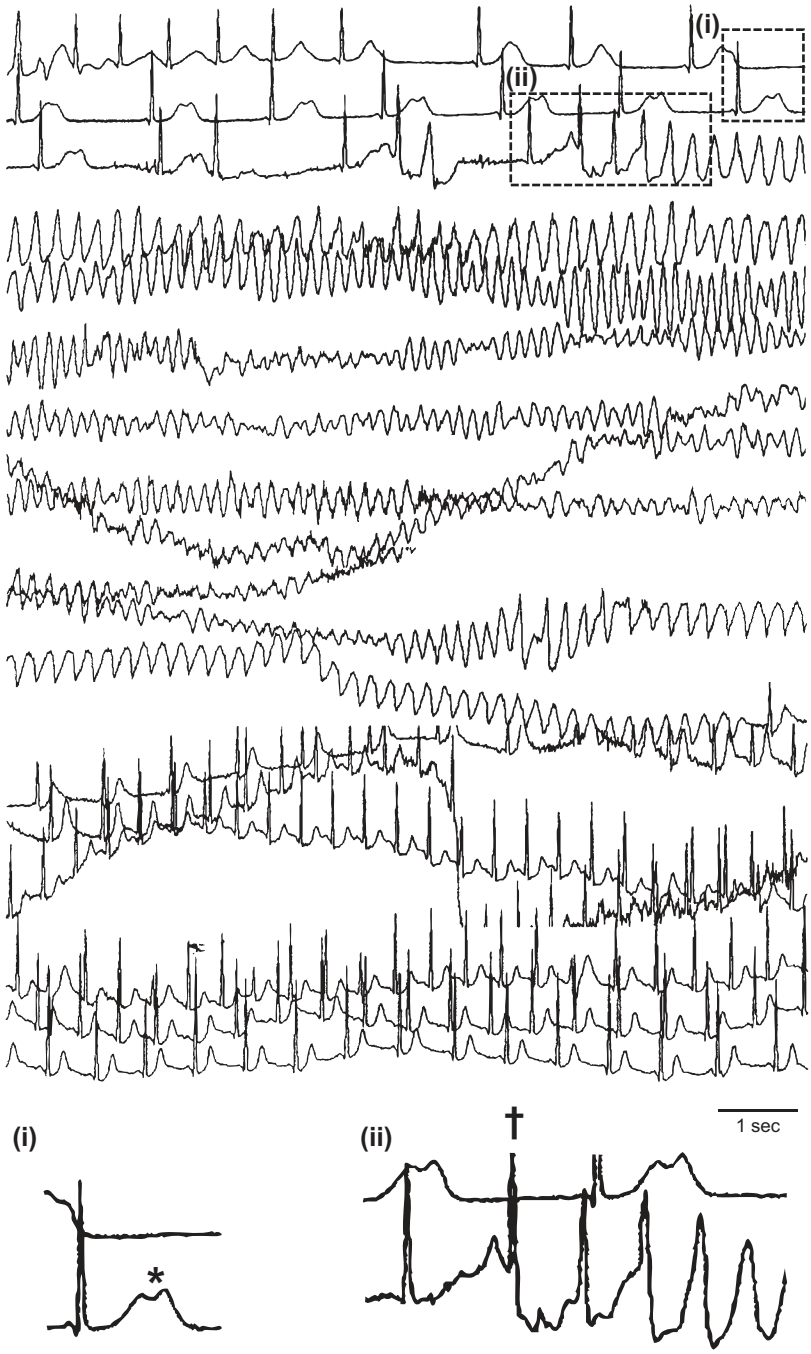

FIGURE 6. Holter recording from a patient with congenital long QT syndrome during an episode of ventricular arrhythmia that spontaneously reverted. The highlighted regions show (i) the bifid or notched T-wave (*), characteristic of patients with long QT syndrome type 2, and (ii) the arrhythmia episode is initiated by a premature beat (†). [From Benhorin and Medina (58), copyright The Massachusetts Medical Society.]

erly are tagged for degradation and transferred to the proteasome (216) (see sect. III, *B* and *E*).

Many of the studies of hERG protein trafficking have leaned very heavily on what has been learned from the very extensive studies of trafficking of CFTR (332, 520). There is, however, one very important difference between Kv11.1 and CFTR channels. Kv11.1 channel subunits must coassemble as tetramers to function, whereas CFTR functions as a monomer. This adds a very important clinical dimension as mutations in Kv11.1 can result in haploinsufficiency (loss of 50% of channel function) or a dominant negative phenotype if the presence of any abnormal subunits in a tetrameric channel results in abnormal trafficking of the entire channel and hence degradation of both the normal and abnormal subunits (175, 310, 728).

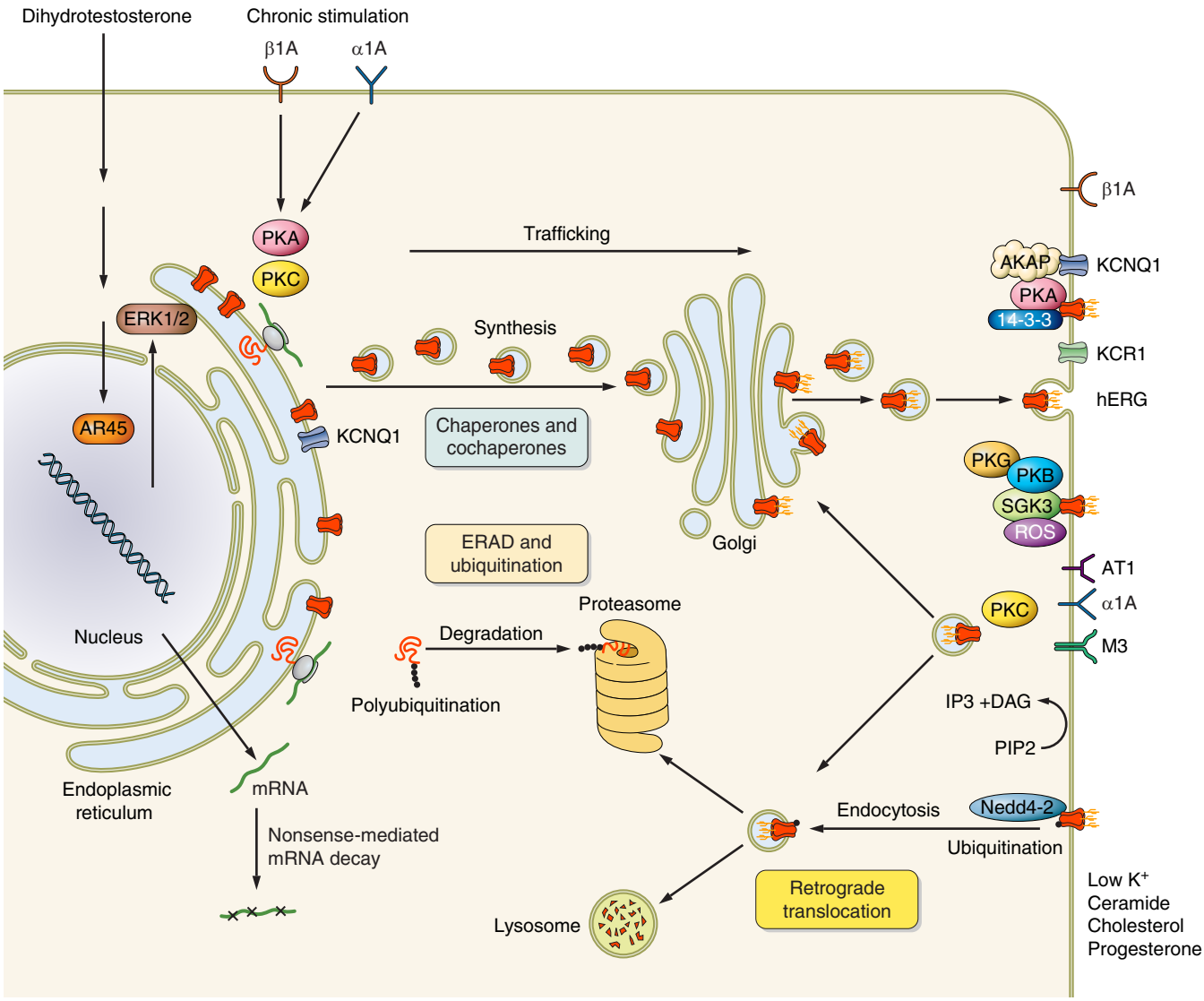

FIGURE 7. Biogenesis of hERG K^+ channels. mRNA transcribed in the nucleus is exported to the cytoplasm. Folding and assembly of the hERG polypeptide (red) occurs in the endoplasmic reticulum, assisted by chaperones (see **TABLE 1**). Folded channels are trafficked to the Golgi where glycosylation is completed. Mature channel complexes are trafficked to the cell membrane via membrane vesicles. Numerous proteins can interact with the channel during its biogenesis (see text for details).

There are numerous comprehensive reviews of general mechanisms of protein biogenesis (see, e.g., Refs. 142, 287, 537). Here, the focus is on those aspects of biogenesis as they relate to Kv11.1 channels and the mechanisms by which mutations in *KCNH2* result in channels not reaching the plasma membrane.

A. mRNA Biogenesis

1. mRNA transcription

There are at least three alternative transcription start sites for KCNH2 (see sect. IIA). These encode transcripts referred to as KCNH2–1a (the predominant transcript expressed in the heart), KCNH2–1b (also expressed in the heart), and KCNH2–3.1 (more highly expressed in neuronal tissues). Relatively little is known about how KCNH2 transcription is regulated, but clearly it must be, as levels of KCNH2 transcripts are spatially and temporally distinct (see sect. IIIF).

2. mRNA splicing

The mature KCNH2–1a isoform contains 15 exons. KCNH2–1b lacks the first five exons of KCNH2–1a but contains the final 10 exons along with an additional exon 1b. KCNH2–3.1 lacks exons 1 and 2 and has an extended exon 3 (at the 5′ end), resulting in a total of 13 exons (see **FIGURE 2**). At least 12 *KCNH2* mutations that are predicted

to have an effect on splice acceptor or donor sites have been identified (315), (http://www.fsm.it/cardmoc/). In four cases, in vitro studies have confirmed that the mutations result in abnormally spliced mRNA (125, 217, 598, 716). Such splice site mutations invariably lead to frameshifts and/or premature termination. These findings also highlight the importance of screening the 5′ and 3′ ends of introns as well as exons when screening for mutations in clinical populations. An additional trap to be aware of when designing primers for detecting mutations is that the presence of intronic polymorphisms in the sites covered by primers can result in failure of the primers to bind, leading to allelic dropout and failure to detect mutations in the affected exon (626).

3. mRNA decay

The steady-state level of KCNH2 mRNA is influenced by rates of transcription and stability. From a clinical perspective, the major interest in KCNH2 mRNA stability relates to the role of nonsense mediated mRNA decay (NMD) in patients with mutations that result in premature termination codons, which is almost always the case with frameshift mutations as well as most deletions and insertions (68). Proteins involved in the exon junction complex that determine splicing also play a critical role in quality control of mRNA transcripts including detection of premature termination codons. A premature termination codon that occurs more than ~50 nucleotides upstream of an exon-exon boundary will undergo NMD. The exon junction protein complex cannot accurately scan the last 50 nucleotides of an exon (629, 713, 714) so premature termination codons in the last 50 bp of an exon may escape NMD. NMD protects the cell from production of proteins that would either be nonfunctional or, worse still, cause dominant negative effects. In the case of KCNH2, NMD of mutant transcripts would result in 50% loss of function, which is, however, still sufficient to reduce I_{Kr} function and hence cause clinical LQTS. NMD has been documented for a number of KCNH2 mutations including Q1078X (67), Y652X (609), W1001X and R1014X (218), and P926AfsX14 (708), but it is likely to occur in ~30% of mutations in this gene (see sect. VII).

B. Protein Biogenesis

1. Protein synthesis

When the mRNA reaches the cytosol, it associates with ribosomes where translation is initiated. Once a transmembrane signal sequence is recognized, the RNA/ribosome/polypeptide complex is targeted to the ER where it engages the translocation machinery and the transmembrane segment is translocated across the ER membrane (see **FIGURE 7**). The specific steps involved have been much more extensively studied for canonical VGK channels (142), but it is likely that the same processes are involved in biogenesis of Kv11.1 channels.

2. Protein folding and trafficking

Folding of the nascent hERG polypeptide is assisted by molecular chaperones (176, 439, 655, 656) that reside in the ER or cytoplasm (see **TABLE 1**). Folding intermediates are recognized and associated with chaperones, which prevent protein misfolding by binding to exposed hydrophobic residues that typically become buried in the correctly folded structure. Chaperones will remain bound until the channel achieves its native structure. The corollary of this is that mutant channels that do not fold correctly will remain bound to chaperones for much longer and this is indeed the case for trafficking defective hERG mutant proteins (176, 674).

Protein trafficking through the ER is tightly regulated (651). In general, proteins contain motifs that promote export, as well as motifs that if exposed are indicative of misfolded proteins and result in the misfolded protein being retained in the ER or returned to the ER if it manages to escape. Thus trafficking undergoes both positive and negative regulation. The best characterized motif for ER retention is the Arg-X-Arg (RXR) motif (710) and for ER export is the diacidic export motif (413). HERG contains multiple RXR motifs. Not all of the hERG RXR motifs have been characterized, but those that have [including the RXR motif at residues 1005–1007 in hERG-1a (340) and the RXR motif at residues 15–17 in hERG–1b (301, 495)] play classical roles in ER retention. From this, one can presume that these motifs are normally hidden in correctly folded proteins but provide a quality checkpoint for detecting locally misfolded protein structure. There are no specific studies of the role of the numerous diacidic motifs in hERG, but it is reasonable to presume that they will contribute to ensuring that only correctly folded proteins are exported from the ER.

3. Glycosylation

Once the proteins are correctly folded, the chaperones dissociate and the channels can be trafficked to the Golgi apparatus where they undergo higher order glycosylation before being trafficked to the plasma membrane. The core-glycosylated hERG protein has a molecular mass of ~135 kDa and is sensitive to deglycosylation by Endo H (214, 733). An additional ~20 kDa of complex glycosylation is added in the Golgi resulting in an ~155 kDa band, which is sensitive to PNGase treatment (10, 216). HERG contains two putative *N*-linked glycosylation sites in the extracellular region, Asn598 and Asn629 (492). Further studies using site-directed mutagenesis revealed that Asn598 is the only site required for *N*-linked glyco-

Table 1. *Proteins interacting with hERG*

Protein	Location	Function	Reference Nos.
		Chaperones	
Hsp70	Cytosolic	Promoter trafficking WT hERG, retain mutants	176, 366
Hsc70	Cytosolic		176, 655
Hsp90	Cytosolic	Increase trafficking of WT hERG, retain mutants	176, 655
Calnexin	ER membrane	Retention of misfolded hERG	215, 655
Grp78	ER membrane	ER stress/unfolded protein response	319
Grp94	ER membrane	ER stress/unfolded protein response	319
Calrecticulin	ER membrane	ER stress/unfolded protein response	319
Hsp-organizing protein	Cytosolic		655
Sigma 1 rceptor	ER membrane	Enhance herg maturation and stability	124
Bag-2	Cytosolic	Binds and inhibits Hsc70 ATPase domain	655
		Cochaperones	
DnaJA-1/2/4	Cytosolic	Quality control, modulates herg degradation	655, 656
FKBP38	ER membrane	Quality control, folding and export	655
KCNE1	ER/plasma membrane	Modulates Kv11.1 current	405
KCNE2	ER/plasma membrane	Modulates Kv11.1 current	1
KCNQ1	ER/plasma membrane	Modulates Kv11.1 current	161, 250, 516
		ER export/endosomal recycling	
Sar1	ER, cytosolic, plasma membrane	Regulates ER export of hERG	140
Rab11B	ER, Golgi, plasma membrane	Golgi processing of hERG	140
		Ubiquitination/deubiquitinylation	
CHIP	ER membrane	Ubiquitinate chaperone bound hERG	656
Nedd4-2	ER plasma membrane	Reduces cell surface expression of hERG	13
STAMBP	ER membrane	hERG endocytosis from plasma membrane	607
		Retrotranslocation	
Vps24	MVBs	Accelerate degradation of mature hERG	607
Caveolin-1, -3	plasma membrane, endosomes	Endocytosis of mature hERG	402
Dynamin-2	Plasma membrane, endosomes	Endocytosis of mature hERG	402
		Others	
EDEM	ER membrane	Degradation of misfolded glycoproein	216
ARHGAP6	Cytosolic	Acts on PLC to reduce hERG current	505
GM130 (Golgin-95)	Golgi	Vesicle trafficking to *cis*-Golgi	532
14-3-3ϵ	Cytosolic	Regulate PKA modulation of Kv11.1	308
KCR1	Plasma membrane	Reduce the sensitivity of HERG to drug blockers	339

sylation (214). Abolishing glycosylation does not prevent trafficking to the cell membrane, but it decreases the stability of hERG protein at the plasma membrane (214). Conversely, mutation of Asn629 causes a trafficking defect, and the mutant protein is retained in the ER (214).

The molecular weight difference between the fully glycosylated mature protein and core-glycosylated immature protein provides a very convenient assay for determining whether mutations result in misfolding, i.e., misfolded proteins do not reach the Golgi and so only give rise to the smaller 135-kDa band (192, 733). Simple western blot assays also provide a convenient means of determining whether mutant channels exhibit a dominant negative effect on wild-type channels (175, 310, 728). By including separate antibody epitopes on the wild-type and mutant channels, one can detect individual subunits separately after coexpression experiments, to determine whether wild-type channels get trapped in the ER and/or whether mutant channels can be rescued. The majority of KCNH2 missense mutations that have been studied to date result in defective trafficking (19). The study from Anderson and colleagues (19) predominantly involved mutants occurring in the transmembrane regions (28 of the 34 mutants studied). There are, however, numerous studies of mutations in

both the NH_2-terminal (209, 478, 531) and COOH-terminal (9, 129, 181, 437, 733) cytoplasmic domains that have trafficking defects as well.

4. Degradation

Mature wild-type hERG has a half-life of ~10 h when expressed in heterologous systems (176, 310, 366). Degradation of hERG can occur via both polyubiquitination-proteasomal degradation (216) as well as ubiquitin-dependent lysosomal degradation (94). Exposure of cells to reduced extracellular K^+ also promotes degradation via ubiquitination and caveolin-dependent endocytosis (227, 401, 402, 607) (see sect. III*E*). Misfolded hERG proteins remain associated with chaperones and are tagged by CHIP (COOH terminus of Hsc70-interacting protein), an E3 ubiquitin ligase that contacts Hsc70 and ubiquitylates chaperone-bound proteins (656). The channels are then degraded in the proteasome via ER-associated degradation (ERAD) (533, 651), a process involving recognition and active removal of misfolded protein from the ER.

Immature (core glycosylated) wild-type hERG disappears during pulse chase experiments with a half-life of ~4 h (216). However, a large portion of the immature hERG is converted into the mature form during a 24-h chase period (216). On the contrary, trafficking defective hERG channels do not undergo maturation and are completely degraded within 24 h (216, 733). Coexpression of the dominant negative trafficking mutant A561V also results in accelerated degradation of wild-type hERG subunits that are retained in the ER as a result of assembling with the mutant subunits (310).

C. Assembly

1. Tetramerization

Individual hERG isforms can form homotetramers or coassemble to form heterotetramers (301, 383, 494). The assembly of the tetrameric channel also occurs within the ER. This can be deduced from observations that many misfolded mutant channels that are retained in the ER bind to wild-type subunits and exert a dominant negative effect on channel expression (175, 310, 728).

In canonical VGK channels, subunit assembly is facilitated by the cotranslational interactions of the NH_2-terminal T1 domain (365, 570). In Kv11.1 channels however, deletion of most of the NH_2 terminus does not prevent normal trafficking (661). Nevertheless, it has been suggested that the NH_2 terminus may still contribute to tetramerization, as purified recombinant NH_2-terminal constructs containing the PAS domain can form tetramers in solution (369).

With the early studies suggesting that the NH_2 terminus may not be essential for tetramerization, many workers switched their attention to the COOH-terminal domain. By using a deletion and rescue strategy, Kupershmidt et al. (338) showed that ligation of a region of the distal COOH terminus (residues 1018–1122) into channels lacking the entire COOH terminus (hERG-ΔC), rescued the trafficking of the hERG-ΔC channels. Furthermore, the rescued channels produced typical Kv11.1 currents (338). A conserved coiled-coil domain (residues 1036–1074, termed TCC) within this region was later shown to form a tetramer in vitro (289). However, the role of residues 1018–1122 in channel assembly has been questioned by other workers. For example, Akhavan and colleages (9, 10) have shown that this sequence is dispensable for the formation of functional tetramers. It may be that, like the PAS domain, the distal COOH terminus is not essential but does contribute to stabilization of tetrameric channels. More recently, attention has shifted to the role of the cNBD domain located in the proximal end of the cytoplasmic COOH-terminal domain. Numerous missense mutations and partial deletions within the cNBD cause trafficking defects (9, 10, 598). More recently, Gustina and Trudeau (231) have also provided evidence for intersubunit interactions between the PAS domain and the cNBD. Whether these interactions are important for assembly and/or are involved in regulating gating remains to be determined.

Overall, there appear to be multiple cytosolic domains that can contribute to assembly and tetramerization of hERG proteins. However, none of them appears to be essential; rather, a model is emerging of multiple interacting domains, in which the absence of one can be at least partially compensated for by other domains.

2. hERG 1a/1b heterotetramers

The hERG-1b isoform lacks the first 373 amino acids of the 1a isoform but contains a unique 36-amino acid sequence at its NH_2 terminus. It was initially thought that hERG 1b isoform was not expressed at very high levels in human cardiac tissue (504). However, with the aid of improved antibody reagents, expression of hERG-1b protein has been detected in human cardiac tissue (301). Subsequently, Robertson et al. (494) showed that 1a and 1b subunits preferentially coassemble with each other mediated via a cotranslational interaction between the NH_2-termini of 1a and 1b during biogenesis. The NH_2-terminal interaction between the two isoforms promotes ER exit of the 1b containing channel complex by masking an RXR ER retention signal that is present in the NH_2 terminus of the 1b isoform (495). Recently, mutations have also been found in the 1b specific exon strongly suggesting that the 1b isoform is indeed clinically important (542). Thus it is likely that the native I_{Kr} in human tissue is composed of 1a/1b heterotetramers (301, 542). The presence of hERG 1b subunits in Kv11.1 channels also alters responses to thyrotropin releasing hormone (328), acidosis (153), oxidative stress (331), and cGMP

(411) as well as altering the sensitivity and kinetics of drug binding (542) and modulation by agonists (351).

3. Accessory subunits

KCNE1 and KCNE2 are single transmembrane domain proteins that interact with the pore-forming subunits of KCNQ1 and hERG proteins (1, 2, 18, 405). Whereas KCNE1 subunits are essential components of the I_{Ks} channel complex (51, 546), the role of KCNEs in regulating Kv11.1 function is still a topic of debate (2). Both KCNE1 and KCNE2 have been shown to associate with hERG (1, 405) and alter gating kinetics of Kv11.1 both in oocytes and mammalian cell lines (403). KCNE1 antisense oligos also reduce I_{Kr} density in the atrial tumor cell line (AT1 cell) (695). A study in horse heart has provided additional evidence that KCNE1 can coimmunoprecipitate with hERG in native tissue (184). However, it is not clear whether these observed interactions are direct or via an undetermined adaptor protein. One possibility is that KCNQ1 acts as the bridge between hERG and KCNE1 (see below).

Mutations in KCNEs are associated with both inherited long QT syndrome (LQTS) (3, 72, 441, 589) as well as drug-induced QT prolongation (1, 565), which is consistent with KCNEs modulating I_{Kr} in native tissue. Conversely, some workers have found that coexpression of KCNE2 has no effect on Kv11.1 kinetics (679). This apparent discrepancy may though be resolved by a recent report from Zhang et al. showing that KCNE2 may modulate Kv11.1 by accelerating the degradation of hERG protein (722). In addition, KCNE2 has been shown to modulate the activity of many other cardiac ion channels (2) including HCN channels (704), Kv4.x channels (717), and Kv2.x channels (404). Thus it is also possible that mutations in KCNE2 could alter cardiac repolarization via effects on channels other than Kv11.1.

4. Other interacting partners

In addition to the KCNE family of β-subunits, KCNQ1 has been shown to alter hERG function. Ehrlich et al. (161) showed that coexpression of KCNQ1 with hERG in CHO cells (transient transfection) resulted in a significant acceleration of Kv11.1 channel deactivation that more closely resembled native I_{Kr}. Furthermore, they showed that coexpression with KCNQ1 resulted in an approximately twofold increase in plasma membrane expression of hERG (161). They also showed that the interaction between hERG and KCNQ1 was mediated by the COOH-terminal domain. Hayashi et al. (250) subsequently showed that the positive influence of KCNQ1 coexpression on Kv11.1 current density was not observed with trafficking defective KCNQ1 mutants. In contrast to this, Brunner et al. (81) showed that transgenic overexpression of dominant negative pore-mutants of hERG or KCNQ1 in rabbit hearts resulted in a downregulation of I_{Ks} or I_{Kr}, respectively, without altering the steady-state levels of the native polypeptides. They followed this up with studies in CHO cells showing that coexpression of KCNQ1 caused downregulation of Kv11.1 current (516). The origin of the discrepancy between the studies of Ren et al. (516) and the studies from Erhlich et al. (161), and Hayashi et al. (250), is not immediately obvious, although Ren and colleagues suggest that it could be related to the transfection technique (a combination of stable and transient expression in their study compared with double transient transfection in the Erlich et al. and Hayashi et al. studies).

The K^+ channel regulator KCR1 is a 12 transmembrane domain protein that associates with hERG and rat EAG channels (273, 339). When coexpressed in heterologous systems, KCR1 associates with hERG at the plasma membrane and renders it less sensitive to classic hERG blockers, including dofetilide, quinidine, and sotalol (339). In addition, a gain of function polymorphism in KCR1, which enhances KCR1 protection against drug block of hERG, has been linked to a reduced risk of drug-induced QT prolongation (491). The protective action of KCR1 against drug-induced QT prolongation is linked to its α-1,2-glucosyltransferase activity, which was discovered after it was noticed that it had high sequence homology to yeast α-1,2-glucosyltransferase ALG10 (436). Subsequently, a loss of function variant of KCR1 was linked with an increased susceptibility to drug-induced prolongation of the QT interval (249).

D. Posttranslational Modifications

In addition to glycosylation, hERG channels have been shown to be phosphorylated via numerous signaling pathways. Phosphorylation of hERG has important roles in biogenesis (see sect. III*G*), as well as acute regulation of gating under a variety of physiological and pathophysiological conditions (see sect. VI*E*). HERG contains multiple putative consensus phosphorylation sites for protein kinase A (PKA), protein kinase C (PKC), and protein tyrosine kinases. Other kinases, including PKB and PKG, have also been implicated in regulating hERG function. In this section, the focus is on signaling/phosphorylation pathways that regulate hERG and how these alter assembly and trafficking. The effects of phosphorylation on gating are discussed in section VI.

1. PKA

PKA is activated by increases in cAMP concentration, which in the heart typically occurs following stimulation of the β-adrenergic pathway (524). HERG contains four consensus phosphorylation sites for PKA: Ser283 in the NH_2 terminus as well as Ser890, Thr895, and Ser1137 in the COOH terminus. All four sites can be phosphorylated in

vitro (130). In addition to these four sites, there is a common SNP (RS1805123) that introduces another phosphorylation site, K897T (204).

A number of accessory proteins are involved in PKA-dependent substrate phosphorylation. For example, the A-kinase adaptor protein (AKAP) Yotiao plays an essential role in mediating adrenergic regulation of KCNQ1 activity (398). A peptide that specifically disrupts interactions between PKA and AKAPs has been shown to diminish phosphorylation of hERG by PKA (370). AKAPs have also been shown to cosediment with hERG in subcellular fractionation experiments from both HEK293 cells and porcine ventricular tissue, although a direct interaction between hERG and an AKAP has not been detected (370).

The family of 14–3-3 proteins are highly conserved regulatory molecules expressed in all eukaryotic cells (188). 14–3-3ε is the most abundant isoform expressed in cardiac tissue, and it has been shown to associate with hERG to potentiate effects of cAMP/PKA stimulation (309). Binding of 14–3-3ε to hERG requires intact PKA phosphorylation sites at Ser283 in the NH_2 terminus and at Ser1137 in the COOH terminus. Binding of 14–3-3 prolongs the adrenergic effects on Kv11.1 gating possibly by shielding phosphorylated Ser283 and Ser1137 from cellular phosphatases (308). Mutations that impair 14–3-3-hERG binding have also been implicated in pathogenesis of LQTS type 2. A series of frameshift or truncation mutations in the distal COOH terminus that remove Ser1137 exhibit normal gating kinetics but do not exhibit the hyperpolarizing shift in voltage dependence of activation when coexpressed with 14–3-3ε (104).

2. Protein kinase B and phosphatidylinositol 3-kinase signaling

Kv11.1 channels are regulated through a signaling cascade involving phosphatidylinositol 3 (PI3) and phosphoinositide-dependent kinases, which subsequently activates downstream serum and glucocorticoid inducible kinase (SGK) and protein kinase B (PKB) (393). Both SGK and PKB are members of the AGC protein kinase superfamily. Kinases in this superfamily share a high degree of homology in their protein sequences especially within the catalytic kinase domain (480). SGK and PKB also share many common upstream effectors as well as downstream targets in their signal cascades (14, 330, 355, 585). Maier et al. (393) reported that coexpression of SGK3, but not SGK1, with hERG in *Xenopus* oocytes enhanced steady-state current and cell membrane protein abundance, without altering gating kinetics. This effect was not abolished by mutating the consensus sites for SGK phosphorylation, suggesting that the SGK3 effects were independent of direct channel phosphorylation. Similarly, the expression of constitutively active PKB also increases Kv11.1 current in HEK293 cells (725), although it is unclear whether this requires direct channel phosphorylation. Conversely, direct phosphorylation by PKB may have a role in downregulating hERG protein in which a PKB site is generated through the K897T polymorphism (204). Furthermore, in pituitary cells, thyroid hormone T_3 stimulates hERG via activation of PI3 kinase, which reduces phosphorylation at residue Thr895 (203, 204).

The downstream targets of SGK3 and PKB that regulate Kv11.1 are not known. However, given what is known about how SGK3 and PKB regulate other ion channels, including, e.g., the epithelial sodium channels (533), it is likely that they will act through other proteins, such as the E3 ubiquitin ligase Nedd4–2. Nedd4–2 is expressed in cardiac tissue, and a possible role of Nedd4–2 in regulating plasma membrane expression of hERG protein has started to emerge (13), although disparity in opinion exists regarding a direct interaction between hERG and Nedd4–2 (535).

3. PKC

The acute effects of PKC activation have been examined in several different experimental systems, using either activators of PKC such as diacylglycerol (DAG)/l-oleoyl-2-acetyl-*sn*-glycerol (OAG) and phorbol 12-myristate 13-acetate (PMA) (53, 113, 633) or by studying G protein-coupled receptors linked to PKC activation, including TRH receptor (213), angiotensin II receptor AT1 (676), α-adrenoceptors (631, 671), and muscarinic receptors (113, 260, 407). Acute activation of PKC typically results in reduced KV11.1 current in oocytes (53, 630, 633) and HEK293 cells (113, 513, 676), as well as isolated guinea pig ventricular myocytes (671). These changes are mediated in part by changes in gating properties as well as increased endocytosis (513).

The major controversy regarding PKC regulation of Kv11.1 channels is whether the channel is directly phosphorylated. Thomas et al. (633) identified 18 consensus sites for PKC phosphorylation in hERG using PROSITE software (Ser26, Thr74, Thr162, Thr174, Ser179, Ser250, Ser278, Ser354, Thr371, Thr526, Ser606, Ser636, Thr670, Ser890, Thr895, Ser918, Ser960, and Thr1133). Mutating each of these sites to alanine (with the exception of Thr74, as the alanine mutation prevented correct folding and assembly) did not abrogate acute regulation by PKC, suggesting that direct phosphorylation of hERG protein is not required. Cockerill et al. (113) confirmed that Kv11.1 channels with all the PKC consensus phosphorylation sites mutated to alanine are still regulated by PKC. Furthermore, they showed that PKC activation resulted in an increased level of phosphorylation of hERG protein (113). Whilst they were not able to identify the specific phosphorylation sites they showed that deletion of the NH_2 terminus (Δ2–354) prevented the PKC-stimulated increase in phosphoprotein levels and prevented the acute effects on Kv11.1 function, which suggests that residues in the NH_2 terminus are directly phosphorylated by PKC. One possibility could be that there is an atypical

PKC site in the NH_2 terminus of the hERG protein. Subsequently, Chen et al. (96) showed that intact PKC phosphorylation sites were required for the enhanced rates of synthesis seen with chronic stimulation of PKC. Together, these studies suggest that PKC-mediated phosphorylation of hERG protein can occur, but to what extent it contributes to the functional effects observed remain to be defined. Furthermore, the specific sites phosphorylated by PKC remain to be determined.

4. cGMP/ANP, BNP/PKG

Atrial natriuretic peptide (ANP) and brain natriuretic peptide (BNP) are two hormones secreted by the atria in response to atrial stretch/dilatation and increased levels are hallmarks of heart failure (406). ANP, signaling via cGMP, has been shown to modulate Kv11.1 function, in particular channels containing the hERG-1b isoform. In heterologus cell lines, cGMP or ANP has no effect on Kv11.1 channels composed entirely of hERG 1a subunits (130, 411, 613), but cGMP potently suppresses Kv11.1 channels composed of ERG1b or ERG1a/1b subunits in a PKG-dependent manner (130, 411, 613). In the mouse heart, cGMP exhibits a striking regional difference by suppressing I_{Kr} in atrial but not ventricular myocytes, suggesting that cGMP and its physiological activators ANP and BNP may have significant roles in arrhythmogenesis under pathophysioloigcal conditions such as heart failure (130, 411, 613).

5. Tyrosine kinases/Src/EGFR

Stimulation of the tyrosine kinase Src increased Kv11.1 current in the rat microglial cell line MLS-9 (732). Cayabyab and Schlichter (90) subsequently showed that hERG and Src can be coimmunoprecipitated and may form a multimeric regulatory complex. Zhang et al. (711) also showed that Kv11.1 current amplitude was reduced following inhibition of EGFR kinase and the Src family of kinases. They suggested that the effects of the inhibitors occurred through decreased phosphorylation of Tyr475 and/or Tyr611. Given that Tyr475 is located on the intracellular S2-S3 loop, whereas Tyr611 is potentially buried within the membrane and has been suggested to point towards the membrane interior (359), it would seem that Ty475 is the more likely candidate.

E. Regulation of Biogenesis

1. Developmental changes in KCNH2 expression

The levels of KCNH2 mRNA expression change during development. In rodents, I_{Kr} current density (665) as well as KCNH2 mRNA (45) and ERG protein levels (672) decrease from fetal to neonatal and to adult levels. This is consistent with numerous studies showing that I_{Kr} blockers have minimal or no effect on QT interval duration in adult mice (45). There are no comparable studies in higher mammals. However, it is clear that KCNH2 expression is important for development in both mice and humans as genetic ablation of KCNH2 mRNA, either in knockout mice (622) or homozygous loss of function in humans (67), results in embryonic lethality. Furthermore, in mice, there is evidence to suggest that mERG function contributes to early embryo development with I_{Kr} specific blockers resulting in reduced incidence of blastocyst formation (685). Wang et al. (672) have also shown that the subunit composition of I_{Kr} changes during development with levels of mERG1b expression high in neonates but not detectable in adults, whereas mERG1a expression is higher in adults compared with neonates.

Despite the importance of I_{Kr} for cardiac function and the multiple studies highlighting significant I_{Kr} expression changes during development, there are few studies that have investigated the molecular basis of these changes. Wang and colleagues (158) have shown that treating young mice (10–15 day) with dexamethasone (a synthetic glucocorticoid) prevents the normal loss of I_{Kr} function and dofetilide binding sites during this time period in mice. The specific mechanisms by which glucocorticoids regulate I_{Kr} expression, however, remain to be determined. In adults, I_{Kr} current density as well as KCNH2 transcript levels also vary between males and females (194), which suggests regulation by sex hormones, with the strongest evidence indicating that there is a positive influence of testosterone (381, 519, 688) resulting in higher KCNH2 levels and in turn shorter QT intervals in men.

2. Regulation of mRNA biogenesis

Mammalian gene promoters are typically either GC rich or contain canonical TATA box or CCAAT box motifs that bind components of the RNA polymerase complex of proteins required for initiation of transcription (581). DNA sequences immediately upstream of the transcription initiation sites for KCNH2–1a and -1b lack canonical TATA and CCAAT boxes but are GC rich (64–68% GC content). The KCNH2–3.1 promoter lacks canonical TATA and CCAAT boxes and is not particularly GC rich. The level of KCNH2–3.1 expression, however, is considerably lower than the 1a or 1b transcripts in most tissues, with the exception of hippocampal and prefrontal cortical regions of the brain where KCNH2–3.1 and 1a are expressed at similar levels (279).

Recently, Lin et al. (373) showed that the length of a TG repeat polymorphism ~1 kb upstream of the KCNH2–1a transcription start site is inversely correlated with the level of KCNH2 transcription and QT prolongation. Given that the levels of functional hERG protein expression can have a marked influence on cardiac electrical activity, further study of the regulation of transcription of KCNH2 is clearly warranted.

3. Regulation of protein biogenesis

Sustained elevation of cAMP increases hERG biogenesis (98). A 24-h exposure to CPT-cAMP (a direct activator of PKA) resulted in a two- to fourfold increase in steady-state levels of protein expression in HEK293 cells and ~25–40% in isolated rabbit cardiomyocytes (98). This increase in hERG synthesis is due to an increase in translation, as demonstrated by increased incorporation of ^{35}S-methinonine, which was blocked by treating cells with cycloheximide, an inhibitor of translation. The stability of hERG at the plasma membrane however remained unaltered. At least in HEK293 cells, the increase in Kv11.1 current density was delayed relative to the increase in synthesis in the ER, suggesting that trafficking of hERG through the ER and Golgi apparatus is the rate-limiting step of forward trafficking (98). More recently, McDonald et al. (590) have shown, using a FRET-based PKA biosensor, that PKA located at the ER membrane surface, as opposed to the plasma membrane, is responsible for the changes in protein synthesis. In addition to the direct effects of PKA on KV11.1 channels, one has to take into account the fact that chronic β-adrenergic stimulation eventually results in downregulation of many components of the signaling pathway (171), so the overall effect may be much more modest than that seen in relatively short term (order of days) tissue culture experiments. Thus the pathophysiological relevance of the chronic effects of PKA stimulation on Kv11.1 remain to be fully determined (see sect. VI).

Acute PKC activation (15–60 min) results in increased endocytosis and reduced plasma membrane expression of hERG (513). Conversely, chronic stimulation of α1-adrenergic receptors leading to chronic stimulation of PKC causes an increase in hERG biogenesis in HEK293 cells (96). Although smaller, this effect is also observed in neonatal rat cardiomyocytes (96). Stimulation of the NH_2-terminal truncated isoform of the androgen receptor has also been shown to stabilize hERG protein half-life (688). This effect is mediated by phosphorylation of ERK1/2 and is observed both in CHO cells and in isolated rabbit cardiac myocytes.

In contrast to the upregulation of hERG synthesis observed with chronic PKA/PKC phosphorylation, Nanduri and colleagues (439, 440) have shown that rates of protein synthesis are reduced by chronic hypoxia. They subsequently showed that hypoxia inhibited the interaction of hERG with Hsp90, a chaperone required for maturation. Furthermore, they showed that this effect could be reversed by reactive oxygen species scavengers (439).

4. Regulation of protein degradation

Until recently, there has been relatively little known about the regulation of hERG channel degradation. Ceramide has been shown to cause ubiquitin-dependent lysosomal degradation of hERG (94), and more recently, Ramstrom et al. (513) have also shown that acute stimulation of PKC can increase endocytosis of hERG channels thereby reducing levels at the plasma membrane. In the last few years, a series of elegant studies from Zhang and colleagues has highlighted an important role played by hypokalemia in regulating hERG turnover at the plasma membrane (227, 401, 402, 607). Furthermore, this effect of hypokalemia occurred at pathophysiologically relevant levels (227, 401, 402, 607). Exposure to reduced extracellular K^+ results in the channels entering a long-lived nonconducting state that promotes ubiquitination, caveolin-dependent endocytosis, and degradation (227, 401, 402, 607). Changes in extracellular K^+, however, have no effect on the stability of the intracellular pool of hERG (227, 401, 402, 607). The E3 ubiquitin ligase that mediates this process has not been identified.

IV. GATING OF I_{KR}/Kv11.1

A. Principles of Gating

Like other VGK channels, Kv11.1 channels can exist in closed, open, and inactivated states. Kv11.1 channels, however, have some unusual gating kinetics. For instance, transitions between open and closed states are unusually slow, whereas transitions between the open and inactivated states are both very fast and voltage dependent (see **FIGURE 5**). The unusual kinetics result in some distinctive features, such as hooked tail currents, but also cause some difficulties in accurately quantifying gating kinetics. Here, the properties of I_{Kr} in cardiac cells are compared with the properties of Kv11.1 channels expressed in heterologous expression systems. This is followed by a review of the protocols used and pitfalls to be aware of in the experimental determination of the kinetics of gating before discussing what is known about the molecular and structural basis of gating.

B. Gating of I_{Kr} in Cardiac Myocytes

Between 1969 and the mid 1980s, there were numerous reports of a rectifying K^+ current contributing to repolarization of the cardiac action potential (79, 145, 448, 449). But it was not until 1987 that Shibasaki, using the then recently developed patch-clamp technique (237) to study both the macroscopic and single-channel I_K from rabbit sinoatrial node cells (572), provided the first insights into the gating properties of what is now known as the rapid component of the delayed rectifying current (I_{Kr}). In macroscopic current recordings he noted the presence of a "hook" following repolarization and correctly surmised that the hook was caused by "a quick removal of inactivation of I_K which had occurred during the depolarizing pulse" (see **FIGURE 1**). Furthermore, he demonstrated that the current had a voltage-dependent activation gate and the voltage at which half-maximal activation occurred ($V_{0.5}$)

was −25 mV. He also noted that the voltage dependence of activation was insensitive to the concentration of K^+ at the extracellular face of the channel, as were the rates of current deactivation. Shibasaki also examined the microscopic basis of I_K gating, using the cell-attached configuration to record single-channel currents. He noted that no channels appeared to open at stronger depolarized potentials, while channels opened during the subsequent repolarizing step. He also noted that the open burst duration decreased as the holding potential was made more negative. Ensemble averages of single-channel records mirrored the rates of I_K activation and deactivation obtained from direct fitting to the time course of macroscopic current, indicating that these single channels were the microscopic basis of I_K. Lifetime analysis of single-channel activity revealed the presence of one open lifetime with a time constant of 2.5 ms and two closed lifetimes with time constants of 0.7 and 17.6 ms at −90 mV. Shibasaki also noted that the lifetime of the open state was shorter than what would be expected from the decay of the macroscopic tail current and also got shorter with more positive potentials, the opposite to what would be predicted for a channel whose gating is just controlled by a single activation/deactivation gate. Based on this, Shibasaki suggested the presence of a second gating process, inactivation, and proposed that this might be the basis of the observed rectification of I_K.

Three years later, Horie et al. (271) noted that the I_K from guinea pig atrial cells could be separated into two components based on single-channel conductance, with one of these components sharing many characteristics with the I_K reported by Shibasaki (572). Notable among these features were a single-channel conductance of 10 pS in 150 mM K^+ (compared with 11.1 pS reported by Shibasaki), the presence of 1 open lifetime (τ_o = 9 ms) and 2 closed lifetimes (τ_{x1} = 1.2 ms and τ_{x2} = 37 ms at −100 mV) similar to those reported by Shibasaki, and a $V_{0.5}$ of −15 mV, compared with −25 mV reported by Shibasaki. Horie et al. also noted a similar hook, rectification, and voltage-dependent deactivation. Sanguinetti and Jurkiewicz subsequently used E-4031, a drug now known to be a highly selective I_{Kr} channel blocker, to pharmacologically isolate a component of the guinea pig ventricular myocyte I_K (548) that had very similar characteristics to those described by Shibasaki and Horie et al., including the hook, rectification, and $V_{0.5}$ for activation of −21.5 mV. Sanguinetti and Jurkiewiecz performed a more extensive analysis of the voltage dependence of gating and showed that the time constants of activation and deactivation followed a bell-shaped distribution peaking between −30 and −40 mV. However, the activation time constants were derived by fitting a single exponential function to the current recorded during a simple depolarization step, a method that is now accepted as inaccurate, due to the coincident nature of activation and inactivation (see sect. IV*D*). They also presented the first approximation of the voltage dependence of the rectification process by measuring the degree of rectification relative to the maximal conductance of a fully activated *I-V* plot. The reported $V_{0.5}$ of −9 mV for rectification is right shifted compared with subsequent characterizations of I_{Kr} and Kv11.1 (380, 547), most likely due to the fact that the *I-V* relationship was only measured down to −100 mV, meaning the maximal conductance and therefore the degree of rectification was underestimated (see sect. IV*D*). Based on these experiments, Sanguinetti and Jurkiewicz coined the term I_{Kr} (rapid component of the delayed rectifier current) to describe this component of the repolarizing I_K.

Subsequently, Liu et al. (380) used the pharmacological isolation method to characterize fully the voltage-dependent kinetics of I_{Kr}. Most notably they used a modified envelope of tails protocol (448) to separate the activation and inactivation processes, which permitted the first measurement of the rates of I_{Kr} activation at depolarized voltages (see sect. IV*D*). Their data indicated that activation of I_{Kr} must involve multiple steps, similar to what had been reported for other voltage-gated K^+ currents (263, 275), and had recently been shown for the cloned Kv11.1 channel (643; see below). They also showed that the rates of activation saturated at highly depolarized voltages, which suggested the presence of a voltage-independent step in the activation pathway.

There have been very few studies of I_{Kr} in human ventricular myocytes (302, 454). O'Hara and colleagues performed a partial characterization of I_{Kr} in undiseased human ventricular myocytes including steady-state activation and rates of activation and deactivation (454). Although it should be noted that rates of activation were measured from a holding potential of −40 mV (which will result in faster apparent rates of activation as the channels will not have to transit through all closed states, see sect. IV*D* for more details). In addition, the inactivation characteristics of human I_{Kr} remain to be determined.

C. Gating of Kv11.1 Channels

1. Macroscopic currents

The properties of Kv11.1 channels, expressed in *Xenopus* oocytes, were first described in 1995 (547, 643). These papers showed that the biophysical properties of Kv11.1 were very similar to those of I_{Kr} in cardiac myocytes (271, 380, 572). The $V_{0.5}$ for Kv11.1 activation was −15.1 mV compared with −22 mV (548), −25 mV (572), and −18 mV (271) for I_{Kr} in native myocytes. It should be noted that the value for $V_{0.5}$ will depend on the length of the depolarization steps (see sect. IV*D*). Also in common with I_{Kr}, Kv11.1 showed a time course of deactivation best described by two exponential components, inward rectification of the current and paradoxical "activation" of the current by external K^+. This last characteristic is in contrast to what would be ex-

pected for a K^+ conducting channel as the outward driving force is reduced. In hindsight, this is now known to be due to the effect of extracellular K^+ on inactivation (668).

The two studies differed with respect to their explanations for the current rectification at depolarized potentials. Sanguinetti et al. (547) investigated the hypothesis originally proposed by Shibasaki, that the current rectification was due to fast voltage-dependent inactivation. Although they were unable to directly measure inactivation, they reasoned they should be able to measure its recovery as a way of interrogating the process. The authors measured recovery from inactivation at a range of holding potentials and noted that the $V_{0.5}$ for the voltage dependence of recovery from inactivation was very similar to the $V_{0.5}$ for the rectification process of I_{Kr} in rabbit nodal cells (572), with a slope factor identical to that in guinea pig (548). Although these data are consistent with the hypothesis that rectification is caused by fast voltage-dependent inactivation, they could not rule out block by an endogenous cytoplasmic moiety. In contrast, Trudeau et al. (643) favored the possibility that Kv11.1 may be a classic inward rectifier, i.e., that rectification was caused by a soluble cytoplasmic moiety such as Mg^{2+} or polyamines (643). Their conclusion was based on sequence homology within the core channel region as well as similar profiles for Kv11.1 and inward rectifier block by Cs^+ and Ba^{2+} (235, 236). Like Sanguinetti et al. though, they could not rule out other mechanisms such as C- or N-type inactivation.

In 1996, three groups independently identified the mechanism of inward rectification (558, 583, 588). Each of these groups ruled out so-called ball and chain or N-type inactivation (274, 706) since the process was insensitive to both internal application of TEA (583) and to deletion of the cytoplasmic NH_2 terminus (558, 588). Channel block by intracellular Mg^{2+} (as reported for inward rectifiers) was also discounted (583, 584, 588). Instead, they concluded it was more analogous to "C-type" (106, 276). Like C-type inactivation in *Shaker*, Kv11.1 inactivation is sensitive to external application of TEA and ion occupancy of the selectivity filter (558, 583), both of which were thought to physically prevent "collapse" of the selectivity filter. In addition to this, mutation of the serine at position 631 to alanine markedly affected inactivation. Ser631 is equivalent to Thr449 in *Shaker*, a residue critical for C-type inactivation (388, 700). However, while bearing features analogous to C-type inactivation, Kv11.1 inactivation clearly has features that are unique. Most notably, the rates of inactivation and recovery from inactivation are both fast and voltage-dependent (583, 588). In contrast, C-type inactivation as reported in *Shaker* channels is slow and voltage insensitive (276). Wang et al. (668) later reasoned that the voltage sensitivity of Kv11.1 inactivation could not be explained by coupling to activation since: *1*) Kv11.1 inactivation continues to show voltage dependence at voltages where activation is complete, *2*) the slopes of the equilibrium activation and inactivation curves are markedly different (compare **FIGURES 9** and **14** below), and *3*) inactivation is sensitive to changes in external K^+ while activation is insensitive to changes in extracellular K^+ (668).

In 1997, Wang et al. (668) provided the first full quantitative description of all the kinetic parameters of Kv11.1 gating based on experiments in *Xenopus* oocytes, consolidating much of the previous data. Among other features, they recapitulated the bell-shaped distribution of the forward and reverse rates of inactivation reported by Spector et al. (588), the potassium sensitivity of inactivation, and the saturation effect of voltage on the rate of activation (380). This compilation of kinetic descriptions allowed the authors to develop the first fully characterized model for simulation of Kv11.1 current, discussed below in section IV*H*.

Each of the descriptions of Kv11.1 gating outlined above was based on expression of the hERG1a isoform in heterologous systems. However, some recent studies have suggested that native I_{Kr} is a heterotetrameric assembly of hERG1a and hERG1b subunits (358, 383). The hERG1a and 1b isoforms are identical in their transmembrane and cytoplasmic regions, but the 1b isoform is significantly truncated in the NH_2-terminal cytoplasmic region, being 340 amino acids shorter. In heterologous expression systems, heterotetramers of hERG1a and hERG1b show faster activation, deactivation, and recovery from inactivation than Kv11.1 channels composed of hERG1a subunits alone (542). These differences in kinetics are not surprising given the role of the NH_2-terminal domain in regulating Kv11.1 gating (see sect. IV*F*). These characteristics of the heterotetramer, particularly the faster deactivation, potentially explain the observed differences between the gating kinetics of I_{Kr} in myocytes compared with Kv11.1 channels composed only of hERG1a subunits (421, 679).

2. Single-channel recordings of Kv11.1 channels

In 1996, Kiehn et al. (324) presented the first single-channel recordings from recombinant Kv11.1 channels expressed in *Xenopus* oocytes. As with single-channel recording from I_{Kr} (572), Kv11.1 channel activity was only apparent during repolarization, and ensemble averages of multiple single-channel records recapitulated the typical hooked Kv11.1 tail current (323) (see **FIGURE 8**). Analysis of single-channel lifetimes revealed the presence of a single open state with a mean open time of 3.2 ms and two closed states with time constants of 1.0 and 23 ms (at −100 mV in the presence of 100 mM K^+ at the external face of the channel). Zou et al. (738) carried out parallel experiments and reported similar closed state kinetics: two closed states with lifetimes of 0.54 and 14.5 ms. However, they reported two open states with lifetimes of 2.9 and 11.8 ms at −90 mV. This was the first suggestion of multiple open states for the Kv11.1 channel, which the authors ascribe to simply acquiring more events for analysis. A potentially important methodological differ-

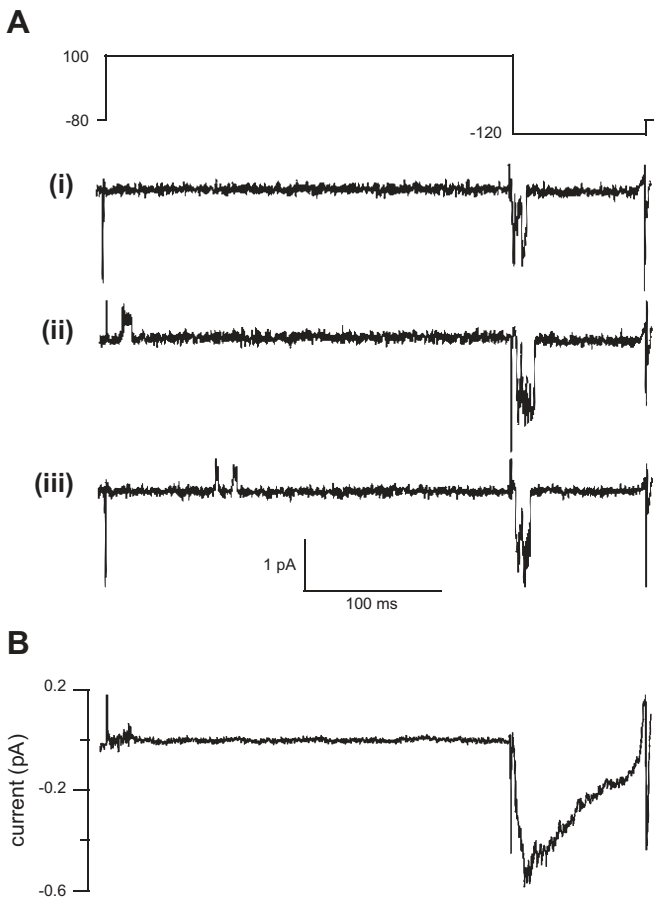

FIGURE 8. Kv11.1 single-channel recordings. *A*: typical cell-attached patch current traces recorded during a 1 s depolarization to 100 mV followed by a hyperpolarization step to −120 mV. Patch pipette contained 100 mM K^+. The depicted traces illustrate the three types of recordings observed: (i) no channel openings, (ii) early openings, and (iii) late channel openings during the depolarization step. *B*: average of 32 traces from patches that had at least four channels in the patch. Note the hooked tail current recorded at −120 mV, similar to that seen in whole cell currents (see **FIGURE 1**). [From Kiehn et al. (323).]

ence between the Zou and Kiehn studies is that Zou used a cell attached configuration compared with excised patches used by Kiehn; it is possible that the presence of accessory proteins and/or scaffold proteins that are lost upon excision of the patch could alter the gating kinetics. The time constants for the closed states reported for Kv11.1 in the above two studies are very similar to those reported for I_{Kr} in nodal (572) and atrial cells (271). The data from Zou also suggests a possible explanation for the discrepancy in mean open times reported for I_{Kr} in nodal (2.5 ms; Ref. 572) and atrial (9 ms; Ref. 271) cells, i.e., differences in sampling rate and durations of data acquisition may have resulted in one of the two life times being missed in the previous studies. The Sanguinetti group recapitulated their finding of multiple open states in an inactivation deficient mutant, S631A, where they reported open lifetimes of 0.6 and 5.9 ms and closed lifetimes of 0.5 and 3 ms, clearly different from their measurements of wild-type Kv11.1 (739, discussed above). Given the authors show that the S631A mutation does not alter activation/deactivation, these differences in lifetimes presumably reflect changes in inactivation gating even at negative membrane potentials in the presence of high extracellular K^+.

Subsequently, Kiehn et al. (323) analyzed the kinetics of Kv11.1 single-channel activity over multiple voltages, with a view to understanding how the unique kinetics contribute to the observed macroscopic currents. In considering the previously observed phenomenon that channels rarely opened at the onset of depolarization, but produced bursts of opening upon repolarization (as channels recover from inactivation before deactivating), they noticed that recordings fell into three categories: in 55% of recordings there were no openings during a depolarizing pulse to +100 mV, in 24% of recordings there were early openings, with a mean latency of 12 ms and in the remainder of recordings there were late openings with a mean latency of 122 ms. Kiehn et al. suggested that the lack of openings in the majority of sweeps at depolarized potentials was due to closed-state inactivation, as initially suggested by Shibasaki in 1987 (572). Based on this observation, they suggested that the openings with the shortest latency are the bursts responsible for the transient peak during depolarization, while those with longest latency contribute to the small steady-state current at depolarized potentials. This theory was supported by experimental recordings of ensemble averages from macropatches that showed that the magnitude of the transient peak was dependent on the holding potential from which depolarization occurred; that is, cells depolarized from more negative potentials showed a greater peak magnitude, as fewer channels were resident in the closed-inactivated state at more negative potentials there were more channels available to open (323). The authors also reported that a five-state kinetic model incorporating closed to inactive transitions provided the best fit to their macroscopic data (discussed in sect. IV*H*).

The differences in mean open times between different studies, together with the finding that the minimal number of states required in a Markov state model to reproduce both macroscopic and single-channel data was more than the number of states that could be directly observed in Kv11.1 single-channel recordings (323), highlight the technical difficulties in studying Kv11.1 at the single-channel level. Most notably, the channel inactivates very quickly and has very small unitary conductance, particularly at physiological extracellular K^+ concentrations, estimated at ~1 pS using noise analysis (256, 324). This has meant that each of the above studies has used a high concentration of extracellular potassium to slow inactivation and increase unitary conductance (323, 324, 738) or used inactivation deficient mutants (739). Because of these difficulties, the vast majority of work relating to Kv11.1 channels, and a corresponding majority of the functional insight into the structural and molecular basis of Kv11.1 gating as discussed below, has come from studies of macroscopic currents.

D. Experimental Measurement of Kv11.1 Gating: Protocols and Pitfalls

The kinetics of Kv11.1 gating, in particular the temporal and electrical coincidence of activation and inactivation, mean that it is not straightforward to measure these characteristics. However, there are now well-established and routinely used protocols. This section outlines the protocols, as well as potential difficulties associated with them. It is also important to note that while the protocols below are discussed in the context of the wild-type channel, the individual experimental parameters, such as the voltages and durations of particular pulses, may need to be adjusted based on the particular mutant or experimental conditions of the study.

1. Steady-state activation

The voltage-dependence of Kv11.1 activation is assessed using tail current analysis (**FIGURE 9*A***). From a holding potential of −90 mV, channels are activated with a series of depolarizing P1 pulses (typically from −80 mV to +60 mV for wild-type Kv11.1), and tail currents are recorded during a repolarizing P2 pulse (typically −60 mV). Inactivation of Kv11.1 at depolarized potentials means significant rectification is seen during the P1 pulse, while fast recovery from inactivation relative to deactivation ensures that the magnitude of the tail current during P2 is an accurate representation of the proportion of channels activated during the preceding P1 pulse **(FIGURE 9)**. A fit of the Boltzmann equation to the peak tail current measured during P2 allows an assessment of the $V_{0.5}$ of activation as well as a slope factor that approximates the activation gating charge.

As a consequence of the slow kinetics of Kv11.1 activation, it is important to ensure the P1 pulse is of sufficient duration to allow activation to reach as close as possible to steady state. Indeed, the data obtained from a tail pulse protocol should really be referred to as isochronal activation data with specific mention of the duration of the P1 pulse duration. As illustrated in **FIGURE 8*C***, the apparent $V_{0.5}$ of "steady-state activation" varies by over 20 mV as the P1 duration is increased from 0.5 to 16 s. The duration of the P1 pulse is particularly important when characterizing mutants that alter the activation process, as mutants that slow activation may result in an apparent depolarizing shift in the $V_{0.5}$ of "steady-state activation" and mutants that increase the rate of activation may result in a hyperpolarizing shift of steady-state activation. Another point to consider when comparing results from different studies is the composition of the perfusion solutions. Divalent and trivalent cations have a profound effect on gating properties including the voltage dependence of activation (261, 262, 300, 543, 547). While these effects are most pronounced for trivalent ions, such as La^{3+} and Co^{3+} (543), significant effects are also observed with Ca^{2+} (300) and Mg^{2+} (503) in the low millimolar range. For example, going from 1.8 to 10 mM Ca^{2+} results in a +22 mV shift in the voltage dependence of activation as measured from 2 s isochronal activation curves (300).

In regard to estimating the gating charge, the fit of a simple Boltzmann distribution to activation data can lead to underestimation of the effective number of charges moved. A more accurate estimation of gating charge can be made using the limiting slope method (16, 65, 577). In this case, the natural logarithm of the open probability (P_o), the peak

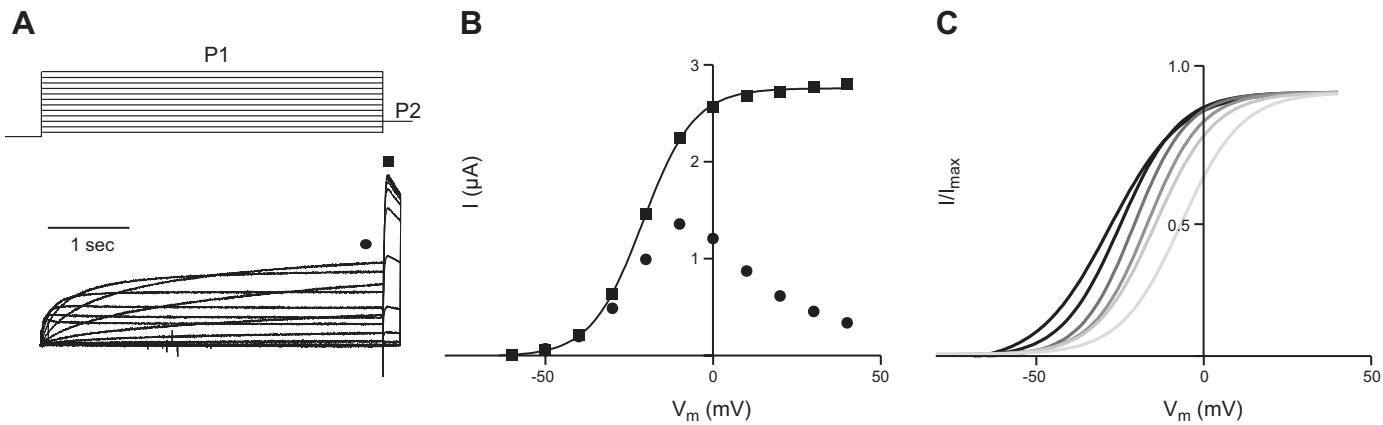

FIGURE 9. Measurement of steady-state activation of Kv11.1 channels. *A*: voltage protocol and typical example of current traces recorded from a *Xenopus laevis* oocyte injected with KCNH2–1a mRNA. Cells are depolarized from a holding potential of −90 mV to voltages in the range −80 to +40 mV (P1 pulse), then stepped back to −60 mV (P2 pulse) to allow channels to recover from inactivation back to the open state and so reveal the relative proportion of channels that had been activated during the P1 pulse. *B*: plot of current at the end of the 4 s P1 voltage step (closed circles, shows a typical n-shaped curve) and peak tail currents during the P2 pulse (closed squares, shows typical sigmoidal shaped curve). *C*: isochronal activation curves where duration of the P1 voltage step was 0.5, 1, 2, 4, 8, and 16 s. This highlights the leftward shift in the voltage dependence of activation with longer P1 voltage steps.

tail current measured during P2, is plotted against voltage and fitted with a Boltzman equation

$$P_o = \frac{1}{1 - e^{-z_g q_e V / k_B T}} \quad (1)$$

where z_g is the gating charge, q_e is the elementary charge, V is the membrane potential, k_B is the Boltzmann constant, and T is absolute temperature. At low open probabilities the P_o-voltage relationship is linear when plotted on semi-logarithmic axes **(FIGURE 10)** and hence the gating charge z_g can be calculated as

$$z_g = \frac{k_B r}{q_e} \times \text{Slope} \quad (2)$$

The accuracy of this method is dependent on a good spread of P_o measurements in the linear part of the curve. Therefore, when acquiring data for this type of analysis, P1 pulses should be spaced at tight voltage intervals (every 2–5 mV for example) and the voltage range extended more negative than the $V_{0.5}$ for activation (at least to −60 mV for wild-type Kv11.1, **FIGURE 10**).

2. Rates of activation

Due to the coincident nature, both temporally and electrically, of the activation and inactivation processes, particularly at more depolarized potentials, it is not possible to obtain rates of activation by simply fitting current records with exponential functions (380). As an alternative to direct fitting, Liu et al. (380) used an "envelope of tails" protocol as shown in **FIGURE 11**. Under these experimental conditions, the membrane voltage is stepped from a holding potential (typically −90 mV or more negative) to an activating P1 test potential for successively increasing durations. At the end of each P1, the membrane is repolarized and the peak tail current during the P2 pulse is plotted against the duration of the preceding P1. **FIGURE 11*B*** illustrates the extent to which the observed activation of macroscopic Kv11.1 current at 0 mV differs from the actual rate as measured using the envelope of tails protocol. The envelope of tails protocol also reveals the sigmoidal nature of the initial activation phase, which is representative of the multiple closed states that Kv11.1 channels must transition through before opening. A single exponential fitted to the latter half of this time course yields a time constant for the slowest (or rate-limiting) step of the activation process **(FIGURE 11*B*)**. An extrapolation of this exponential fit, back to the baseline, provides an estimate of the time taken to traverse all the other steps in the activation process. To characterize the activation time course over a range of test potentials, this process is repeated in its entirety with the voltage of the P1 pulse altered.

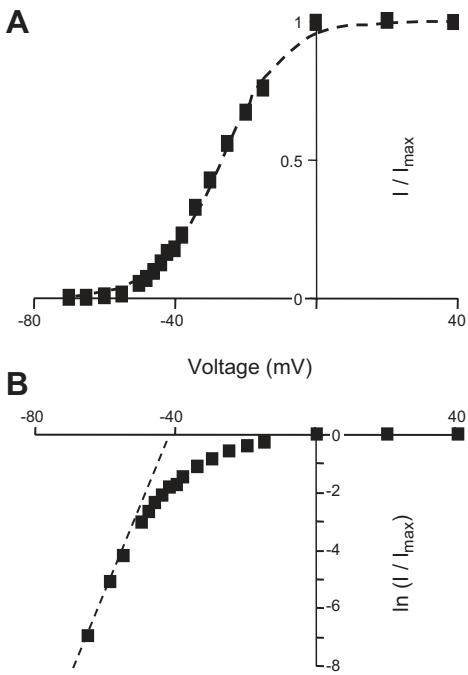

FIGURE 10. Limiting slope method for estimation of gating charge movement during activation. *A*: plot of I/I_{max} versus voltage for a 30-s isochronal activation curve for Kv11.1 channels expressed in CHO cells. The line of best fit is a Boltzman distribution. *B*: same data as in *A* with the I/I_{max} data plotted on a logarithmic scale. The dashed line shows fit of a straight line to the data at the most hyperpolarized potentials to obtain limiting slope estimate of gating charge. The estimates for z_g were 3.4 and 5.9 electronic charges for the analyses in *A* and *B*, respectively. [Redrawn from Vandenberg et al. (649).]

3. Rates of deactivation

Rates of deactivation of Kv11.1 channels are measured using a two-step voltage protocol and fitting tail currents with two exponential functions. Channels are activated with a P1 pulse (typically +40 mV for 500 ms) followed by a series of P2 pulses at voltages ranging from −50 to −160 mV for wild-type Kv11.1 potentials (see **FIGURE 12**). During this P2 pulse, a sharp increase in current is observed as channels quickly recover from inactivation, before tail currents decay as channels deactivate. Fits to this deactivation phase have been made using a single (390, 659, 735), or more commonly a biexponential function (446, 601, 668, 670). There are several reports in the literature where the separation between the fast and slow components of deactivation can be individually altered by mutations or drugs (487, 648), suggesting the two components have their roots in separate mechanistic processes. Thus it is prudent to use a biexponential function to obtain rates of deactivation. It is important to note though that at more negative test potentials the majority of wild-type deactivation occurs via the fast component **(FIGURE 12*C*)** while at less negative potentials (typically above −60 mV), the slower component is more dominant. In experiments where accurate measurement of the slow time constant is critical, the duration of the P2 pulse should be long enough to ensure a faithful fit of the current decay, and as a guide should be three times longer than the slowest time constant. Furthermore, if estimating the proportions of fast and slow components of deactivation, it is important that as much of the tail current is used as possible

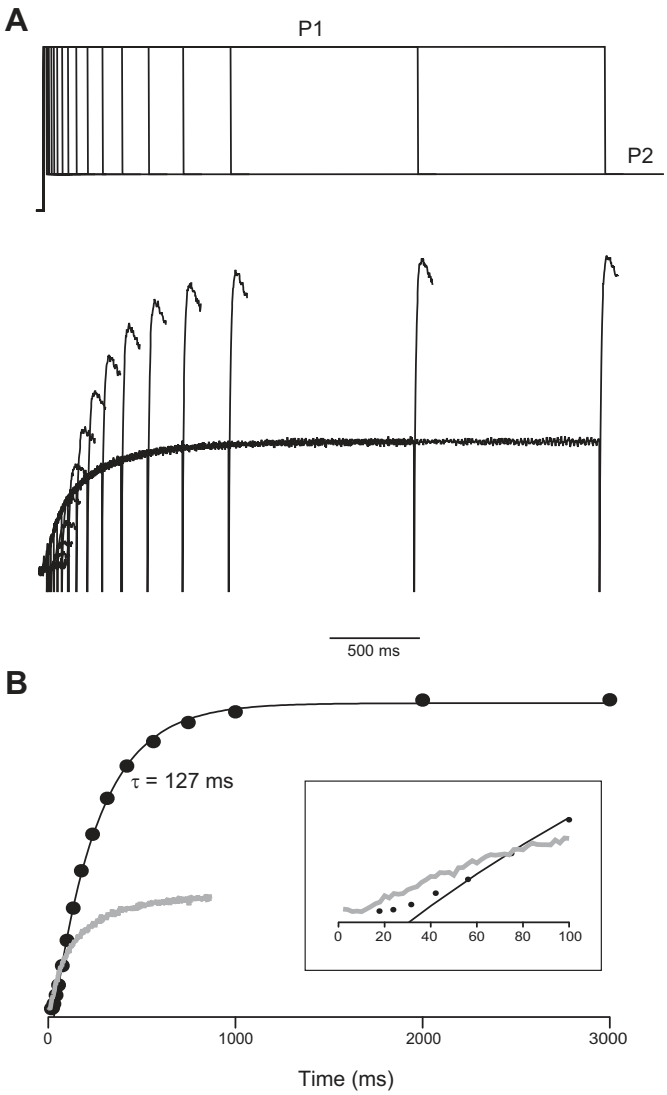

FIGURE 11. Measurement of rate of activation of Kv11.1 channels. *A*: family of current traces recorded during an envelope of tails voltage protocol, where cells were depolarized to 0 mV (P1) for varying durations before stepping back to −60 mV (P2) to reveal the proportion of channels that had been activated during the preceeding P1 step. *B*: plot of peak tail current (closed circles) from current traces shown in *A* plotted against preceding P1 duration. The black line is a fit of a single exponential to the latter part of the activation time course. For comparison, the gray line shows macroscopic hERG current recorded from a depolarizing pulse to 0 mV, highlighting the different shape due to overlapping activation and inactivation. *Inset* shows an expansion of the first 100 ms highlighting the sigmoidal nature of the early activation time course.

and that the fits be extrapolated back to the start of the P2 pulse to allow correct estimation of the relative proportions of the fast and slow components.

4. Rates of inactivation

Since inactivation in Kv11.1 occurs so quickly and is concurrent with or even precedes channel opening (323), it is necessary to use more complex voltage protocols to electrically manipulate the state occupancy of the channel to enable measurement of the kinetics of inactivation. To determine the rate of channel inactivation, a triple pulse protocol, first employed by Smith and Yellen (583), is now routinely used **(FIGURE 13)**. Cells are depolarized using a P1 pulse (typically +40 mV for 500 ms) to ensure channels are fully inactivated. A short P2 pulse (−90 mV for 25 ms) is then used to allow channels to recover from inactivation into the open state. The duration of the P2 pulse may need to be modified for mutants or specific experimental conditions (e.g., using different temperatures) and the extent to which channels undergo deactivation during the P2 pulse needs to be corrected for (see below). The membrane potential is then stepped to a series of P3 test pulses, typically between +60 and −80 mV. Since the channels are in the open state at the end of P2, the rate of inactivation at each potential can be measured directly by fitting a single exponential function to the decay of the current during P3 **(FIGURE 13*A*)**.

5. Rates of recovery from inactivation

To measure the rate of recovery from inactivation, a two-step voltage protocol is used (**FIGURE 13*Aii***). A depolarizing P1 pulse (typically +40 mV for 500 ms) drives all the channels to an inactivated state. The membrane is then repolarized to a series of increasingly negative P2 test pulses (typically +40 mV to −160 mV for 500 ms). During repolarization a transient increase in current is observed as channels quickly recover from inactivation, before the current slowly decays as channels deactivate. The current profile during P2 is therefore a sum of recovery from inactivation and deactivation which is fit with a double exponential to extract the individual components (see **FIGURE 13*Aii***).

It is important to note that the observed rate constants for inactivation and recovery from inactivation are actually the sum of the unidirectional rates constants at that voltage. This gives rise to the typical "bell-shaped" curve for plots of time constants of inactivation and recovery from inactivation **(FIGURE 13*B*)**. If, instead of plotting time constants, the observed rate constants are plotted on a logarithmic axis, then the observed rates show a typical chevron shape (see **FIGURE 13*C***) indicative of a reaction that is dominated by a single transition state between the two end states (open and inactivated in this case) (658). The chevron plot can be fitted with the equation

$$k_{\mathrm{obs,V}} = k_{\mathrm{inact,V}} + k_{\mathrm{rec,V}} \quad (3)$$

where $k_{\mathrm{obs,V}}$ is the measured rate constant at voltage V, and $k_{\mathrm{inact,V}}$ and $k_{\mathrm{rec,V}}$ are the unidirectional forward (inactivation) and reverse (recovery) rate constants. It is clear from **FIGURE 13*C*** that at more negative voltages, the observed rate tends towards the true unidirectional rate of recovery, while at more positive potentials, the observed rate tends to the unidirectional rate of inactivation.

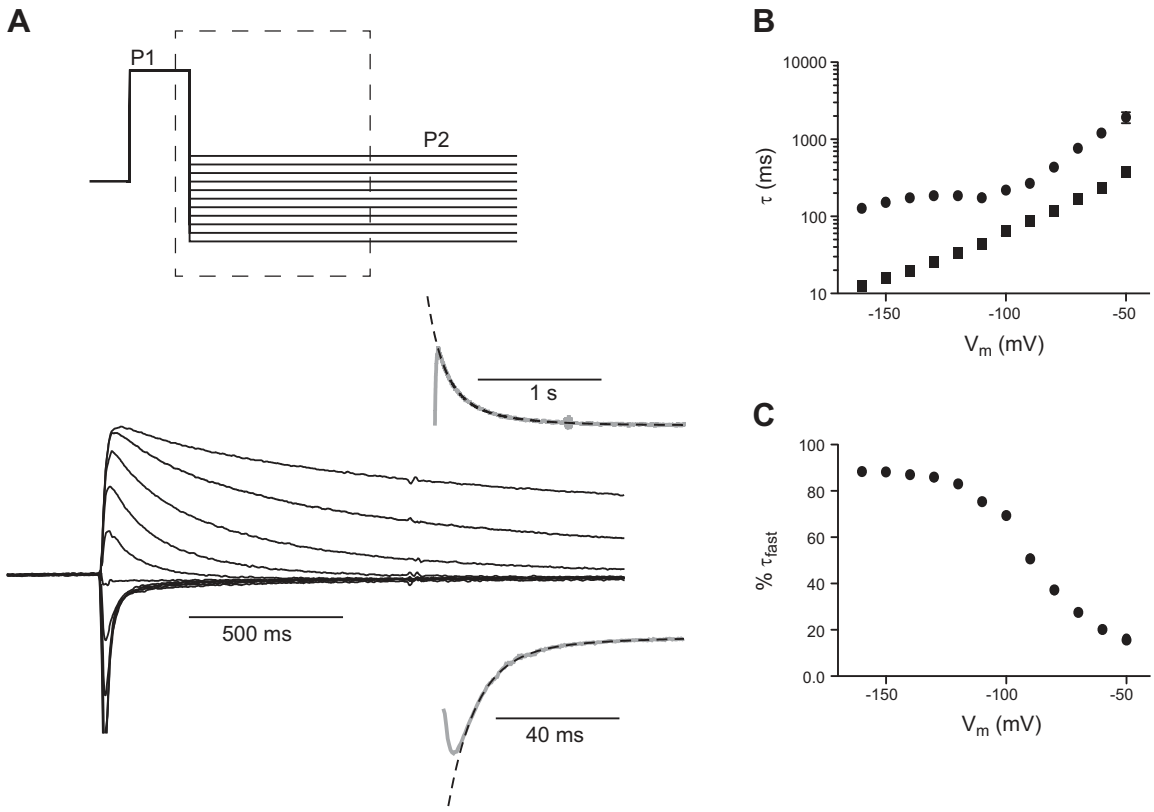

FIGURE 12. Measurement of rates of deactivation. *A*: typical family of current traces recorded from Kv11.1 channels in response to the voltage protocol shown. *Insets* show examples of fits of biexponantial functions to P2 tail currents at −80 mV (*top*) and −160 mV (*bottom*). Dashed lines show fits of double exponential functions to the decaying current phase. *B*: plot of time constants of the two components of deactivation, denoted τ_{fast} and τ_{slow} versus voltage. *C*: plot of the voltage dependence of the relative amplitudes of τ_{fast} and τ_{slow}.

It should be noted that when measuring the kinetics of any fast process such as the rate of inactivation in Kv11.1 channels, particular attention should be paid to experimental technique. Inactivation occurs on a millisecond timescale that can often be coincident with experimental artefacts. For example, in two electrode voltage-clamp recordings from *Xenopus* oocytes, at extreme voltages (>+40 mV) it can be difficult to differentiate current inactivation from decay of capacitive currents. In addition, care should be taken to ensure good voltage control, since a combination of large currents and high electrode resistance can mean the membrane is not clamped to the desired voltage until well after most of the inactivation process has occurred. Likewise, in whole cell patch-clamp experiments, proper compensation of series resistance as well as selection of cells expressing appropriately sized currents can help ensure a faithful voltage clamp and allow proper measurement of fast kinetics.

6. Steady-state inactivation

Several different approaches are routinely used in the literature to measure the voltage dependence of steady-state inactivation. Examples of each of these protocols are shown in **FIGURE 14**. The first two, the "rectification method" (547, 548) and the "extrapolation method" (649) both use the same two-step protocol described above for measuring the rate of recovery from inactivation, but with different approaches to extracting the relevant data. In each of these two cases, the proportion of channels that recover from inactivation, a reflection of the steady state, is assessed during the P2 test pulse. For the rectification method, the peak current during P2 is plotted against voltage and the degree of inactivation is determined by the extent of deviation of the *I-V* relationship from a linear fit to the most extreme negative voltages where no inactivation occurs **(FIGURE 14*A*)**. This rectification factor is then fitted with the Boltzmann function to give a $V_{0.5}$ for inactivation **(FIGURE 14*C*)**. The "extrapolation method" takes a different approach. In this case, the deactivation phase of the current during P2 is extrapolated back to the point where the membrane voltage is stepped from P1 to P2. This method aims to get a better representation of the degree of recovery from inactivation at each test potential by taking into account the small amount of deactivation that has already occurred before the current reaches its peak. The contaminating effect of deactivation is most prominent at more negative potentials where deactivation is faster (compare *I-V* relationships in **FIGURE 14*A***).

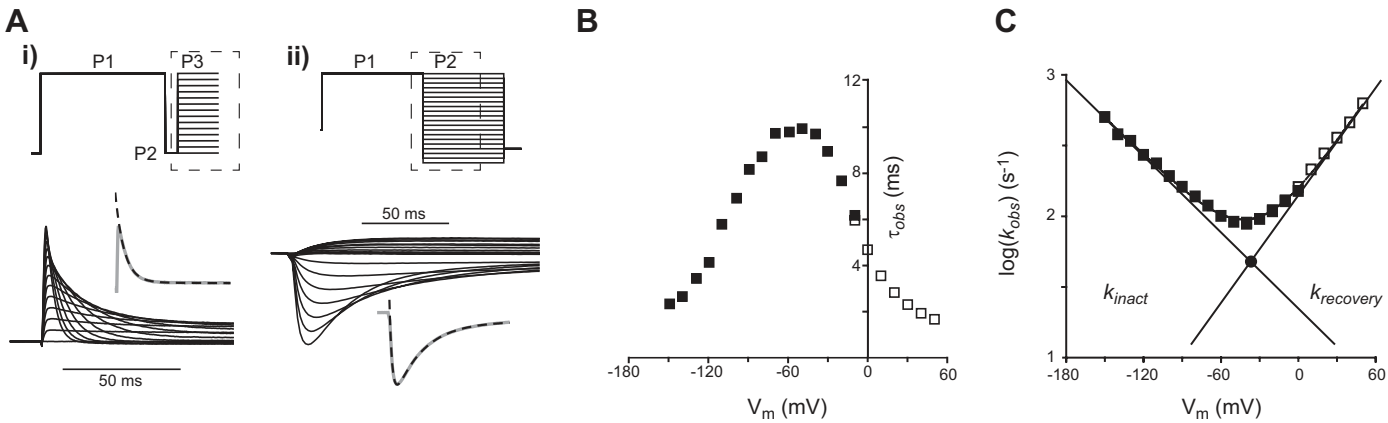

FIGURE 13. Measurement of rates of inactivation and recovery from inactivation. *A*: Kv11.1 currents recorded in response to i) triple pulse protocol to measure rate of inactivation and ii) two-pulse protocol to measure rates of recovery from inactivation. *Insets* show example fits of a single exponential function to the current record at +20 mV to derive the time constant of inactivation and a biexponantial function at −140 mV to derive the time constant for recovery from inactivation. *B*: plot of time constants for inactivation (open squares) and recovery from inactivation (closed squares) showing typical bell-shaped curve. *C*: plot of the observed rates ($1/\tau$) for inactivation (open sqaures) and recovery from inactivation (closed squares). Solid lines show unidirectional rate constants derived from the fit to the chevron plot as described in the text. The closed circle highlights the voltage at which the two unidirectional rate constants are equal.

To assess the $V_{0.5}$ of inactivation, this *I-V* relationship is first converted to a conductance and then fitted with the Boltzmann function **(FIGURE 14*C*)**.

A third method uses a triple pulse voltage protocol. Cells are depolarized to (+40 mV for 500 ms) to ensure all channels are inactivated. The channels are then allowed to relax to a steady state of inactivation during a series of short P2 pulses (typically +20 mV to −150 mV for 30 ms). The peak current is then measured at the start of a P3 "revelatory step" (+20 mV) to assess the extent to which channels are inactivated at each P2 voltage **(FIGURE 14*Bi*)** (583). Analysis of inactivation using this protocol necessitates the use of an extra step. At more negative voltages, a proportion of the channels also deactivate during the P2 pulse, leading to the observed decrease in the peak current at negative potentials **(FIGURE 14*B*)**. Before fitting of the Boltzmann equation, this deactivation must be corrected for. Since the duration of P2 is too short to fit and acquire an accurate reflection of the rate of deactivation, a separate protocol such as that shown in **FIGURE 12** must also be analyzed to obtain the rates of deactivation at each P2 voltage. In our experience, using a two-exponential function to correct for deactivation gives more reproducible sigmoidal steady-state inactivation relationships that can then be well-fitted with a Boltzmann function (see *Eq. 1*).

Each method gives a different value for the $V_{0.5}$ of steady-state inactivation. These discrepancies are due in part to methodology differences, such as underestimation of recovery during the P2 pulse in the triple pulse protocol and inconsistent extrapolation or correction for the deactivation in the different protocols. It is also possible that some of the difference may also be due to the fact that there may be multiple open and multiple inactivated states, and that the voltage-dependent occupancy of these different states may be interrogated differently by each protocol. In any case, each of the methods provides an equally good means of comparison for the effects of system perturbations on the steady state of inactivation so long as a single method is used throughout a particular set of experiments. When comparing different studies though, it is important to be aware that if different methods have been used these will contribute to any apparent differences.

A fourth method that has been used to estimate the equilibrium constant for inactivation, K_{inact}, is that of measuring the ratio of the forward and reverse rate constants, i.e.

$$K_{\mathrm{inact,V}} = k_{\mathrm{inact,V}}/k_{\mathrm{rec,V}} \qquad (4)$$

For this method, the $V_{0.5}$ can then be calculated as the voltage at which $k_{\mathrm{inact,V}} = k_{\mathrm{rec,V}}$, which corresponds to the minimum on the chevron plot depicted in **FIGURE 13*C***. This method invariably gives more positive values for $V_{0.5}$ than those obtained with the triple pulse and two pulse extrapolation methods (but not too dissimilar to that obtained using the rectification method). It has been argued that the $V_{0.5}$ measured using the rates method reflects inactivation occurring from the open state, i.e., inactivation that occurs whilst the voltage sensors are in the up conformation (658).

As mentioned in the previous section, expression of overly large membrane currents has consequences for good voltage control in electrophysiological experiments. In *Xenopus* oocyte recordings, large currents coupled with the heavily invaginated surface membrane can also result in local accumulation of K^+, which is particularly problematic as

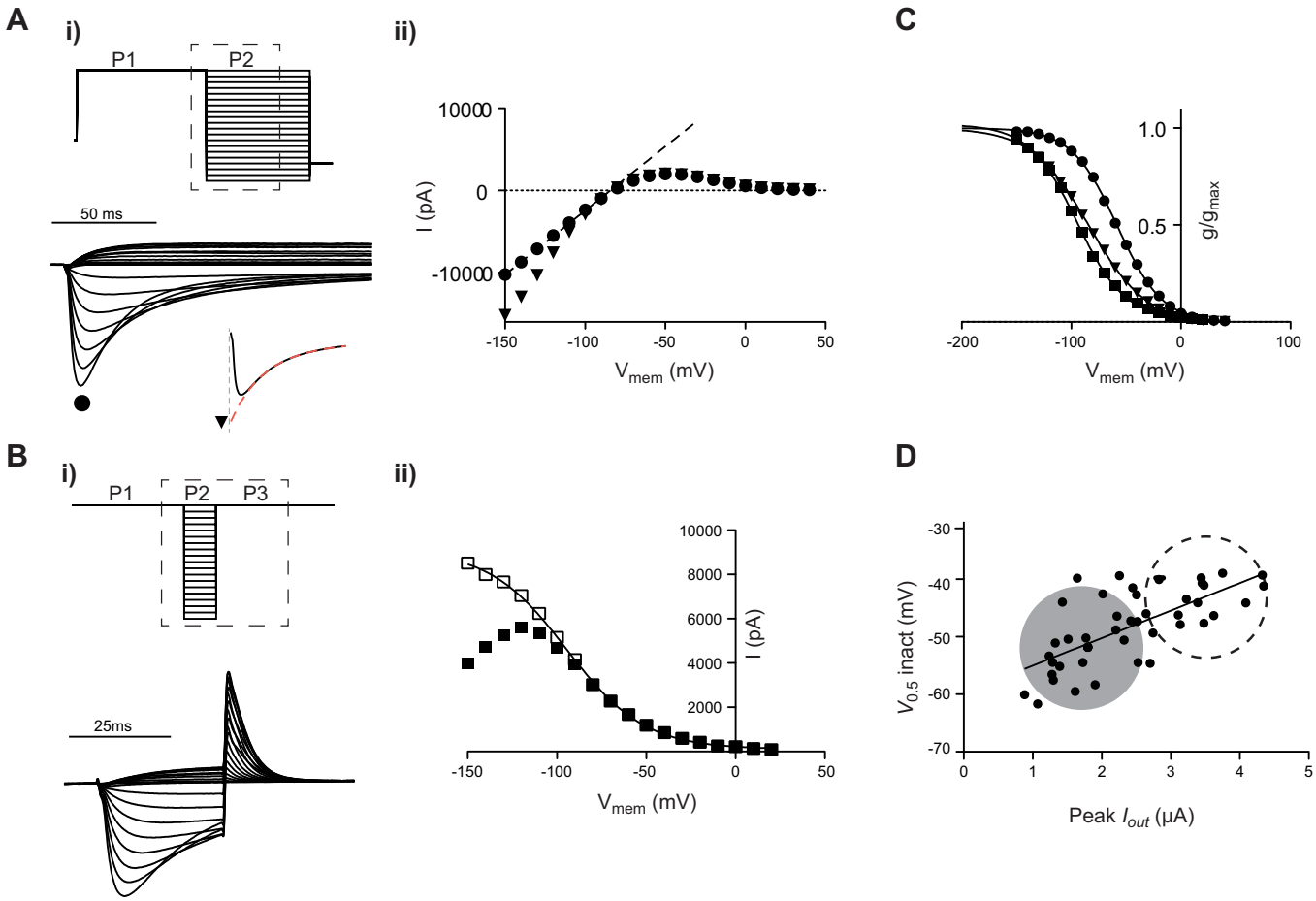

FIGURE 14. Measurement of steady-state inactivation. *A*, *i*: a family of Kv11.1 current traces recorded during the portion of the two pulse voltage protocol highlighted by the dashed box. For the "rectification method," peak current is measured directly from the current trace (closed circles in *panel ii*). For the "extrapolation method," the current recorded during the P2 pulse is extrapolated back to the onset of the P2 pulse (red line on *inset*, triangles in *panel ii*). The dashed line in *panel ii* is a linear fit to the nonrectifying part of the *I-V* relationship for the direct fit (closed circles) data. *B*, *i*: a family of Kv11.1 current traces recorded in response to the boxed area of the triple pulse voltage protocol shown (*top*). *ii*: *I-V* relationship of peak P3 current before (closed squares) and after (open squares) correction for deactivation. *C*: comparison of steady-state inactivation curves obtained using the three methods. The $V_{0.5}$ for inactivation were −60 mV (rectification, circles), −84 mV (extrapolation, triangles), and −94 mV (three-step, squares). *D*: dependence of $V_{0.5}$ of inactivation on current size. The $V_{0.5}$ of inactivation plotted against the size of the peak outward current (measured at −70 mV). Each point represents a different oocyte. The circles show the mean ± 2SD for the $V_{0.5}$ of inactivation measured in a separate set of oocytes perfused with 2 mM K^+ (gray circle) and 5 mM K^+ (dashed circle) illustrating the effect that increasing bath K^+ has on inactivation.

Kv11.1 inactivation is very sensitive to changes in extracellular [K^+] (668). **FIGURE 14*D*** shows the relationship between the $V_{0.5}$ for inactivation (assessed by the "rectification factor method") and the magnitude of peak outward current, showing a depolarized shift in the $V_{0.5}$ with increasing current magnitude. This phenomenon most likely occurs as a result of an accumulation of K^+, which inhibits the inactivation process and so shifts the equilibrium to more positive potentials (see **FIGURE 14*D***).

E. Molecular Basis of Activation

The process of opening and closing of voltage-dependent ion channels, in particular VGK channels, has been the subject of a plethora of studies over the past 60 years (65, 640). Broadly speaking, changes in the transmembrane electric field result in an outward displacement of the voltage-sensing domain (VSD) that is comprised of the first four transmembrane helices, S1-S4 (see **FIGURE 3** above), and this movement is electromechanically coupled to opening of an activation gate at the cytoplasmic entrance of the ion conducting pore. It is generally accepted that the structural rearrangements that occur in the VSD are transferred to the pore domain via a physical interaction of the S4-S5 linkers with the cytoplasmic terminals of the S6 helices, which acts to open and close the activation gate (385, 642). However, there is less agreement in regard to the exact structural rearrangements that occur between the "up" and "down"

states of the voltage sensor domain, and more specifically the magnitude of movement of the voltage sensor between these states (640). These general principals of activation gating also apply to Kv11.1 with regards to the role of the VSD (601, 602, 720); S4S5 (173, 642, 648); S6 activation gate (245, 417, 689). The discussion below will therefore focus on what distinguishes Kv11.1 activation gating from that of other VGK channels.

1. The activation gate

Comparison of the crystal structures of several different potassium channels in either the open [e.g., MthK (296), KvAP (297), Kv1.2 (384), KirBac3.1 (57)] or closed state [KcsA (150), KirBac3.1 (337)] shows that the COOH-terminal part of the inner helices are tightly packed in the closed state but splayed apart in the open state, thus allowing passage of ions. The extent of this splaying probably varies between families (57, 111, 128), and the specific details of the hinge site and extent of hinge motion probably vary between channels. Two putative hinge points have been identified. First there is a highly conserved glycine residue (corresponding to Gly99 in KcsA, Gly466 in *Shaker* and Gly648 in hERG; see **FIGURE 15**). Mutations of this glycine to alanine or proline (392) have confirmed its importance as a hinge residue in multiple K^+ channels. Second, in canonical voltage-gated K^+ channels, there is a Pro-X-Pro motif just COOH terminal to the conserved glycine discussed above that has also been demonstrated to play an important role in opening and closing of the activation gate (137, 234, 345, 346). HERG, however, lacks the Pro-X-Pro motif, but instead contains a second glycine (Gly657) in a position corresponding to the second proline (see **FIGURE 15**).

In a scan of the S6 transmembrane helix, Mitcheson et al. (417) found that substitution of either Gly648 or Gly657 with alanine did not prevent channel opening in Kv11.1. More recently the same group showed that when both hERG S6 glycine residues were mutated to alanine, this did not substantially alter the voltage dependence or the rates of Kv11.1 activation, and did not affect block of Kv11.1 by terfenadine (a 10 Å diameter molecule which requires opening of the activation gate to reach its binding site) (245). These data suggest that unlike other potassium channels, flexibility in these hinge regions is not a prerequisite for channel opening in Kv11.1. Conversely, replacing these glycine residues with proline, or larger hydrophobic residues, destabilizes the closed conformation and shifted the equilibrium toward the open state of the channel (245). Hardman et al. (245) also used molecular dynamics simulation techniques to examine the conformational dynamics of the S6 helices of G648A, G657A, G648A/G657A, compared with wild-type Kv11.1 channels. These simulations showed that regardless of the presence of alanine at either position 648 or 657 there was inherent flexibility in the Kv11.1 S6 linker close to position Gly648 that was comparable in degree of swivel and kink to the open state of the KvAP

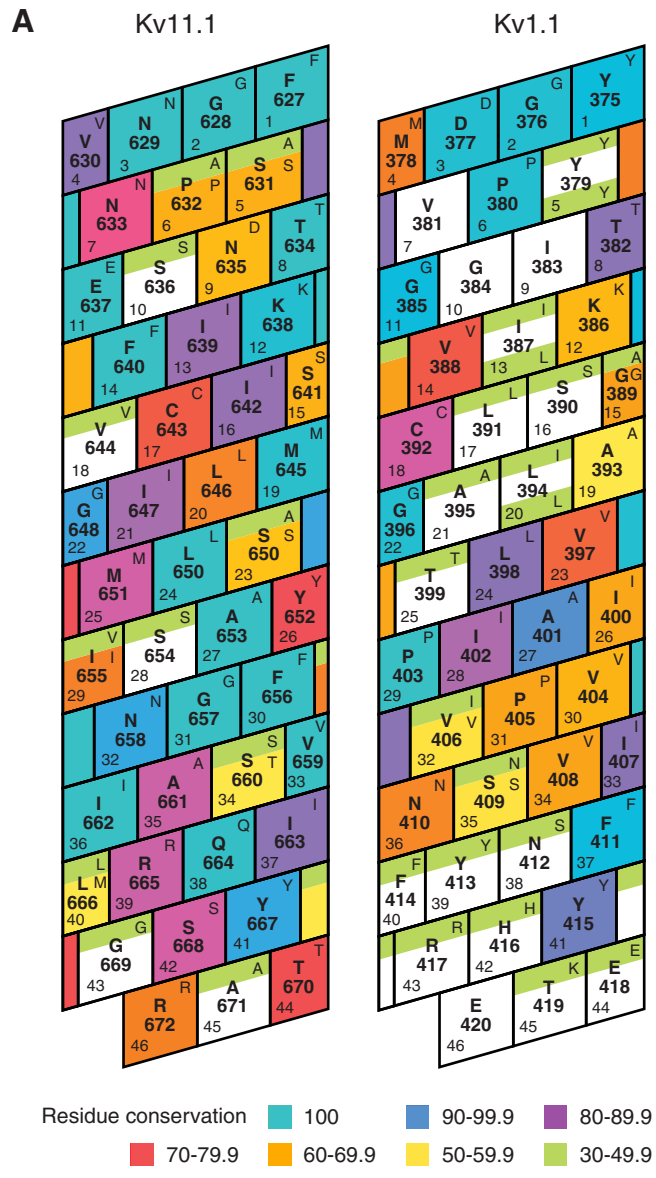

FIGURE 15. Sequence alignment of S6. *A*: sequence conservation in S6 segments for *1*) EAG subfamily and *2*) canonical VGK channels generated as described in Ju et al. (275). The helical net diagrams represent each position as a rhomboid with 3.6 residues per turn. The sequence shown is that for *1*) Kv11.1 and *2*) Kv1.1. The color coding indicates the degree of sequence identity at each position. The most frequent residue at each position within the whole family is shown in the top right corner of each rhomboid. *B*: sequence alignment for Kv11.1 and Kv1.1. Solid lines indicate identity, and dashed lines indicate homology. The only residue that is >90% conserved in all EAG and VGK channels is a glycine (G648 in Kv11.1 and G396 in Kv1.1). Residues in Kv11.1 that affect deactivation gating are highlighted in blue. Val659 and Gln664 are 100% conserved within the EAG subfamily (see *A*). Tyr667 and Ser668 are less highly conserved, which suggests that they may be important for deactivation gating in Kv11.x channels rather than in the whole EAG subfamily.

channel (297). The authors concluded that the Kv11.1 pore, in contrast to other VGK channels, is more stable in the open conformation, and that the presence of glycine at positions 648 and 657 was important for helical packing rather than as a hinge.

Further differences in the COOH-terminal region of S6 between hERG and other voltage-sensitive channels were highlighted by Wynia-Smith et al. (689) using cysteine-scanning mutagenesis to investigate the role of the COOH-terminal end of the S6 helices in Kv11.1 gating. They found that the most important residues clustered into two S6 micro domains. The innermost of these, containing residues Gln664, Tyr667, and Ser668 (see **FIGURE 15**), formed a ringed domain, with the side chain of Gln664 occluding the conduction pathway in the closed state. Critically, this is more than a full helical turn away from the predicted gate, as determined through alignment with *Shaker* residue Val478 (382). Moreover, amino acid substitutions at the position corresponding to the *Shaker* gate (Ser660 in hERG) had little effect on gating, suggesting that the molecular location of the S6 activation gate is different in Kv11.1 channels. The second microdomain contained the residue Val659, which was sensitive to a wide range of substitutions. Their structural modeling showed this side chain buried in a pocket formed by the S5, S6, and S4S5 linker in the closed state, and interpreted the reduced slope in the voltage dependence of current activation for many mutants at this position to be indicative of a disruption of coupling between the voltage sensor and the activation gate. Overall, both the study by Hardman et al. and Wynia-Smith et al. highlight that mutagenesis in the S6 primarily disrupts the closed state of Kv11.1, suggesting specific interactions are necessary to stabilize Kv11.1 in the closed state (245).

2. The voltage sensing domain

It has been shown in a wide range of VGK channels that the first three or four positively charged residues in the S4 domain are predominantly responsible for sensing changes in the transmembrane electrical field (6, 372, 471, 483, 564). The first comprehensive study of the S4 region in Kv11.1 involved mutating each of the S4 charged residues, Lys525, Arg528, Arg531, Arg534 and Arg537, to glutamine (601). Neutralization of any of these charges shifted the voltage dependence of activation gating. A thermodynamic analysis of the shifts in activation equilibria showed that of the two positions where mutants caused the largest perturbation of activation, Arg531Q shifted the equilibrium towards the closed state, while Lys525Q shifted the equilibrium toward the open state compared with wild-type channels. These data suggest that Lys525 stabilizes the closed and Arg531 stabilizes the open state in wild-type Kv11.1 channels. The mutations at position Arg531 also highlighted some clear differences with the activation process in *Shaker* channels. R531Q caused a depolarizing shift in the $V_{0.5}$ of activation, whereas the equivalent mutation in *Shaker* (R371Q) causes a hyperpolarizing shift (6, 564). It is also worth noting that in all voltage-gated ion channels the vast majority of S4 charged residues are arginine but in the case of the outermost S4 charge in Kv11.1 it is lysine. By mutating Lys525 to cysteine and assessing the effects of different MTS reagents, Subbiah et al. (601) also showed that replacing the lysine with other positively charged residues did not restore the wild-type phenotype, suggesting that the specific lysine side chain rather than charge per se was important at this residue.

Soon after this initial characterization, Zhang and Tseng (720) used a Boltzmann analysis of the voltage dependence of current activation, coupled with cysteine scanning accessibility mutagenesis, to examine the contribution to the gating charge of each of the charged residues in the Kv11.1 S4 domain (720). They showed that only the three outermost charged residues contributed to activation gating charge, and this was supported by the state dependence of MTS accessibility of these three residues during activation. Piper et al. (500) subsequently used gating current measurements to show that Arg531 likely contributes to activation gating charge whilst residues Arg534, Arg537, and Lys538 do not. Unfortunately, the level of expression for K525A and R528A was too low to permit recording of gating currents (500). Nevertheless, the results of Piper et al. are consistent with those of Zhang and Tseng (720).

These initial characterizations suggested that in a broad sense, the overall contribution of the voltage-sensing domain to Kv11.1 activation is similar to other VGKs. But why then is the activation of ionic current so much slower in Kv11.1? Experiments on *Shaker* channels have shown that the S4 region moves rapidly in response to voltage and that channel activation quickly follows this movement (91, 353, 395). Slow activation gating in Kv11.1 could therefore be due to slower movement of the VSD, less efficient coupling between VSD movement, and opening of the S6 activation gate, or a comination of both factors. Smith and Yellen (584) addressed this question, using voltage clamp fluorometry. They attached a fluorescent probe to the extracellular end of the S4 domain to monitor conformational changes in this region in response to changes in membrane voltage, whilst simultaneously monitoring changes in ionic currents. In this study, the kinetics of the changes in fluorescence were slow and very similar to the kinetics of current activation. These data strongly supports the hypothesis that the slow kinetics of Kv11.1 activation, relative to other VGK channels, can be attributed to slow VSD movement rather than poor coupling between the VSD and the intracellular activation gate. The following year, these data were corroborated by the first measurement of gating currents in Kv11.1 channels. Using the cut open oocyte technique (65), Piper et al. (500) showed that the bulk (>95%) of charge movement associated with the Kv11.1 voltage sensor movement was slow (see **FIGURE 16**).

These data raise the question as to the origin of the slow movement of the voltage sensor. Is it an intrinsic property of the domain, and/or due to additional constraints placed on the voltage sensor limiting its movement? Subbiah et al. (602) investigated whether the environment surrounding S4 could have a significant impact on the rate at which the S4 domain can traverse the transmembrane electrical field. They hypothesized that if the Kv11.1 S4 helix was tightly abutted against surrounding protein domains, then its motion would be limited through steric hindrance. The authors examined this hypothesis using tryptophan-scanning mutagenesis, reasoning that the side chain of the tryptophan residue, being *1*) bulky and *2*) hydrophobic, should be poorly tolerated if there is close packing around the helix or there are tight protein-protein interactions. Surprisingly, mutation to tryptophan was tolerated in the entire region studied, from Leu524 to Leu539, suggesting the entire domain is loosely packed and not consistent with especially close interactions with other domains in the voltage sensor.

Zhang et al. (719) also investigated whether internal constraints, specifically whether a network of internal salt bridges between the positively charged residues in S4 and negative charges in the S1-S3 transmembrane helices, affected voltage sensor movement. In *Shaker*, and related VGKs, three conserved negative charges in the VSD,

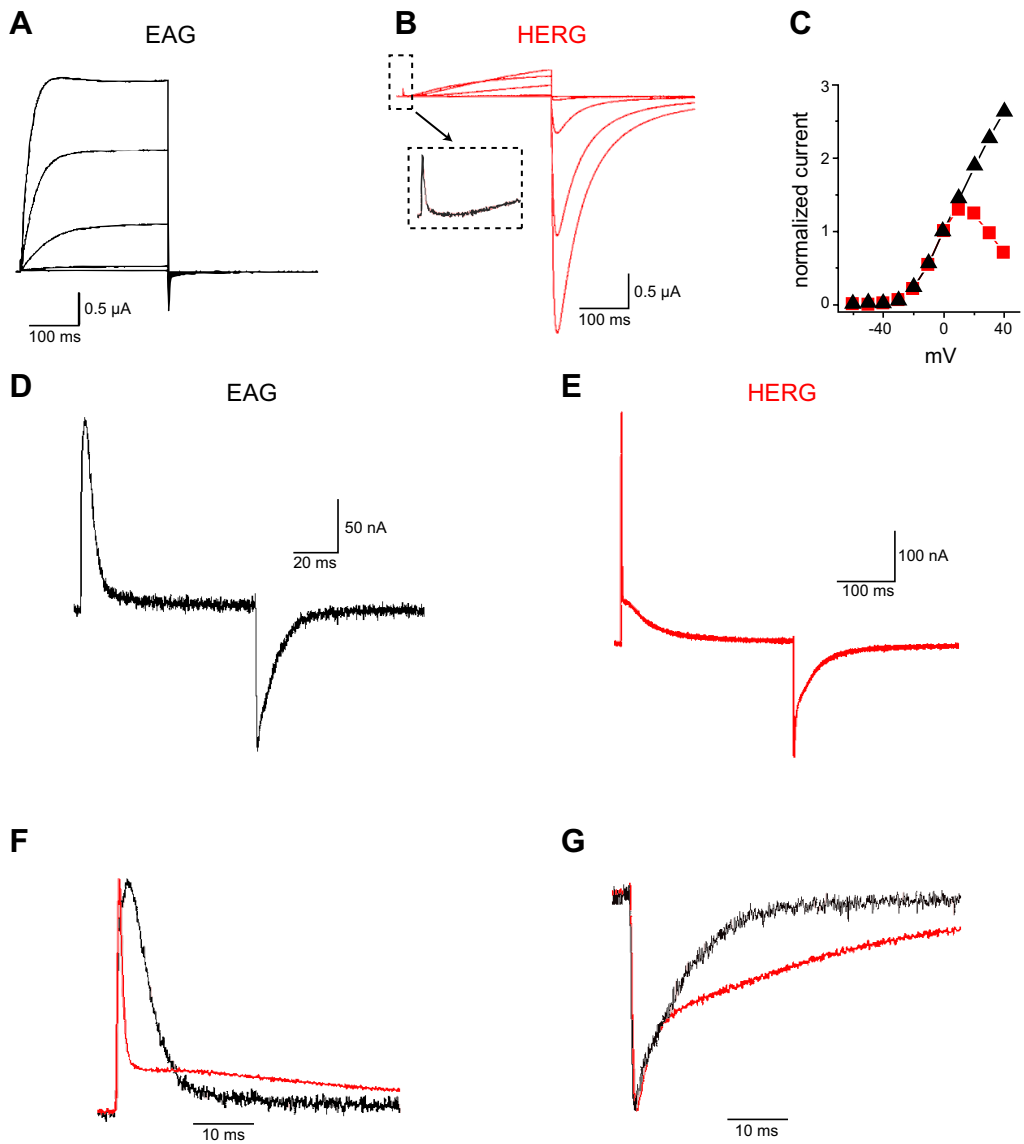

FIGURE 16. Comparison of gating current recordings for Kv11.1 (HERG) and Kv10.1 (EAG) channels. *A*: typical examples of Kv10.1 ionic currents. *B*: examples of Kv11.1 ionic currents during step depolarizations to potentials in the range −40 to +40 mV. *C*: plot of normalized ionic currents for Kv10.1 (black) and Kv11.1 (red). Typical examples of Kv10.1 (*D*) and Kv11.1 (*E*) gating currents for step depolarization to 0 mV and return to −120 mV. q_{on} (F) and q_{off} (G) for Kv10.1 (black) and Kv11.1 (red) plotted on the same time scale. Note the two very distinct components for Kv11.1 gating charge movement. [From Piper et al. (502), copyright National Academy of Sciences.]

Glu283 and Glu293 in S2 and Asp316 in S3, are involved in proper folding of the voltage sensor (637) as well as contributing to gating charge movement (564). In Kv11.1, the equivalent residues are Asp456 and Asp466 in S2 and Asp501 in S3. In addition, there are three negative charges unique to the EAG family of VGK channels, Asp411 in S1, Asp460 in S2, and Asp509 in S3 (see **FIGURE 17**). Neutralization of Asp466 (377, 719) or Asp501 (377) by mutation to cysteine resulted in a change in the slope of the Boltzmann equation fitted to the steady-state activation curves, indicating that there may be a change in the gating charge of these channels. Mutation of Asp460 and Asp509 shifted the $V_{0.5}$ for activation in the depolarizing direction as well as slowing the rate of activation, i.e., shifted the equilibrium toward the closed state, suggesting these residues stabilize the open state in wild-type channels. Conversely, D411C shifted the $V_{0.5}$ of activation in the hyperpolarizing direction and accelerated activation, suggesting this residue was involved in stabilizing the closed state in the wild-type channel. Together with previous data showing that Lys525 stabilizes the closed state and Arg531 the open state (601), Lys525-Asp411 and Arg531-Asp460/Asp509 were suggested as possible salt bridge pairings in the closed and open states, respectively (501, 719). An alternative pairing for Asp411 in the closed state would be with Lys538, as mutations to Lys538 also cause significant hyperpolarizing shifts in steady-state activation (500, 602).

In addition to the internal constraints described above, multiple studies have shown that external factors also limit VSD movement in Kv11.1 channels. Van Slyke et al. (648) showed, using voltage clamp fluorometry, that mutants in the S4S5 linker, which they proposed to reduce the constraint on VSD movement, increased the rate and shifted the voltage dependence of both S4 movement and ionic current activation. These data again indicate that VSD movement limits the rate of current activation in Kv11.1, but that in turn, the movement of the VSD is constrained by other factors, in this case the S4S5 linker. Saenen et al. (538) reported that deletion of a charge cluster, KIKER, beginning at position 362 in the proximal NH_2-terminal domain, immediately prior to the S1 transmembrane helix, resulted in a hyperpolarizing shift in the voltage-dependence of activation and increased the rate of the voltage-independent transition in the activation gating sequence. They proposed that the local electric field within this region modulates activation gating via electrostatic interactions with the gating machinery. The specific sites of interaction, however, remain to be identified.

3. Coupling of VSD to activation gate

The voltage-dependent rearrangements of the voltage-sensing domain are transmitted to the activation gate via a physical interaction of the S4S5 linkers with the cytoplasmic terminals of the S6 helices (385, 642). In Kv11.1, multiple mutations at two acidic positions in this linker, Asp540 and Glu544, have been shown to alter both activation and deactivation gating (551). The most dramatic of these, D540K, showed a U-shaped dependence of activation on voltage; that is opening at both depolarized and hyperpolarized potentials (420). Tristani-Firouzi et al. (642) used this novel background to probe the interaction between the S4S5 and the S6 helices and found that a single residue, Arg665 at the distal end of S6, was involved in the unique activation gating of D540K. The authors suggest that the activation at hyperpolarized potentials is mediated via charge repulsion between these sites, while in the wild-type channel, an electrostatic interaction between Asp540 and Arg665 provides a direct interaction between S4S5 and S6 which mediates coupling between the VSD and the S6 activation gate to stabilize the closed state. Interestingly though, more subtle mutations to Asp540 (551) and Arg665 (689) do not have dramatic effects on steady-state activation, but instead affect only the rates of activation and deactivation. This suggests that these residues may not necessarily be involved in stabilizing the closed or open end states but rather may be important for stabilizing intermediate states in the activation process.

F. Molecular Basis of Slow Deactivation in Kv11.1 Channels

While the molecular basis of Kv11.1 activation gating is understood in a broad sense, this is in large part due to the similarities between Kv11.1 and other VGK channels. The mechanism of slow closure of Kv11.1 channels, however, cannot be explained by slow movement of the VSD alone. The Kv11.1 channel has unique cytosolic domains, compared with other VGK channels, and many of these domains have been shown to modulate deactivation kinetics.

1. Role of the NH_2 terminus in slow deactivation of Kv11.1

Shortly after Kv11.1 was discovered, two groups independently reported that deletion of the NH_2-terminal cytoplasmic domain resulted in acceleration of deactivation (558, 588). Initially it was thought that the PAS domain in the NH_2 terminus (see **FIGURE 3**) was responsible for slow deactivation gating (425). Morais Cabral et al. (425) showed that the fast deactivation phenotype of Δ2–373 channels could be substantially slowed by the addition of a recombinant protein corresponding to the PAS domain (residues 1–135). In addition to the deletion studies, several groups have shown that point mutations within the PAS domain result in an acceleration of the deactivation kinetics (99, 232, 425).

A small but important finding in the Morais-Cabral study was the observation that following patch excision, the recombinant PAS domain remained tightly bound to the Δ2–373 channels, suggesting that binding and unbinding

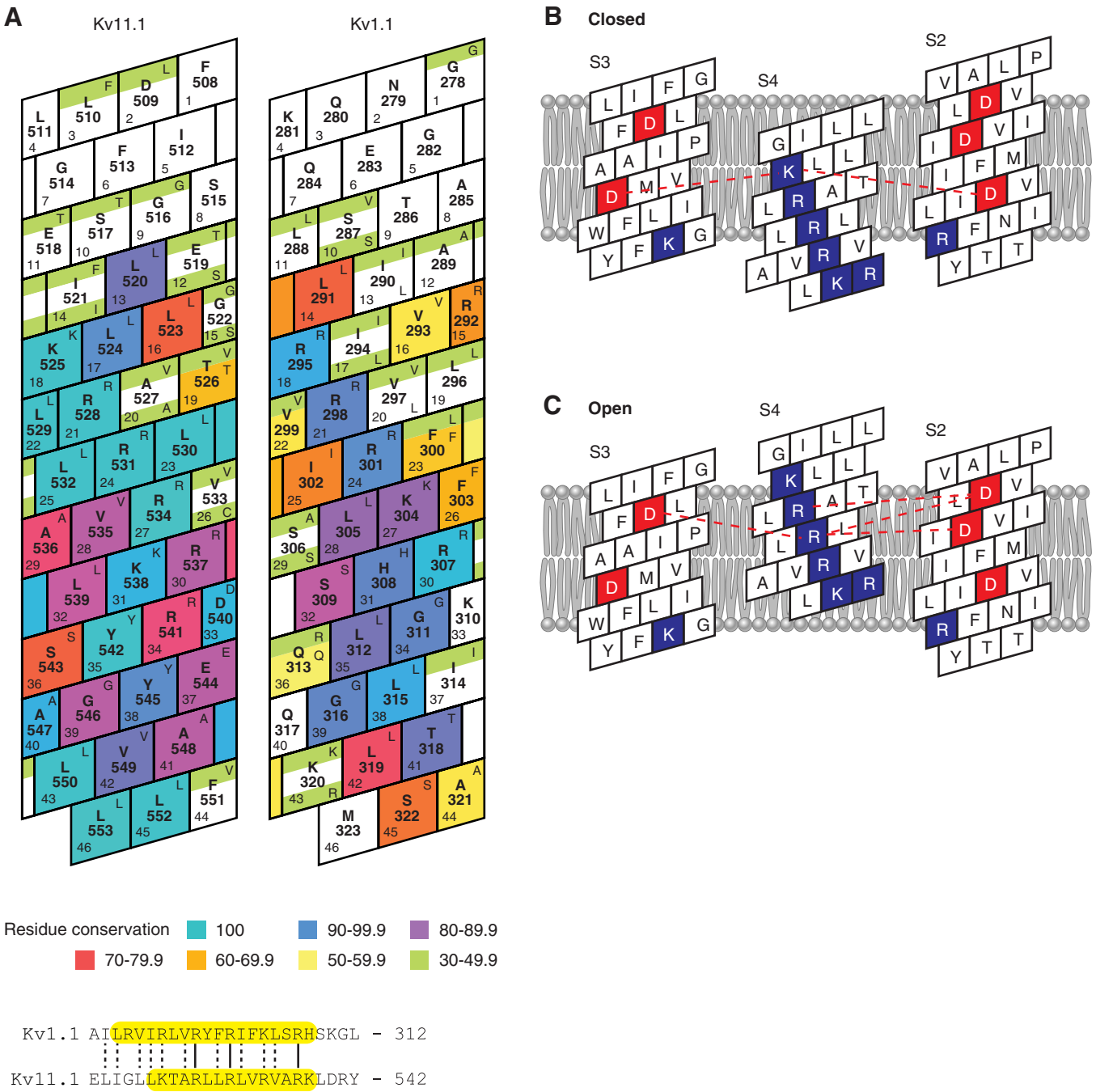

FIGURE 17. Voltage sensor domain of Kv11.1. *A*: sequence conservation in S4 segments for *1*) EAG subfamily and *2*) canonical VGK channels generated as described in Ju et al. (275). The helical net diagrams represent each position as a rhomboid with 3.6 residues per turn. The sequence shown is that for *1*) Kv11.1 and *2*) Kv1.1. The color coding indicates the degree of sequence identity at each position. The most frequent residue at each position within the whole family is shown in the top right corner of each rhomboid. *Bottom panel* shows the sequence alignment for Kv11.1 and Kv1.1. Solid lines indicate identity and dashed lines indicate homology. *B*: proposed salt bridges in VSD in closed state with S4 in the down position and open state (*C*) with S4 in the up position. Proposed salt bridges are based on cysteine scanning (719) and mutant cycle analysis (501) experiments. The two critical basic residues for these interactions Lys525 and Arg531 are 100% conserved within the EAG subfamily (*A*). Similarly, four of the five acidic residues depicted in *B* are 100% conserved, the exception being the middle aspartate in the S2 domain which is a glutamate (i.e., still acidic) in 23% of EAG family members.

of the PAS domain cannot be directly responsible for deactivation gating which takes place over tens to hundreds of milliseconds. Recently, Gustina and Trudeau (232) confirmed the importance of the PAS domain by showing that a genetically encoded PAS domain restored wild-type-like slow deactivation kinetics to a "core" Kv11.1 construct missing the entire NH_2-terminal cytoplasmic domain (Δ2–354), while mutant PAS domain

constructs could not restore the slow deactivation kinetics.

The PAS domain commences at residue 26. The preceding NH_2-tail 25 residues also play an important role in regulating Kv11.1 deactivation. Deletion of just the 25 residue NH_2-tail region results in a very similar phenotype to that seen for deletion of the entire NH_2-terminal cytoplasmic domain. Indeed, even deletion of just 9 (446) or 16 (659) residues can also cause significant acceleration of deactivation. There are also numerous point mutants within this 25-residue tail domain that result in significantly faster rates of deactivation (431, 446). Wang et al. (659) have also shown that in inside-out macropatches, exogenous application of a peptide corresponding to residues 1–16, to "core" Kv11.1 constructs (Δ2–354) could substantially restore slow deactivation kinetics by stabilizing the open state. The authors noted, however, that the 1–16 peptide only slowed deactivation to an intermediate level, which they suggested could indicate that this peptide may be just one component of a more complex multidomain cytosolic arrangement that is needed for full restoration of function. Recently, three separate groups solved the structure of the hERG PAS domain using NMR spectroscopy (367, 431, 446), and each has noted that the NH_2-terminal tail formed by the first 25 amino acids contains a helical element (see **FIGURE 18**). Disruption of the α-helix, by substitution with a glycine/serine linker, whilst leaving the NH_2-terminal 14 residues intact, dramatically accelerated deactivation to a level comparable with the truncation of the entire 25 residue tail. This highlights the importance of this helical element in positioning the NH_2-terminal tail at its appropriate site of action (446). Li et al. (367) and Muskett et al. (431) reported broadly similar results.

From the foregoing discussion it is clear that the NH_2-terminal domain, comprising both the PAS domain as well as the NH_2-terminal tail, is critically involved in slow deactivation of Kv11.1 channels. A plausible hypothesis to explain these data would be that the PAS domain forms a stable interaction with the core of the channel, bringing the flexible NH_2-terminal tail close to the central conduction axis where it is in an appropriate position to regulate gating of the activation gate. Where then do the PAS domain and the NH_2-tail interact with the channel?

Gustina and Trudeau (231) have shown that deletions in the COOH-terminal region of the channel, specifically the cNBD, resulted in rapid deactivation kinetics similar to the deleted PAS domain construct. They also showed that when both the NH_2-terminal amino acids 1–135 and the cNBD were deleted, addition of a recombinant EAG domain could no longer restore slow deactivation. These data strongly suggest that the PAS domain binds to the cNBD. In 2009, Al

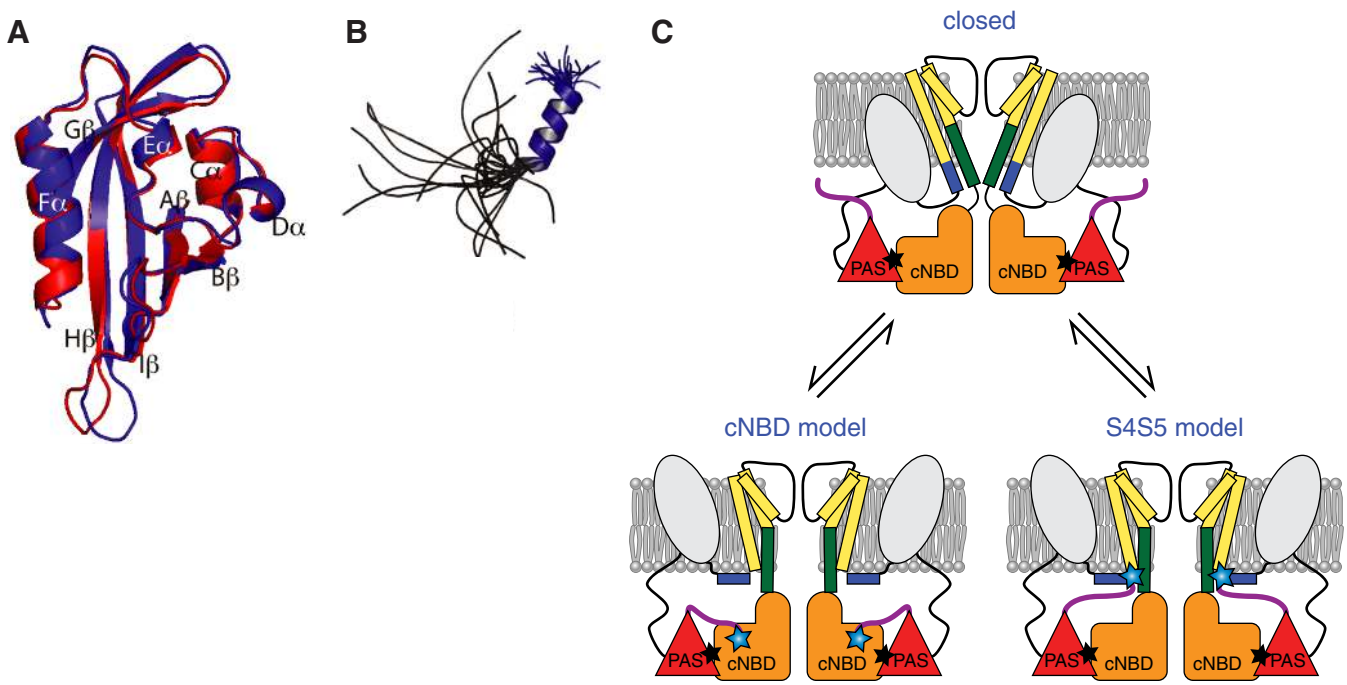

FIGURE 18. Structure and function of hERG NH_2-terminal domain. *A*: solution structure of hERG PAS domain (residues 26–135) shown in blue (445) superimposed on the crystal structure of the PAS domain shown in red (425). *B*: 20 lowest energy structures of the NH_2-terminal 25 residues, superimposed on residues 12–23, which forms an amphipathic α-heli. *C*: putative models of role of PAS domain and NH_2-tail in regulating Kv11.1 deactivation. In both the open and closed states, the PAS domain remains bound to the cNBD. In the S4S5 model, the flexible NH_2-tail transiently binds to the S4S5 linker to stabilize the open state directly (367). In the cNBD model, the NH_2-tail binds to the "cAMP binding pocket" of the cNBD and regulates deactivation allosterically (431). [*A* and *B* from Ng et al. (445).]

Owais et al. (11) identified a hydrophobic patch predicted to be on the surface of the cNBD (residues V794-I798) where introduction of charge mutants resulted in up to a sixfold increase in the rate of deactivation. They also noted that a similar hydrophobic patch had previously been identified on the surface of the PAS domain (425) and so suggested that these patches may provide a site for a stable interaction, although this remains to be verified experimentally.

There has also been extensive investigation of the role of the S4S5 linker in slow deactivation. Numerous studies have shown that mutations in the S4S5 linker can affect deactivation (642, 659, 661). Notably, Wang et al. (661) showed that NEM modification of a cysteine introduced at position Gly546 in the S4S5 linker accelerated deactivation in a similar manner to deletion of the NH_2 terminus (Δ2–354). Furthermore, the effects of the NEM modification and the NH_2-terminal deletion were not additive, indicating they likely disrupt the same process (661). More recently however, van Slyke et al. (648) used voltage-clamp fluorometry to show that the rate of VSD return during deactivation was altered by other mutations at position Gly546 (most notably G546V). The effect of the G546V mutation was not dependent on any NH_2-terminal interaction with the S4S5 as the effect was the same in NH_2-terminal truncated (Δ2–354) Kv11.1 channels (648). In an alternative experimental approach, Li et al. (367) noted that titration of the PAS domain protein in the presence of a nine residue peptide corresponding to the S4S5 linker, shifted peaks in the HSQC spectrum. This change in chemical shift was taken to indicate specific interactions between the S4S5 peptide and several PAS domain residues. Yet another model for sites of interaction between the NH_2 terminus and remainder of the channel has been proposed by de la Pena et al. (135). Using cysteine mutagenesis, they demonstrated that V3C in the NH_2-tail could interact with Y542C in the S4S5 linker. This interaction appeared to preferentially occur when the channels were in the closed state. The fact that these residues are close enough to form disulfide bridges is evidence of proximity in the functional channel; however, it does not show whether this is a physiologically and functionally relevant interaction. Furthermore, the preference for interaction in the closed state is at odds with the data from Wang et al. indicating that the 16-residue peptide preferentially binds to the open state of NH_2-terminally truncated (Δ2–354) channels (659).

Such diversity in the predictions for how the EAG domain may interact with the remainder of the channel simply highlights that the structural basis of slow deactivation gating is one of the least understood aspects of Kv11.1 gating. While it may be some way off, a crystal structure of the full-length Kv11.1 channel, including these intracellular assemblies, would help resolve these discrepancies and help guide the future direction of study in this area.

G. Molecular Basis of Inactivation Gating

The rapidity and voltage-dependence of inactivation is perhaps the most important kinetic component of gating in regard to the role of Kv11.1 channels during the cardiac action potential (see sect. II*D*). Inactivation in Kv11.1 is most analogous to C-type inactivation in *Shaker*, yet it also has several unique features, most notably much faster and voltage-dependent kinetics (558, 583, 668).

1. Role of selectivity filter in inactivation

The importance of the selectivity filter in fast inactivation of Kv11.1 was first demonstrated in 1996, when Smith et al. (583) showed that the double mutation S631C-G628C abolished inactivation and Schonherr et al. (558) showed that mutation of Ser631 to alanine (the equivalent residue in the noninactivating Kv10.1 channel) largely eliminated inactivation. Two years later, Herzberg et al. (254) showed that transfer of a region encompassing the pore helix and selectivity filter between Kv11.1 and Kv10.1 channels conferred rapid inactivation to Kv10.1 and abolished it in Kv11.1 channels. The authors also showed that the S620T mutation in Kv11.1 (i.e., converting it to the equivalent residue in Kv10.1) removed inactivation. Ficker et al. reported similar findings for the S620T Kv11.1 mutant (178) and later showed that the replacement of Thr432 and Ala443 in Kv10.1 channels with serine (equivalent to Ser620 and Ser631 in Kv11.1) was sufficient to introduce fast inactivation (177).

In the last decade, our understanding of the molecular basis of gating at the selectivity filter has been revolutionized by the use of X-ray crystallography. First, Doyle et al. (150) revealed a network of hydrogen bonds and van der Waals interactions between two tryptophan residues at the NH_2-terminal of the pore helix (residues 67 and 68 in KcsA, equivalent to 434 and 435 in *Shaker*) and the tyrosine in the selectivity filter (residue 78 in KcsA, 445 in *Shaker*) which they suggested act as a "molecular spring" that exerts radial forces to maintain the selectivity filter in a conformation relevant for selecting K^+ over Na^+. More recently, Perozo and co-workers (116, 127) identified residues Glu71 and Asp80 as critical for C-type inactivation in KcsA. The authors also suggest that this mechanism was likely conserved in voltage-gated channels since introducing glutamate at position Val370 in Kv1.2, a noninactivating channel in the absence of its β-subunit, recapitulated slow C-type inactivation. Further weight is added to this theory when considering that similar mutations in the selectivity filter and the proximal pore domain in several voltage-gated and inward rectifying potassium channels also have considerable effects on their gating properties (12, 178, 702). Interestingly, of the five residues in KcsA that have been proposed to be involved in hydrogen bond networks stabilizing the structure of the selectivity filter in the open and/or inactivated states, none of them is conserved in Kv11.1 (see **FIGURE 19**).

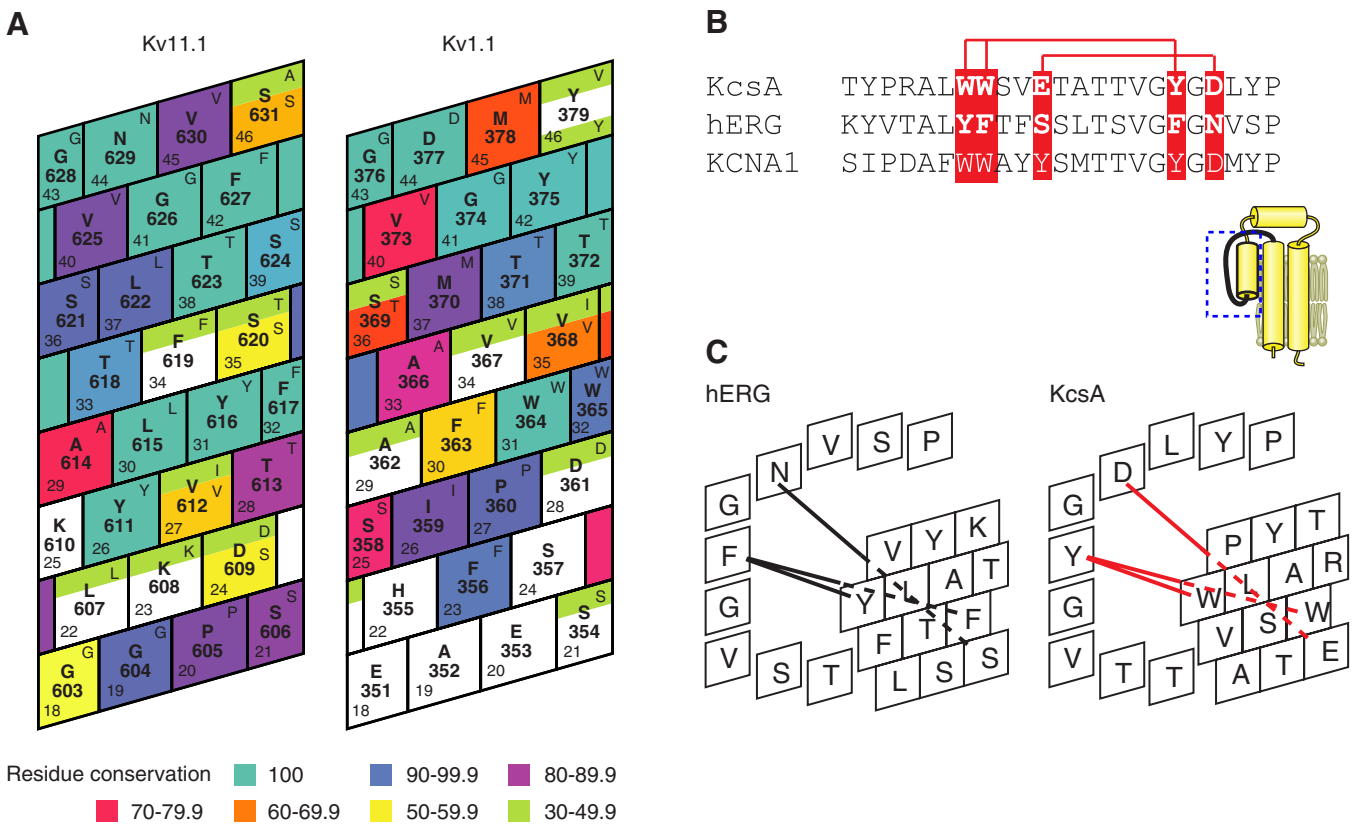

FIGURE 19. Selectivity filter hydrogen bond networks. *A*: sequence conservation in pore-helix segments for *1*) EAG subfamily and *2*) canonical VGK channels generated as described in Ju et al. (275). The helical net diagrams represent each position as a rhomboid with 3.6 residues per turn. The sequence shown is that for *1*) Kv11.1 and *2*) Kv1.1. The color coding indicates the degree of sequence identity at each position. The most frequent residue at each position within the whole family is shown in the top right corner of each rhomboid. *B*: sequence alignment for KcsA, Kv11.1, and Kv1.1. H-bond networks identified in KcsA are highlighted in red. Note that none of the five H-bonding residues is present in Kv11.1, whereas four of five are present in Kv1.1. Although not all EAG subfamily channels inactivate, the residues at four of these five positions are 100% conserved, with the exception being Ser620 (see *A*). This is consistent with the well-established critical role for Ser620 in inactivation properties of Kv11.1 (see text for details). *C*: cartoon representation of selectivity filter region of Kv11.1 and KcsA showing how H-bond networks contribute to stabilization of selectivity filter in KcsA.

The equivalent residues in Kv11.1 are Tyr616 (Trp67 in KcsA), Phe617 (Trp68), Ser620 (Glu71), Phe627 (Tyr78), and Asn629 (Asp80) (see **FIGURE 19**). It has been postulated that the lack of these hydrogen bond networks in Kv11.1 contributes to the selectivity filter being more inclined to "collapse" leading to a faster rate of inactivation (167).

Molecular dynamic simulations of the pore helix and selectivity filer regions of Kv11.1, based on homology model of KcsA, have provided some insights into the molecular basis of Kv11.1 inactivation (592). In wild-type Kv11.1, the backbone carbonyl of the selectivity filter residue Phe627 often flips away from the central axis of the conduction pathway, disrupting the S0 K^+ coordination site and so perturbing conduction. Conversely, in the presence of the S620T mutation, a water molecule stabilizes the backbone of the selectivity filter by sitting at the center of a network of hydrogen bonds between the pore helix and selectivity filter residues, similar to that previously identified in the crystal structure of KcsA (116). Specifically, the water molecule bridges Ser620 and Asn629. The equivalent residues in KcsA, Asp71 and Glu80, have been shown to be very important for C-type inactivation in KcsA (178, 254, 357).

A point worth considering here is the relationship between ionic selectivity and inactivation. With the process of inactivation seemingly so closely tied with the conformation of the selectivity filter, it is unsurprising that the two processes overlap. Several mutations that have been shown to alter inactivation gating in Kv11.1 have also been shown to alter ionic selectivity (295, 357, 378, 644, 645). Gang and Zhang (197) examined this relationship in Kv11.1 channels, invoking the concept of separate P- and C-type steps to inactivation, where P-type refers to the initial closure of the selectivity filter and C-type refers to a stabilization of the inactive conformation (387). This multistep process has been associated with a decrease in selectivity for K^+ over Na^+ in other voltage-gated channels (593, 594) that can be observed as Na^+ currents when recorded in K^+-free conditions. In Kv11.1 channels, the fast transition to the P-type

state usually manifests as the termination of K^+ conductance, but can be detected as a transient Na^+ conductance in K^+-free conditions. The second slower transition to a stable C-type inactivated state, impermeable to either K^+ or Na^+, can be detected in K^+-free conditions as a slow decay in the Na^+ conductance. These experiments illustrate the tight interplay between inactivation gating at the selectivity filter and permeability. Given that in wild-type channels, the P-type and C-type inactivated states can only be separated in nonphysiological solutions, that is in the absence of K^+, most groups still continue to use the term C-type inactivation as a general description of the overall process.

2. Role of the pore outer mouth

In early studies of C-type inactivation in *Shaker* K^+ channels, Thr449 in the outer mouth region was identified as a key regulator. The equivalent residue in Kv11.1, Ser631, had been identified in early studies as important (see above). Heinemann et al. (558) initially suggested that the mutation S631A abolished inactivation. However, a subsequent study from Zou et al. (739) showed that the S631A mutation does not abolish inactivation, but results in a shift of the $V_{0.5}$ for inactivation by approximately +100 mV. A more in-depth investigation of the S631 position in Kv11.1, carried out by Fan et al. (167), identified some additional distinctions in the role of this position between Kv11.1 and *Shaker* channels. For example, mutation of this residue to either glutamate or lysine in Kv11.1 disrupted inactivation, while mutation of the equivalent residue in Shaker (Thr449) to either of these residues facilitated inactivation. Furthermore, in *Shaker*, Thr449 is an important determinant of sensitivity to TEA and has been shown to interact directly with the TEA molecule (252, 474). Conversely, in Kv11.1, TEA block is insensitive to mutations at this position, (474) and indeed, the mechanisms of block by TEA are likely to be quite different between Shaker and Kv11.1 (167, 573). Lastly, cysteine mutants at Ser631 in Kv11.1 form disulfides across the mouth of the pore much more readily than T449C in *Shaker*, suggesting that the outer mouth region in Kv11.1 is either narrower (167) or more flexible.

3. Role of S5P domain in inactivation

Beyond the subtle changes in structure of the outer mouth region of Kv11.1 compared with *Shaker*, there is of course a much more significant difference in the turret region between the EAG subfamily and other members of the VGK channel family. KV11.1 has a much longer linker between the outer helix of the pore domain and the pore helix (i.e., the S5P linker, ~40 residues in Kv11.1) than in VGK channels (typically 12–15 residues).

Jiang et al. (294) first suggested that the longer S5P linker may be involved in Kv11.1 inactivation when they discovered that mutations of the two histidine residues in this region (His578 and His687) altered inactivation characteristics (294). In a subsequent paper, the authors examined the individual roles of these positions and noted that while His578 tolerated mutation to proline, cysteine, or lysine without affecting Kv11.1 gating properties, similar mutations at His587 altered inactivation as well as ion selectivity (159). This begged the question, how do mutations in the S5P linker, which is relatively far from the pore and selectivity filter in the primary sequence, impact inactivation and selectivity?

To examine the role of the S5P linker in more depth, Liu et al. (378) performed a cysteine scan of the entire region. Based on the accessibility of substituted cysteines to MTS modification, Tseng et al. suggested that the middle part of the linker (from Ile583 to Tyr597) forms a helical structure, which runs parallel to the membrane and is exposed to the extracellular environment along its whole length. The authors also proposed that the helix was orientated such that its NH_2 terminus was sitting close to the pore, since MTS modification of G584C caused a similar phenotype to modification of two residues near the pore entrance (T613C and S631C). In addition, many of the cysteine mutant channels could form intersubunit disulfide bonds (295), with disulfide bonds forming more readily for mutants in the NH_2-terminal half of the helix. They interpreted these data as indicating that the NH_2 terminus pointed towards the central pore (and therefore each other). However, introduction of many of these disulfides disrupted selectivity, and while this may reflect the previously discussed link between inactivation and selectivity, it is also possible that these channels may have been locked in nonnative conformations, so conclusions about native structure drawn from these experiments should be made with that caution in mind.

The prediction of a helical component in this region was confirmed in NMR studies from Torres et al. (641) who solved the structure of a 42-amino acid peptide corresponding to the S5P linker using two-dimensional NMR spectroscopy. They also showed that this helical region was amphipathic and was only seen in the presence of the membrane mimetic SDS micelles, but was unfolded in aqueous solutions. Interestingly, when CHO cells expressing wild-type Kv11.1 channels were superfused with exgenous S5P peptide, inactivation of the channels was disrupted. Furthermore, the interaction was voltage-dependent, with the off rate seemingly more voltage sensitive that the on rate. However, binding of the exogenous S5P peptide also resulted in disruption of selectivity and so again some caution needs to be applied to the interpretation of these experiments. Subsequently, Jiang et al. (295) used a combination of circular dichroism and NMR studies to show that the structure of the S5P domain was quite dynamic and suggested that it may switch between helical and unstructured conformations depending on its interaction with hydrophobic or

aqueous environments. They also proposed that the S5P helical domains themselves were physically involved in terminating conduction during inactivation, either through stearic hindrance or though a local electrostatic potential formed as a result of the NH_2-terminal positive helical dipoles being orientated towards the ion conduction pore preventing K^+ conduction. While the S5P linker is clearly important, whether it is involved directly or is an allosteric regulator of the structure of the selectivity filter remains to be finalized.

4. Voltage sensitivity of inactivation

One of the most intriguing features of Kv11.1 inactivation gating is the origin of the voltage-dependence (547, 658, 668). Two main hypotheses have been considered. First, the voltage-dependence of inactivation arises from coupling to the S4 voltage sensor (502), and second, there is an inactivation voltage-sensing domain that is distinct from the activation voltage sensor (110).

As discussed in section II*E*, the major component of voltage sensor motion in Kv11.1, as detected by gating current measurements, is slow and, moreover, is proposed to be the rate-limiting step for slow activation (502). There is, however, also a fast component of voltage sensor movement (see **FIGURE 16**), which could couple to inactivation. In wild-type channels, this fast component is first detected at −80 mV, well before the apparent threshold for channel opening, but consistent with the equilibrium voltage-dependence of inactivation. However, gating currents in wild-type and S631A Kv11.1 channels (a mutant that shifts the $V_{0.5}$ of inactivation by ~+100 mV) were indistinguishable, suggesting that either the voltage-dependence of ionic inactivation was not derived from this fast component of the S4 gating charge or that mutations to Ser631 affect a later part of the inactivation process (658). Zhang et al. (720) also examined the contribution of S4 gating charge to inactivation voltage sensing, using the charge component of the Botzmann equation as a reflection of the gating charge. In these experiments, neutralization of any of the six positive charges in the S4 transmembrane helix did not alter the apparent gating charge during inactivation.

Taking an alternative approach to monitoring voltage sensor motion, Smith and Yellen (584) used voltage-clamp fluorometry to simultaneously monitor ionic current and fluorescent emission from a probe attached to the external end of S4. In these experiments, both the kinetics and the voltage dependence of the fluorescent change mirrored that of ionic inactivation. However, again they were not able to demonstrate a causal link between the two, since the fast fluorescent changes were not affected by external application of TEA, which slows Kv11.1 inactivation (583), nor by the S631C-G628C double mutation that eliminates Kv11.1 inactivation. However there are possible confounding factors in these experiments. Changes in the environment of the fluorophore (which lead to the observed changes in fluorescence) do not necessarily reflect movement of the S4 itself, but could report movement of other domains relative to this position. Even so, both the pharmacological and mutational disruptions of inactivation did not alter the fluorescent report, suggesting that the shared kinetics of the fluorescence and ionic inactivation may be purely coincidental and unrelated. More recently, Es-Salah-Lamoureux et al. (165) reexamined these fluorescent reports in the background of removal of endogenous cysteines and reported that the fast component of the signal actually related to fast VSD movement, with the slow component reporting opening of the activation gate but were unable to find direct evidence of a report of inactivation gating. The exact nature of the motion of the VSD of Kv11.1 and its role in inactivation is therefore unresolved.

In the absence of any concrete link between VSD movement and the voltage-dependent kinetics of the inactivation process, the extracellular S5P linker is a region that has been considered a possible candidate for the inactivation voltage sensor (110, 641). In their initial cysteine scanning mutagenesis experiments of the S5P linker, Tseng et al. (378) proposed that the S5P helical region may act as a bridge to couple the VSD and the outer mouth of the pore, i.e., upon depolarization, upward motion of the voltage sensors shift the S5P α-helices toward the pore resulting in a physical and/or electrostatic barrier to ion conduction through the pore and hence inactivation of ion conduction. In 2006, Clarke et al. (110) showed that swapping the S5P domains between Kv11.1, Kv12.2 (hELK-2), and Kv10.1 (hEAG) had a large effect on the voltage-dependence of inactivation. They followed up on this observation by introducing different positive and negative charged residues at all the hydrophilic residues in the S5P α-helix (His587, Asn588, Asp591, and Gln592) showing that the voltage range of Kv11.1 inactivation could be tuned over ~150 mV. Most dramatically, substitution of a lysine residue at either position 588 or 592 shifted the $V_{0.5}$ of inactivation by 120 mV in the depolarized direction, whereas introduction of a glutamate at position Asn588 shifted inactivation ~30 mV in the hyperpolarized direction (110). Furthermore, the introduction of lysine residues into the S5P linker increased the slope of the Boltzmann fit to steady-state inactivation data, whereas introduction of negative charges decreased the slope. This would be consistent with the S5P being directly involved in voltage sensing. However, given the uncertainties of measuring changes in gating charge from Boltzmann fits to steady-state data, one cannot make definitive conclusions from these data.

Most recently, using voltage-clamp fluorometry studies of probes attached to R582C, which is located close to the NH_2-terminal end of the S5P helix, Fougere et al. (187) reported a fast component of the fluorescent change that was coincident with rectification of the macroscopic

Kv11.1 current, i.e., between −20 and +60 mV (187). One problem with these data is that direct measurements of inactivation indicate that it is substantially completed by −20 mV (547, 583) even in the R528C mutant (187). Therefore, while these findings add more weight to the notion of the S5P helix contributing to Kv11.1 inactivation, perhaps as the voltage-sensing domain, this process is yet to be fully described.

5. Summary of voltage dependence

There is compelling evidence to suggest that voltage sensing for inactivation is distinct from the voltage sensing for activation. First, the two processes occur over quite distinct voltage ranges (668). Second, there are numerous mutations that have profound effects on the voltage sensitivity of activation but minimal effect on inactivation, such as mutations of charged residues in the S4 domain (500, 601). Vice versa, there are mutations that have profound effects on inactivation but minimal effect on activation, such as S631A (739) and N588K (110, 115). Third, changes in temperature have very different effects on the two processes, causing a hyperpolarizing shift in the midpoint of steady-state activation but a depolarizing shift in steady-state inactivation (649). It is important, however, to make the distinction between the differences in the range over which the voltage sensor operates and the molecular basis of the voltage sensor. It is possible that the S4 domain, in addition to being the voltage sensor for activation, could also be the voltage sensor for inactivation (either alone or in combination with other domains of the channel), despite the two processes occurring over different voltage ranges. An initial outward movement could contribute to activation gating, and a susbsequent relaxation could contribute to inactivation. At this stage it seems most likely that both the S4 and S5P linker contribute to the voltage sensing for inactivation, but the specific mechanisms remain to be determined.

6. Macromolecular rearrangements in inactivation

Until recently, studies of C-type inactivation have focused on localized structural rearrangements in the vicinity of the selectivity filter. However, two recent cystallographic studies on KirBac (111) and KcsA (128) have shown that "collapse" of the selectivity filter may be linked to much more extensive macromolecular rearrangements involving domains throughout the channel protein. This has led to the suggestion that "collapse of the selectivity filter" may represent the final movement in a much more complex process. The concept that domains throughout the channel could be involved in inactivation came as no surprise to people working on Kv11.1 channels, given that mutations in so many disparate domains of the channel affected inactivation. In addition to the examples detailed above, there are also reports of deletions within the cytoplasmic COOH-terminal and NH_2-terminal domains altering Kv11.1 inactivation (44).

In 2011, Wang et al. (658) reported an analysis of the contribution of different domains to the energetics of inactivation in Kv11.1, using Φ-value analysis (658). Φ-Value analysis compares the relative effects of an exogenous perturbation, such as a mutation, on the energetics of rates and equilibrium of a two-step reaction, to elucidate the relative temporal order with which different components (in this case domains of the channel) move during the transition between two stable end states. The authors showed that inactivation in Kv11.1 was initiated by exit of K^+ from the selectivity filter, followed in order by conformational rearrangements of the S5 helix, extracellular turret region, S4 domain, S4S5 linker, and pore domain inner helix. They were not able to identify the final step but hypothesized that a collapse of the selectivity filter stabilized the final inactivated state. This seemingly complex allosteric process involving communication between extracellular, intracellular, and transmembrane domains is reminiscent of a Japanese puzzle box. Why the inactivation process is apparently so complex is an unresolved question, but one which would certainly open up multiple possibilities for regulation. If a similar mechanism is present in other channels, then there would be ample opportunity for kinetic fine-tuning, explaining why the rates of C-type inactivation vary by many orders of magnitude between different channels.

H. Models of Kv11.1 Gating

Kinetic modeling of ion channel activity serves two purposes. First, it provides a formal, quantitative mechanism for testing hypotheses about how channels work. Second, by building up models for all the different ion channels expressed in a cell, one can reproduce the electrical activity of an entire cell and ultimately build cells into models of organs and organisms. These models can then be used to interrogate the link between molecular defects and whole organ phenotypes. Cell and organ models, however, are only as good as the individual components that they are based on.

The biophysical accuracy of Kv11.1 models in reproducing gating kinetics is particularly important for several reasons. While simpler models may be able to approximate the global characteristics of the current, they are less effective in reproducing more complex time- and voltage-dependent effects (323, 390). It is also now widely accepted that binding of drugs to Kv11.1 channels (overwhelmingly the most common cause of drug-induced QT prolongation; see sect. VIII) is state dependent. In each of these scenarios, the accuracy of the model in predicating voltage-dependent changes in state occupancy is critical.

Over the past 25 years, models of I_{Kr}/Kv11.1 behavior have developed from Hodgkin-Huxley type descriptions (524),

via relatively simple linear Markov schemes (668), to more complex Markov descriptions containing multiple closed, open, and inactive states (323, 390) as well as subunit cooperativity (502). While this increase in complexity has clearly arisen in parallel with a more in depth understanding of Kv11.1 gating, it is also a result of the availability of more powerful computer hardware that has facilitated the fitting of such models in a realistic time frame. This technological development is allowing more and more complex and realistic in silico simulations, meaning the coming years hold a huge amount of promise for this research field both in terms of how it drives our understanding of how ion channels work and in terms of clinical benefit felt from applied use of models.

The earliest models of I_{Kr} were based on experimental data obtained for I_K in cardiac myocytes (448, 572). However, in these early studies, researchers were still grappling with technical difficulties such as dissecting the multiple components to I_K and trying to tease out the unique kinetics of I_{Kr}. As a result, these models are not commonly used today and are not discussed in detail here.

The simplest, and perhaps most used, model of voltage-gated ion channel behavior is based on the formalism introduced by Hodgkin and Huxley 60 years ago (263). In these formulations, the current passed through the channel is simply a function of two gating variables, an activation gate and an inactivation gate. These models can incorporate pseudo second-order kinetics by including power functions for each rate constant. The parameters used for simulation in **FIGURE 20** are taken from ten Tusscher et al. (620). While there are earlier instances of Hodgkin-Huxley descriptions of I_{Kr} (119, 506), this is the first that is based on fits to expressed Kv11.1 current. The authors note that their implementation is dramatically different from previous uses, with shifts of up to 60 mV in its steady-state gating characteristics (620).

In 1997, Wang et al. (668) developed a simple linear Markov scheme based on experimental data obtained from Kv11.1 currents expressed in oocytes. In contrast to the Hodgkin-Huxley type models, Markov schemes can allow incorporation of multiple open, closed, and inactive states, with transitions between each individual state determined by a voltage-dependent rate constant. To determine the number of pre-open closed states, the authors used an envelope of tails protocol to describe the onset of current activation (see sect. IV*D*) with depolarizations to the activating potential of +50 mV taken from −120 mV to ensure that the resting potential of each step reflected the fully deactivated state. The activation time course was fitted with a series of activation models ($C_0 \rightarrow C_1 \ldots C_n \rightarrow O$) with a varying number of pre-open closed states, and it was found that a minimum of three closed states was required to achieve good fits to the experimental data (668).

As the rates of activation reach a plateau at positive potentials, Wang et al. (668) included a voltage-independent step in the Kv11.1 activation pathway. The rationale for choosing the C_1-C_2 transition to be voltage independent was based on the fact that rates of deactivation are strongly voltage dependent, meaning that the final C_2-O transition had to be voltage-dependent. And second, the duration of the sigmoidal phase in activation time courses continues to shorten at the most positive depolarization steps, which they interpreted as the first C_0-C_1 transition being weakly voltage-dependent. This model for activation was then fitted to activation time courses for multiple voltages, steady-state activation data, and deactivation time constants. Finally, an inactivation state was included in this linear gating scheme. Since the authors were able to fit their measured forward and reverse rate constants for inactivation with first-order voltage-dependent models, this is included as a simple single state transition from the open state.

Two years later, Kiehn et al. (323) published an expansion of this model that included inactivation from the final pre-open closed state (see **FIGURE 20**). The authors proposed that this transition was necessary to explain *1*) the presence of channel openings upon repolarization when no channel openings had occurred during the preceding depolarization step and *2*) the voltage-dependence of the magnitude of the transient peak upon depolarization. The authors evaluated several Markov model structures by fitting to macroscopic Kv11.1 currents and showed that a closed to inactive transition was necessary to accurately reproduce the transient peak observed experimentally upon depolarization. The model, however, was only used to simulate a few simple voltage protocols.

The "closed state inactivation model" was not parameterized fully, or used to simulate more physiologically relevant action potential waveforms until two years later when an adaptation of the model proposed by Kiehn et al. was used in an in silico evaluation of long QT syndrome (108, 403) and in evaluating the effects of premature stimulation on Kv11.1 gating (390). In these cases a five-state model with inactivation between both the closed and open states was employed **(FIGURE 20)**. Each of these groups took different approaches to constraining the parameters in the model. Lu et al. fitted the model to activation, deactivation, and inactivation data recorded from Kv11.1 currents recorded in CHO cells at 37°C, (390), Mazhari et al. (403) fitted their model to similar data acquired at 22°C and scaled the transition rates with a Q_{10} of 3.3, whilst Clancy and Rudy (108) used data obtained from guinea pig cardiac myocytes to constrain their models. As a result, the models in each of these publications, despite having the same structure, have different rate constants and hence different current outputs during simulation.

In 2003, Piper et al. (502) proposed a more complex model based on measurement of gating currents in relation to activa-

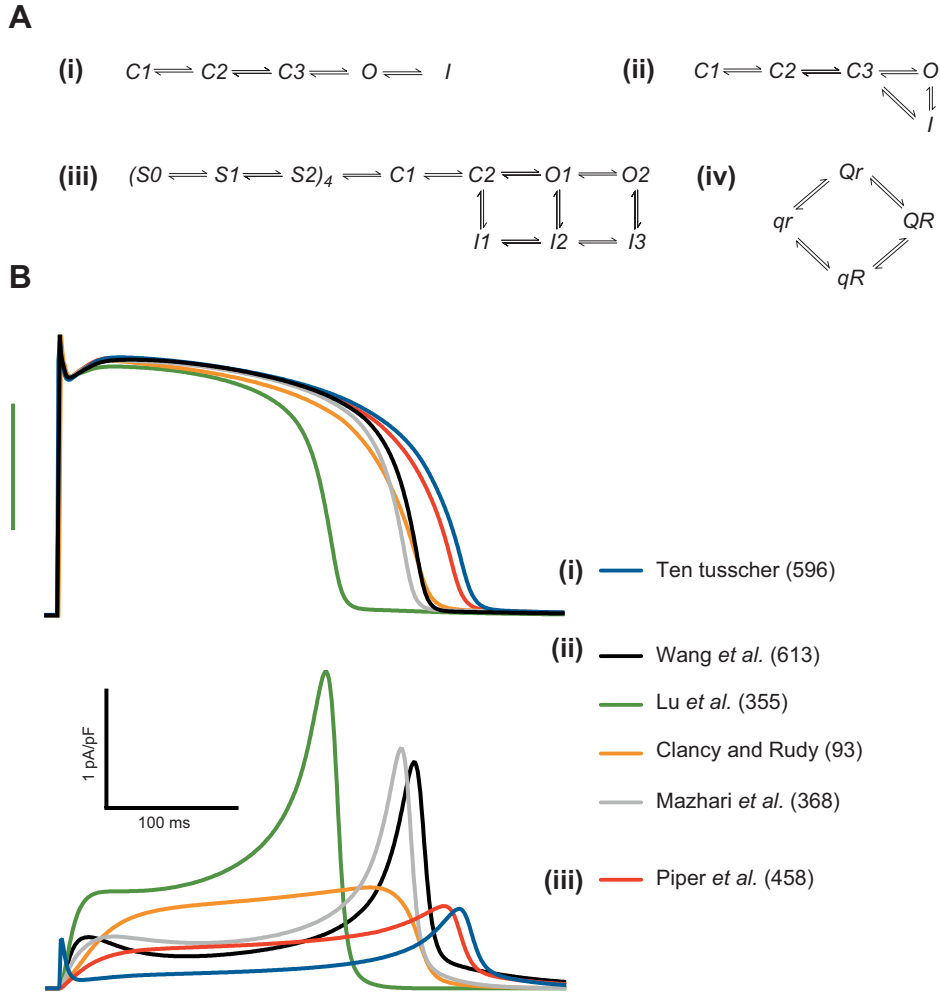

FIGURE 20. Models of hERG gating. *A*: Markov state descriptions of hERG kinetics: (i) linear scheme (668), (ii) branched scheme (108, 390, 403), (iii) subunit scheme (502), and (iv) relaxed-activated state scheme (584). *B*: action potentials (*top panel*) and Kv11.1 currents (*bottom panel*) simulated using different hERG gating models. In each case, the Hodgkin-Huxley formulation of the I_{Kr} component in the ten Tusscher description of the ventricular action potential (621) was replaced with the model shown. For comparison, the maximum I_{Kr} conductance was equivalent in each case. Simulations were carried out at 37°C. Where models were derived from data at different temperatures, rate constants were corrected using a Q_{10} of 3.3 (403). Waveforms shown are the 10th beat of pacing at 1 Hz.

tion and inactivation gating (see **FIGURE 20**). In particular, this model includes an extra closed state as well as transitions for individual VSDs between the up and down configurations. As a result, the first two closed state transitions were treated independently for each of four subunits of the channel with a statistical factor for both steps (S0→S1 and S1→S2) and positive cooperativity included in the S1→S2 transition. For each of the first two transitions, $S_n \rightarrow S_{n+1}$ the transition sequence is considered as

$$S0000 \underset{1\cdot\beta}{\overset{4\cdot\alpha}{\rightleftharpoons}} S0001 \underset{2\cdot\beta\cdot c^{-1}}{\overset{3\cdot\alpha\cdot c}{\rightleftharpoons}} S0011 \underset{3\cdot\beta\cdot c^{-2}}{\overset{2\cdot\alpha\cdot c^{2}}{\rightleftharpoons}} S0111 \underset{4\cdot\beta\cdot c^{-3}}{\overset{1\cdot\alpha\cdot c^{3}}{\rightleftharpoons}} S1111 \quad (5)$$

The four steps represent the four individual subunit transitions. For the first step, the "four" multiple reflects the availability of four subunits while in the second transition, this drops to three and a cooperativity factor, c, is included. Under this scenario, the model predicts that the fast component of the gating charge (see discussion in sect. IV*E*) is derived from the S0→S1 subunit transition, and not inactivation. The remaining transitions were all considered concerted rearrangements involving all of the subunits. This model also incorporates two open states based on single-channel data previously reported (323, 738), as well as closed state inactivation (323). In this regard, based on their transition rates, the C2→I0 transition is dominant over the C2→O1 transition at depolarized potentials.

The final model summarized here is that presented by Smith and Yellen (584) that has its roots in a very different dataset, and hence has a different structure (see **FIGURE 20**). The

authors developed this model to specifically represent changes in conformational state of the VSD based on fluorescent measurements reporting the movement of this domain in response to voltage (see sect. IV*E*). For illustration we have only shown the structure of the model they suggest reproduces ionic current more faithfully, although both of their original models describe the fluorescent datasets equally well. In this model the VSD is supposed to have four conformational states: qr, Qr, qR, and QR and two types of conformational change q→Q and r→R, where the first of these is fast and the second slow. Upon depolarization, the VSD quickly changes conformation between qr and Qr before slowly transitioning to QR. Conversely, upon repolarization, the VSD quickly transitions from QR to qR before slowly transitioning to qr. In the original paper, these fast and slow transitions, occurring in parallel, account for the fast and slow components of the fluorescent report of VSD movement (see **FIGURE 20**). Based on prior knowledge of Kv11.1 kinetics, the authors suggest that slow q-Q transitions reflect slow activation/deactivation while fast r-R transitions reflect fast inactivation/recovery from inactivation as annotated in the model. For the purpose of simulation of ionic current, the occupancy of qR is considered proportional to the open state. However, since this is solely a model for VSD movement, and does not include any coupling to gates in the conduction pathway, this model cannot be considered a true description of channel gating and is not routinely used as such.

1. Comparison of model outputs

I_{Kr} currents and corresponding ventricular action potential waveforms simulated using each of the models discussed above are shown in **FIGURE 20**. The I_{Kr} profiles described by the different models are quite diverse, and as a result, the action potential waveforms have significantly different durations and shapes. It should be noted that in these examples, an identical conductance value for I_{Kr} was used in each case; hence, the magnitudes of the currents could potentially be scaled to be more similar. The kinetics, however, are largely unaffected by this parameter, except indirectly via altered contribution to the cellular membrane potential. The important consequence of these varied current profiles is that in interrogating physiological and pathophysiological questions, each of these models would be expected to make different predictions, but clearly not all of the models can be correct. Recent advances in computational hardware are making organ level simulations incorporating more complex biophysically accurate cellular models possible on practical time scales. Simulations at this level of scale and complexity have the potential to give us an unprecedented level of insight into the electrical system of the heart in the coming years. However, before we can take advantage of these technological gains in relation to the role of Kv11.1 channels in arrhythmogenesis, there is clearly a need for an examination of these kinetic models to provide accurate descriptions of Kv11.1 gating under both physiological and pathophysiological conditions.

V. PHARMACOLOGY OF Kv11.1 CHANNELS

The pharmacology of Kv11.1 has become a subject of intense interest following the discovery that this channel is the molecular target for the vast majority of drugs associated with drug-induced arrhythmias (see sect. VIII). In this section we will discuss the pharmacology of Kv11.1 channels and review how understanding the gating of these channels has provided insights into the molecular basis of drug-induced QT prolongation.

A. Drug Binding to Kv11.1 Channels

Voltage-gated ion channels are not static structures but instead undergo substantial conformational changes as they open, close, and inactivate. Determining how drugs bind to ion channels and how the affinity or kinetics of drug block are influenced by the gating state of the channel has been of significant interest for nearly half a century. Many of the classical principles of state-dependent drug block originate from studies examining the action of quaternary ammonium (QA) compounds on the delayed rectifier K^+ current of squid giant axons (32–36) or local anesthetic block of the sodium current in frog myelinated nerve or muscle fibers (120, 258, 259, 268, 561, 597). Insights gained from these studies have had a significant influence on how people think about drug block of Kv11.1 channels. There are, however, some subtle differences between how drugs block Kv11.1 compared with other voltage-gated ion channels as discussed below.

1. Drug block requires channel opening

Spanning a decade (1965–74), Armstrong published a series of seminal papers investigating the block of delayed rectifier K^+ current (I_K) by QA compounds (32–36). The key findings were as follows: *1*) block by QA from the intracellular side requires channel opening by membrane depolarization (33, 36); *2*) the onset of voltage-dependent block by hydrophobic QA compounds can be directly observed by a decrease in outward I_K (32, 34, 35); and *3*) at membrane potentials more negative than the reversal potential for potassium, a rapid dissociation of QA ions from open channels is observed because the inward flow of K^+ ions helps remove QA ions from the permeation pathway, an effect that is accelerated by increasing the external K^+ concentration (32–34). In a study using positively charged derivatives of local anesthetics (namely QX-314), which do not easily cross the lipid membrane, Strichartz (597) demonstrated a form of open channel block of Na^+ current that, like the QA block of I_K, is strongly voltage-dependent. Consistent

with these findings, Armstrong (33) and Strichartz (597) proposed simple models which assert that blockers, acting from the intracellular side, must pass through an internal gate to gain access to their receptor site within the ion conducting pathway of the channel pore. Moreover, the blockers are prevented from exiting through the external side by a narrowing of the pore which allows only the passage of permeant ions (33, 34). Subsequently, these models of the pore have been validated by crystal structures of multiple K^+ channel proteins (111, 150, 244, 297, 337, 384, 386, 619, 682), as well as a bacterial voltage-gated Na^+ channel (479).

Similar to QA block of I_K or local anesthetic block of Na current, the vast majority of drugs which target Kv11.1 channels require channels to open before they can gain access to the receptor site within the inner cavity of the channel pore, between the selectivity filter on the external side and the internal activation gate (86, 325, 420, 587, 698, 738). Two exceptions to this rule are drugs that inhibit trafficking of Kv11.1 channel protein (discussed in sect. VC) and Kv11.1 channel toxins (sect. VF).

2. Modulated receptor hypothesis for drug block

In 1977, Hille (258) extended the open channel block model by proposing the modulated receptor hypothesis for local anesthetic block of sodium current in frog axons. The hypothesis centered around earlier findings that the binding of local anesthetics promoted inactivation gating of sodium channels and that block was reduced by procedures that alleviated inactivation, i.e., membrane hyperpolarization (120, 258, 259, 321, 680) or pronase treatment (83). In the modulated receptor hypothesis, which is analogous to the model for allosteric modulation of enzyme activity proposed by Monod et al. (424), local anesthetics preferentially bind to the inactivated state of sodium channels and, in turn, local anesthetic binding promotes inactivation (258).

Whether Kv11.1 channel blockers preferentially bind to the open or the inactivated state has been the subject of many studies. Binding to the inactivated state was initially thought to be unfavorable because strong depolarizations actually reduced the affinity for dofetilide (324, 586, 697). However, reduced block at strong depolarizations could also occur if drug binding was voltage dependent, although this remains to be formally tested. Wang et al. (669) and Suessbrich et al. (604) showed that block by E4031 or LY97241 was reduced in mutant Kv11.1 channels which lack C-type inactivation. Subsequently, a variety of Kv11.1 mutations that impair or remove inactivation have been shown to alter the affinity of a multitude of drugs (178, 356, 452, 694), especially those of high affinity such as dofetilide (484). Other factors that alter inactivation, such as the addition of divalent cations (Cd^{2+}) or the removal of extracellular sodium, also reduce block (55, 452). Together, these studies provide evidence that inactivation plays a role in Kv11.1 channel block. Although it is important to remember that for some drugs the affinity for binding to the open and inactivated states is very similar (e.g., quinidine), the preference for binding to the inactivated state appears to be drug-dependent (484). An important difference between Kv11.1 channels and sodium channels with respect to drug binding to the inactivated state is that Kv11.1 channels undergo C-type inactivation rather than N-type inactivation (see sect. VC).

3. Drug trapping

To fully understand the relationship between drug binding and channel gating, we also need to consider the dissociation of the drug from its receptor. When examining recovery of I_K from QA block, two distinct phases were observed, a prominent rapid phase that was enhanced by increased extracellular potassium or membrane hyperpolarization, and an additional, much slower phase that was slower at hyperpolarized potentials (32–34). Armstrong (33) suggested that the initial rapid phase represents dissociation of QA compounds through the open gate of the channel, whereas the slower phase represents dissociation of drugs which had been retained within the pore of the channel by closure of the gate during repolarization, which was termed drug trapping. The smaller the side chain of the QA compound, the slower the second phase of recovery, meaning that smaller compounds are more easily trapped (33). Larger compounds may prevent closure of the activation gate, analogous to a foot-in-a-door effect (84, 258, 699). Local anesthetics too can be trapped within the pore of sodium channels at resting membrane potentials (i.e., −80 mV) (597), although this may also depend on the size of the compound (258). As a consequence of drug trapping, repetitive depolarizations, such as those associated with a train of action potentials, can cause block to accumulate because unbinding between depolarizations is minimal. This phenomenon was termed use-dependent block and is also observed with uncharged local anesthetics (120), although alternative pathways may also exist for more rapid recovery from block by more hydrophobic drugs (258, 259, 268, 561).

Recovery from block, at least for some Kv11.1 channel blockers, occurs relatively slowly compared with the rate of onset of block (86, 311, 420, 485, 596, 698). However, accurately assessing rates for recovery from block by different drugs is complicated by the use of different experimental protocols and the differences in state-dependent binding. It was noted by Yang and co-workers (698) that the slow recovery from block could mean that drugs are "trapped" within the inner cavity of the channel in the closed state following membrane repolarization. This would require closure of the activation gate while the drug remained bound within the cavity (420), which would be problematic for many of the larger Kv11.1 blockers. Studies utilizing a novel point mutation that allows Kv11.1 channels to open

both with depolarization and again in response to strong hyperpolarization show that recovery from block by some drugs is augmented at negative potentials in these channels (311, 420, 596). If drug trapping in the closed state does exist, it may require reorientation of the drug compared with open or inactivated state binding modes (591, 705). Increasingly though, it is evident that trapping in the closed state is not necessarily true for all drugs (418, 485, 596). For example, the slow recovery from block by clofilium was not improved in D540K mutant Kv11.1 channels. This suggests that clofilium is held within the inner cavity of the channel even when the activation gate is open and membrane repolarization favors exit of the drug (485). One intriguing possibility is that the drug is held in the inactivated state via stronger binding to some residues (485). Further studies are required to further understand these phenomena.

B. Molecular Basis of Drug Binding

We now know that the majority of drugs bind within the inner cavity of Kv11.1 to block conduction of potassium ions through the central pore of the channel. In 2000, a mutagenesis study of four residues within the S6 helix, chosen based on homology differences with other Kv channels, reported the importance of a single aromatic residue (Phe656) for block by dofetilide (356). Alanine scanning mutagenesis subsequently revealed a more substantial binding site for the anti-arrhythmic agent MK-499 (419). This includes polar residues located at the base of the pore helix (Thr623 and Ser624), as well as aromatic residues on the S6 helix (Tyr652 and Phe656) both of which line the inner cavity of the channel (see **FIGURE 21**). The relative contribution of polar pore helix residues to drug binding appears compound-specific (419, 485). Indeed, mutation of polar residues can decrease the potency of ibutilide analogs between 30- and 1,000-fold depending on the para-substituent attached to the phenyl ring (489). In contrast, numerous studies have confirmed that aromatic S6 residues Tyr652 and Phe656 are crucial for high-affinity block by a range of different chemical entities (172, 356, 419). Systematic mutations at these two key positions indicate that high-affinity block by cisapride or terfenadine requires an aromatic side chain at position 652 and a hydrophobic side chain at position 656 (172). The aromatic side chain requirement at position 652 suggests that the π-electrons of the ring may form π-cation or π-π interactions with the drug molecule via charged nitrogen or aromatic ring structures, respectively (172, 591). Experiments using tandem dimers indicate that drugs such as cisapride can interact with Tyr652 residues on multiple subunits of the channel (432) and that the exact nature of these multisubunit interactions may be drug-specific (282). In silico modeling of drug-channel interactions using a homology model of Kv11.1 support these conclusions, and also suggest that individual drugs could adopt a multitude of binding conformations (168, 591). Certainly the concentric arrangement of aromatic side chains (Tyr652, Phe656) from each of the four subunits that line the cavity, together with the eight polar residues just below the selectivity filter, would allow for ample variability in the binding site of diverse drugs.

Whereas polar residues at the base of the pore helix are highly conserved among members of the VGK channel family, the aromatic residues (Tyr652, Phe656) on the S6 helices are not (568). These aromatic residues explain much of the extraordinary sensitivity of Kv11.1 channels to block by a diverse range of chemical entities. One problem with this hypothesis, however, is that the closely related Kv10.1

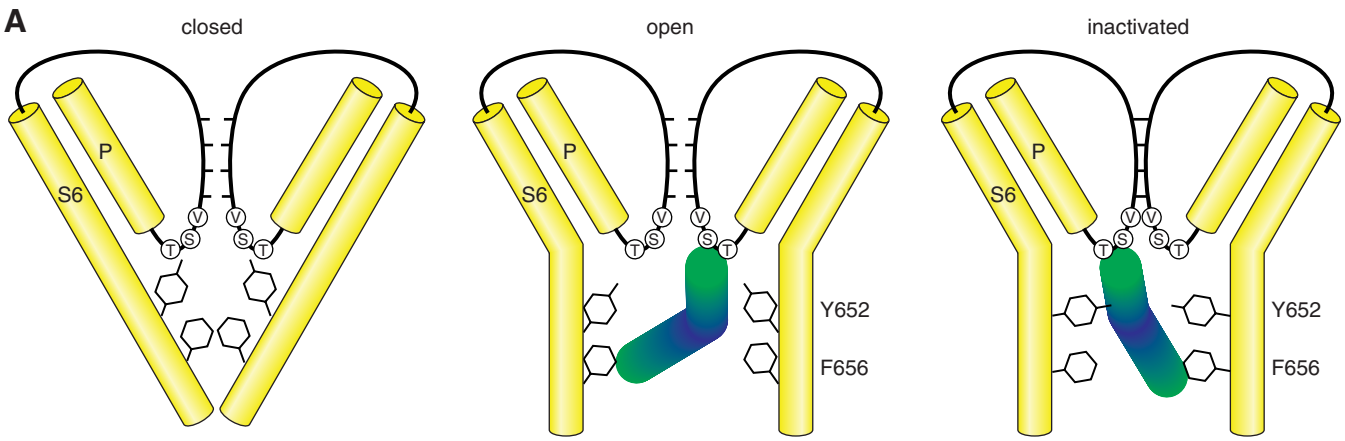

FIGURE 21. Drug binding in the pore cavity of Kv11.1 channels. Cartoon representation of the pore region of Kv11.1 in the closed, open, and inactivated states. Residues involved in drug binding include Thr623, Ser624, and Val625 close to the intracellular entrance to the selectivity filter as well as two aromatic residues Tyr652 and Phe656. Channels have to open before drugs can enter the pore cavity. Once open, drugs can enter the pore cavity and interact with one or more drug binding residues. Channel inactivation involves reorientation of drug binding residues such that drugs may bind in different orientations in the open and inactivated states.

channel also possesses Tyr and Phe residues in analogous positions to Kv11.1, but the Kv10.1 channels are substantially less sensitive to block by most drugs (177, 254). One important difference between Kv10.1 and Kv11.1 is that the former do not exhibit the same rapid C-type inactivation process observed in Kv11.1 channels (177, 254). Indeed, transfer of the pore and upper S6 helix (Val612-Leu650) from Kv11.1 into Kv10.1 channels not only introduces rapid C-type inactivation it also increases the sensitivity to drug block such that it is now comparable with that of Kv11.1 channels (254). Indeed, mutation of just three residues in Kv10.1 (T432S/A443S/A453S) is enough to observe inactivation and drug binding phenotypes that are closer to Kv11.1 than wild-type Kv10.1 (177). Together with the earlier observations that Kv11.1 channel mutations that impair C-type inactivation also reduce sensitivity to block, these studies in Kv10.1 strongly suggested that rapid C-type inactivation was a requirement for high-affinity block. However, it is not quite as simple as that. First, not all high-affinity drugs favor binding to the inactivated state. Clofilium, for example, can block Kv10.1 channels with the same affinity as it blocks Kv11.1 channels (206, 208). Second, mutations that enhance inactivation can still reduce sensitivity to block (419). Third, and most important, the reduced sensitivity to block exhibited by mutant Kv11.1 channels with impaired inactivation is relatively minor compared with mutations to key binding residues such as Tyr652 or Phe656 (452, 484, 669). This would suggest that the predominance of inactivated state binding is not necessarily critical, and it may vary from drug to drug (484).

If, as seems likely, at least some drugs bind preferentially to the inactivated state, what is the mechanism that underlies this phenomenon? One possibility is that inactivation alters the side chain position of residues at the base of the pore helix (Thr623, Ser624), which then could facilitate drug binding. Two recent in silico studies have suggested that relaxation of the pore helix (282) or reorientation of pore helix polar residue side chains (592) is associated with inactivation. While this possibility is still valid, an important study by Chen et al. (97) demonstrated that repositioning of key binding residues, Tyr652 and Phe656, one position (100°) down the S6 helix, substantially increased sensitivity of Kv10.1 channels to cisparide even if inactivation was absent. This suggests that it is the positioning of the S6 aromatic residues and not the inactivation process itself that is important. Interestingly, the repositioning of residues in Kv10.1 did not confer sensitivity to block by MK-499 (97). One possible explanation is that the repositioning occurs relative to other important binding residues within the cavity, in particular the pore helix residues, which are important for binding MK499 but less so for cisapride. A subtle repositioning of the side-chains of Tyr652 and/or Phe656, which favors binding of some drugs, could occur naturally during transition from the open state to the C-type inactivated state of Kv11.1 channels (97). In support of this proposition, removal of inactivation by mutation is not additive to removal of Phe656, an important binding residue (391). Computer modeling using a Kv11.1 channel model suggests that rotation of the S6 helix from Gly648 downwards can reposition Tyr652 and Phe656 in a more favorable orientation for drug binding. A second in silico model, suggesting an alternative perpendicular binding mode, infers that the rotameric flexibility of Tyr652 side chains is critical during inactivation, and that rotation of at least one of the four Tyr652 side chains during inactivation could enhance binding (705). In either case, the dynamic nature of the drug-binding site of Kv11.1 offers even more possibilities for variations to drug binding conformations.

C. Drugs Can Alter hERG Protein Trafficking

The vast majority of drugs reduce I_{Kr} via block of potassium conduction through the pore as outlined above. Another potential mechanism by which drugs can reduce I_{Kr} is through a reduction in the number of Kv11.1 channels in the membrane. Several drugs that confer loss of function through reduced trafficking have recently been identified (179). Some drugs, including arsenic trioxide (179), pentamidine (117, 342), and probucol (226), used at concentrations known to cause QT prolongation and arrhythmia, disrupt hERG trafficking without direct channel block. Others, such as fluoxetine and ketoconazole, can acutely block Kv11.1 channels and reduce hERG protein at the cell membrane following long-term exposure (512, 614). It is worth noting that mutation of Phe656 abolished channel block but had no effect on the impaired trafficking of hERG protein by either drug (512, 614). This may reflect either alternative binding sites on the channel (663) or targeting of a distinct pathway that in turn regulates hERG protein trafficking (176). In any case, it is important to consider impaired trafficking as an alternative mechanism for drug-induced QT prolongation, especially as conventional compound screening procedures for Kv11.1 block liability may not detect reductions in current through this mechanism.

D. In Silico Modeling of Kv11.1 Drug Block

To determine a drug's liability for causing prolongation of the QT interval, the pharmaceutical industry uses an initial nonclinical multitier approach to screen all new chemical entities as laid out by the ICH (International Conference on Harmonization of technical requirement for registration of pharmaceuticals for human use) guideline S7B (375). However, prior to this, in silico modeling can be used to assess the likelihood that any given drug will block Kv11.1 channels. Most of the modeling approaches to date have exploited ligand-based approaches, like (QSAR) and/or classification models, to build pharmacophores that highlight chemical moieties on a drug that positively or negatively correlate with block (39).

In 1992, Morgan and Sullivan published a pharmacophore model, based on a limited number of class III antiarrhythmic agents which are now known to preferentially block Kv11.1 channels (426). At the core of this pharmacophore lies a basic amine core attached by a short linker (1–4 atoms) to a phenyl ring. The nature of a para-substituent attached to the phenyl ring, in addition to two lipophilic substituents of the amine (one or more of which may be aromatic), were also acknowledged as important determinants of function. Remarkably, these key features are in general agreement with three pharmacophore models published 10 years later using 3D-QSAR modeling of known Kv11.1 channel blockers (89, 162, 481). Subsequent 2D- and 3D-QSAR models developed based on much larger and more diverse training sets did not dramatically improve their predictive capacity (201, 562), and one model exhibited lower prediction accuracy as new compound sets of diverse class and structure were added over time (201). One explanation is that structurally diverse compounds may preferentially bind to the channel during distinct gating states (open or inactivated). A rigid pharmacophore model may therefore not be the best solution, despite the apparent homogenous nature of the binding site (146, 320, 336, 617, 703). Recent studies have attempted to address the problem of multiple binding modes for different drugs (146, 320, 336, 617, 703). One approach taken by Kramer et al. (336) was to produce a composite model of two pharmacophores for high-affinity Kv11.1 blockers, as well as a third model for compounds that did not fit either of the first two pharmacophores (labeled nonspecific). This multimodel approach contrasts that of Tan et al. (617) who produced an ensemble pharmacophore derived from 5 best in class models distilled down from an initial 47. Both methods offer promising approaches to overcome the problems with static pharmacophore models.

A second approach, statistical classification, aims to predict the potency of compounds based on a variety of parameters such as fragmental partition coefficient and hydrophobicity. Various classification methods have now been used to examine parameters associated with Kv11.1 block potency (40, 156, 320, 368, 453, 523, 606, 627, 638). In general, classification models appear to have greater accuracy for inactive (nonpotent) than active (potent) compounds (40, 156, 320, 368, 453, 523, 606, 627, 638). This is not surprising as most studies use training compound datasets that contain many more inactive than active compounds, so skewing the statistical analysis. Recent support vector machine based classification models using large compound datasets exhibit much improved prediction power (291, 569).

Overall, the pharmacophore models generated by either method highlight some key physiochemical features of high-affinity Kv11.1 channel blockers: *1*) hydrophobicity, in the form of aliphatic chains or aromatic rings, probably due to strong hydrophobic and/or π-stacking interactions with Tyr652 and Phe656 on the S6 helix of the channel (156, 523, 569, 617, 627, 638); *2*) flexibility (562, 617, 638), which could reflect the ability of small molecules to take a variety of conformations within the inner cavity of the channel (105, 168, 399, 705); *3*) increasing the number of aromatic rings has a positive correlation with block potency (447, 569, 606, 617); and *4*) the presence of a charged amine shows strong correlation with high potency but is not necessarily crucial (38, 617). In contrast, molecular features that in general negatively correlate with block include the presence of polar entities (156, 447, 569, 638, 703) and hydrophilic groups close to hydrophobic regions of the drug (562, 569). On this note, distances between features (such as proximity between nonpolar atoms or between hydrogen bond donors and polar groups) may also be significant factors (569, 599).

One of the principle challenges in understanding Kv11.1 block using in silico modeling is interpreting the wealth of ligand-based modeling data within the context of a receptor model. Part of this challenge is due to the absence of direct structural information for the Kv11.1 channel. Instead, researchers must rely on homology models based on potassium channels for which there are crystal structures but where the degree of homology can be highly questionable for some regions of the protein potentially important for drug block (378, 641). Even when accurate alignments can be made, homology models based on crystal structures are a static picture of the channel in a single state and do not provide information regarding structural rearrangements that occur during gating transitions that likely contribute to state dependent drug binding (591, 592). A further complication is the inclusion of lipid membranes into these models using molecular dynamics simulations, which may be important for a stable Kv11.1 channel model (399, 595). Despite these significant problems in obtaining an accurate receptor model of Kv11.1, several sophisticated in silico models of drug binding exist (74, 160, 168, 282, 399, 591, 595, 705). The different docking strategies and diverse test structures used in these studies makes a comparison of binding conformations difficult. However, a few key points can be made. First, the predicted orientation of drugs within the inner cavity of the channel is variable. Relative to the conduction axis, there are three principle conformations: "curled" (168, 591), parallel (399, 591), and perpendicular (705). This variation may stem from the different homology models used for docking simulations (591, 705). Second, all studies highlighted the importance of multiple π-stacking and hydrophobic interactions with the aromatic side chains of two S6 helix residues, Tyr652 and Phe656. Furthermore, the simulations suggest that drugs can form aromatic and hydrophobic interactions with more than one subunit of the channel (74, 168, 282, 399, 591, 705). This fits well with ligand-derived models which indicate that multiple aromatic and/or aliphatic chains are critical for high-affinity

block (156, 523, 569, 617, 627, 638). Positioning the side chains of Phe656, and particularly Tyr652, is then critical for drug interaction (591, 705). This may corroborate suggestions that repositioning of these residues during inactivation allows for a higher affinity interaction between drug and channel (97, 591, 705). Finally, some of the docking simulations noted the absence of a cation-π interaction between protonated nitrogen on the drug and an aromatic side chain of Tyr652 (74, 168, 282). Although ligand-based models suggest that this charged nitrogen is not crucial, its presence does correlate well with high-affinity block (447, 569, 606, 617). Docking models have suggested other potential roles for this positively charged group, including interaction with pore helix residues (168, 705), interaction with water molecules within the cavity in place of a potassium ion (74), and attraction to the overall negative electric field within the electric field (168).

It is important to note at this stage that accurate predictions for the arrhythmogenic profile of a compound require a multitude of considerations beyond just Kv11.1 block liability. Simple simulations of Kv11.1 channel block (approximated by reducing I_{Kr} conductance) in models of human ventricular cells have recapitulated some of the pro-arrhythmogenic biomarkers that are associated with drug-induced prolongation of the QT interval (219, 286, 454, 621). However, these models do have some problems such as the relative contributions of I_{Kr} and I_{Ks} to AP repolarization, especially in regard to adrenergic tone, and the lack of adequate incorporation of calcium handling mechanisms. A further consideration is the nonspecific actions of drugs. Verapamil for example blocks Kv11.1 with relatively high affinity but has little arrhythmogenic risk due, at least in part, to its effects on other cardiac ion channels (7). In this regard, Mirams et al. (416) recently used a human cardiac myocyte model to correctly characterize drugs into one of four categories of arrhythmogenic risk based on their modulatory effects on I_{Kr}, the fast sodium channel (I_{Na}), and the L-type calcium channel ($I_{Ca,L}$). Interestingly, the only drug that did not fall into any of the categorizations was amiodarone, which is known not only to directly block Kv11.1 but also to impair trafficking of the channel to the cell surface (416). This acts as a reminder that direct channel block is not the only mechanism by which drugs can reduce I_{Kr} and prolong the QT interval, and we know very little regarding which types of structures can mediate these alternative effects.

Given these problems, the development of a computational model that accurately predicts the arrhythmogenic potential of a chemical entity will likely require a wider and more integrative approach that includes all levels of the system. To this end, a recent study used 3D-QSAR and docking simulations to predict block of both I_{Kr} (Kv11.1) and I_{Ks} (Kv7.1), before incorporating this information into a guinea pig ventricular tissue model (455). This integrated model then allowed the simulation of individual action potentials, pseudo-ECGs, and 2D-maps of action potential propagation through simulated ventricular tissue. The generation of even more complex integrative models will be extremely challenging but may in future provide an in silico screen for the arrhythmogenic potential of drugs.

E. High-Throughput Screens for Kv11.1 Drug Block

The development of lead compounds in any pharmaceutical program involves screening large numbers of chemical entities. The mandated need to ensure that any potential therapeutic does not have an unacceptably high affinity for Kv11.1 therefore requires a medium- or preferably high-throughput screening method for Kv11.1 channel block. The full gamut of high-throughput screening technologies have been applied to this problem. These include radioligand binding, ion efflux, and fluorescence-based assays that indirectly measure channel function, as well as automated parallel patch-clamp electrophysiological assays that allow direct measurement of ionic current.

1. Radioligand binding assays

Competitive radioligand binding assays are one of the most common in vitro screening tools used within the pharmaceutical industry. Several radiolabeled Kv11.1 blockers have been characterized, including [^{3}H]dofetilide (92, 143, 182, 183), [^{3}H]astemizole (103), [^{35}S]-MK-499 (509), and [^{125}I]-BeKm1 (21). A nonradioactive fluorescent tracer polarization assay, which also works through competitive binding, has been reported to produce similarly accurate results, albeit using a small test drug dataset (499). Competitive binding assays can provide reasonably accurate estimations of Kv11.1 block liability, although it is important to note their limitations. Importantly, as these assays rely on competitive binding with high-affinity blockers, they cannot be used to identify drugs that bind outside of the channel cavity. For example, alternative binding sites have been proposed for drugs that impair hERG protein trafficking (512, 614), Kv11.1 agonists (488), and Kv11.1 toxins (646). The assays also do not take into account relative differences in state-dependent binding for the test drug compared with the drug being displaced. Finally, the kinetics of binding, which could be important when it comes to predicting proarrhythmic risk, are also not accounted for. It is clear therefore that this type of assay cannot be used in isolation when assessing action of a drug.

2. Rubidium (Rb^+) efflux assay

Potassium channels like Kv11.1 are able to conduct Rb ions, so decreased Rb^+ flux in the presence of a drug allows an indirect measure of channel block (618). While this technique can accurately predict relative potency between

drugs, it tends to substantially underestimate the IC_{50} of most drugs (78, 430, 518, 618). At least some of this underestimation can be attributed to impaired inactivation caused by Rb^+ (518).

3. Fluorescence-based assays

Fluorescence-based dyes that measure changes in membrane potential can be used to assess Kv11.1 channel function indirectly (149, 430, 618). Three commercially available dyes have been assessed using stable Kv11.1-expressing cell lines and a fluorometric imaging plate reader (FLIPR, Molecular Devices, Sunnyvale, CA), with all three dyes giving IC_{50} values that showed relatively poor correlation with those obtained by patch-clamp analysis (149, 430). Two of the three studies reported a high number of false negatives in the fluorescence assay (618), while the third reported a number of false positives (149, 430, 618). Two of the main reasons for the less than satisfactory results with this technique are the low signal-to-noise ratio and a substantial quenching of the fluorescent signal by many of the test compounds that bind to the fluorescent dyes. Hopefully, some of these problems may be overcome by the generation of more accurate dyes and better fluorometric plate readers. Recently, Tian et al. (634) reported use of the dye di-8-ANNEPS and a genetically encoded fluorescent voltage sensor (Mermaid) to measure action potentials in rat cardiomyocytes. Addition of the drug E4031 prolonged action potential duration, suggesting that this type of technique could be used as a screen for drug-induced QT prolongation.

A combination of ion flux and fluorescence-based approaches forms the basis of newly proposed thallium flux assay (635). On one hand, this works similarly to the rubidium flux assay in that thallium can permeate through the channel once opened. Channel activity is indirectly measured using a dye (FluxOR, Life Technologies, Carlsbad, CA), trapped in the cell, which is excited in the presence of thallium. This technique can be ultra high-throughput if used in conjunction with a plate reader that enables fast (~10 min) detection of fluorescence in 1,536-well plates. In initial studies, the accuracy of IC_{50} values was highly variable, with underestimations of potency by more than 1,000-fold for some drugs compared with the IC_{50} values obtained using automated patch clamp (77, 278, 635). However, small alterations to the protocol of thallium flux studies, such as increasing the external KCl concentration used to open the channels, appears to improve these inaccuracies, at least for high-affinity compounds (557). One major benefit of flux assays compared with competitive binding assays is the possibility of identifying Kv11.1 channel agonists (278). Moreover, by incubating cells with drug for a longer time period, these assays may also detect compounds which impair trafficking of Kv11.1 channels to the cell membrane (278).

4. hERG-Lite

A specific assay named hERG-Lite, which measures cell surface expression of hemagglutinin (HA)-tagged hERG protein in HEK293 cells, has been developed to detect inhibitors of hERG trafficking (683). In this assay, Kv11.1 channel block can be indirectly assessed at the same time by measuring the capacity of a drug to rescue a trafficking defective mutant hERG protein. A total of 26 of 100 compounds were shown to induce hERG trafficking inhibition, of which 20 also exhibited channel block (683). This assay though cannot measure IC_{50} values directly and at present is relatively low throughput.

5. Automated patch-clamp techniques

The major problem with high-throughput assays for Kv11.1 channel block discussed above is the lack of direct voltage control and hence inability to accurately assess the state dependence of drug binding. At the present time, only electrophysiological techniques allow for direct control of the membrane potential, and these assays are considered the "gold standard" for assessing Kv11.1 block liability (238). Traditionally though, electrophysiological screens do not have sufficiently high throughput to be considered as primary screening tools. The development of automated planar patch-clamp systems that allow parallel recordings from multiple cells has significantly improved the screening potential of such systems. Several systems exist including Ionworks Barracuda and PatchXpress 7000A (both Molecular Devices), Patchliner and SynchroPatch 96 (Nanion), QPatch HTX (Sophion Biosciences), and IonFlux (Fluxion). These systems are now being extensively used in the pharmaceutical and biotechnology industries. Furthermore, the data for large numbers of drugs screened for hERG binding are now publically available (see, e.g., www.hergcentral.org; Ref. 155).

6. In vivo screening assays

While high-throughput screens like those discussed above are important tools for measuring Kv11.1 block by drugs in vitro, it is important that potential new drugs are subsequently tested for liability to cause QT interval prolongation and arrhythmias in an in vivo system, as per the ICH guidelines. Isolated ventricular wedge preparations (693) and Langendorff-perfused heart preparations (266) are commonly used for this purpose. These are, however, by their very nature more expensive and much lower throughput and have been reviewed in detail elsewhere (210, 313). More recently, the use of zebrafish as an in vivo screening assay for arrhythmic potential has been explored (54, 349, 414, 422). When coupled with medium- to high-throughput screening techniques for the assessment of cardiac function (82), zebrafish may provide an interesting in vivo model for this purpose, although its efficacy requires further evaluation (422).

F. Toxin Binding to Kv11.1 Channels

1. ERG specific toxins

Several short peptide toxins isolated from various species of scorpion are high-affinity blockers of Kv11.1 K^+ channels (118, 528). Despite sharing little amino acid homology, both BeKm-1 (334) and ErgTx-1 (also known as CnErg1; Refs. 229, 473) specifically target the ERG subfamily of K^+ channels with nanomolar affinity. Together with their various analogs, BeKm-1 and ErgTx-1 form a subfamily of scorpion toxins termed γ-KTx (528). A sea anemone toxin APETx1 (148) also demonstrates specificity for ERG channels over other channel types, but this toxin has been less extensively studied. Although less potent than the peptide toxins, the organic quanidine-based alkaloid saxitoxin (STX) can also reduce the function of Kv11.1 channels (660).

The venom of most venomous animals contains a wide range of toxins, many of which specifically target different ion channels. These toxins presumably subserve different tasks, from rapidly immobilizing their prey (e.g., through inhibition of neuronal/muscle sodium channels) to killing the prey. One would not expect an ERG-specific toxin to cause rapid immobilization of a small animal, but induction of a cardiac arrhythmia would certainly contribute to rapid cardiac arrest.

2. Mechanisms of block

Ion channel toxins typically exhibit either one of two modes of action. Pore blockers bind to a region of the channel where they directly prevent conduction of ions through the pore (212), whereas gating modifiers alter channel function by modifying the kinetics and/or voltage dependency of one or more gating transitions (611). There are several common features of Kv11.1 inhibition by γ-KTx-subfamily toxins BeKm-1 and ErgTx-1, which allude to their mechanism of action. Both toxins inhibit Kv11.1 in a concentration-dependent manner with an apparent toxin-channel stoichiometry of 1:1 (229, 334). Contrary to drug-induced pore block, binding of BeKm-1 or ErgTx-1 shows reverse state dependence, with reduced affinity at more depolarized potentials (229, 415, 718). The rapid onset and reversibility of action (229, 334) indicates that both toxins bind to an external site on the channel and crucially, their inhibitory effect can be attenuated by outer pore mutations and external TEA, both of which strongly implicate direct pore block (473, 474, 718).

Direct pore block of other voltage-gated potassium channels by KTx-family toxins is sensitive to changes in the permeant cation concentration. Charybdotoxin, for example, blocks deep within the pore of *Shaker* channels to "plug" the selectivity filter and prevent conduction of potassium ions (212). In this case, a positively charged lysine residue, which together with a hydrophobic patch forms a functional dyad group on the toxin, plugs the pore by substituting for a potassium ion at the outermost coordination site of the channel selectivity filter (212). A high external potassium concentration leads to increased occupancy of the outermost potassium coordination site and thereby reduces the affinity for toxin binding (212). In contrast, the inhibition of Kv11.1 by γ-KTx-subfamily toxins, BeKm-1 and ErgTx-1, was unaffected by elevated external potassium concentration (474, 718). Further, Kv11.1 inhibition by either toxin was incomplete, even at concentrations 100-fold greater than the IC_{50} (334, 474, 718). At first glance, the lack of sensitivity to potassium and incomplete block suggest that γ-KTx act as gating modifiers (718). However, while the residual current (~10% of total) following maximal inhibition exhibits altered gating parameters (256, 718), these are insufficient to account for the inhibition of Kv11.1 by γ-KTx (256, 718). Neither is there a significant alteration to single-channel conductance, at least in the case of ErgTx-1 (256, 718). An alternative explanation is that the primary mechanism is one of pore block rather than gating modification, but Kv11.1 toxins may not bind as deep within the pore as occurs in other KTx-family scorpion toxins (see **FIGURE 22**). In support of this, a point mutation (S631A) in the outer mouth of the Kv11.1 pore introduced sensitivity of toxin binding to external potassium concentration (255). It is possible that the S631A mutation alters the conformation of the outer mouth, which allows the toxin to bind deeper within the pore, possibly through a dyad binding motif (255). A "weaker" binding mechanism for Kv11.1 toxins may also underlie their fast dissociation kinetics from the channel. This is important because a fast dissociation rate (relative to binding rate) from the Kv11.1 pore can account for the incomplete block by ErgTx-1 (256).

APETx1 may act more as a gating modifier of Kv11.1 rather than a direct pore blocker (148, 721). Unlike the more direct pore blockers, APETx-1 exhibits a much higher affinity for Kv11.1 over Kv11.2 or Kv11.3 K^+ channels (517). This specific inhibition of Kv11.1 current by APETx-1 occurs through a concentration-dependent depolarizing shift in the voltage dependence of activation and a reduction in maximal conductance (148, 721). As with γ-KTx-subfamily toxins, the inhibition of Kv11.1 current by APETx-1 is incomplete even at high concentrations (148, 721).

The organic molecule saxitoxin also reduces Kv11.1 current via a mechanism that is reminiscent of APETx-1 (660). One important difference though is that saxitoxin also induces a depolarizing shift in the voltage dependence of C-type inactivation, which paradoxically causes an enhancement of Kv11.1 function at very depolarized potentials where activation is maximal (660). This effect is not observed with APETx-1, and it is likely that these toxins have

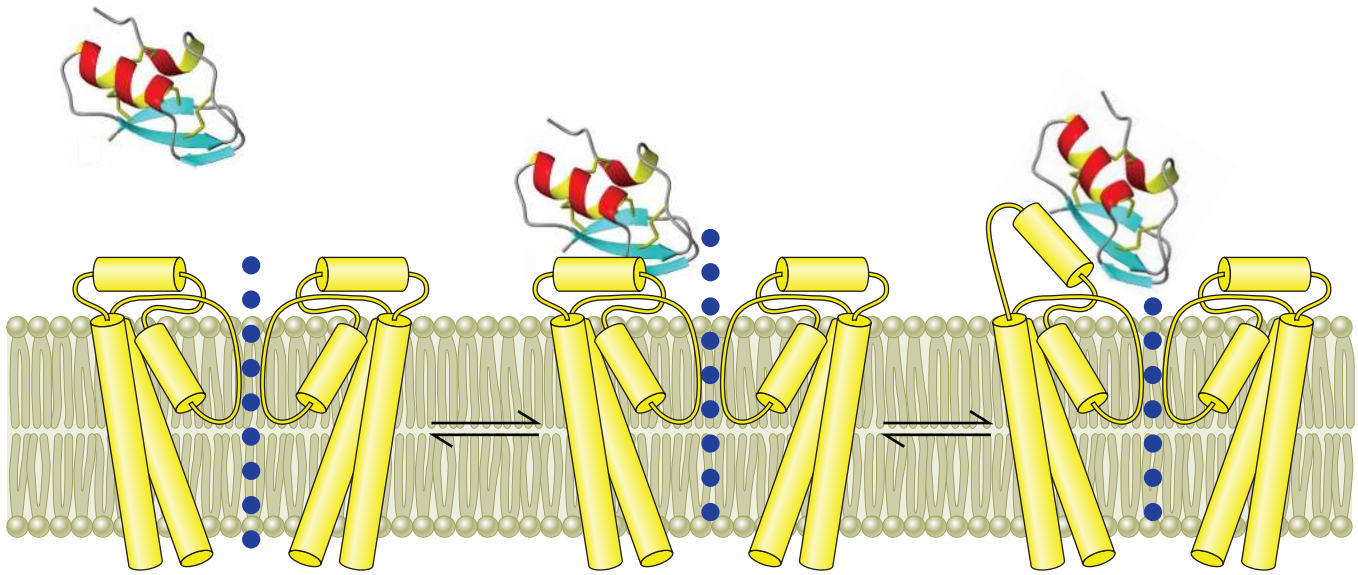

FIGURE 22. Two step model for CnErg1 binding to Kv11.1 channels. Toxin binds to the channel, interacting with the S5P helix (335, 646, 701). Block of ion conduction, however, requires a second step, which is hypothesized to be conformational rearrangements of the external mouth of the channel (256). Note the toxin can unbind from the nonblocked conformation, and this can explain the incomplete block of conductance even at high concentrations of toxin (256).

distinct binding sites on the hERG protein. Interestingly, several naturally occurring small molecule agonists of Kv11.1 channels also reduce inactivation by shifting the voltage dependence to more depolarized potentials but do not produce the concomitant depolarizing shift in voltage dependence of activation (see sect. VG).

3. Binding site for erg toxins

The rapid onset and reversibility of γ-KTx-subfamily toxins clearly indicates an external binding site on the hERG protein (229, 334). Mutagenesis studies of Kv11.1 identified the outer mouth of the pore, as well as the four S5-P linkers of the channel as the likely binding regions for both BeKm-1 (646, 718) and ErgTx-1 (474), with at least partial overlap in binding sites for these toxins (718).

Mutant cycle analysis and NMR spectroscopy have highlighted the importance of residues with hydrophobic (Tyr11 and Phe14) and positively charged (Lys18 and Arg20) side chains in γ-KTx binding to Kv11.1 channels (333, 646). In particular, the positively charged Lys18 and Arg20 appear to play a key role in BeKm-1 toxin binding.

It has been suggested that binding of ERG toxins to Kv11.1 is mediated by interactions with hydrophobic residues in the amphipathic helix of the S5P linker (474). Given that mutations of the S5P linker hydrophobic residues resulted in significant perturbations to inactivation gating and selectivity (474), one must be cautious with assuming that they have maintained the normal tertiary structure. Conversely, mutation Q592C within the S5P linker exhibits reduced affinity for CnErg1 but still has normal inactivation and selectivity (474). Thus there is no doubt that the S5P linker is important for CnErg1 (and BeKm1) binding, although the precise site of binding remains to be determined. Nevertheless, various models predicting the binding conformation of both γ-KTx-subfamily toxins have been postulated, and a general picture of γ-KTx binding to Kv11.1 channels is emerging. This consensus appears to involve binding to the outer mouth of the pore and the S5-P linker through hydrophobic interactions, but with the positively charged lysine or arginine residues interacting with the hydroxyl group of Ser631 (255, 646). This is distinct from other KTx-family toxins (like charybdotoxin) that bind into the selectivity filter of Kv channels to plug the pore. This can explain why Kv11.1 block by γ-KTx-subfamily toxins is incomplete and lacks sensitivity to external potassium concentration.

Unlike the pore blocking γ-KTx-subfamily of toxins outlined above, the gating modifier toxin APETx-1 appears to impair activation of Kv11.1 channels through an interaction with the voltage sensor paddle (721). Crystal structures of other voltage-gated potassium channels indicate that the voltage sensor paddle is comprised of S3b to S4 helices, which play a critical role in opening the channel in response to membrane depolarization. Targeted binding to the S3b appears to be a common mechanism for gating modifiers of a range of ion channels (610). Cysteine scanning mutagenesis of residues within the outer S3b region of the Kv11.1 channel highlighted a negatively charged residue (Glu518) as important for binding of APETx-1, probably through an interaction with a basic residue (Lys18) on the toxin (721).

In addition, several hydrophobic residues on APETx-1 may help stabilize this interaction (93, 721). The binding site for another gating modifier, saxitoxin, has not yet been identified but is likely separate from that of APETx-1 due to their distinct effects on C-type inactivation of the channel (660, 721).

G. Kv11.1 Activators

High-throughput screening techniques used to test compound libraries for Kv11.1 block have led to the serendipitous discovery of small molecules that enhance current passed through Kv11.1 channels. In principle, an increase in ventricular repolarization currents such as I_{Ks} or I_{Kr} could provide a useful treatment for ventricular arrhythmias associated with both congenital LQTS and acquired QT interval prolongation. Moreover, this mechanism for shortening action potential duration (APD) would be favorable over the use of calcium channels blockers as it would not be expected to alter contractility of the myocardium.

Several partial agonists of Kv11.1 have been identified since 2005 (88, 205, 240, 241, 312, 600, 729). The exact mechanistic profile of each appears to be subtly different and may reflect specialized binding interactions for each agonist with the channel. This seems in direct contrast to Kv11.1 channel blockers that show a remarkable degree of conformity in blocking conduction by binding within the inner cavity of the channel (see sect. V*B*). Based on the primary mode of action, Kv11.1 activators can be separated into two groups, types 1 and 2.

The first reported Kv11.1 activator was RPR260243 {(3*R*,4*R*)-4-[3-(6-methoxyquinolin-4-yl)-3-oxo-propyl]-1-[3-(2,3,5-trifluoro-phenyl)-prop-2-ynyl]-piperidine-3-carboxylic acid}, a small molecule that primarily slows the rate of channel deactivation and is designated a type 1 activator (312, 487). Secondary effects on channel gating include an attenuation of C-type inactivation and a slowing of channel opening upon depolarization (312, 487). Site-directed mutagenesis identified a putative binding site for RPR26043 formed by the intracellular ends of the S5 and S6 helices that form the pore domain (487). Molecular modeling showed that four key binding residues (Leu553, Phe557 on the S5; Asn658, Val659 on the S6) face away from the conduction pathway of the channel. Knowing that the S6 helices of each subunit (4 in total) come together to block conduction upon repolarization of the membrane potential (deactivation), it seems intuitive that binding of RPR260243 at this location could severely restrict the rate of channel closure.

So far most activators primarily act on the C-type inactivation mechanism that begets inward rectification of Kv11.1/I_{Kr}. By slowing the normally rapid-onset, in addition to shifting the voltage dependence to more depolarized potentials, these designated type 2 activators profoundly impair the inactivation process of Kv11.1 channels (88, 205, 240, 241, 600, 729). A secondary mechanism for some type 2 activators, revealed under conditions where inactivation is minimal, is cautiously identified as an increase in single-channel open probability (486). Other, comparatively small effects on channel gating appear to be somewhat activator specific, including slowed deactivation and a hyperpolarizing shift in the voltage dependence of activation (88, 205, 240, 241, 600, 729). These small differences in mode of action could reflect subtle differences in binding interactions of type 2 activators with the channel protein. For example, a combination of mutagenesis and molecular modeling suggests that binding of PD118057, a type 2 activator that attenuates inactivation but has no effect on deactivation, occurs within a small hydrophobic pocket formed between the pore helix and S6 helix of adjacent subunits (486). Another type 2 activator, NS1643, that does slow deactivation, is proposed to bind in a similar region but shares only some binding residues with PD118057 (namely Leu622 on the pore helix and Leu646 on the S6 helix) (222). Subtle differences in binding residues within this pocket have also been identified for a more potent activator, ICA105574 (200). Further studies to map the binding sites of other type 2 activators may reveal the exact nature of these activator specific effects in more detail. In any case, the primary effect of impaired inactivation is likely mediated through drug interaction with the pore helix, a region proposed to stabilize the inactivation gate of the channel (592).

Other Kv11.1 activators have been identified that fit neither type 1 nor type 2 categories. For example, mallotoxin and KB130015 (a derivative of amiodarone) do not affect inactivation but promote channel opening by accelerating the kinetics of activation and shifting the voltage dependence of activation in the hyperpolarizing direction (207, 709). As yet their site of interaction with Kv11.1 channels is unclear, but it is known that the effects of these two drugs are synergistic, suggesting that they occupy separate but functionally coupled binding sites (207, 709). Similar effects on activation are observed with some class III antiarrhythmics (Almokalent, azimilde, nifekalent), although only after a strong depolarizing prepulse (85, 272, 293). In this case "facilitation" of Kv11.1 current is only observed at potentials less than −30 mV due to the voltage-dependent block that concomitantly occurs at more positive potentials. Facilitators are considered distinct from activators like mallotoxin and KB130015 due to the prerequisite depolarizing prepulse (85, 272, 293).

VI. REGULATION OF Kv11.1 CHANNELS

There are dozens of reports in the literature looking at regulation of Kv11.1/I_{Kr} by pathological stimuli such as oxi-

dative stress, acidosis, and altered electrolytes as well as acute and chronic stimulation of signaling pathways. There are many disparate and, in some cases contradictory, findings in these studies. Rather than critiquing each study one by one, discussion of these studies is focused on what will happen to cardiac I_{Kr} activity during *1*) acute adrenergic regulation (such as occurs during exercise), *2*) acute ischemia (oxidative stress, acidosis, hyperkalaemia), and *3*) heart failure (chronic stimulation of multiple signaling pathways). Studies that have specifically focused on regulation of Kv11.1/I_{Kr} in noncardiac tissue are covered in section X. In the last section some miscellaneous regulatory pathways including the effects of lipid messengers, temperature, and steroid hormones are reviewed.

A. Adrenergic Tone and Circulating Catecholamines

Exercise is the prototypic example of the fight-or-flight response resulting from activation of the sympathetic nervous system. During exercise, in addition to circulating catecholamines, there is a significant release of catecholamines from local sympathetic nerve terminals (121) which activate adrenergic receptors resulting in activation of adenylate cyclases, increases in cAMP, and activation of PKA. The increase in intracellular cAMP stimulates HCN channels directly resulting in an enhanced rate of diastolic depolarization and hence increased heart rate in sinoatrial node cells (144). The increased PKA activity also results in phosphorylation of numerous proteins involved in calcium handling, including plasma membrane L-type calcium channels and ryanodine receptors, resulting in enhanced calcium cycling and hence contractility of the myocardium (*555*).

During exercise, the increase in heart rate demands that repolarization duration shortens so that there is still a sufficient diastolic interval for the heart to refill with blood before the next contraction. To a large extent, this is achieved by enhanced activity of I_{Ks}. I_{Ks} has a very strong adrenergic response (624, 657) and represents one of the best examples of a well-characterized macromolecular complex governing phosphorylation (398, 625). In addition to contributing directly to shortening of APD, the enhanced I_{Ks} is also sufficient to counteract the enhanced I_{Ca} activity, which contributes to increased contractility but also tends to lengthen the APD.

β-Adrenergic and/or PKA stimulation of isolated guinea pig ventricular myocytes has been reported to cause no change in I_{Kr} activity (*549*), a decrease (72% reduction in tail current amplitude after 12 min application of isoproterenol; Ref. 316), or a small increase that was dependent on a rise in intracellular Ca^{2+} and activation of PKC (251). Given that these three studies were undertaken in guinea pig ventricular myocytes, one cannot evoke species differences as a possible explanation. There were, however, slight differences in protocols used, such as differences in the level of calcium buffering in the patch pipette. The studies are also complicated by difficulties in completely isolating the I_{Ks} and I_{Kr} components, which is problematic given that I_{Ks} is very sensitive to activation by both PKA and PKC (657). Additionally, guinea pig myocytes contain a robust cAMP-activated chloride current (46, 247) that can complicate analyses. More recently, Harmati et al. (246) have provided evidence for β-adrenergic/PKA-mediated stimulation of I_{Kr} in canine ventricular myocytes. Whereas 100 nM isoprenaline caused a 293% increase in I_{Ks}, it caused only 37% increase in I_{Kr}. Thus, based on studies in isolated myocytes, it appears that I_{Kr} can be modulated by PKA, although there may be some species variation. Perhaps more importantly though, the modulation of I_{Kr} by PKA is relatively modest, and it is certainly not as important as changes in I_{Ks} for shortening APD during exercise.

To overcome some of the problems of overlapping currents and inadequacy of pharmacological tools for separating different channel activities, a number of groups have investigated the effects of PKA on Kv11.1 channels (±the putative β-subunit, KCNE2) in heterologous expression systems. When expressed in *Xenopus* oocytes, Kv11.1 currents are modestly reduced following activation of PKA by the PDE IV inhibitor Ro-20–1724 (100 μM) or forskolin (400 μM), and this is associated with ~10 mV depolarizing shift in the $V_{0.5}$ of steady-state activation (632). These effects were largely abrogated by mutation to alanine of all four of the putative PKA phosphorylation sites (Ser283, Ser890, Thr895, and Ser1137). Similarly, Cui et al. (130) showed that Kv11.1 channels expressed in CHO cells are modestly inhibited by PKA activation, while cAMP could have a direct stimulatory effect, presumably via binding to the cAMP-binding domain of the channels. The overall effect of this inhibition caused by phosphorylation and cAMP-mediated activation is a small decrease in current amplitude (130). Conversely, when Kv11.1 channels are coexpressed with either KCNE1 or KCNE2, the overall effect of adrenergic stimulation was an overall increase in current amplitude (129). A further complicating factor is that whilst Cui et al. were clearly able to show that cAMP bound to Kv11.1 channels, the affinity was as high as 40 μM. A similar value of ≥50 μM was reported by Brelidze et al. (76). These values, 40–50 μM, are more than an order of magnitude greater than the concentrations of cAMP determined in cardiac myocytes (280). The low affinity for cAMP has been attributed to the lack of a critical arginine residue in the cAMP binding pocket that coordinates binding of the phosphate moiety (76). Whilst it is possible that there may be compartmentalization of cAMP production (114), it is difficult to imagine that one could get local concentrations of cAMP exceeding a few micromolar. More recently, the Zagotta group has determined the crystal structure of the cyclic nucleotide binding homology domain (cNBHD) of the zebrafish ether-a-go-go like (zELK) channel and found that the "cAMP binding pocket" was occupied by a short β-sheet strand at the COOH-terminal end of the domain,

which they suggested acted as an endogenous ligand for the channel (75).

In recent years there has been increasing awareness that ion channels do not function in isolation but rather exist as part of macromolecular complexes. One of the best-studied examples of this is the KCNQ1 channel, which forms a complex with A-kinase adaptor proteins, PKA, and phosphatases (625). The net effect is that signaling process can be effectively localized to specific regions in the cell and is not dependent on diffusion of second messengers and/or effector proteins across significant distances. Another corollary of this arrangement is that the local concentration of signaling molecules such as cAMP may be much higher in the vicinity of the effector protein than in the general cytoplasm (363). Although not as extensively investigated as I_{Ks}, there is evidence to suggest that components of PKA signaling complexes are attached to hERG proteins. McDonald and co-workers (309) have shown that the 14–3-3 protein can bind to hERG but only if Ser283 and Ser1137 have been phosphorylated (104). Binding of 14–3-3 results in a hyperpolarizing shift in $V_{0.5}$ of steady-state activation (thus counteracting the effect of PKA alone) and prolongs the effect of PKA stimulation. More recently, McDonald and co-workers (370) have also shown that hERG proteins in porcine cardiac membranes cosediment with a range of PKA RI and RII domains, although they have not been able to confirm these interactions by coimunoprecipitation; thus any interactions may require additional partners (370).

Another complicating factor when considering acute regulation of Kv11.1 by PKA is that the common polymorphism (L897T, minor allele frequency ~23%) results in introduction of an additional PKA consensus phosphorylation site. Numerous groups have investigated the effect of the K897T polymorphism on gating, with reports of very modest loss (22, 468) or gain of function (66). Similarly, in clinical studies, the K897T polymorphism has been associated with slight lengthening of the QT interval (496), shortening of QT interval (397, 444, 493), or no statistically significant change (510). The larger studies suggest a 1–3 ms shortening for each copy of the Thr allele (397, 444, 493). This suggests that the Thr allele may result in a slightly enhanced I_{Kr}. Recently, Gentile et al. (204) have shown that Thr897 is phosphorylated following PKA stimulation, resulting in reduced channel activity. If the overall effect of K897T is to increase I_{Kr} function when nonphosphorylated, but decrease it when phosphorylated, then the population studies (397, 444, 493) suggest that under the conditions in which they made their ECG measurements, the increased activity of the nonphosphorylated K897T is relatively more important than the reduced activity of the phosphorylated K897T.

From the studies in heterologous expression systems, one can conclude that it is possible for Kv11.1 channel activity to be influenced by PKA. However, whether such modulation occurs in native cells is still not known for certain. To help resolve these issues, more needs to be known about the macromolecular complexes hERG proteins are part of in native cells and whether the level of adrenergic activation that occurs in vivo is sufficient to modulate Kv11.1 activity within the context of its native macromolecular environment. Irrespective of whether the overall effect under in vivo conditions is a small increase, small decrease, or no change, what is certain is that the relative balance between I_{Kr} and I_{Ks} is very different, with I_{Ks} being the major repolarizing current during exercise, whereas I_{Kr} is much more important at rest.

Another possible interaction between adrenergic stimulation of the heart and I_{Kr} function is that ERG proteins are expressed in rat chromaffin cells and blockade of I_{Kr} in these cells leads to enhanced epinephrine (but not norepinephrine) release (225).

B. The Alarm Clock Stimulus

One of the arguments used to support the hypothesis that I_{Kr} is regulated by acute sympathetic nerve stimulation is that patients with LQTS type 2 are particularly prone to arrhythmias triggered by loud noises, such as being awoken from sleep by an alarm clock (684). There is no doubt that unexpected auditory stimuli are associated with activation of the sympathetic nervous system and that this leads to an acute increase in heart rate (433). However, it is important to bear in mind that following sympathetic stimulation the increase in heart rate occurs relatively rapidly (as it only requires production of cAMP which binds directly to HCN channels), whereas there is a significant lag between activation of HCN channels and activation of channels that require phosphorylation (363). More recently, Liu et al. (376) have also shown that there is a significantly longer lag in the increase in I_{Ks} compared with I_{Ca} following adrenergic stimulation in rabbit cardiac myocytes. Thus, in the first 5–10 s after an alarm clock going off, one would expect to see significant changes in heart rate but minimal changes in APD. This is indeed what is observed. However, after correcting for the change in heart rate, there is up to a 20% prolongation of the corrected QT interval (QT_c) in the 5–10 s after an alarm clock goes off (433).[2] This time frame is important, as in cases where arrhythmias have been recorded on Holter monitors following an alarm clock going off, the arrhythmia is initiated within 5–10 s (684). At rest, one would expect there to be minimal sympathetic tone such that I_{Ks} would make a minimal contribution to repolarization. Conversely, I_{Kr} is relatively more important for

[2]As heart rate increases, the absolute QT interval necessarily shortens. To enable comparison of QT intervals at different heart rates, a corrected QT interval is calculated. The most popular correction formulas are Bazett's formula: $QT_c = QT/\sqrt{RR}$, and Fridericia's formula: $QT_c = QT/\sqrt[3]{RR}$, where RR is the interval between successive R-waves (134).

repolarization at slower heart rates, so one would expect that an alarm clock might cause an exaggerated QT_c prolongation in patients with LQTS type 2 but not in LQTS type1 (i.e., LQTS caused by loss of I_{Ks} function). Clearly sympathetic stimulation is an important component of the stimulus, such that β-blockers would still be useful therapy (211); however, this need not be because there is direct modulation of I_{Kr} by sympathetic nerve stimulation.

Overall, the accumulated data in the literature suggest that if I_{Kr} is modulated by sympathetic nerve activity it is only modestly so (perhaps a maximum ~30% change in current magnitude), compared with the effects observed for I_{Ks} (246). Furthermore, the sensitivity of patients with LQTS type 2 to arrhythmias triggered by adrenergic stress does not necessarily support a direct role of regulation of I_{Kr} by adrenergic activity. Rather, there are multiple mechanisms, via actions on other channels, by which adrenergic stress can trigger arrhythmias in patients with LQTS type 2. For example, simple prolongation of the action potential and increased duration of SR Ca^{2+} release coupled with the sensitivity of Ca^{2+} release channels to adrenergic stress (360, 507) could increase risk of arrhythmias in patients with LQTS type 2.

C. Myocardial Ischemia

Acute ischemia, with or without reperfusion, is associated with many metabolic changes that result in altered electrical activity and in increased risk of arrhythmia. Many of these metabolic changes can influence I_{Kr} activity, which consequently increases arrhythmia risk.

1. Oxidative stress

Generation of reactive oxygen species (ROS) using hydrogen peroxide (62) results in an acceleration in rates of both activation and deactivation, with the changes in activation occurring more quickly than the changes in deactivation. Xanthine plus xanthine oxidase (662), hyperglycemia (723), TNF-α (662), and ceramide (47) have all been reported to increase ROS and decrease Kv11.1 channel activity. In contrast to these studies, Tagliatela et al. (612) showed that extracellular application of $FeSO_4$ and ascorbic acid caused an increase in ROS in oocytes but resulted in increased Kv11.1 activity secondary to reduced inactivation. Yet, in guinea pig ventricular myocytes, hypoxia has been reported to have no effect on I_{Kr} activity (270). Given the multitude of stimuli that have been used, it is perhaps not surprising that the observed effects vary between studies. Whilst generation of ROS may be common to each study, it is quite likely that other factors that differ between stimuli come into play as well. For example, Ganapathi et al. (196) recently showed that the effects of ceramide were in part mediated by translocation of Kv11.1 channels into lipid rafts, and this is presumably unrelated to any observed effects on ROS generation. In addition to differences in the acute effects of ROS generation, prolonged (i.e., order of many hours) generation of ROS can also affect Kv11.1/I_{Kr} activity. The chronic effect is likely to be a result of reductions in the level of fully mature hERG protein reaching the plasma membrane. In the case of TNF-α, there was no decrease in total protein, which suggests that the defect may be at the level of trafficking rather than synthesis. Overall, these studies suggest that large increases in ROS are likely to have multiple effects on Kv11.1/I_{Kr} kinetics, and prolonged exposure to ROS will lead to reduced Kv11.1 current density. Oxidative stress is known to induce early afterdepolarizations (EADs) and triggered activity, likely mediated by effects on multiple ion channels but in particular through impaired inactivation of Na^+ current (i.e., enhanced late sodium current) (305, 541). Kv11.1 channels are believed to play a significant role in suppressing EADs (390); therefore, any reduction in Kv11.1 current by oxidative stress will exacerbate the propensity for EADs.

The molecular basis of the effects of ROS on Kv11.1/I_{Kr} has not been completely elucidated. Pannaccione et al. (469) showed that modulation of inactivation, following extracellular application of $FeSO_4$ and ascorbate, requires two histidine residues in the extracellular S5P linker (His578 and His587). This mechanism, however, does not account for the reduced current density seen with production of intracellular ROS (331). Conversely, Kolbe et al. (331) showed that cysteine residues in the cytoplasmic COOH-terminal domain of Kv11.1, in particular Cys723 in the COOH-linker domain, play a role in the acute regulation of Kv11.1 currents by intracellular ROS. Cysteine residues are commonly associated with responses to oxidative stress as they can react with glutathione to form glutathionylated adducts or react with other cysteine residues to form disulfide bonds. The reactivity of thionyl side chains is promoted by having neighboring basic residues (650), which lower the pK_a of the thionyl group. Cys723, however, is surrounded by a triad of acidic residues (Glu722, Asp727, and Asp767 from a neighboring subunit); thus it is unlikely that Cys723 would be directly modulated by oxidative stress.

Oxidative stress is also a major component of the diabetic heart. Acute hyperglycemia has been shown to reduce Kv11.1/I_{Kr} function (723) and prolonged hyperglycemia to reduce Kv11.1/I_{Kr} density (726). Furthermore, insulin has been shown to reduce some of these effects, and thus it has been postulated that ROS regulation of Kv11.1/I_{Kr} function may be an important component of the electrical remodeling that occurs in diabetic hearts and makes them more susceptible to arrhythmias in the context of ischemic heart disease (303).

2. Acidosis

Kv11.1 currents, whether expressed in mammalian cells or oocytes, are reduced by extracellular acidosis (26, 154, 262,

294), whereas selective alteration of intracellular pH does not affect gating (154). Although there are subtle differences between studies, all have reported an acceleration of the rate of deactivation (262, 294). A range of other effects have also been reported including suppression of G_{max} (26, 64, 262), slowing of activation (26, 623, 730), a depolarizing shift in steady-state activation (26, 64, 262), and a modest increase in rate of recovery from inactivation (294). Multiple groups have also reported that the changes in deactivation and suppression of G_{max} had different pH sensitivities (26, 64, 262), and this likely explains some of the discrepancies between studies in which different pH ranges were used. Nevertheless, the overall effect is to cause a reduction of the amount of I_{Kr} that will flow during the action potential (152), which contributes to the action potential prolongation observed during acidosis (63).

The observation that intracellular acidosis does not affect Kv11.1 gating is consistent with the suggestion that extracellular acidosis alters Kv11.1 gating by modifying extracellular residues (294). The pK_a for changes to the rate of deactivation, ~6.2 (294), and modification of the voltage-independent step in activation, ~6.4 (730), are similar to the pK_a of histidine. However, when the two extracellular histidines in Kv11.1 (His578, His587) are mutated to glutamate, the extracellular pH effects on deactivation remained (294). It should be noted though that the pK_a of amino acid side chains in proteins can be very different to those measured in free solution, e.g., the active site aspartate in *Escherichia coli* thioredoxin is buried in a hydrophobic environment and has a pK_a of 7.5 (350). It is possible that charged residues within the transmembrane region of Kv11.1 could have pK values closer to 6.5. Consistent with this, Tseng and co-workers (377) showed that mutating aspartate residues in the S1 (Asp411), S2 (Asp460, Asp466), or S3 (Asp501, Asp509) of Kv11.1 largely abrogated the effects of extracellular pH on accelerated deactivation (377). Two recent voltage-clamp fluorometry studies (165, 648), showing that extracellular acidosis slows voltage sensor return during deactivation, are also consistent with the primary site of action of extracellular protons being within the voltage sensor.

3. Hyperkalemia

I_{Kr}/Kv11.1 activity is very sensitive to changes in extracellular K^+ (547), primarily due to effects on inactivation (658, 668, 670). In contrast, hyperkalemia does not affect rates of activation nor steady-state activation (668, 670). Increasing extracellular K^+ from 5 to 100 mM increases the single-channel conductance [~10–12 pS in symmertrical high K^+ (324, 738) compared with 1–2 pS at physiological K^+ (256, 738)]. There are relatively few studies that have examined the effect of changes in K^+ within the physiologically relevant range. Wang et al. (658) showed that changes in extracellular K^+ between 2 and 10 mM caused dramatic changes in rates of inactivation but minimal changes in rates of recovery from inactivation, with a consequent modest shift in steady-state inactivation. Overall, mild hyperkalemia will lead to an increase in Kv11.1 current flow during the cardiac action potential, and this would counteract the reduced current flow caused by acidosis and oxidative stress.

4. Summary

During myocardial ischemia, accumulation of extracellular K^+ will result in an increase in I_{Kr} that would likely counteract any decrease caused by extracellular acidosis and oxidative stress. It is also worth noting that the accumulation of extracellular K^+ occurring during myocardial ischemia is predominantly the result of activation of K_{ATP} channels (198), and the magnitude of these fluxes would overwhelm any changes in Kv11.1/I_{Kr} activity. Conversely, during reperfusion, changes in extracellular K^+ and acidosis are rapidly corrected, whereas oxidative stress will be exacerbated by the reintroduction of oxygen. Thus, during early reperfusion, there is likely to be a suppression of I_{Kr}.

That I_{Kr} still makes significant contributions to cardiac repolarization during ischemia is confirmed by findings using guinea pig ventricular muscle strips showing that low doses of dofetilide (5 nM) can prevent APD shortening during early ischemia (534). Conversely, dofetilide, at doses ranging from 5 to 50 nM, did not alter the incidence of reperfusion-induced arrhythmias (534). These results suggest that either reduced I_{Kr} contributes to reperfusion-induced arrhythmias (and therefore reducing it further does not prevent them) or that the magnitude of I_{Kr} during reperfusion is insufficient to modulate the occurrence of reperfusion-induced arrhythmias. In a more recent study, Gerard et al. (157) found that when extracellular K^+ was increased during simulated ischemia (and reperfusion), a low dose of dofetilide caused significant action potential prolongation and, either had a neutral or protective effect against reperfusion-induced arrhythmias. This later study indicates that the effects of hyperkalemia can have a significant impact on I_{Kr} function, although one should probably be cautious in extrapolating the results from the in vitro model used by Gerard et al. to the clinical environment where ischemic insults are likely to be much more heterogeneous than in well-controlled in vitro models.

D. Heart Failure

Heart failure is associated with activation of numerous signaling pathways (48). Many groups have investigated the effects of stimulating these pathways on Kv11.1 channels (see sect. III). Almost invariably these studies have focused on the effects of acute stimulation. In general, acute stimulation has resulted in reduced Kv11.1 function (see sect. III*E*) with the exception being the PIP_2/PIP_3 pathway that can significantly upregulate Kv11.1 function (see below).

More recently, the McDonald group has started to look into the effects of chronic (24 h) stimulation. Interestingly, both chronic β-adrenergic (activating PKA) and α-adrenergic stimulation (activating PKC/PLC/PKA) resulted in significantly increased levels of hERG protein at the plasma membrane (96, 98). These changes are primarily mediated by an increase in the rate of synthesis of protein with no change in the rate of degradation of channels. In the case of β-adrenergic stimulation, the increased protein synthesis could be prevented by transfection of cells with a protein kinase A inhibitory (PKI) peptide. Furthermore, when the PKI peptide was targeted to the mitochondrial outer membrane, it was ineffective but, when it was targeted to the ER membrane it was effective and completely suppressed the enhanced protein synthesis in both HEK cells and neonatal rat ventricular myocytes (590).

In the two studies to date that have looked at KCNH2 mRNA expression in human heart failure samples, no change in mRNA levels was found (221, 307). This does not, however, preclude the possibility that there are changes in the level of hERG protein or Kv11.1 current density. In a rat model of cardiac hypertrophy, which is a precursor to heart failure, it has been reported that KCNH2 mRNA and protein levels are decreased (277). This is not necessarily incompatible with the data from McDonald et al. showing that chronic (24 h) neurohormonal stimulation of myocytes leads to increased hERG protein synthesis, as in heart failure chronic stimulation usually leads to downregulation of signaling pathways (348). Indeed, it is thought that one of the benefits of β-adrenergic blockers in heart failure is to reverse the downregulation of the intracellular signaling pathways induced by chronic stimulation.

Patients with heart failure are prone to develop hypokalemia, both as a result of the activation of neurohormonal pathways that regulate renal K^+ handling and as a consequence of diuretic therapy. Hypokalemia in the setting of heart failure is known to increase mortality (362). Indeed, Leier et al. (362) have suggested that "effective potassium management with properly targeted serum potassium concentrations . . . probably represents the most effective and safe antiarrhythmic intervention" in heart failure. Recently, Zhang et al. have shown that hypokalemia is a potent stimulus for proteasomal degradation of hERG protein, and this contributes to the prolongation of APD seen in hypokalemia (see sect. III*F*). It is important to note that the changes seen in cultured cells after 24 h were much more dramatic than those seen in vivo. Nevertheless, rabbits treated with a low K^+ diet for 4 wk (sufficient to reduce K^+ from 4.88 to 2.4 mM) resulted in a marked reduction of fully glycosylated hERG protein and an ~30% prolongation of QT interval, clearly sufficient to markedly increase the risk of lethal arrhythmias (227).

E. Miscellaneous Regulation of I_{Kr} Function

1. Temperature

The cardiac action potential is very sensitive to changes in temperature, with the duration at 95% repolarization approximately doubling as temperature is dropped from ~34 to ~24°C (329). This can be largely explained by the observation that repolarizing K^+ currents during the action potential are more sensitive to changes in temperature than the depolarizing current through L-type calcium channels (329). Noble et al. noted that I_K was particularly sensitive to temperature with a Q_{10} value of 4.4, i.e., its magnitude changed 4.4-fold for every 10°C change in temperature. This large temperature sensitivity was confirmed for Kv11.1 channels heterologously expressed in CHO cells (649). The origin of the very high temperature sensitivity for Kv11.1 current magnitudes measured during depolarizing pulses (see **FIGURE 23**) can be primarily attributed to the opposing effects of temperature on steady-state activation and inactivation. As temperature increases, the $V_{0.5}$ for activation shifts to more negative potentials (i.e., it is activated more easily), whereas the $V_{0.5}$ for inactivation shifts to more positive potentials. As a consequence, there is a very large in-

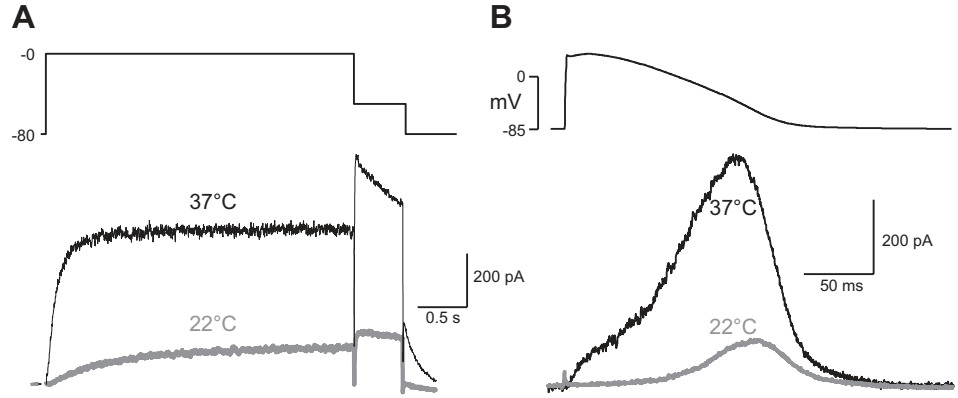

FIGURE 23. Temperature dependence of Kv11.1 current magnitude. Currents recorded from CHO cell expressing Kv11.1 at 22 and 37°C in response to square pulse voltage waveform (*A*) and AP waveform (*B*). [From Vandenberg et al. (649).]

crease in the range of potentials where the channels are open, i.e., the so-called window current (649). This result has two important implications. First, it suggests that patients with loss of I_{Kr} caused by mutations or drug-block may be particularly prone to arrhythmias when they have high fevers (17, 228). Second, when constructing kinetic models of Kv11.1 based on gating parameters derived from recordings at room temperature, it is inadvisable to use a single temperature correction factor to obtain predicted outputs at 37°C.

2. Sex hormones

Adult females have longer QT_c (288, 514, 724) and are at higher risk for developing life-threatening torsades de pointes ventricular arrhythmias, especially after taking medications that block Kv11.1 channels (394). Recent epidemiological studies indicate that QT_c in men is significantly correlated with testosterone levels (724). Such studies do not, however, provide insight into the molecular mechanism. Animal models provide strong evidence for male sex hormones causing an increase in I_{Kr} and a shorter QT interval (189, 381, 688). In rabbits, the increase in I_{Kr} was not associated with any changes in KCNH2 mRNA (381); rather, dihydrotestosterone causes an increase in rabERG protein stability at the plasma membrane which is likely to involve an ERK1/2-dependent mechanism (688). Female sex hormones do not appear to have significant effects on Kv11.1/I_{Kr} levels (189), although progesterone increases basal I_{Ks} activity and this may contribute to the variation in QT interval during the menstrual cycle (438). The Koren group have also shown that in the Rabbit LQTS2 model, progesterone reduces the incidence of arrhythmias whilst estrogen increases the risk of arrhythmias, although these effects are likely mediated by changes in calcium current density (456).

Recently, it has been shown that β-estradiol can inhibit Kv11.1 channels expressed in HEK293 cells (20). If this were to occur in native cells, then it may contribute to the greater sensitivity of women to drug-induced arrhythmias. On the other hand, Shuba et al. (576) have shown that testosterone can reduce the sensitivity of Kv11.1 channels to drug block. Overall, these studies suggest that it may be a combination of females being slightly more susceptible and males slightly less susceptible that leads to the marked gender divide with respect to susceptibility to drug-induced arrhythmias.

3. Lipid second messengers

Phosphatidylinositol 4,5-bisphosphate (PIP_2) is a minor component of the plasma membrane but serves many important functions. It is the substrate of phospholipase C (PLC), leading to the production of IP_3 and DAG, two important second messengers. PIP_2 also directly modulates the function of many proteins and a number of ion channels (for recent review, see Ref. 605) including Kv11.1 (71). In most cases, as a result of activation of PLC, depletion of PIP_2 acts on the target ion channels in concert with PI3 kinase and PKC (which are activated in response to IP_3 and DAG, respectively) to exhibit synergistic effects. Elevation of PIP_2 results in an increase in current amplitude, as well as enhancing the rate of activation and decreasing the rate of inactivation of Kv11.1 channels (69). Bian et al. (69) also showed that exposing Kv11.1 channels in excised inside-out patches to PIP_2 largely abrogated channel run down, a phenomenon that has dogged attempts to study Kv11.1 channels in this configuration. The effect of PIP_2 is independent of Ca^{2+} and PKC and is thought to involve a cluster of basic amino acid residues just distal to the cNBD domain in the COOH terminus of Kv11.1 (70).

Kv11.1 is localized in cholesterol- and sphingolipid-enriched membrane microdomains of cardiomyocytes (49). Depletion of membrane cholesterol causes a positive shift in the voltage dependence of activation and an acceleration of the rate of deactivation (49). These effects are opposite to that observed with PIP_2, and it has been suggested that increasing cholesterol may activate PLC resulting in reduced levels of PIP_2 (107). Probucol, a cholesterol-lowering agent, also reduces Kv11.1 activity in heterologous cell lines and native cardiomyocytes (226). Probucol also decreases cell membrane caveolin, a Kv11.1 interacting protein found in cholesterol- and sphingolipid-rich lipid rafts. Thus it has been suggested that the increased degradation of cell surface Kv11.1 channels in the presence of probucol may be related to altered cholesterol metabolism (226). An argument against this hypothesis, however, is that statins, which are very effective cholesterol-lowering drugs, result in shortening of QT intervals rather than a lengthening (654).

Ceramide, another minor component of phospholipid membranes, has been shown in some studies to modulate Kv11.1 kinetics (196). In contrast, other studies suggest that ceramide does not affect kinetics (47, 94), but prolonged exposure leads to increased degradation, although the specific mechanism of this decreased protein half-life is debated (47, 94, 196).

VII. Kv11.1 CHANNELS AND CONGENITAL LONG QT SYNDROME TYPE 2

A. Historical Perspective

"Wenigstens hatten die Aeltern des Kindes, nachdem ihnen möglichst schonend das unglückliche Lebensende ihrer Tochter mitgetheilt worden war sich gar nicht darüber gewundert sondern geradezu geantwortet dass diese Nachricht sie durchaus nicht befremdet habe, da schon einige solche Zufälle in ihrer Familie früher vorgekommen seien ein Kind war nehmlich nach einem heftigen Schreck, ein

zweites nach heftigem Zorn splötzlich todt niedergefallen" (410).

The parents of the child were given the unfortunate news of the death of their daughter, but they were not surprised, as this had happened twice before in their family: one child had died suddenly during a sudden shock and another during a violent rage.

Writing in 1856 on the education of the "deaf-mute," Friedrich Ludwig Meissner recounted the case of a young girl who died suddenly during an emotional upset. His short account, including details of the untimely deaths of her brothers, captured key features of our current understanding of the congenital LQTS: its genetic basis; an association, in some cases, with deafness; its lethality; and symptoms during times of acute emotion (410). However, 100 years passed before a synthesized description of the condition was made.

Anton Jervell and Fred Lange-Nielsen reported, in 1957, the "combination of deaf-mutism and a peculiar heart disease" in three girls and a boy among six children of a family (290). Each suffered congenital deafness and fainting spells in association with prolongation of the QT interval on the electrocardiogram. Three of the four died before the age of 10. The appellation, Jervell Lange-Nielsen was attached to this evidently autosomal recessive disorder. A short time after, Romano (1963) (529) and Ward (1964) (677) described a syndrome characterized by a long QT interval and episodes of syncope or sudden cardiac death. However, in such families, the mode of inheritance was autosomal dominant, and no child suffered from a hearing deficit. It is now understood that the Romano-Ward form of congenital LQTS is considerably more common than the Jervell Lange-Nielsen form.

While QT prolongation was a necessary component for diagnosis of the condition, the underlying cardiac arrhythmia responsible for syncope and sudden death was not recorded. Dessertenne, in 1966, published the case of an 80-year-old woman presenting with complete atrioventricular block, prolongation of the QT interval, and a unique form of polymorphic ventricular tachycardia that appeared to twist around the isoelectric line, "torsades de pointes" (TdP) (141). His complete and careful analysis ensured the survival of this eloquent description. A few years later, this arrhythmia was shown to be the cause of symptoms in congenital LQTS (429).

A landmark in LQTS research occurred in 1979 with the establishment of the LQTS registry (427). It provided the first long-term, prospective follow-up of families with well-defined clinical phenotypes. It has also enabled molecular discoveries made in subsequent years to be understood immediately in their clinical context, and strong genotype-phenotype relationships established in short time. The first genetic locus for congenital LQTS was identified on chromosome 11 in 1991 by the Keating group (318), and they suggested that the affected gene was the Harvey ras-1 gene, although this was later shown to be incorrect (see below). Later in 1991, the Keating group identified a further six families with linkage to the same locus on chromosome 11 and suggested that the syndrome may be genetically homogeneous. However, in 1994, a LQTS family with linkage to chromosome 7 (LQTS type 2) and another with linkage to chromosome 3 (LQTS type 3) were identified (292), confirming the genetic heterogeneity of the syndrome. In the short space of a year, the three genes responsible for >90% of congenital LQTS were identified: *KCNH2*, the cause of LQTS type 2 (131); *SCN5A*, the cause of LQTS type 3 (667); and *KCNQ1* (not the previously suspected Harvey ras-1 gene, which is located in a very similar region of chromosome 11), the cause of LQTS type 1 (666).

Douglas Zipes (737) had remarked that just as Wolf-Parkinson-White was the Rosetta Stone of reentrant arrhythmia, LQTS might be the Rosetta Stone of ventricular tacchyarrhythmias dependent on sympathetic simulation. This prediction has very much proved to be correct; molecular insights into LQTS have become the paradigm for understanding the normal processes that underscore repolarization in the heart and which, in their dysfunction, predispose to sudden cardiac death in a host of common cardiac diseases (396).

Mutations in *KCNH2* account for ~40% of cases of genetically confirmed congenital LQTS. As will be described, the risk for sudden cardiac death, the efficacy of therapy, the triggers for symptomatic episodes, the ECG appearance, and the phenotypic response to exercise are individual to this genotype.

B. Loss of Function Mutations in hERG

From the discussion of the crucial role of Kv11.1 channels in cardiac repolarization (see sect. II*D*), it is easy to understand how mutations that reduce Kv11.1 channel function may have a harmful effect on cardiac electrical activity. Over 459 putative disease-causing mutations in *KCNH2* have been identified (http://www.fsm.it/cardmoc/; Ref. 315; see **FIGURE 24**). However, very few of these have been characterized at an in vitro level, and it is quite possible that at least some of these putative mutations may not be the cause of disease. The magnitude of current (I) passing through a given ion channel type is determined by four parameters:

$$I = N \cdot \gamma \cdot P_o \cdot V \qquad (6)$$

Where N is the total number of channels on the membrane, γ is the single-channel conductance, P_o is the open probability, and V is the transmembrane voltage. Theoretically then, mutations in *KCNH2* may result in a loss of function

by four mechanisms: *1*) reduced or defective protein synthesis ($\downarrow N$ in *Eq. 1*), *2*) defective trafficking ($\downarrow N$), *3*) defective channel gating ($\downarrow P_o$), and *4*) reduced ion permeation ($\downarrow \gamma$) (139).

1. Reduced synthesis

Around 25% of *KCNH2* mutations (http://www.fsm.it/cardmoc/) result in premature stop codons (see **FIGURE 24**). A relative absence of truncated protein in the cell is likely the result of nonsense-mediated mRNA decay (344) (see sect. III*B*). Truncated KCNH2 transcripts resulting in mutations R1014X and W1001X have been shown to undergo nonsense mediated decay (218), and it is reasonable to assume that this will also apply to the vast majority of other mutants that result in premature stop codons.

2. Defective trafficking

In the most comprehensive survey of mutants to date, Anderson et al. (19) showed that 28 of 34 missense mutants (i.e., ~80% of the mutants studied) result in a hERG trafficking defect. For hERG trafficking mutants there are examples that exert a dominant negative suppression of wild-type channels (19, 181, 310) and others that appear to cause haploinsufficiency (192). Lastly, it should also be noted that numerous proteins, including chaperones, are involved in the trafficking of hERG (176, 655) (see sect. IIIC). To date, no mutations in chaperone proteins have been associated with congenital LQTS; however, this is likely to be because most chaperones assist with the trafficking of multiple proteins, so any defects in the chaperones would be expected to have multiple defects and quite likely a severe phenotype.

3. Abnormal gating

Abnormal gating can lead to reduced Kv11.1 current by one of two mechanisms: reduced activation (i.e., slower activation kinetics/accelerated deactivation kinetics, or shift in the voltage dependence of activation to more depolarized voltages) (61, 99, 545) or enhanced inactivation (435, 552, 728). Many mutations affect the gating of Kv11.1 channels when assayed in *Xenopus* oocytes (545). However, as *Xenopus* oocytes are incubated at low temperatures (typically ~17°C), mutant proteins that would be misfolded and consequently degraded in mammalian systems maintained at 37°C will often reach the cell membrane. This problem is

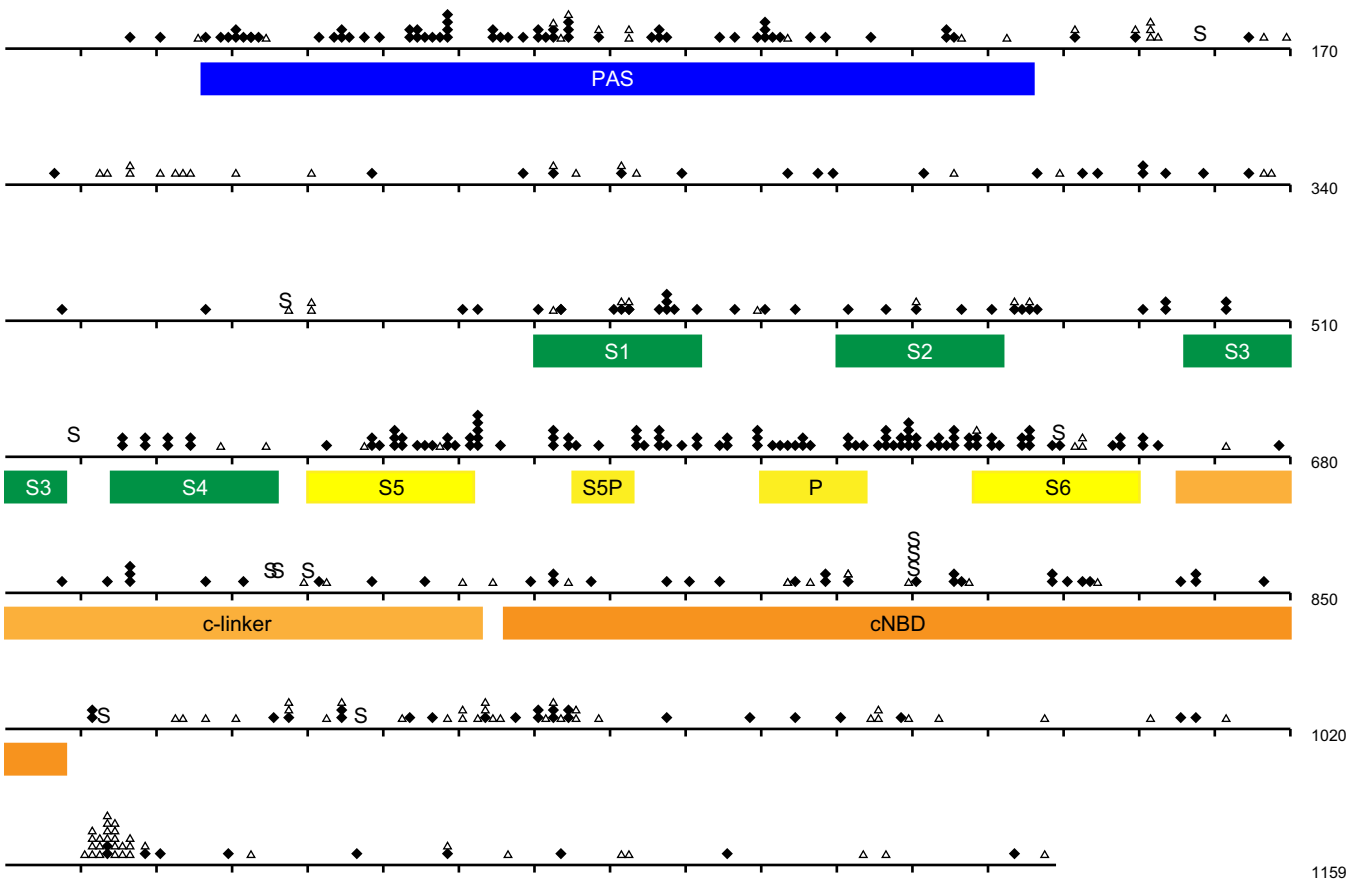

FIGURE 24. Location of LQTS type 2 mutations. Missense mutations (closed diamonds), nonsense mutations (includes deletion/insertion/frameshift; open diamonds), and splice site mutations (S). Note the high incidence of mutations in the PAS domain and pore domain regions.

most clearly exemplified by the study of the R534C mutant Kv11.1 channel. When expressed in *Xenopus* oocytes, the mutation results in an increased open probability, i.e., a gain of function, yet clinically the mutant causes loss of function (434). Subsequently, it was shown that the R534C mutant when expressed in mammalian cells is retained in the ER, explaining the clinical loss of function (19). The most important implication of these results is that it is essential when characterizing mutant channels to perform assays in mammalian cells. This is not trivial as studying ion channels in mammalian systems has a much lower throughput than studies in *Xenopus* oocytes. Nevertheless, a number of mutations that result in gating defects have been characterized in mammalian cells (61, 552, 728). The Berecki study of the R56Q mutant is especially noteworthy for the use of the dynamic action potential clamp technique that is a particularly elegant means of characterizing the effect mutant channels will have on the cardiac action potential.

4. Abnormal conduction

Mutations in proximity to the selectivity filter of Kv11.1 may result in altered ion selectivity and/or altered single-channel conductance (521). In 2000, it was reported that the mutation N629D resulted in altered ionic selectivity and proposed that an inward current during terminal repolarization was the cause of prolonged repolarization in these patients (357). However, these studies were performed in *Xenopus* oocytes, and a subsequent study showed that the N629D mutation resulted in defective trafficking (19). More recently, it has been shown that the G628S mutant channel trafficks normally and gates normally, as assessed by voltage-clamp fluorometry (166), but does not conduct in normal physiological solutions. The channels can, however, pass Na^+ current when extracellular K^+ is removed, consistent with the channels adopting a partially collapsed selectivity filter that is incapable of supporting normal K^+ conduction.

C. Rescue of Trafficking Defective Mutant Channels

Many mutant Kv11.1 channels can give rise to channels with normal or near normal gating properties, if they reach the plasma membrane (192, 434). This has led to considerable interest in the possibility of developing pharmacological chaperones to rescue trafficking defective mutant channels (174, 317, 522), similar to what has been shown for trafficking defective CFTR channels (202). Broadly speaking there are three classes of compounds that can rescue misprocessed Kv11.1 channels. First, there are small molecules, such as glycerol and DMSO, that are thought to help stabilize correctly folded proteins, i.e., act as chemical chaperones, and have been shown to improve trafficking for multiple different proteins, including CFTR (553), aquaporin-2 (616), and Kv11.1 (734). Second, many Kv11.1 blockers including E-4031, astemizole, cisapride, terfenadine, and fexofenadine (180, 511, 734) can rescue trafficking by binding to the inner vestibule of the channel pore, i.e., the same site as drugs that block the channels (180). As such this would therefore not appear to be clinically useful as the rescued channels would be nonconducting (317). However, fexofenadine is an exception to this rule, in that it can rescue trafficking at a dose more than two orders of magnitude lower than the dose that causes channel block (180, 511, 734). The mechanism underlying this particular property of fexofenadine, however, remains to be determined. Third, there are a series of non-protein specific drugs such as the sarcoplasmic/ER Ca^{2+}-ATPase inhibitor thapsigargin that can improve trafficking of many types of mutant channels including Kv11.1 (138). To date there have been no whole animal or clinical studies to determine whether any of these drugs could be useful in vivo.

An interesting feature of the studies looking at pharmacological rescue of trafficking defective Kv11.1 channels is that the efficacy of different drugs to rescue mutant proteins appears to be domain specific. For example, pore-blocking drugs are more effective at rescuing channels with mutations in transmembrane domains, whereas thapsigargin does not rescue N470D but is effective at rescuing channels with mutations in the cNBD (180). More recent studies, however, suggest that these differences may not be quite as clear-cut, with both drugs showing more similarities than differences in terms of the mutant channels they can rescue (19). Nevertheless, the differences that do occur may well be telling us something about how different mutant channels fold as it is possible that different conformational states of the channel (e.g., open versus inactivated) are more stable than others, and this warrants further investigation.

D. Genotype-Phenotype Relationships in LQTS Type 2

The International Long-QT Syndrome Registry has been an important resource for investigating genotype-phenotype relationships in the three most common forms of the disorder (LQTS type 1 casued by mutations in KCNQ1, LQTS type 2 caused by mutations in KCNH2, and LQTS type 3 caused by mutations in SCN5a). There are some common features in all genotypes, for example, an early age of onset and a long baseline QT interval carry an increased risk of sudden cardiac arrest (SCA) irrespective of genotype (508). There are also many differences between genotypes.

Each LQTS subtype manifests an idiosyncratic T-wave morphology on the surface electrocardiogram (ECG).

These are as follows: LQTS type 1, low amplitude and broad; LQTS type 2, notched or bifid; LQTS type 3, late onset and peaked (428, 715) (see **FIGURE 6** above). A refined subdivision of these general descriptions into 10 "typical" T-wave appearances (4 for LQTS type 1, 4 for LQTS type 3, and 2 for LQTS type 3) is accurate for identifying genotype from T-wave morphology (715). An affected individual's ECG may not show a typical T-wave morphology; however, ECGs of affected family members often reveal a predominant, typical form. Furthermore, individuals with LQTS type 2 and normal T-waves at rest may develop the typical bifid or notched appearance during exercise (615). It is, at present, uncertain why reduced Kv11.1 function manifests with a bifid or notched T wave. An arterially perfused wedge preparation modeling LQTS type 2 has been advanced to explain the appearance based on an increase in transmural dispersion of repolarization with reduced Kv11.1 current (574). However, the whole animal applicability of such experiments is controversial (see Ref. 463 for discussion).

In LQTS type 2, standing from the supine position prolongs the QT interval despite tachycardia; in contrast, the QT interval shortens in LQTS type 1 (653). The QT_c in LQTS type 2 prolongs early in exercise, before falling to normal duration at peak exertion (686). Catecholamine and gating augmentation of I_{Ks} (578) at high heart rates is able to compensate for reduced Kv11.1 current, but is evidently delayed in onset. Kv11.1-mediated repolarization, then, is critical during sudden increases in heart rate and upon exercise inception. This insight informs our understanding of the common triggers for cardiac events in LQTS type 2: sudden sympathetic surge (loud noises/emotion), and exercise (see sect. VI*B*).

In congenital LQTS, triggers for syncope and SCA show significant genotype specificity (560). In LQTS type 1, exercise was the predominant risk factor for cardiac events (62% of total) and SCA (68%), with swimming being a particularly notable risk factor. In LQTS type 2, arousal (e.g., loud noises or sudden emotion) was the major trigger for cardiac events (43%), although exercise and rest/sleep were also common. Interestingly, in LQTS type 3, exercise was never a trigger for SCA, which was frequently in the setting of arousal (29%) or rest/sleep (49%). In each genotype, a low but significant percentage of cases had no obvious antecedent for the cardiac event.

Pregnancy is associated with a reduction in arrhythmic risk in LQTS type 1 and LQTS type 2, but the postpartum period is a time of very high risk. This increase is especially pronounced in LQTS type 2 compared with LQTS type 1 (322, 566). The cause is not known but stress, change in sex hormone levels, reduced sleep, and the intensity of auditory stimuli (crying babies) are possible contributors.

1. Mutation specific phenotypes

There have been numerous case reports of *KCNH2* mutations with a malignant phenotype (310, 545, 728). However, this hypothesis had not been thoroughly tested until quite recently. Kim et al. (327) studied 634 patients with LQTS type 2, from 158 proband-identified families; each subject was followed from diagnosis to the age of 40. During this time period, 204 patients had a first cardiac event; the trigger to this event was mutation-site specific: mutations in the pore domain had the highest risk for arousal triggers, and a high risk for exercise triggers; while mutations in non-pore transmembrane domains had a strong predilection to exercise-triggered events, mutations in the PAS domain were significantly associated only with nonarousal/nonexercise triggered events. Events were more common in those with long QT_c intervals, and in women, regardless of mutation site (327).

A full understanding of mutation-specific phenotype would require the in vitro characterization of each mutant, an exercise of considerable time and resource. However, some general insights may be gleaned from the existing data. First, mutations causing defects in synthesis, i.e., premature truncation mutations that undergo nonsense-mediated decay, would be expected to result in a ~50% reduction in Kv11.1 current, assuming that the wild-type allele is unaffected. Conversely, trafficking mutants that result in misfolded monomers, but which associate with wild-type subunits and are then retained in the ER and targeted for degradation, could result in up to 93% reduction in Kv11.1 current (175); these mutants would be expected to cause severe disease. At this stage it is not known how many trafficking defective mutants result in dominant negative suppression of current, but based on the data of Anderson et al. (19), one would expect most trafficking mutants to be dominant negative, although not necessarily causing complete dominant negative suppression. Almost all mutants within the transmembrane core of the channel are trafficking defective, (19), although there is at least one in the extracellular S5P linker that results in a gating defect (728) and another mutant close to the selectivity filter that results in abnormal conduction (166). Fewer mutants in cytoplasmic domains have been studied, but they are likely to contain a mixture of defective synthesis (218), trafficking (340), and gating (61) phenotypes (see **FIGURE 24** above). Given the overlap of phenotypes defined by mutation site, it is quite possible that the mechanism of Kv11.1 current reduction is of more importance than the mutation site per se.

Considerable progress has been made in refining our understanding of genotype-phenotype associations in LQTS type 2, in particular in regard to risk profiling. Risk is now understood as a function of the patient's clinical history and baseline ECG, as well as their age, gender, pregnancy status, and most intriguing of all, mutation site. Further work is required to understand the influence of an individual's "ge-

netic loading," for instance, the effect of common polymorphisms to modulate the QT interval and the implications for individual risk (639). Genetic influences on the autonomic system are also likely to influence the triggers to cardiac events.

E. Animal Models of LQTS Type 2

Despite impressive progress in the characterization of LQTS type 2 in humans, the absence of an animal model has hampered efforts to understand the complex interplay of genetic and environmental modifiers of phenotype expression. The first animal model developed was that from Colatsky et al. (45) who bred transgenic mice overexpressing the Kv11.1 pore mutant G628S. In *Xenopus* oocytes, G628S exerts a dominant-negative effect on channel function (545). Correspondingly, transgenic mice showed absent I_{Kr} and, at slow cycle lengths and 20°C, a prolonged APD. However, recordings from strips of ventricular muscle were unchanged between wild-type and G628S mice, and there was no change in QT interval. Furthermore, no mice developed cardiac arrhythmia. Given the much higher heart rates in mice (500–600/min in the unanesthetized mouse) compared with humans (60–90/min), and consequently very different repolarization characteristics, the mouse may not be a good model system to use for studying arrhythmias related to abnormalities of repolarization. Furthermore, it is worth noting that I_{Kr} is relatively unimportant in adult mice (664, 665), so one would not expect to see any significant change in the QT interval of G628S Kv11.1 mice.

ZERG, the zebrafish ortholog of hERG, is expressed in the atrium and ventricle of zebrafish; the zebrafish heart has only two chambers and has very similar amino acid sequence in the pore and drug-binding regions (349). Coupled with ease of breeding, rapid development, and straightforward generation of genetic knockdowns, this makes zebrafish a very attractive model for the investigation of LQTS type 2. Additionally, the heart rate, QT interval, rate-adaptation of QT interval, and action potential duration recorded from zebrafish hearts are all similar to those measured in humans (37). Zebrafish Kv11.1 expressed in *Xenopus* oocytes also shows similar characteristics to human Kv11.1. Consequently, reduced I_{Kr} in zebrafish displays a similar electrophysiological phenotype to human I_{Kr} block: markedly prolonged action potential duration, to the extent of producing 2:1 conduction; and a prolonged QT interval on the surface ECG (37). Complete absence of I_{Kr} results in a "silent ventricle," with a depolarized membrane near 0 mV perhaps explaining the apparent rarity of live human births with homozygous LQTS type 2, i.e., embryonic/fetal lethality (67). These results suggest that zebrafish may be a useful animal model system for the investigation of LQTS type 2 and the genetic milieu that shift its phenotype. Langheinrich et al. (349) have also demonstrated that zebrafish may to be used to screen for drugs, which block Kv11.1. Drug application commonly produced 2:1 atrioventricular conduction; however, several false-negative results were obtained, including sotalol, quinidine, and erythromycin, all important causes of TdP in humans, perhaps as a result of poor drug penetration to its site of action.

A transgenic rabbit model of LQTS type 2 expressing G628S has been described (81). Half of rabbits with this mutation died suddenly from polymorphic ventricular tachycardia within 12 mo of birth. Optical voltage mapping demonstrated that susceptibility to arrhythmia was correlated with an increase in the spatial heterogeneity of epicardial action potential duration across the anterior wall of the heart. Interestingly, many of the female rabbits died during lactation, a correlate of the increased risk of LQTS type 2 arrhythmia in postpartum women (see above). Transgenic rabbits expressing KvLQT1:Y315S (a model of LQTS type 1) showed prolonged QT, but did not develop arrhythmia under resting conditions. Thus several distinct features of LQTS type 2 and LQTS type 1, and their phenotypic differences, are reproduced in these transgenic animal models.

VIII. DRUG-INDUCED QT PROLONGATION AND KV11.1 CHANNELS

In clinical practice, prolongation of the QT interval on the surface electrocardiogram is most commonly seen in patients taking medications that block the Kv11.1 channel and/or electrolyte abnormalities that alter repolarizing currents. This scenario, sometimes referred to as acquired long QT syndrome (aLQTS), encompasses any noninherited form of QT prolongation beyond the clinically defined normal range (>440 ms in men, >460 ms in women). Patients with so-called aLQTS do not have any of the noncardiac features seen in some patients with congenital long QT syndrome. Accordingly, it is more accurate to refer to this condition as drug-induced prolongation of the QT interval. However, in keeping with common practice, the term aLQTS is used in this review. More common than the congenital form, aLQTS is similarly associated with the development of life-threatening arrhythmias such as torsades de pointes (TdP). A variety of medical conditions including myocardial infarction, as well as electrolyte abnormalities such as hypomagnesemia and hyokalemia, can lead to QT prolongation. However, drug administration is by far the most commonly identified cause of aLQTS and will be the focus of this section.

Congenital long QT syndrome is genetically heterogeneous (see sect. VII*A*). In contrast, the overwhelming majority of cases of aLQTS are caused by drug block of I_{Kr}. Drug-induced QT prolongation can occur as a direct consequence of Kv11.1 channel block and/or impaired trafficking of Kv11.1 channels to the cell membrane.

A. Historical Perspective

Levy (364) reported the first cases of syncope and sudden death linked to treatment of patients with the antimalarial drug quinidine, in 1922. The clinical basis for these phenomena was revealed in 1964, when Selzer and Wray (563) observed polymorphic ventricular tachycardia on electrocardiograms from patients with quinidine-related syncope. This observation clearly demonstrates TdP arrhythmia associated with use of a drug that is now known to block Kv11.1 channels.

In 1970, Vaughan-Williams (579) introduced a classification system for antiarrhythmic drugs, which, as the name implies, are used to restore normal heart rhythm and contraction. It was triggered by the finding that amiodarone, an antianginal drug, caused considerable prolongation of the action potential duration in isolated rabbit atrial or ventricular muscle fibers (579). Newly identified drugs like amiodarone, which delayed repolarization and thereby prolonged both action potential duration and the effective refractory period, were categorized as class III antiarrhymic drugs (580). Quinidine, on the other hand, was identified as a class I antiarrhythmic due to its reduction in the magnitude of APD and slowing of conduction velocity (298). However, as early as 1957 it was suggested that quinidine could slow repolarization by reducing potassium conductance in isolated rabbit heart and atria (31). Subsequent studies showed that quinidine prolonged repolarization of the action potential in a manner similar to class III antiarrhythmic drugs (527). It is now well known that a significant overlap exists between all four classes of the Vaughan-Williams system, and much of this is due to the high susceptibility of Kv11.1 channels to block by antiarrhythmic drugs.

The first noncardiac drug associated with ventricular tachycardia was the antipyschotic thioridazine (559). Subsequently, a large number of non-cardiac-related medications, spanning a number of therapeutic classes and with a wide variety of chemical structures, have been demonstrated to induce life-threatening arrhythmia through QT prolongation (listed at www.torsades.org). As a consequence of this potentially fatal unwanted side effect, several noncardiac medications have been severely restricted in their use, or removed from the pharmaceutical market altogether (525). Predicting whether new chemical entities carry the risk of drug-induced QT prolongation and TdP before substantial time and expenditure has been spent on their development has been, and remains, an important scientific goal.

B. Predicting Risk of Drug-Induced TdP

In theory, the relationship between Kv11.1 channel block, QT_c prolongation, and TdP offered an attractive approach to identify the proarrhythmic risk of new and existing drugs. High-throughput assays for detecting Kv11.1 drug block are discussed in section V*E*. However, due to a complex interplay of factors, these relationships are not as straightforward as initially thought. Drugs, for instance, can target more than one molecular entity that underlies the complex depolarization-repolarization relationship of an action potential. This means that Kv11.1 channel block does not necessarily always lead to prolongation of the action potential duration and QT interval. One example of this is the Kv11.1 channel blocker verapamil, which also blocks L-type calcium channels and reduces depolarization current thereby preventing QT interval prolongation (170, 697). Block of L-type calcium channel current [$I_{Ca\ (L)}$] will also severely restrict the formation of EADs and could explain why verapamil very rarely results in TdP (7). The relationship between QT prolongation and the generation of arrhythmia is even less certain. It is true that drug-induced TdP most often results from Kv11.1 block and QT interval prolongation, but QT interval prolongation alone is not sufficient to cause the development of TdP in patients. In fact, it has been estimated that most antiarrhythmic drugs that prolong the QT interval carry only a 1–3% risk of TdP over a 2-year exposure and that this risk is even less for non-cardiac-related drugs (313, 525). Indeed, some class III antiarrhythmic drugs, such as amiodarone, which prolongs the QT interval by high-affinity block of Kv11.1 channels, have almost no propensity to be proarrhythmic (265, 697). An even further level of complexity is added by the suggestion that drug-induced ventricular tachyarrhythmias which fit the description of TdP can occur without QT prolongation, but are not labeled TdP for this very reason (567).

Despite this uncertainty, progress has been made in the development of a predictive model for the proarrhythmic risk of drugs. In particular, a number of interlinked electrophysiological biomarkers for TdP have been identified using an automated Langendorff-perfused rabbit heart preparation called SCREENIT (266, 267, 567). Known by the acronym TRIaD these biomarkers are: triangulation, reverse use-dependence, instability, and dispersion. Drug-induced prolongation of action potential duration by slowing phase 3 repolarization (defined as APD_{30-90}) results in a triangulation of action potential morphology. As discussed previously, this occurs predominantly though reduced outward I_{Kr}, but can also occur through enhanced inward sodium or calcium currents. Triangulation is proarrhythmic because it both increases the propensity for arrhythmogenic triggers such as EADs (due to increased time in calcium and sodium window currents) and for substrates of arrhythmia like reentry and transmural dispersion of repolarization (TDR) (266, 267, 567). Clinically, triangulation manifests as wider, flatter, and often notched T-waves that precede TdP, although caution must be taken in using T-wave morphol-

ogy as an indicator of TdP as there may be other causes for this phenotype (451, 467).

Reverse use dependence refers to the tendency of most class III antiarrhythmic drugs to prolong the APD to a greater degree during bradycardia (slower heart rates) when it is least required (269). Several explanations for reverse use dependence have been postulated, but the exact molecular mechanism underlying this phenomenon has not been resolved (50, 306, 687, 696). One intriguing possibility is that the inherent reverse rate dependence of currents that constitute the cardiac action potential (50), in particular the late sodium current, favors a greater degree of action potential prolongation with I_{Kr} block at slow heart rates (687). This would explain why the I_{Kr} blocker amiodarone, which also blocks the late sodium current, shows little reverse use dependence (540). In addition to being a highly predictive preclinical marker for arrhythmia, reverse use dependence also causes beat-to-beat variation in repolarization that is known as instability (266, 267, 567). This cyclic phenomenon results in alternate long-short lengths of action potential duration and QT interval. Although some degree of instability is normal, due to intrinsic reverse rate dependence of currents, its proarrhymic potential is greatly enhanced with I_{Kr} block (267). On an ECG, instability is represented by T-wave alternans prior to arrhythmia, thereby making it a powerful predictive biomarker for TdP (186).

One of the most important biomarkers for TdP is dispersion of repolarization (24). Essentially, dispersion refers to gradients in the action potential duration that exist between different areas of the cardiac muscle including from apex to base, from right to left ventricle, and in regions of scar tissue. Transmural dispersion between the epicardium (shortest APD) and the mid-myocardium (longest APD) appears to be of particular importance (23). An imbalance of depolarizing and repolarizing ionic conductances underlies these transmural differences, i.e., midmyocardial cells (M-cells) have a reduced I_{Ks} repolarizing conductance and enhanced depolarizing conductances, both of which contribute to a longer action potential duration (24, 443). Block of I_{Kr} therefore produces larger alterations to M-cell action potential duration than in epi- or endomyocardium, which creates a strong substrate for reentry arrhythmia (23, 24). Since repolarization of the epicardium coincides with the peak of the T-wave on an ECG, while midmyocardial repolarization coincides with the end of the T-wave, prolongation of the distance between T-peak and T-end can be a powerful biomarker for increased transmural dispersion of repolarization (25, 691). These studies have been largely conducted in arterially perfused isolated wedges of canine heart. Other studies using intact pig and canine hearts have added a note of caution, in that T-peak to T-end may represent dispersion of repolarization across the entire ventricle, rather than being a direct measure of transmural dispersion (464, 690). It is also important to note that none of the biomarkers listed is an absolute predictor of the arrhythmogenic potential of a drug. Further studies are required to examine the predictive abilities of these and other possible biomarkers of drug-induced QT prolongation and TdP.

Marked variations in QT prolongation and proarrhythmic risk are observed not only for different drugs but also between patients taking comparable doses of the same drug. At least some of this variation can be attributed to drug-drug interactions. Inadvertent prescriptions for multiple QT-prolonging drugs may be a fairly common problem that could lead to increased clinical manifestations of drug-induced QT prolongation (133). Other problems may occur in relation to impaired metabolism of a QT-prolonging agent. A common example is the antihistamine terfenadine that is metabolized by cytochrome *P*-450 3A4 (CYP3A4) to its active agent, which at standard doses has little proarrhythmic risk (239). Inhibition of CYP3A4 by grapefruit juice or a number of other commonly used drugs can significantly elevate serum concentrations of terfenadine and increase the incidence of Kv11.1 block and QT prolongation (60, 151, 731). Such increased arrhythmic risk is unacceptable for a drug used in treatment of non-life-threatening conditions, and for which safer alternatives are available, so terfenadine was withdrawn from the pharmaceutical market in 1998.

Various patient specific factors can also influence susceptibility to drug-induced QT prolongation and the onset of TdP (525). A concept known as "repolarization reserve" may help explain the basis of this individual variation (526). In essence, repolarization is coordinated by a number of mechanisms so a natural redundancy exists. As such, there is little substrate for arrhythmia to occur. In this context, block of I_{Kr} may not, on its own, represent a significant risk for QT prolongation. However, if combined with other stressors that reduce the repolarization reserve, then a significant increase in risk is expected. Genetic factors, such as gender or common polymorphisms in LQTS causing genes, are likely common stressors. Pathophysiological conditions including various forms of heart disease, renal failure, and hepatic insufficiency have also been identified as risk factors.

C. Clinical Management

Incidence rates for drug-induced QT prolongation are hard to accurately evaluate, although estimations suggest that 2–3% of drug prescriptions may carry some risk (136). Perhaps the best study in this regard is that from Ray et al. (515) looking at the incidence of sudden cardiac death (SCD) in patients taking antipsychotic medications. The incidence of SCD was closely correlated with the dose of drug used, and in those patients taking higher doses of drugs, the incidence of SCD was up to three times higher

than in a comparable patient group not taking medication (515).

Regulatory agency approval and clinical use of any drug with suspected liability to cause QT prolongation is clearly dependent on the benefits of the primary therapy and the availability of alternatives. In addition, clinical evaluation of risk factors that increase susceptibility to arrhythmia is important. If assessed prior to treatment, at least some of these risk factors, such as electrolyte imbalances, could be reduced. Computer algorithms that combine analysis of patient- and drug-specific risk factors could be an important tool for clinicians in TdP risk avoidance (525).

Current therapies for acute episodes of drug-induced QT prolongation are limited to intravenous administration of magnesium sulfate (647) or in extreme cases cardiac pacing (95). Magnesium therapy prevents recurrence of TdP without correction of the QT interval, even in patients with serum concentrations within the normal range (647). The underlying mechanism for the effectiveness of magnesium remains unclear, although one plausible hypothesis is that it suppresses EADs by blocking L-type calcium channels (27). Discontinued use of the suspected problematic medication appears an obvious concomitant step to alleviate TdP risk. However, if the primary use of the medication is for an otherwise fatal condition and there is no alternative therapy available, continued use of the drug with adequate supervision may be a necessity (525).

The discovery of a series of Kv11.1 channel agonists (see sect. VG) has raised the possibility that these drugs may be used as antiarrhythmic drugs (223). Another interesting question is whether Kv11.1 agonists have potential as alternative pharmacological treatments for drug-induced QT prolongation. Reversal of drug-induced reductions in I_{Kr} may occur if only a portion of channels are blocked (so the remaining unblocked channels can be activated) or if the agonists are able to displace blockers from their binding sites (possibly by inhibiting inactivation and reducing affinity for block). In this regard, both type 1 and 2 agonists have been shown to reverse drug-induced APD prolongation in vitro (312, 729), although this effect is minimal for other Kv11.1 agonists (205). In vivo, NS3623 can prevent E4031-induced QT prolongation in conscious guinea pigs (243), while NS1643 substantially reduced the number of ectopic beats and tachycardic episodes in a methoxamine-sensitized rabbit model of TdP (147). A note of caution is that agonists may be proarrhythmic in some conditions (389, 476, 482). One concern is that by enhancing repolarization current some of these agents could induce arrhythmia through shortening of the QT interval (389). Kv11.1 agonists produce only a moderate effect on Kv11.1 channel inactivation compared with the inherited mutations (N588K or T618I) that are known to induce SQTS (80, 115, 608). However, computational modeling of Kv11.1 mutations that induce shifts in the voltage dependence of inactivation similar to the level of Kv11.1 agonists (~+20mV) suggests that such drugs could cause sufficient shortening of the QT interval to induce SQTS (<360 ms) (59). Whether agonist-shortened QT intervals could result in arrhythmia is therefore uncertain and requires further exploration. A second problem that may inhibit the therapeutic use of Kv11.1 channel agonists is their relative low potency (low micromolar range). Indeed, most are partial agonists that also block Kv11.1 at high concentrations (88, 486, 487). Specificity of action may also be a problem. For example, agonists may not show sufficient specificity for Kv11.1 over other *ether-a-go-go* family members (163) or ion channels (223). Additional unwanted side effects may arise from targeting of noncardiac Kv11.1 channels (see sect. X). Despite these potential problems, potassium channel agonists (either Kv11.1, KCNQ1, or Kir6) still present a potentially interesting pharmacological alternative for the treatment of LQTS. Increased knowledge regarding their mechanisms of action, binding sites, and therapeutic potential may in the future allow us to tailor the use of these compounds to specific LQTS phenotypes (223).

There are also a few reports of noncardiac drugs that result in shortening of the QT interval. In a recent study, Schimpf et al. (556) reported that the antiepileptic drug rufinamide caused ~20 ms shortening of corrected QT interval in a sample of 19 patients. There were, however, no adverse events (cardiac arrhythmias or sudden cardiac arrest) observed in this group over an average 3-yr follow up. Nevertheless, given the risk of sudden death in patients with short QT intervals (see below), it is reasonable to sound a note of caution with the use of drugs that shorten the QT interval (556).

IX. SHORT QT SYNDROME

People with short QT intervals (<400 ms) on the electrocardiogram have as high a risk of SCD (~2.4 increase risk of SCD in the subsequent 2 yr) as do people with long QT intervals (>440 ms) (15). It was not until 2000, however, that Gussak et al. (230) suggested a new inherited arrhythmia syndrome characterized by shortened QT intervals and atrial fibrillation, which they termed short QT syndrome (SQTS). Today the consensus for how short the QT interval needs to be to define STQS is <360 ms in females and <350 ms in males (477). Inherited SQTS, however, is likely to be very rare with relatively few families identified worldwide.

A. Genetic Basis

In 2004, Brugada et al. (80) identified mutations in *KCNH2* in two families with SQTS. Although the gene mutations were different in the two families, they both resulted in the same protein change, N588K (80). The N588K mutation

results in reduced inactivation and hence greater current flow during the plateau potentials of the cardiac potential (see **FIGURE 25**). As a consequence of the greater current flow at plateau potentials, the ventricular (and atrial) action potential has a shorter duration and thence a shorter QT interval (see **FIGURE 25**). Recently, Sun et al. (608) reported another *KCNH2* mutation, resulting in a mutation T618I that also results in loss of inactivation, although the phenotype is less severe than that seen for N588K. The only other *KCNH2* mutation reported to be associated with SQTS is R1135H (284). R1135H channels display significantly slower deactivation than wild-type channels without significant changes in any other gating parameters (284). Such a phenotype would not be expected to cause significant shortening of the action potential at low heart rates, but it is possible that at high rates the accumulation of Kv11.1 current could contribute to a significant shortening of the action potential.

Recently, McPate et al. (409) have shown that the in vitro phenotype of the SQTS mutation N588K was more severe when coexpressed with hERG1b subunits rather than hERG1a subunits. Given that the midpoint of the voltage dependence of inactivation of Kv11.1 channels composed of hERG1b subunits is shifted by ~+20 mV compared with channels composed of hERG1a subunits (542), it is reasonable to presume that coexpression of N588K, in either the hERG1a or hERG1b background, with hERG1b subunits would exacerbate the loss of inactivation seen with the N588K mutant subunits.

Since 2004, a total of five genetic loci associated with SQTS have been identified. These include mutations in three K^+ channel subunits: *KCNH2* (SQTS1), *KCNQ1* (SQTS2), and *KCNJ2* (SQTS3) as well as two Ca^{2+} channel subunits: *CACNA1C* (SQTS4) and *CACNB2b* (SQTS5). A more comprehensive review of these SQTS subtypes has been reviewed elsewhere (477).

B. Pharmacological Treatment of SQTS1

Given the large number of drugs that can inhibit Kv11.1 K^+ channels, intuitively one would think that it would be relatively easy to treat patients with SQTS1. As noted earlier (see sect. V), however, the N588K mutation results in a marked reduction of channel inhibition by a wide range of drugs (408, 484). Nevertheless, there have been some promising results in small clinical trials. For example, Gaita et al. (195) showed that hydroquinidine was effective in prolonging the QT interval to normal levels and eliminating inducibility of ventricular fibrillation in patients with SQTS.

C. Models of SQTS

In 2008, Hassel et al. (248) identified a zebrafish mutation, *reggae* (reg), which displays clinical features of SQTS. The

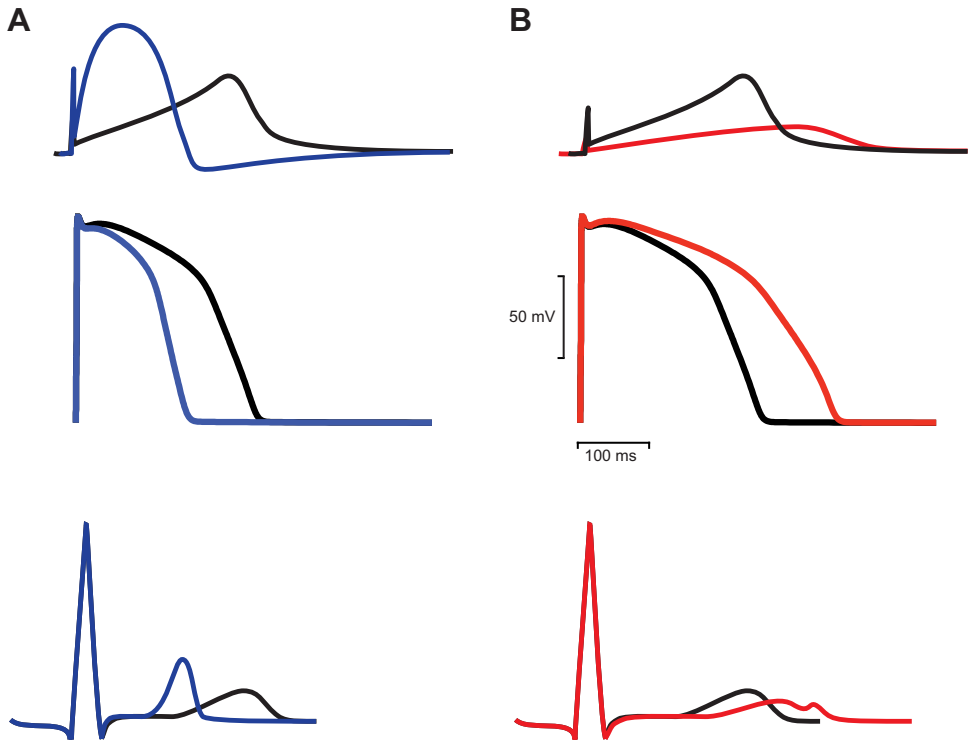

FIGURE 25. Electrical phenotype of short QT syndrome compared with long QT syndrome. *A*: representation of effect of N588K on Kv11.1 current, epicardial AP, and ECG (blue) compared with wild type (black). Note the shortening of the action potential duration and QT interval. In addition, patients with short QT syndrome typically have peaked T-waves (80). *B*: representation of effect of reducing Kv11.1 conductance by 50%. In addition to the prolonged QT interval, the T-wave is depicted as having a bifid T-wave (715).

reg mutation was found to be located in the voltage sensor of zERG (248) and resulted in a mutation equivalent to L532P in human Kv11.1. Characterization of both the zERG mutant (248) as well as the equivalent human mutation (727) revealed a complex gating phenotype resulting in a marked increase in the window current, i.e., the voltage range at which the channels would be constitutively open. The Kv11.1 agonists, PD-118057 (476) and NS3623 (352), have also been used to mimic SQTS in cardiac tissues. It is interesting to note that NS3623 was also found to impair cardiac conduction in guinea pig hearts, consequent to reduced sodium channel availability. Whether this is due to a direct effect on sodium channels or an indirect effect caused by the altered K^+ conductance remains to be determined.

An alternative to animal models is to use in silico models of the N588K mutation (283, 681, 712). These models have reproduced the shorter action potential duration and QT interval; however, the earlier models did not reproduce the altered dispersion of repolarization or the taller T-waves typical of SQTS1. In a more recent study, Adeniran et al. (4) found that these features could only be reproduced if they incorporated a heterogeneous distribution of I_{Kr} among the subtypes of ventricular myocytes (epicardial:mid-myocardial:endocardial in ratio 1.5:1:1 or greater). Whether such a gradient really exists is uncertain (193). Nevertheless, the Adeniran study clearly illustrates the importance of combining tissue heterogeneity into any cardiac electrophysiology studies.

X. DISTRIBUTION OF KV11.1 CHANNELS IN DIFFERENT TISSUES

Although Kv11.1 channels have been most extensively studied with respect to cardiac function, they are also quite widely expressed in brain regions, smooth muscle cells of the gastrointestinal and genitourinary tracts, as well as a range of endocrine cells (see **TABLE 2**).

A. Nervous System

Most of what is known about Kv11.1 in the central nervous system has come from studies in rats. In addition to ratERG-1 (Kv11.1), adult rat brain expresses two closely related members of the EAG superfamily, ERG2 (Kv11.2) and ERG3 (Kv11.3) (571) (see **FIGURE 4,** sect. II). ratERG2 and ratERG3 appear to be exclusively expressed in neuronal tissue. All three ratERG subtypes are strongly expressed

Table 2. *Tissue distribution of hERG outside the heart*

Tissue	Species	Isoforms	Reference Nos.
	Nervous tissue		
F11 DRG neuron x neuroblastoma hybrid cell line	Mouse x rat hybrid	Unknown	102
Hippocampus/prefrontal cortex	Human, primate	hERG1a+b, hERG 3.1	279
Hippocampus	Rat	rERG1a+b, rERG2, rERG3	224
Developing ventral horn GABAergic interneurons	Mouse	mERG1a+b, mERG2, mERG3	190
Glomus cells (carotid body)	Rabbit, rat	Unknown	326, 465
Astrocytes	Rat, mouse	ERG1a+b, ERG2, ERG3	164, 224, 470
Taste buds (young β2/M5 cells)	Rat	Unknown	457
	Smooth muscle		
Esophagus	Opossum	Unknown	8
Stomach smooth muscle	Rat	rERG1, rERG2	458
Small intestinal smooth muscle	Mouse, human, rabbit, horse	Unknown	347, 371
Colonic smooth muscle	Human, rabbit	ERG1	575
Gallbladder smooth muscle	Human, mouse, guinea pig	ERG1*	475
Portal vein	Mouse	mERG1b >> mERG1a	459
Urinary bladder	Guinea pig	Unknown	281
Myometrium	Mouse	mERG 1a, 1b	220
Epididymal duct	Bovine	bERG1b > bERG1a	412
	Endocrine		
Pancreatic beta-cells	Human	hERG1 found, hERG2+3 unknown	530
Pituitary	Rat	In lactotrophs: rERG1, rERG2, rERG3	52, 56, 554
Cromaffin cells	Rat	rERG1	225
Lactotroph cells	Rat	rERG1, rERG2, rERG3	554
	Miscellaneous		
Kidney (proximal tubule, distal tubule, collecting duct)	Rat	rERG1a+b (rERG2&3 not tested)	87

in the olfactory bulb, while ratERG1 is the only isoform present in brain stem nuclei, and ratERG3 is the dominant isoform in cerebral cortex and hippocampal pyramidal cells (539). Subsequent RT-PCR, in situ hybridization, and immunohistochemistry studies confirmed and extended these results (224) and additionally detected expression of KCNH2 transcripts in hippocampal astrocytes (164, 470), cerebellar Purkinje cells (164, 470, 536), and vestibular nucleus neurons (490). Papa et al. (470) also found that KCNH2 transcripts appeared at very high levels in individual, scattered neurons throughout the cortex and speculated that these cells possibly represent inhibitory interneurons. A similar pattern of scattered, high levels of KCNH2 expression are also found in interneuron populations of the hippocampus (470, 539).

During a single neuronal action potential, only a small fraction of I_{Kr} channels will be activated, due to the slow activation and rapid inactivation properties of these channels (see sect. IV). Therefore, the effect of I_{Kr} on an individual neuronal action potential is minimal. However, during prolonged bursts of action potentials, the amount of I_{Kr} increases as a consequence of the slow deactivation kinetics. Chiesa et al. (102) have shown that current injection into rat F11 cells results in brief, self-terminating trains of action potentials, but after blocking I_{Kr} with WAY-123,398, these trains became long lasting and more regular. This indicates that the gradual increase in I_{Kr} during prolonged bursts can eventually counteract Na^+ influx and decrease spiking frequency or even terminate a burst (see **FIGURE 26**). This spike-frequency adaption has also been demonstrated in cerebellum Purkinje neurons (224, 536) and in neurons from the medial vestibular nucleus (490).

Another example of I_{Kr} channels influencing the membrane potential and firing rate has been shown in glomus cells of the adult rabbit carotid body (466). In whole cell current-clamped glomus cells, application of 150 nM dofetilide caused a significant 13 mV depolarizing shift of the membrane potential. Voltage-clamp experiments showed a concentration-dependent block of I_{Kr} by dofetilide with an IC_{50} of 13 ± 4 nM. In carotid sinus nerve preparations, dofetilide was also able to increase the basal sensory discharge. I_{Kr} has also been demonstrated in rat carotid body chemoreceptor cells (326). The current density in these cells decreases with age, and this could be implicated in increased sensitivity to hypoxia during maturation.

In addition to expression in neurons, I_{Kr} is also present in astrocytes (164). In hippocampal slices, E-4031 inhibited both hyperpolarization- and depolarization-activated glial currents resulting in impaired clearance of extracellular potassium (164, 736). From these results, Emmi et al. (164) concluded that Kv11.1 encoded I_{Kr} currents are important in the process of "spatial buffering" of extracellular potassium ions, which accumulate during high neuronal activity.

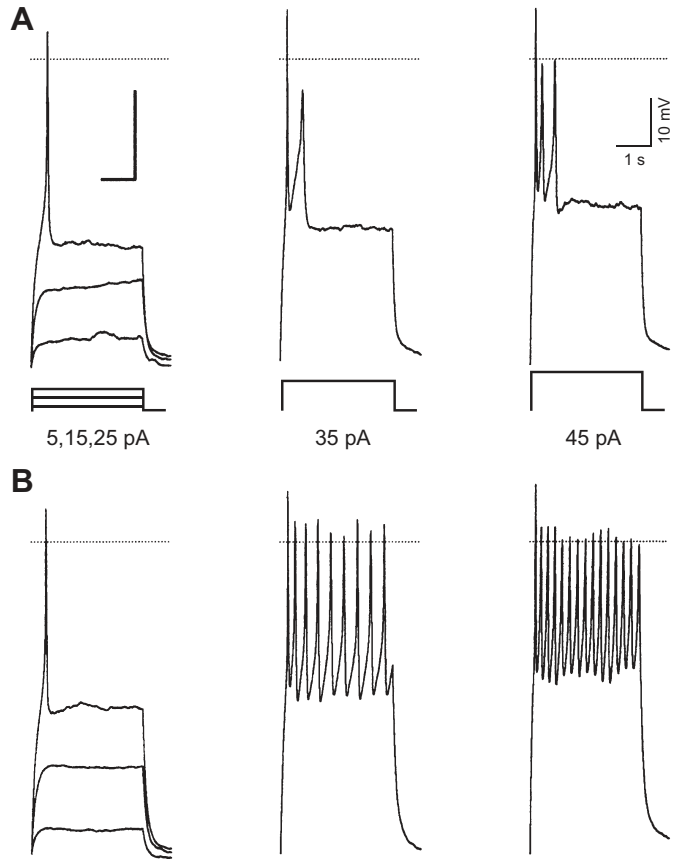

FIGURE 26. Kv11.1 channels regulate AP firing rates in neuronal cells. *A*: voltage responses of an F-11 cell in response to current injections of 5, 15, 25, 35 and 45 pA. *B*: effect of Kv11.1 blocker, WAY-123,398, on F-11 voltage responses. After inhibition of Kv11.1 currents, cells respond to current stimuli with repetitive AP firing. [From Chiesa et al. (102), copyright John Wiley and Sons Ltd.]

1. Potential role in neuropathophysiology

Mutations in *KCNH2* have been linked to both LQTS type 2 and a high incidence of seizures (169, 461). In many cases, the "seizures" may be caused by cardiac arrhythmias. However, recent work has demonstrated that the incidence of true seizures is significantly higher in patients with LQTS type 2 than in patients with LQTS type 1 or LQTS type 3 (47% in LQTS type 2 vs. 22% in LQTS type 1 and 25% in LQTS type 3, sample size 343 patients; Ref. 299). While there is no definitive proof of the idea, one possible reason for this high incidence of seizures in LQTS type 2 could be the effect of Kv11.1 mutations on K^+ buffering properties of astrocytes (164) as discussed above.

Two recent studies have found a link between schizophrenia and *KCNH2* (43, 279). A SNP in the chromosomal 7q36.1 region was linked to a novel KCNH2–3.1 isoform (see **FIGURE 2**), in which the first 102 NH_2-terminal amino acids are replaced by 6 unique amino acids. In control patients, mRNA levels of the KCNH2–3.1 isoform and the KCNH2–1a isoform were comparable in the brain, while in the heart KCNH2–1a mRNA is three orders of magnitude

more abundant than mRNA of the KCNH2–3.1 isoform. In brains of some schizophrenia patients, however, the KCNH2–3.1 isoform expression levels were 2.5-fold higher than KCNH2–1a expression (279). Given the critical role that the NH_2-terminal regions play in Kv11.1 deactivation (see sect. IV*F*), it is not surprising that the 3.1 isoform displays a significantly faster deactivation rate than channels composed of hERG1a subunits. Huffaker et al. (279) showed that expression of the 3.1 isoform in rodent cortical neurons results in high-frequency nonadapting firing patterns. This is precisely what one would expect for a channel that has rapid deactivation and so will show significant less accumulation during repetitive action potential firing. Kv11.1 channels have of course been of keen interest in the schizophrenia field for many years as almost all anti-psychotics used clinically have the unwanted side effect of blocking Kv11.1 channels in the heart, resulting in a significantly increased risk of sudden death (515). The discovery of an increased expression of a hERG isoform in the brains of at least some schizophrenia patients raises the intriguing question as to whether antipsychotic drug block of Kv11.1 in the brain may influence the clinical course of schizophrenia either in a beneficial or harmful way?

B. Smooth Muscle

Both full-length hERG1a and the COOH-terminally truncated hERG-USO variant have been identified in a range of smooth muscle tissue (see **TABLE 2**). HERG-USO has distinct biophysical properties compared with the cardiac Kv11.1 channels, in particular, a much accelerated rate of deactivation (169, 338). Smooth muscle I_{Kr} channels contribute to regulation of the resting membrane potential as well as affecting either the force or frequency of contraction. Studies in human jejunum revealed that block of I_{Kr} channels with 1 μM E-4031 and increase in the extracellular potassium to 45 mM caused very similar effects on phasic contractile amplitude (169). This suggests that influence of I_{Kr} on contractile function is mediated by membrane potential, which leads to an increase in intracellular Ca^{2+}. This theory is further supported by the observation that nifedipine, an L-type Ca^{2+} channel blocker, completely abolished phasic contractile activity, even in the presence of high concentrations of E-4031 (169). In this context it is interesting to note that the prokinetic drug cisapride, in addition to its action as a 5-HT_4 receptor agonist, is a strong Kv11.1 blocker (423), and this could explain part of its prokinetic activity in the digestive system.

In mice, mERG1a and mERG1b, but not mERG2 or mERG3, are expressed in nonpregnant myometrium (220). Application of E-4031, dofetilide, or Be-KM1 increases spontaneous contractility of mouse myometrium, whereas Kv11.1 activators PD118057 and NS1643 had the opposite effect and suppressed spontaneous contractility. This suggests that Kv11.1 channels help to keep the myometrium quiescent during early pregnancy (220). mERG protein expression levels appear to be constant throughout pregnancy and comparable to nonpregnant animals. However, preparations of smooth muscle strips from late pregnant mice show strong spontaneous contractions that are insensitive to either Kv11.1 blockers or activators (220). Greenwood et al. (220) suggested that the apparent insensitivity to Kv11.1 modulators may be related to a marked upregulation of KCNE2 and KCNE4 transcripts during pregnancy. These accessory subunits could alter the properties of Kv11.1 in a way that reduces its importance during late pregnancy (220). Given the marked effect that changes in microRNA expression can have on levels of protein expression independent of changes in transcript levels (see sect. III*B*), it would be worth investigating whether changes to microRNA expression during pregnancy may explain the reduced role Kv11.1 channels play in the late stages of pregnancy.

In bovine epididymal duct, KCNH2–1a and KCNH2–1b transcripts are found throughout the length of the duct, with higher levels of KCNH2–1b relative to KCNH2–1a (412). Application of E-4031, dofetilide, or cisapride enhanced spontaneous contractions, while NS-1643 suppressed spontaneous contractions. Experiments with nifidipine (L-type Ca^{2+} channel blocker) and thapsigargin (SR Ca^{2+} reuptake inhibitor) suggest that Ca^{2+} influx and not internal Ca^{2+} release is responsible for the muscle contractions modulated by I_{Kr} channels. Given the importance of correct epididymal duct contractile function for the male reproductive system, these findings raise the interesting possibility that Kv11.1 activators could have contraceptive effects.

C. Endocrine Cells

Blockade of I_{Kr} channels in some endocrine cells has a similar effect as that seen in smooth muscle cells, i.e., depolarization of the resting membrane potential and/or an increase in the frequency of action potential firing leading to increased release of hormones. This has been shown in human pancreatic islet cells, where blockade of I_{Kr} channels causes a 77% increase in insulin secretion (530). Similarly, in rat chromaffin cells, E-4031 causes increased release of epinephrine but not norepinephrine (225), and in rat lactotrophs, ERG block is associated with increased prolactin release (554). The corollary of each of these studies is that in patients with loss-of-function mutations in KCNH2, one might expect to see increased blood levels of insulin, epinephrine, and prolactin. In general, there are no clinical studies to corroborate this. However, it is well known that a side effect of many neuroleptic drugs that inhibit Kv11.1 channels is an increase in blood prolactin levels (554).

D. Kv11.1 Channels and Cancer

1. hERG in cell cycle regulation

VGK channels in general, and Kv11.1 channels in particular, have been implicated in the regulation of apoptosis and proliferation, both during normal development and in cancer. For example, in early embryonic stages, I_{Kr} channels are expressed at high levels in quail neural crest and are replaced by inward rectifier currents during maturation (30, 122). Also, in mouse embryonic heart, mERG expression levels are high, but downregulated during development (664, 665). Interestingly, ERG protein reappears in tissue that has undergone dedifferentiation (112), and in tissue samples from tumors, KCNH2 transcript and hERG protein expression is usually found to be more frequent than in the noncancerous control tissue (101, 497). These findings correlate well with the fact that most terminally differentiated cells display a membrane potential more negative than −60 mV, while nondifferentiated cells are usually more depolarized and have a membrane potential in the Kv11.1 window current range (8).

Arcangeli et al. (29) demonstrated that the recorded membrane potentials of unsynchronized mammalian neuroblastoma cells vary considerably from cell to cell, and that these variations correlate well with cell-to-cell differences in the steady-state activation curves of "K_{IR}" inward rectifier currents. After synchronization of the cells in the G_1 phase with retinoic acid, the variation in steady-state activation curves as well as membrane potentials was much less. In the same publication, Arcangeli et al. (29) also first proposed that "K_{IR} channels might be a relevant target in the transformation process" (29). At the time the group had no information about the molecular identity of the channels that carried the K_{IR} current. In a later study, Crociani et al. (123) found that the hERG subunit mix varies at different points in the cell cycle of synchronized cells: the NH_2-terminally truncated hERG1b isoform was dominant during the S phase, while hERG1a subunit was dominant during the G_1 phase. This result provides a molecular correlate to the apparent differences of biophysical parameters of "K_{IR}" at different phases of the cell cycle.

2. Evidence for hERG expression in cancer tissue

KCNH2 mRNA has been detected in numerous cancer cell lines (73, 472) (see **TABLE 3**). Smith et al. (582) also showed that, in various leukemia cell lines, incubation with E-4031 could reduce the rate of proliferation in these cells. This was the first demonstration of a functional effect of Kv11.1 in a cancer cell line (582).

3. Mechanism of hERG action in cancer

The emerging picture is that Kv11.1 has important implications for the invasiveness of cancers. In human colorectal cancer, Kv11.1 was found to regulate invasion of tumor cells, and Kv11.1 expression was observed more often in

Table 3. *Cancer cell lines positive for hERG*

Cell Line	Cancer Type	Reference Nos.
CEM	Leukemia	582
U937	Leukemia	582
K562	Leukemia	582
SK-OV-3	Ovarian cancer	41, 42
SH-SY5Y	Human neuroblastoma	29, 73
N18TG2	Mouse neuroblastoma	29, 73
NG108-15	Mouse neuroblastoma	29, 73
TE-671	Human rhabdomyosarcoma	73
SK-BR-3	Human mammary adenocarcinoma	73
NCI-N592	Human lung microcytoma	73
FLG29	Human monoblastic leukemia	73
SK-N-BE	Human neuroblastoma	73
41A3	Mouse neuroblastoma	73
F11	Rat DRG x mouse N18TG2 neuroblastoma	73
NG108-15	Mouse-rat neuroblastoma x glioma	73
PC12	Rat pheochromocytoma	73
GLC8, H69	Small cell lung cancer	73
GH3, GH4, MMQ	Pituitary tumor	73
RIN, INS-1	Pancreatic beta-cell tumor	73
MCF-7	Human breast cancer	472
EF119	Breast cancer	472

metastatic cancers with a bad prognosis than in less aggressive cancers (354). This trend was also observed in human leukemia cases, in which patients with Kv11.1 positive tumors had a higher mortality and higher likelihood of relapse than patients with Kv11.1 negative tumors (498). It appears that interaction of Kv11.1 with integrins is an important factor in this phenomenon. Hofmann et al. (264) showed that in the leukemic prosteoclastic cell line FLG29.1, fibronectin can transiently increase Kv11.1 current density and alter membrane potential via integrin action. Both mRNA and membrane protein levels appeared to be unchanged, so most likely a posttranslational mechanism was involved in the Kv11.1 current increase. Interestingly, the Kv11.1 activation in turn led to an increased expression of $\alpha_v\beta_3$ integrins, indicating that Kv11.1 is involved both in outside-in and inside-out signaling in these cells. The addition of G protein inhibitor pertussis toxin prevented both the current density increase and the upregulation of $\alpha_v\beta_3$ integrins. Later work added further evidence for the interaction of Kv11.1 channels with the β_1 subunit of the integrin receptor in leukemia and neuroblastoma cells, and that this complex could influence downstream signaling targets such as tyrosine kinases and GTPases (28, 100). Cherubini et al. (100) showed that β1 integrin and Kv11.1 colocalize in close proximity to caveolin-1, indicating an involvement of lipid rafts/caveolae. They also showed that the focal adhesion kinase (FAK) associates with Kv11.1 and becomes tyrosine phosphorylated after exposure of the cell to fibronectin (100), an effect that could be blocked with Kv11.1 blockers. In a model of Kv11.1-transfected HEK-293 cells, cell migration after seeding on fibronectin was clearly impaired in mock-transfected cells compared with Kv11.1 transfected cells (100).

Currently the most plausible hypothesis for how Kv11.1 channels activate integrins is that Kv11.1 channels and integrins are conformationally coupled, i.e., gating transitions of the Kv11.1 protein could be directly transmitted to integrins in close proximity. While there are no data available that would support this hypothesis at present, in EAG channels there is evidence for ion-channel signaling that does not involve ion flux across the membrane, such as in fibroblasts and myoblasts where overexpression of EAG has a proliferative effect. This effect persists even when the nonconducting EAG mutant F456A is expressed instead of wild-type channels. Hegle et al. (253) were able to demonstrate involvement of p38 MAP kinase in this proliferative signaling. Furthermore, they showed that the conformational state of the EAG channels is important for signaling, since mutants with increased open-state occupancy inhibited proliferation (253). Another piece of evidence comes from work on melanoma cells. In these cells, block of Kv11.1 channels with E-4031 or cisapride disrupted proliferation and cell migration as does Kv11.1 knockdown with siRNA. Similar to the previous experiments, the signaling appears to go via mitogen-activated protein (MAP) kinase and expression of c-*fos* transcription factor. Block of Kv11.1 reduced MAP kinase phosphorylation and reduced c-*fos* levels (5).

Solid tumors are often characterized by a lack of oxygen, because growth of the cancerous tissue outpaces development of new vasculature. Kv11.1 channels might play a role here as well. First, it has been shown that Kv11.1 channel gating can be modulated by hypoxic conditions (185). The authors of this study speculated that the Kv11.1 PAS domain could be involved in sensing hypoxic conditions, but to date, no experimental evidence for this has been found. Second, in glioblastoma multiforme, Kv11.1 channels are overexpressed and modulate VEGF secretion, which is critical for angiogenesis (400).

4. hERG as a potential treatment target in cancer

Given its frequent expression and functional relevance in cancerous tissue, Kv11.1 appears to be a possible target for anticancer drugs. The antihistamine and known Kv11.1 blocker astemizole has been suggested as a possible candidate (199). This drug is particularly interesting, because it has been used in humans before, and it has two distinct properties that make it a good candidate: histamine favors proliferation of normal and cancerous cells, and astemizole is a strong Kv11.1 blocker. Both attributes combined have been shown to be antiproliferative both in vitro and in vivo (199). The use of Kv11.1 blockers in combating cancer is a novel and promising concept. Another example in this regard is the use of arsenic trioxide, which has been shown to induce apoptosis in MCF-7 cells via inhibition of Kv11.1 and activation of caspase-3 (675).

XI. CONCLUSIONS

In the first 12 months after Kv11.1 channels were identified there was some initial confusion as to how Kv11.1 channels gated. Were they inward rectifiers, canonical voltage-gated K^+ channels, or a hybrid of the two? It turns out that they are classical voltage-gated K^+ channels, but they have "upside-down" kinetics. The consequence of these unusual kinetic properties is that these channels are ideal for determining the repolarization duration of the cardiac action potential. The underlying basis of the unusual kinetic properties of Kv11.1 channels continues to fascinate physiologists. Conventional patch-clamp techniques, gating current measurements, voltage-clamp fluorometry, and phi-value analysis have all contributed to reveal significant insights into the molecular basis of gating of Kv11.1 channels. The next challenge will be to determine the structural basis of gating by combining high-resolution structural biology methods with electrophysiology studies. In the clinical sphere, Kv11.1 channels are also a topic of immense interest, as mutations in *KCNH2* are one of the most common causes of congenital long QT syndrome. Most *KCNH2* mutations

result in defective trafficking of the mutant channels. Consequently, there are considerable efforts underway to try and unravel the molecular basis of normal assembly and trafficking of these channels with the hope that one day it will be possible to restore trafficking in mutant channels. Perhaps the area of greatest interest is in the area of pharmacology. Kv11.1 channels are the most dreaded of "anti-targets," and trying to predict the affinity with which drugs will bind to these channels continues to exercise the minds of pharmaceutical chemists everywhere. Hopefully, structural biology, and in particular X-ray crystallography, will open up the analysis of the structural basis of drug binding to Kv11.1 channels. However, the picture that is emerging is that drug binding to Kv11.1 is likely to be a highly dynamic process with multiple drug and channel conformations contributing to binding for any given drug. It is likely that the development of accurate computer models of drug binding kinetics combined with structural studies will be needed to fully understand and ultimately overcome this complex safety-pharmacology problem.

ACKNOWLEDGMENTS

Address for reprint requests and other correspondence: J. I. Vandenberg, Molecular Cardiology and Biophysics Division, Victor Chang Cardiac Research Institute, 405 Liverpool St., Darlinghurst, NSW 2010, Australia (e-mail: j.vandenberg@victorchang.edu.au).

GRANTS

J. I. Vandenberg is supported by a Senior Research Fellowship from the National Health and Medical Research Council (NHMRC; 459401, 1019693). A. P. Hill is supported by a Future Fellowship from the Australian Research Council (ARC; FT110100075). Work in the authors' laboratory is supported by project grant funding from the NHMRC, ARC, National Heart Foundation of Australia, and the St. Vincent's Clinic Foundation.

DISCLOSURES

No conflicts of interest, financial or otherwise, are declared by the authors.

REFERENCES

1. Abbott GW, Sesti F, Splawski I, Buck ME, Lehmann MH, Timothy KW, Keating MT, Goldstein SA. MiRP1 forms IKr potassium channels with HERG and is associated with cardiac arrhythmia. *Cell* 97: 175–187, 1999.

2. Abbott GW, Xu X, Roepke TK. Impact of ancillary subunits on ventricular repolarization. *J Electrocardiol* 40: S42–46, 2007.

3. Ackerman MJ, Tester DJ, Jones GS, Will ML, Burrow CR, Curran ME. Ethnic differences in cardiac potassium channel variants: implications for genetic susceptibility to sudden cardiac death and genetic testing for congenital long QT syndrome. *Mayo Clin Proc* 78: 1479–1487, 2003.

4. Adeniran I, McPate MJ, Witchel HJ, Hancox JC, Zhang H. Increased vulnerability of human ventricle to re-entrant excitation in hERG-linked variant 1 short QT syndrome. *PLoS Computat Biol* 7: e1002313, 2011.

5. Afrasiabi E, Hietamaki M, Viitanen T, Sukumaran P, Bergelin N, Tornquist K. Expression and significance of HERG (KCNH2) potassium channels in the regulation of MDA-MB-435S melanoma cell proliferation and migration. *Cell Signal* 22: 57–64, 2010.

6. Aggarwal SK, MacKinnon R. Contribution of the S4 segment to gating charge in the Shaker K^+ channel. *Neuron* 16: 1169–1177, 1996.

7. Aiba T, Shimizu W, Inagaki M, Noda T, Miyoshi S, Ding WG, Zankov DP, Toyoda F, Matsuura H, Horie M, Sunagawa K. Cellular and ionic mechanism for drug-induced long QT syndrome and effectiveness of verapamil. *J Am Coll Cardiol* 45: 300–307, 2005.

8. Akbarali HI, Thatte H, He XD, Giles WR, Goyal RK. Role of HERG-like K^+ currents in opossum esophageal circular smooth muscle. *Am J Physiol Cell Physiol* 277: C1284–C1290, 1999.

9. Akhavan A, Atanasiu R, Noguchi T, Han W, Holder N, Shrier A. Identification of the cyclic-nucleotide-binding domain as a conserved determinant of ion-channel cell-surface localization. *J Cell Sci* 118: 2803–2812, 2005.

10. Akhavan A, Atanasiu R, Shrier A. Identification of a COOH-terminal segment involved in maturation and stability of human ether-a-go-go-related gene potassium channels. *J Biol Chem* 278: 40105–40112, 2003.

11. Al-Owais M, Bracey K, Wray D. Role of intracellular domains in the function of the herg potassium channel. *Eur Biophys J* 38: 569–576, 2009.

12. Alagem N, Yesylevskyy S, Reuveny E. The pore helix is involved in stabilizing the open state of inwardly rectifying K^+ channels. *Biophys J* 85: 300–312, 2003.

13. Albesa M, Grilo LS, Gavillet B, Abriel H. Nedd4–2-dependent ubiquitylation and regulation of the cardiac potassium channel hERG1. *J Mol Cell Cardiol* 2011.

14. Alessi DR, James SR, Downes CP, Holmes AB, Gaffney PR, Reese CB, Cohen P. Characterization of a 3-phosphoinositide-dependent protein kinase which phosphorylates and activates protein kinase Balpha. *Curr Biol* 7: 261–269, 1997.

15. Algra A, Tijssen JG, Roelandt JR, Pool J, Lubsen J. Heart rate variability from 24-hour electrocardiography and the 2-year risk for sudden death. *Circulation* 88: 180–185, 1993.

16. Almers W. Gating currents and charge movements in excitable membranes. *Rev Physiol Biochem Pharmacol* 82: 96–190, 1978.

17. Amin AS, Herfst LJ, Delisle BP, Klemens CA, Rook MB, Bezzina CR, Underkofler HA, Holzem KM, Ruijter JM, Tan HL, January CT, Wilde AA. Fever-induced QT_c prolongation and ventricular arrhythmias in individuals with type 2 congenital long QT syndrome. *J Clin Invest* 118: 2552–2561, 2008.

18. Anantharam A, Abbott GW. Does hERG coassemble with a beta subunit? Evidence for roles of MinK and MiRP1. *Novartis Found Symp* 266: 100–112, 2005.

19. Anderson CL, Delisle BP, Anson BD, Kilby JA, Will ML, Tester DJ, Gong Q, Zhou Z, Ackerman MJ, January CT. Most LQT2 mutations reduce Kv11.1 (hERG) current by a class 2 (trafficking-deficient) mechanism. *Circulation* 113: 365–373, 2006.

20. Ando F, Kuruma A, Kawano S. Synergic effects of beta-estradiol and erythromycin on hERG currents. *J Membr Biol* 241: 31–38, 2011.

21. Angelo K, Korolkova YV, Grunnet M, Grishin EV, Pluzhnikov KA, Klaerke DA, Knaus HG, Moller M, Olesen SP. A radiolabeled peptide ligand of the hERG channel, [^{125}I]-BeKm-1. *Pflügers Arch* 447: 55–63, 2003.

22. Anson BD, Ackerman MJ, Tester DJ, Will ML, Delisle BP, Anderson CL, January CT. Molecular and functional characterization of common polymorphisms in HERG (KCNH2) potassium channels. *Am J Physiol Heart Circ Physiol* 286: H2434–H2441, 2004.

23. Antzelevitch C. Ionic, molecular, and cellular bases of QT-interval prolongation and torsade de pointes. *Europace* 9 Suppl 4: iv4–15, 2007.

24. Antzelevitch C. Role of transmural dispersion of repolarization in the genesis of drug-induced torsades de pointes. *Heart Rhythm* 2: S9–15, 2005.

25. Antzelevitch C, Sicouri S, Di Diego JM, Burashnikov A, Viskin S, Shimizu W, Yan GX, Kowey P, Zhang L. Does Tpeak-Tend provide an index of transmural dispersion of repolarization? *Heart Rhythm* 4: 1114–1119, 2007.

26. Anumonwo JM, Horta J, Delmar M, Taffet SM, Jalife J. Proton and zinc effects on HERG currents. *Biophys J* 77: 282–298, 1999.

27. Aomine M, Tatsukawa Y, Yamato T, Yamasaki S. Antiarrhythmic effects of magnesium on rat papillary muscle and guinea pig ventricular myocytes. *Gen Pharmacol* 32: 107–114, 1999.

28. Arcangeli A, Becchetti A. Complex functional interaction between integrin receptors and ion channels. *Trends Cell Biol* 16: 631–639, 2006.

29. Arcangeli A, Bianchi L, Becchetti A, Faravelli L, Coronnello M, Mini E, Olivotto M, Wanke E. A novel inward-rectifying K^+ current with a cell-cycle dependence governs the resting potential of mammalian neuroblastoma cells. *J Physiol* 489: 455–471, 1995.

30. Arcangeli A, Rosati B, Cherubini A, Crociani O, Fontana L, Ziller C, Wanke E, Olivotto M. HERG- and IRK-like inward rectifier currents are sequentially expressed during neuronal development of neural crest cells and their derivatives. *Eur J Neurosci* 9: 2596–2604, 1997.

31. Armitage AK. The influence of potassium concentration on the action of quinidine and of some antimalarial substances on cardiac muscle. *Br J Pharmacol Chemother* 12: 74–78, 1957.

32. Armstrong CM. Inactivation of the potassium conductance and related phenomena caused by quaternary ammonium ion injection in squid axons. *J Gen Physiol* 54: 553–575, 1969.

33. Armstrong CM. Interaction of tetraethylammonium ion derivatives with the potassium channels of giant axons. *J Gen Physiol* 58: 413–437, 1971.

34. Armstrong CM. Ionic pores, gates, and gating currents. *Q Rev Biophys* 7: 179–210, 1974.

35. Armstrong CM. Time course of TEA(+)-induced anomalous rectification in squid giant axons. *J Gen Physiol* 50: 491–503, 1966.

36. Armstrong CM, Binstock L. Anomalous rectification in the squid giant axon injected with tetraethylammonium chloride. *J Gen Physiol* 48: 859–872, 1965.

37. Arnaout R, Ferrer T, Huisken J, Spitzer K, Stainier DY, Tristani-Firouzi M, Chi NC. Zebrafish model for human long QT syndrome. *Proc Natl Acad Sci USA* 104: 11316–11321, 2007.

38. Aronov AM. Common pharmacophores for uncharged human ether-a-go-go-related gene (hERG) blockers. *J Med Chem* 49: 6917–6921, 2006.

39. Aronov AM. Ligand structural aspects of hERG channel blockade. *Curr Top Med Chem* 8: 1113–1127, 2008.

40. Aronov AM, Goldman BB. A model for identifying HERG K^+ channel blockers. *Bioorg Med Chem* 12: 2307–2315, 2004.

41. Asher V, Khan R, Warren A, Shaw R, Schalkwyk GV, Bali A, Sowter HM. The Eag potassium channel as a new prognostic marker in ovarian cancer. *Diagn Pathol* 5: 78, 2010.

42. Asher V, Warren A, Shaw R, Sowter H, Bali A, Khan R. The role of Eag and HERG channels in cell proliferation and apoptotic cell death in SK-OV-3 ovarian cancer cell line. *Cancer Cell Int* 11: 6, 2011.

43. Atalar F, Acuner TT, Cine N, Oncu F, Yesilbursa D, Ozbek U, Turkcan S. Two four-marker haplotypes on 7q36.1 region indicate that the potassium channel gene HERG1 (KCNH2, Kv111) is related to schizophrenia: a case control study Behavioral and brain functions. *BBF* 6: 27, 2010.

44. Aydar E, Palmer C. Functional characterization of the C-terminus of the human ether-a-go-go-related gene K^+ channel (HERG). *J Physiol* 534: 1–14, 2001.

45. Babij P, Askew GR, Nieuwenhuijsen B, Su CM, Bridal TR, Jow B, Argentieri TM, Kulik J, DeGennaro LJ, Spinelli W, Colatsky TJ. Inhibition of cardiac delayed rectifier K^+ current by overexpression of the long-QT syndrome HERG G628S mutation in transgenic mice. *Circ Res* 83: 668–678, 1998.

46. Bahinski A, Nairn AC, Greengard P, Gadsby DC. Chloride conductance regulated by cyclic AMP-dependent protein kinase in cardiac myocytes. *Nature* 340: 718–721, 1989.

47. Bai Y, Wang J, Shan H, Lu Y, Zhang Y, Luo X, Yang B, Wang Z. Sphingolipid metabolite ceramide causes metabolic perturbation contributing to HERG K^+ channel dysfunction. *Cell Physiol Biochem* 20: 429–440, 2007.

48. Balakumar P, Jagadeesh G. Multifarious molecular signaling cascades of cardiac hypertrophy: can the muddy waters be cleared? *Pharmacol Res* 62: 365–383, 2010.

49. Balijepalli RC, Delisle BP, Balijepalli SY, Foell JD, Slind JK, Kamp TJ, January CT. Kv11.1 (ERG1) K^+ channels localize in cholesterol and sphingolipid enriched membranes and are modulated by membrane cholesterol. *Channels* 1: 263–272, 2007.

50. Banyasz T, Horvath B, Virag L, Barandi L, Szentandrassy N, Harmati G, Magyar J, Marangoni S, Zaza A, Varro A, Nanasi PP. Reverse rate dependency is an intrinsic property of canine cardiac preparations. *Cardiovasc Res* 84: 237–244, 2009.

51. Barhanin J, Lesage F, Guillemare E, Fink M, Lazdunski M, Romey G. K(V)LQT1 and lsK (minK) proteins associate to form the I(Ks) cardiac potassium current. *Nature* 384: 78–80, 1996.

52. Barros F, del Camino D, Pardo LA, Palomero T, Giraldez T, de la Pena P. Demonstration of an inwardly rectifying K^+ current component modulated by thyrotropin-releasing hormone and caffeine in GH3 rat anterior pituitary cells. *Pflügers Arch* 435: 119–129, 1997.

53. Barros F, Gomez-Varela D, Viloria CG, Palomero T, Giraldez T, de la Pena P. Modulation of human erg K^+ channel gating by activation of a G protein-coupled receptor and protein kinase C. *J Physiol* 511: 333–346, 1998.

54. Barros TP, Alderton WK, Reynolds HM, Roach AG, Berghmans S. Zebrafish: an emerging technology for in vivo pharmacological assessment to identify potential safety liabilities in early drug discovery. *Br J Pharmacol* 154: 1400–1413, 2008.

55. Barrows B, Cheung K, Bialobrzeski T, Foster J, Schulze J, Miller A. Extracellular potassium dependency of block of HERG by quinidine and cisapride is primarily determined by the permeant ion and not by inactivation. *Channels* 3: 239–248, 2009.

56. Bauer CK, Engeland B, Wulfsen I, Ludwig J, Pongs O, Schwarz JR. RERG is a molecular correlate of the inward-rectifying K current in clonal rat pituitary cells. *Receptors Channels* 6: 19–29, 1998.

57. Bavro VN, De Zorzi R, Schmidt MR, Muniz JR, Zubcevic L, Sansom MS, Venien-Bryan C, Tucker SJ. Structure of a KirBac potassium channel with an open bundle crossing indicates a mechanism of channel gating. *Nat Struct Mol Biol* 2012.

58. Benhorin J, Medina A. Images in clinical medicine. Congenital long-QT syndrome. *N Engl J Med* 336: 1568, 1997.

59. Benson AP, Al-Owais M, Holden AV. Quantitative prediction of the arrhythmogenic effects of de novo hERG mutations in computational models of human ventricular tissues. *Eur Biophys J* 40: 627–639, 2011.

60. Benton RE, Honig PK, Zamani K, Cantilena LR, Woosley RL. Grapefruit juice alters terfenadine pharmacokinetics, resulting in prolongation of repolarization on the electrocardiogram. *Clin Pharmacol Ther* 59: 383–388, 1996.

61. Berecki G, Zegers JG, Verkerk AO, Bhuiyan ZA, de Jonge B, Veldkamp MW, Wilders R, van Ginneken AC. HERG channel (dys)function revealed by dynamic action potential clamp technique. *Biophys J* 88: 566–578, 2005.

62. Berube J, Caouette D, Daleau P. Hydrogen peroxide modifies the kinetics of HERG channel expressed in a mammalian cell line. *J Pharmacol Exp Ther* 297: 96–102, 2001.

63. Bethell HW, Vandenberg JI, Smith GA, Grace AA. Changes in ventricular repolarization during acidosis and low-flow ischemia. *Am J Physiol Heart Circ Physiol* 275: H551–H561, 1998.

64. Bett GC, Rasmusson RL. Functionally-distinct proton-binding in HERG suggests the presence of two binding sites. *Cell Biochem Biophys* 39: 183–193, 2003.

65. Bezanilla F. The voltage sensor in voltage-dependent ion channels. *Physiol Rev* 80: 555–592, 2000.

66. Bezzina CR, Verkerk AO, Busjahn A, Jeron A, Erdmann J, Koopmann TT, Bhuiyan ZA, Wilders R, Mannens MM, Tan HL, Luft FC, Schunkert H, Wilde AA. A common polymorphism in KCNH2 (HERG) hastens cardiac repolarization. *Cardiovasc Res* 59: 27–36, 2003.

67. Bhuiyan ZA, Momenah TS, Gong Q, Amin AS, Ghamdi SA, Carvalho JS, Homfray T, Mannens MM, Zhou Z, Wilde AA. Recurrent intrauterine fetal loss due to near ab-

sence of HERG: clinical and functional characterization of a homozygous nonsense HERG Q1070X mutation. *Heart Rhythm* 5: 553–561, 2008.

68. Bhuvanagiri M, Schlitter AM, Hentze MW, Kulozik AE. NMD: RNA biology meets human genetic medicine. *Biochem J* 430: 365–377, 2010.

69. Bian J, Cui J, McDonald TV. HERG K^+ channel activity is regulated by changes in phosphatidyl inositol 4,5-bisphosphate. *Circ Res* 89: 1168–1176, 2001.

70. Bian JS, Kagan A, McDonald TV. Molecular analysis of PIP_2 regulation of HERG and IKr. *Am J Physiol Heart Circ Physiol* 287: H2154–H2163, 2004.

71. Bian JS, McDonald TV. Phosphatidylinositol 4,5-bisphosphate interactions with the HERG K^+ channel. *Pflügers Arch* 455: 105–113, 2007.

72. Bianchi L, Shen Z, Dennis AT, Priori SG, Napolitano C, Ronchetti E, Bryskin R, Schwartz PJ, Brown AM. Cellular dysfunction of LQT5-minK mutants: abnormalities of IKs, IKr and trafficking in long QT syndrome. *Hum Mol Genet* 8: 1499–1507, 1999.

73. Bianchi L, Wible B, Arcangeli A, Taglialatela M, Morra F, Castaldo P, Crociani O, Rosati B, Faravelli L, Olivotto M, Wanke E. herg encodes a K^+ current highly conserved in tumors of different histogenesis: a selective advantage for cancer cells? *Cancer Res* 58: 815–822, 1998.

74. Boukharta L, Keranen H, Stary-Weinzinger A, Wallin G, de Groot BL, Aqvist J. Computer simulations of structure-activity relationships for hERG channel blockers. *Biochemistry* 2011.

75. Brelidze TI, Carlson AE, Sankaran B, Zagotta WN. Structure of the carboxy-terminal region of a KCNH channel. *Nature*. In press.

76. Brelidze TI, Carlson AE, Zagotta WN. Absence of direct cyclic nucleotide modulation of mEAG1 and hERG1 channels revealed with fluorescence and electrophysiological methods. *J Biol Chem* 284: 27989–27997, 2009.

77. Bridal TR, Margulis M, Wang X, Donio M, Sorota S. Comparison of human Ether-a-go-go related gene screening assays based on IonWorks Quattro and thallium flux. *Assay Drug Dev Technol* 8: 755–765, 2010.

78. Bridgland-Taylor MH, Hargreaves AC, Easter A, Orme A, Henthorn DC, Ding M, Davis AM, Small BG, Heapy CG, Abi-Gerges N, Persson F, Jacobson I, Sullivan M, Albertson N, Hammond TG, Sullivan E, Valentin JP, Pollard CE. Optimisation and validation of a medium-throughput electrophysiology-based hERG assay using IonWorks HT. *J Pharmacol Toxicol Methods* 54: 189–199, 2006.

79. Brown HF, Giles W, Noble SJ. Membrane currents underlying activity in frog sinus venosus. *J Physiol* 271: 783–816, 1977.

80. Brugada R, Hong K, Dumaine R, Cordeiro J, Gaita F, Borggrefe M, Menendez TM, Brugada J, Pollevick GD, Wolpert C, Burashnikov E, Matsuo K, Wu YS, Guerchicoff A, Bianchi F, Giustetto C, Schimpf R, Brugada P, Antzelevitch C. Sudden death associated with short-QT syndrome linked to mutations in HERG. *Circulation* 109: 30–35, 2004.

81. Brunner M, Peng X, Liu GX, Ren XQ, Ziv O, Choi BR, Mathur R, Hajjiri M, Odening KE, Steinberg E, Folco EJ, Pringa E, Centracchio J, Macharzina RR, Donahay T, Schofield L, Rana N, Kirk M, Mitchell GF, Poppas A, Zehender M, Koren G. Mechanisms of cardiac arrhythmias and sudden death in transgenic rabbits with long QT syndrome. *J Clin Invest* 118: 2246–2259, 2008.

82. Burns CG, Milan DJ, Grande EJ, Rottbauer W, MacRae CA, Fishman MC. High-throughput assay for small molecules that modulate zebrafish embryonic heart rate. *Nat Chem Biol* 1: 263–264, 2005.

83. Cahalan MD. Local anesthetic block of sodium channels in normal and pronase-treated squid giant axons. *Biophys J* 23: 285–311, 1978.

84. Cahalan MD, Almers W. Block of sodium conductance and gating current in squid giant axons poisoned with quaternary strychnine. *Biophys J* 27: 57–73, 1979.

85. Carmeliet E. Use-dependent block and use-dependent unblock of the delayed rectifier K^+ current by almokalant in rabbit ventricular myocytes. *Circ Res* 73: 857–868, 1993.

86. Carmeliet E. Voltage- and time-dependent block of the delayed K^+ current in cardiac myocytes by dofetilide. *J Pharmacol Exp Ther* 262: 809–817, 1992.

87. Carrisoza R, Salvador C, Bobadilla NA, Trujillo J, Escobar LI. Expression and immunolocalization of ERG1 potassium channels in the rat kidney. *Histochem Cell Biol* 133: 189–199, 2010.

88. Casis O, Olesen SP, Sanguinetti MC. Mechanism of action of a novel human ether-a-go-go-related gene channel activator. *Mol Pharmacol* 69: 658–665, 2006.

89. Cavalli A, Poluzzi E, De Ponti F, Recanatini M. Toward a pharmacophore for drugs inducing the long QT syndrome: insights from a CoMFA study of HERG K^+ channel blockers. *J Med Chem* 45: 3844–3853, 2002.

90. Cayabyab FS, Schlichter LC. Regulation of an ERG K^+ current by Src tyrosine kinase. *J Biol Chem* 277: 13673–13681, 2002.

91. Cha A, Bezanilla F. Characterizing voltage-dependent conformational changes in the *Shaker* K^+ channel with fluorescence. *Neuron* 19: 1127–1140, 1997.

92. Chadwick CC, Ezrin AM, O'Connor B, Volberg WA, Smith DI, Wedge KJ, Hill RJ, Briggs GM, Pagani ED, Silver PJ. Identification of a specific radioligand for the cardiac rapidly activating delayed rectifier K^+ channel. *Circ Res* 72: 707–714, 1993.

93. Chagot B, Diochot S, Pimentel C, Lazdunski M, Darbon H. Solution structure of APETx1 from the sea anemone *Anthopleura elegantissima*: a new fold for an HERG toxin. *Proteins* 59: 380–386, 2005.

94. Chapman H, Ramstrom C, Korhonen L, Laine M, Wann KT, Lindholm D, Pasternack M, Tornquist K. Downregulation of the HERG (KCNH2) K^+ channel by ceramide: evidence for ubiquitin-mediated lysosomal degradation. *J Cell Sci* 118: 5325–5334, 2005.

95. Charlton NP, Lawrence DT, Brady WJ, Kirk MA, Holstege CP. Termination of drug-induced torsades de pointes with overdrive pacing. *Am J Emerg Med* 28: 95–102, 2010.

96. Chen J, Chen K, Sroubek J, Wu ZY, Thomas D, Bian JS, McDonald TV. Post-transcriptional control of human ether-a-go-go-related gene potassium channel protein by alpha-adrenergic receptor stimulation. *Mol Pharmacol* 78: 186–197, 2010.

97. Chen J, Seebohm G, Sanguinetti MC. Position of aromatic residues in the S6 domain, not inactivation, dictates cisapride sensitivity of HERG and eag potassium channels. *Proc Natl Acad Sci USA* 99: 12461–12466, 2002.

98. Chen J, Sroubek J, Krishnan Y, Li Y, Bian J, McDonald TV. PKA phosphorylation of HERG protein regulates the rate of channel synthesis. *Am J Physiol Heart Circ Physiol* 296: H1244–H1254, 2009.

99. Chen J, Zou A, Splawski I, Keating MT, Sanguinetti MC. Long QT syndrome-associated mutations in the Per-Arnt-Sim (PAS) domain of HERG potassium channels accelerate channel deactivation. *J Biol Chem* 274: 10113–10118, 1999.

100. Cherubini A, Hofmann G, Pillozzi S, Guasti L, Crociani O, Cilia E, Di Stefano P, Degani S, Balzi M, Olivotto M, Wanke E, Becchetti A, Defilippi P, Wymore R, Arcangeli A. Human ether-a-go-go-related gene 1 channels are physically linked to beta1 integrins and modulate adhesion-dependent signaling. *Mol Biol Cell* 16: 2972–2983, 2005.

101. Cherubini A, Taddei GL, Crociani O, Paglierani M, Buccoliero AM, Fontana L, Noci I, Borri P, Borrani E, Giachi M, Becchetti A, Rosati B, Wanke E, Olivotto M, Arcangeli A. HERG potassium channels are more frequently expressed in human endometrial cancer compared with non-cancerous endometrium. *Br J Cancer* 83: 1722–1729, 2000.

102. Chiesa N, Rosati B, Arcangeli A, Olivotto M, Wanke E. A novel role for HERG K^+ channels: spike-frequency adaptation. *J Physiol* 501: 313–318, 1997.

103. Chiu PJ, Marcoe KF, Bounds SE, Lin CH, Feng JJ, Lin A, Cheng FC, Crumb WJ, Mitchell R. Validation of a [^{3}H]astemizole binding assay in HEK293 cells expressing HERG K^+ channels. *J Pharmacol Sci* 95: 311–319, 2004.

104. Choe CU, Schulze-Bahr E, Neu A, Xu J, Zhu ZI, Sauter K, Bahring R, Priori S, Guicheney P, Monnig G, Neapolitano C, Heidemann J, Clancy CE, Pongs O, Isbrandt D. C-terminal HERG (LQT2) mutations disrupt IKr channel regulation through 14–3-3epsilon. *Hum Mol Genet* 15: 2888–2902, 2006.

105. Choe H, Nah KH, Lee SN, Lee HS, Jo SH, Leem CH, Jang YJ. A novel hypothesis for the binding mode of HERG channel blockers. *Biochem Biophys Res Commun* 344: 72–78, 2006.

106. Choi KL, Aldrich RW, Yellen G. Tetraethylammonium blockade distinguishes two inactivation mechanisms in voltage-activated K^+ channels. *Proc Natl Acad Sci USA* 88: 5092–5095, 1991.

107. Chun YS, Shin S, Kim Y, Cho H, Park MK, Kim TW, Voronov SV, Di Paolo G, Suh BC, Chung S. Cholesterol modulates ion channels via down-regulation of phosphatidylinositol 4,5-bisphosphate. *J Neurochem* 112: 1286–1294, 2010.

108. Clancy CE, Rudy Y. Cellular consequences of HERG mutations in the long QT syndrome: precursors to sudden cardiac death. *Cardiovasc Res* 50: 301–313, 2001.

109. Clark RB, Mangoni ME, Lueger A, Couette B, Nargeot J, Giles WR. A rapidly activating delayed rectifier K^+ current regulates pacemaker activity in adult mouse sinoatrial node cells. *Am J Physiol Heart Circ Physiol* 286: H1757–H1766, 2004.

110. Clarke CE, Hill AP, Zhao J, Kondo M, Subbiah RN, Campbell TJ, Vandenberg JI. Effect of S5P α-helix charge mutants on inactivation of hERG K^+ channels. *J Physiol* 573: 291–304, 2006.

111. Clarke OB, Caputo AT, Hill AP, Vandenberg JI, Smith BJ, Gulbis JM. Domain reorientation and rotation of an intracellular assembly regulate conduction in Kir potassium channels. *Cell* 1–20, 2010.

112. Claycomb WC, Lanson NA Jr, Stallworth BS, Egeland DB, Delcarpio JB, Bahinski A, Izzo NJ Jr. HL-1 cells: a cardiac muscle cell line that contracts and retains phenotypic characteristics of the adult cardiomyocyte. *Proc Natl Acad Sci USA* 95: 2979–2984, 1998.

113. Cockerill SL, Tobin AB, Torrecilla I, Willars GB, Standen NB, Mitcheson JS. Modulation of hERG potassium currents in HEK-293 cells by protein kinase C. Evidence for direct phosphorylation of pore forming subunits. *J Physiol* 581: 479–493, 2007.

114. Cooper DM. Compartmentalization of adenylate cyclase and cAMP signalling. *Biochem Soc Trans* 33: 1319–1322, 2005.

115. Cordeiro JM, Brugada R, Wu YS, Hong K, Dumaine R. Modulation of I(Kr) inactivation by mutation N588K in KCNH2: a link to arrhythmogenesis in short QT syndrome. *Cardiovasc Res* 67: 498–509, 2005.

116. Cordero-Morales JF, Jogini V, Lewis A, Vasquez V, Cortes DM, Roux B, Perozo E. Molecular driving forces determining potassium channel slow inactivation. *Nat Struct Mol Biol* 14: 1062–1069, 2007.

117. Cordes JS, Sun Z, Lloyd DB, Bradley JA, Opsahl AC, Tengowski MW, Chen X, Zhou J. Pentamidine reduces hERG expression to prolong the QT interval. *Br J Pharmacol* 145: 15–23, 2005.

118. Corona M, Gurrola GB, Merino E, Cassulini RR, Valdez-Cruz NA, Garcia B, Ramirez-Dominguez ME, Coronas FI, Zamudio FZ, Wanke E, Possani LD. A large number of novel Ergtoxin-like genes and ERG K^+-channels blocking peptides from scorpions of the genus Centruroides. *FEBS Lett* 532: 121–126, 2002.

119. Courtemanche M, Ramirez RJ, Nattel S. Ionic mechanisms underlying human atrial action potential properties: insights from a mathematical model. *Am J Physiol Heart Circ Physiol* 275: H301–H321, 1998.

120. Courtney KR. Mechanism of frequency-dependent inhibition of sodium currents in frog myelinated nerve by the lidocaine derivative GEA. *J Pharmacol Exp Ther* 195: 225–236, 1975.

121. Cousineau D, Ferguson RJ, de Champlain J, Gauthier P, Cote P, Bourassa M. Catecholamines in coronary sinus during exercise in man before and after training. *J Appl Physiol* 43: 801–806, 1977.

122. Crociani O, Cherubini A, Piccini E, Polvani S, Costa L, Fontana L, Hofmann G, Rosati B, Wanke E, Olivotto M, Arcangeli A. Erg gene(s) expression during development of the nervous and muscular system of quail embryos. *Mech Dev* 95: 239–243, 2000.

123. Crociani O, Guasti L, Balzi M, Becchetti A, Wanke E, Olivotto M, Wymore RS, Arcangeli A. Cell cycle-dependent expression of HERG1 and HERG1B isoforms in tumor cells. *J Biol Chem* 278: 2947–2955, 2003.

124. Crottes D, Martial S, Rapetti-Mauss R, Pisani DF, Loriol C, Pellissier B, Martin P, Chevet E, Borgese F, Soriani O. Sigma 1 receptor regulates HERG channel expression through a post-translational mechanism in leukemic cells. *J Biol Chem* 2011.

125. Crotti L, Lewandowska MA, Schwartz PJ, Insolia R, Pedrazzini M, Bussani E, Dagradi F, George AL Jr, Pagani F. A KCNH2 branch point mutation causing aberrant splicing contributes to an explanation of genotype-negative long QT syndrome. *Heart Rhythm* 6: 212–218, 2009.

126. Crotti L, Lundquist AL, Insolia R, Pedrazzini M, Ferrandi C, De Ferrari GM, Vicentini A, Yang P, Roden DM, George AL Jr, Schwartz PJ. KCNH2-K897T is a genetic modifier of latent congenital long-QT syndrome. *Circulation* 112: 1251–1258, 2005.

127. Cuello LG, Jogini V, Cortes DM, Perozo E. Structural mechanism of C-type inactivation in K^+ channels. *Nature* 466: 203–208, 2010.

128. Cuello LG, Jogini V, Cortes M, Pan A, Gagnon D, Dalmas O, Cordero-Morales J, Chakrapani S, Roux B, Perozo E. Structural basis for the coupling between activation and inactivation gates in K^+ channels. *Nature* 2010.

129. Cui J, Kagan A, Qin D, Mathew J, Melman YF, McDonald TV. Analysis of the cyclic nucleotide binding domain of the HERG potassium channel and interactions with KCNE2. *J Biol Chem* 276: 17244–17251, 2001.

130. Cui J, Melman Y, Palma E, Fishman GI, McDonald TV. Cyclic AMP regulates the HERG K^+ channel by dual pathways. *Curr Biol* 10: 671–674, 2000.

131. Curran M, Splawski I, Timothy K, Vincent G, Green E, Keating M. A molecular basis for cardiac arrhythmia: HERG mutations cause long QT syndrome. *Cell* 80: 795–803, 1995.

132. Curran ME, Splawski I, Timothy KW, Vincent GM, Green ED, Keating MT. A molecular basis for cardiac arrhythmia: HERG mutations cause long QT syndrome. *Cell* 80: 795–803, 1995.

133. Curtis LH, Ostbye T, Sendersky V, Hutchison S, Allen LaPointe NM, Al-Khatib SM, Usdin Yasuda S, Dans PE, Wright A, Califf RM, Woosley RL, Schulman KA. Prescription of QT-prolonging drugs in a cohort of about 5 million outpatients. *Am J Med* 114: 135–141, 2003.

134. Davey P. How to correct the QT interval for the effects of heart rate in clinical studies. *J Pharmacol Toxicol Methods* 48: 3–9, 2002.

135. De la Peña P, Alonso-Ron C, Machín A, Fernández-Trillo J, Carretero L, Domínguez P, Barros F. Demonstration of physical proximity between the N terminus and the S4–S5 linker of the human ether-a-go-go-related gene (hERG) potassium channel. *J Biol Chem* 286: 19065–19075, 2011.

136. De Ponti F, Poluzzi E, Cavalli A, Recanatini M, Montanaro N. Safety of non-antiarrhythmic drugs that prolong the QT interval or induce torsade de pointes: an overview. *Drug Saf* 25: 263–286, 2002.

137. Del Camino D, Yellen G. Tight steric closure at the intracellular activation gate of a voltage-gated K^+ channel. *Neuron* 32: 649–656, 2001.

138. Delisle BP, Anderson CL, Balijepalli RC, Anson BD, Kamp TJ, January CT. Thapsigargin selectively rescues the trafficking defective LQT2 channels G601S and F805C. *J Biol Chem* 278: 35749–35754, 2003.

139. Delisle BP, Anson BD, Rajamani S, January CT. Biology of cardiac arrhythmias: ion channel protein trafficking. *Circ Res* 94: 1418–1428, 2004.

140. Delisle BP, Underkofler HA, Moungey BM, Slind JK, Kilby JA, Best JM, Foell JD, Balijepalli RC, Kamp TJ, January CT. Small GTPase determinants for the Golgi processing and plasmalemmal expression of human ether-a-go-go related (hERG) K^+ channels. *J Biol Chem* 284: 2844–2853, 2009.

141. Dessertenne F. Ventricular tachycardia with 2 variable opposing foci. *Arch Mal Coeur Vaiss* 59: 263–272, 1966.

142. Deutsch C. Potassium channel ontogeny. *Annu Rev Physiol* 64: 19–46, 2002.

143. Diaz GJ, Daniell K, Leitza ST, Martin RL, Su Z, McDermott JS, Cox BF, Gintant GA. The [^{3}H]dofetilide binding assay is a predictive screening tool for hERG blockade and proarrhythmia: comparison of intact cell and membrane preparations and effects of altering $[K^+]_o$. *J Pharmacol Toxicol Methods* 50: 187–199, 2004.

144. DiFrancesco D. The role of the funny current in pacemaker activity. *Circ Res* 106: 434–446, 2010.

145. DiFrancesco D, Noma A, Trautwein W. Kinetics and magnitude of the time-dependent potassium current in the rabbit sinoatrial node: effect of external potassium. *Pflügers Arch* 381: 271–279, 1979.

146. Diller DJ, Hobbs DW. Understanding hERG inhibition with QSAR models based on a one-dimensional molecular representation. *J Comput Aided Mol Des* 21: 379–393, 2007.

147. Diness TG, Yeh YH, Qi XY, Chartier D, Tsuji Y, Hansen RS, Olesen SP, Grunnet M, Nattel S. Antiarrhythmic properties of a rapid delayed-rectifier current activator in rabbit models of acquired long QT syndrome. *Cardiovasc Res* 79: 61–69, 2008.

148. Diochot S, Loret E, Bruhn T, Beress L, Lazdunski M. APETx1, a new toxin from the sea anemone *Anthopleura elegantissima*, blocks voltage-gated human ether-a-go-go-related gene potassium channels. *Mol Pharmacol* 64: 59–69, 2003.

149. Dorn A, Hermann F, Ebneth A, Bothmann H, Trube G, Christensen K, Apfel C. Evaluation of a high-throughput fluorescence assay method for HERG potassium channel inhibition. *J Biomol Screen* 10: 339–347, 2005.

150. Doyle DA, Morais Cabral J, Pfuetzner RA, Kuo A, Gulbis JM, Cohen SL, Chait BT, MacKinnon R. The structure of the potassium channel: molecular basis of K^+ conduction and selectivity. *Science* 280: 69–77, 1998.

151. Dresser GK, Spence JD, Bailey DG. Pharmacokinetic-pharmacodynamic consequences and clinical relevance of cytochrome P450 3A4 inhibition. *Clin Pharmacokinet* 38: 41–57, 2000.

152. Du CY, Adeniran I, Cheng H, Zhang YH, El Harchi A, McPate MJ, Zhang H, Orchard CH, Hancox JC. Acidosis impairs the protective role of hERG K^+ channels against premature stimulation. *J Cardiovasc Electrophysiol* 21: 1160–1169, 2010.

153. Du CY, El Harchi A, McPate MJ, Orchard CH, Hancox JC. Enhanced inhibitory effect of acidosis on hERG potassium channels that incorporate the hERG1b isoform. *Biochem Biophys Res Commun* 405: 222–227, 2011.

154. Du CY, El Harchi A, Zhang YH, Orchard CH, Hancox JC. Pharmacological inhibition of the hERG potassium channel is modulated by extracellular but not intracellular acidosis. *J Cardiovasc Electrophysiol* 2011.

155. Du F, Yu H, Zou B, Babcock J, Long S, Li M. hERGCentral: a large database to store, retrieve, analyze compound-human Ether-a-go-go related gene channel interactions to facilitate cardiotoxicity assessment in drug development. *Assay Drug Dev Technol* 9: 580–588, 2011.

156. Dubus E, Ijjaali I, Petitet F, Michel A. In silico classification of HERG channel blockers: a knowledge-based strategy. *Chem Med Chem* 1: 622–630, 2006.

157. Ducroq J, Rouet R, Salle L, Puddu PE, Repesse Y, Ghadanfar M, Ducouret P, Gerard JL. Class III effects of dofetilide and arrhythmias are modulated by $[K^+]_o$ in an in vitro model of simulated-ischemia and reperfusion in guinea-pig ventricular myocardium. *Eur J Pharmacol* 532: 279–289, 2006.

158. Duff HJ, Feng ZP, Wang L, Sheldon RS. Regulation of expression of the [^{3}H]-dofetilide binding site associated with the delayed rectifier K^+ channel by dexamethasone in neonatal mouse ventricle. *J Mol Cell Cardiol* 29: 1959–1965, 1997.

159. Dun W, Jiang M, Tseng GN. Allosteric effects of mutations in the extracellular S5-P loop on the gating and ion permeation properties of the hERG potassium channel. *Pflügers Arch* 439: 141–149, 1999.

160. Durdagi S, Duff HJ, Noskov SY. Combined receptor and ligand-based approach to the universal pharmacophore model development for studies of drug blockade to the hERG1 pore domain. *J Chem Inf Model* 51: 463–474, 2011.

161. Ehrlich JR, Pourrier M, Weerapura M, Ethier N, Marmabachi AM, Hebert TE, Nattel S. KvLQT1 modulates the distribution and biophysical properties of HERG. A novel alpha-subunit interaction between delayed rectifier currents. *J Biol Chem* 279: 1233–1241, 2004.

162. Ekins S, Crumb WJ, Sarazan RD, Wikel JH, Wrighton SA. Three-dimensional quantitative structure-activity relationship for inhibition of human ether-a-go-go-related gene potassium channel. *J Pharmacol Exp Ther* 301: 427–434, 2002.

163. Elmedyb P, Olesen SP, Grunnet M. Activation of ERG2 potassium channels by the diphenylurea NS1643. *Neuropharmacology* 53: 283–294, 2007.

164. Emmi A, Wenzel HJ, Schwartzkroin PA, Taglialatela M, Castaldo P, Bianchi L, Nerbonne J, Robertson GA, Janigro D. Do glia have heart? Expression and functional role for ether-a-go-go currents in hippocampal astrocytes. *J Neurosci* 20: 3915–3925, 2000.

165. Es-Salah-Lamoureux Z, Fougere R, Xiong PY, Robertson GA, Fedida D. Fluorescence-tracking of activation gating in human ERG channels reveals rapid S4 movement and slow pore opening. *PLoS One* 5: e10876, 2010.

166. Es-Salah-Lamoureux Z, Xiong PY, Goodchild SJ, Ahern CA, Fedida D. Blockade of permeation by potassium but normal gating of the G628S nonconducting hERG channel mutant. *Biophys J* 101: 662–670, 2011.

167. Fan JS, Jiang M, Dun W, McDonald TV, Tseng GN. Effects of outer mouth mutations on hERG channel function: a comparison with similar mutations in the *Shaker* channel. *Biophys J* 76: 3128–3140, 1999.

168. Farid R, Day T, Friesner RA, Pearlstein RA. New insights about HERG blockade obtained from protein modeling, potential energy mapping, and docking studies. *Bioorg Med Chem* 14: 3160–3173, 2006.

169. Farrelly AM, Ro S, Callaghan BP, Khoyi MA, Fleming N, Horowitz B, Sanders KM, Keef KD. Expression and function of KCNH2 (HERG) in the human jejunum. *Am J Physiol Gastrointest Liver Physiol* 284: G883–G895, 2003.

170. Fauchier L, Babuty D, Poret P, Autret ML, Cosnay P, Fauchier JP. Effect of verapamil on QT interval dynamicity. *Am J Cardiol* 83: 807–808, 1999.

171. Feldman DS, Carnes CA, Abraham WT, Bristow MR. Mechanisms of disease: beta-adrenergic receptors–alterations in signal transduction and pharmacogenomics in heart failure. *Nat Clin Pract Cardiovasc Med* 2: 475–483, 2005.

172. Fernandez D, Ghanta A, Kauffman GW, Sanguinetti MC. Physicochemical features of the HERG channel drug binding site. *J Biol Chem* 279: 10120–10127, 2004.

173. Ferrer T, Rupp J, Piper DR, Tristani-Firouzi M. The S4–S5 linker directly couples voltage sensor movement to the activation gate in the human ether-a'-go-go-related gene (hERG) K^+ channel. *J Biol Chem* 281: 12858–12864, 2006.

174. Ficker E, Dennis A, Kuryshev Y, Wible BA, Brown AM. HERG channel trafficking. *Novartis Found Symp* 266: 57–69, 2005.

175. Ficker E, Dennis AT, Obejero-Paz CA, Castaldo P, Taglialatela M, Brown AM. Retention in the endoplasmic reticulum as a mechanism of dominant-negative current suppression in human long QT syndrome. *J Mol Cell Cardiol* 32: 2327–2337, 2000.

176. Ficker E, Dennis AT, Wang L, Brown AM. Role of the cytosolic chaperones Hsp70 and Hsp90 in maturation of the cardiac potassium channel HERG. *Circ Res* 92: e87–100, 2003.

177. Ficker E, Jarolimek W, Brown AM. Molecular determinants of inactivation and dofetilide block in ether a-go-go (EAG) channels and EAG-related K^+ channels. *Mol Pharmacol* 60: 1343–1348, 2001.

178. Ficker E, Jarolimek W, Kiehn J, Baumann A, Brown AM. Molecular determinants of dofetilide block of HERG K^+ channels. *Circ Res* 82: 386–395, 1998.

179. Ficker E, Kuryshev YA, Dennis AT, Obejero-Paz C, Wang L, Hawryluk P, Wible BA, Brown AM. Mechanisms of arsenic-induced prolongation of cardiac repolarization. *Mol Pharmacol* 66: 33–44, 2004.

180. Ficker E, Obejero-Paz CA, Zhao S, Brown AM. The binding site for channel blockers that rescue misprocessed human long QT syndrome type 2 ether-a-gogo-related gene (HERG) mutations. *J Biol Chem* 277: 4989–4998, 2002.

181. Ficker E, Thomas D, Viswanathan PC, Dennis AT, Priori SG, Napolitano C, Memmi M, Wible BA, Kaufman ES, Iyengar S, Schwartz PJ, Rudy Y, Brown AM. Novel characteristics of a misprocessed mutant HERG channel linked to hereditary long QT syndrome. *Am J Physiol Heart Circ Physiol* 279: H1748–H1756, 2000.

182. Finlayson K, Pennington AJ, Kelly JS. [^{3}H]dofetilide binding in SHSY5Y and HEK293 cells expressing a HERG-like K^+ channel? *Eur J Pharmacol* 412: 203–212, 2001.

183. Finlayson K, Turnbull L, January CT, Sharkey J, Kelly JS. [^{3}H]dofetilide binding to HERG transfected membranes: a potential high throughput preclinical screen. *Eur J Pharmacol* 430: 147–148, 2001.

184. Finley MR, Li Y, Hua F, Lillich J, Mitchell KE, Ganta S, Gilmour RF Jr, Freeman LC. Expression and coassociation of ERG1, KCNQ1, and KCNE1 potassium channel proteins in horse heart. *Am J Physiol Heart Circ Physiol* 283: H126–H138, 2002.

185. Fontana L, D'Amico M, Crociani O, Biagiotti T, Solazzo M, Rosati B, Arcangeli A, Wanke E, Olivotto M. Long-term modulation of HERG channel gating in hypoxia. *Biochem Biophys Res Commun* 286: 857–862, 2001.

186. Fossa AA, Wisialowski T, Wolfgang E, Wang E, Avery M, Raunig DL, Fermini B. Differential effect of HERG blocking agents on cardiac electrical alternans in the guinea pig. *Eur J Pharmacol* 486: 209–221, 2004.

187. Fougere RR, Es-Salah-Lamoureux Z, Rezazadeh S, Eldstrom J, Fedida D. Functional characterization of the LQT2-causing mutation R582C and the associated voltage-dependent fluorescence signal. *Heart Rhythm* 2011.

188. Fu H, Subramanian RR, Masters SC. 14–3-3 proteins: structure, function, and regulation. *Annu Rev Pharmacol Toxicol* 40: 617–647, 2000.

189. Fulop L, Banyasz T, Szabo G, Toth IB, Biro T, Lorincz I, Balogh A, Peto K, Miko I, Nanasi PP. Effects of sex hormones on ECG parameters and expression of cardiac ion channels in dogs. *Acta Physiol* 188: 163–171, 2006.

190. Furlan F, Taccola G, Grandolfo M, Guasti L, Arcangeli A, Nistri A, Ballerini L. ERG conductance expression modulates the excitability of ventral horn GABAergic interneurons that control rhythmic oscillations in the developing mouse spinal cord. *J Neurosci* 27: 919–928, 2007.

191. Furukawa Y, Miyashita Y, Nakajima K, Hirose M, Kurogouchi F, Chiba S. Effects of verapamil, zatebradine, and E-4031 on the pacemaker location and rate in response to sympathetic stimulation in dog hearts. *J Pharmacol Exp Ther* 289: 1334–1342, 1999.

192. Furutani M, Trudeau MC, Hagiwara N, Seki A, Gong Q, Zhou Z, Imamura S, Nagashima H, Kasanuki H, Takao A, Momma K, January CT, Robertson GA, Matsuoka R. Novel mechanism associated with an inherited cardiac arrhythmia: defective protein trafficking by the mutant HERG (G601S) potassium channel. *Circulation* 99: 2290–2294, 1999.

193. Gaborit N, Le Bouter S, Szuts V, Varro A, Escande D, Nattel S, Demolombe S. Regional and tissue specific transcript signatures of ion channel genes in the non-diseased human heart. *J Physiol* 582: 675–693, 2007.

194. Gaborit N, Varro A, Le Bouter S, Szuts V, Escande D, Nattel S, Demolombe S. Gender-related differences in ion-channel and transporter subunit expression in non-diseased human hearts. *J Mol Cell Cardiol* 49: 639–646, 2010.

195. Gaita F, Giustetto C, Bianchi F, Schimpf R, Haissaguerre M, Calo L, Brugada R, Antzelevitch C, Borggrefe M, Wolpert C. Short QT syndrome: pharmacological treatment. *J Am Coll Cardiol* 43: 1494–1499, 2004.

196. Ganapathi SB, Fox TE, Kester M, Elmslie KS. Ceramide modulates HERG potassium channel gating by translocation into lipid rafts. *Am J Physiol Cell Physiol* 299: C74–C86, 2010.

197. Gang H, Zhang S. Na^+ permeation and block of hERG potassium channels. *J Gen Physiol* 128: 55–71, 2006.

198. Ganitkevich V, Reil S, Schwethelm B, Schroeter T, Benndorf K. Dynamic responses of single cardiomyocytes to graded ischemia studied by oxygen clamp in on-chip picochambers. *Circ Res* 99: 165–171, 2006.

199. Garcia-Quiroz J, Camacho J. Astemizole: an old anti-histamine as a new promising anti-cancer drug. *Anti-Cancer Agents Med Chem* 11: 307–314, 2011.

200. Garg V, Stary-Weinzinger A, Sachse F, Sanguinetti M. Molecular determinants for activation of human ERG1 potassium channels by 3-nitro-*N*-(4-phenoxyphenyl) benzamide. *Mol Pharm.* In press.

201. Gavaghan CL, Arnby CH, Blomberg N, Strandlund G, Boyer S. Development, interpretation and temporal evaluation of a global QSAR of hERG electrophysiology screening data. *J Comput Aided Mol Des* 21: 189–206, 2007.

202. Gelman MS, Kopito RR. Rescuing protein conformation: prospects for pharmacological therapy in cystic fibrosis. *J Clin Invest* 110: 1591–1597, 2002.

203. Gentile S, Darden T, Erxleben C, Romeo C, Russo A, Martin N, Rossie S, Armstrong DL. Rac GTPase signaling through the PP5 protein phosphatase. *Proc Natl Acad Sci USA* 103: 5202–5206, 2006.

204. Gentile S, Martin N, Scappini E, Williams J, Erxleben C, Armstrong DL. The human ERG1 channel polymorphism, K897T, creates a phosphorylation site that inhibits channel activity. *Proc Natl Acad Sci USA* 105: 14704–14708, 2008.

205. Gerlach AC, Stoehr SJ, Castle NA. Pharmacological removal of human ether-a-go-go-related gene potassium channel inactivation by 3-nitro-*N*-(4-phenoxyphenyl) benzamide (ICA-105574). *Mol Pharmacol* 77: 58–68, 2010.

206. Gessner G, Heinemann SH. Inhibition of hEAG1 and hERG1 potassium channels by clofilium and its tertiary analogue LY97241. *Br J Pharmacol* 138: 161–171, 2003.

207. Gessner G, Macianskiene R, Starkus JG, Schonherr R, Heinemann SH. The amiodarone derivative KB130015 activates hERG1 potassium channels via a novel mechanism. *Eur J Pharmacol* 632: 52–59, 2010.

208. Gessner G, Zacharias M, Bechstedt S, Schonherr R, Heinemann SH. Molecular determinants for high-affinity block of human EAG potassium channels by antiarrhythmic agents. *Mol Pharmacol* 65: 1120–1129, 2004.

209. Gianulis EC, Trudeau MC. Rescue of aberrant gating by a genetically-encoded PAS (Per-Arnt-Sim) domain in several long QT syndrome mutant human ERG (hERG) potassium channels. *J Biol Chem* 2011.

210. Gintant GA. Preclinical Torsades-de-Pointes screens: advantages and limitations of surrogate and direct approaches in evaluating proarrhythmic risk. *Pharmacol Ther* 119: 199–209, 2008.

211. Goldenberg I, Bradley J, Moss A, McNitt S, Polonsky S, Robinson JL, Andrews M, Zareba W. Beta-blocker efficacy in high-risk patients with the congenital long-QT syndrome types 1 and 2: implications for patient management. *J Cardiovasc Electrophysiol* 21: 893–901, 2010.

212. Goldstein SA, Miller C. Mechanism of charybdotoxin block of a voltage-gated K^+ channel. *Biophys J* 65: 1613–1619, 1993.

213. Gomez-Varela D, Giraldez T, de la Pena P, Dupuy SG, Garcia-Manso D, Barros F. Protein kinase C is necessary for recovery from the thyrotropin-releasing hormone-induced r-ERG current reduction in GH3 rat anterior pituitary cells. *J Physiol* 547: 913–929, 2003.

214. Gong Q, Anderson CL, January CT, Zhou Z. Role of glycosylation in cell surface expression and stability of HERG potassium channels. *Am J Physiol Heart Circ Physiol* 283: H77–H84, 2002.

215. Gong Q, Jones MA, Zhou Z. Mechanisms of pharmacological rescue of trafficking-defective hERG mutant channels in human long QT syndrome. *J Biol Chem* 281: 4069–4074, 2006.

216. Gong Q, Keeney DR, Molinari M, Zhou Z. Degradation of trafficking-defective long QT syndrome type II mutant channels by the ubiquitin-proteasome pathway. *J Biol Chem* 280: 19419–19425, 2005.

217. Gong Q, Zhang L, Moss AJ, Vincent GM, Ackerman MJ, Robinson JC, Jones MA, Tester DJ, Zhou Z. A splice site mutation in hERG leads to cryptic splicing in human long QT syndrome. *J Mol Cell Cardiol* 44: 502–509, 2008.

218. Gong Q, Zhang L, Vincent GM, Horne BD, Zhou Z. Nonsense mutations in hERG cause a decrease in mutant mRNA transcripts by nonsense-mediated mRNA decay in human long-QT syndrome. *Circulation* 116: 17–24, 2007.

219. Grandi E, Pasqualini FS, Bers DM. A novel computational model of the human ventricular action potential and Ca transient. *J Mol Cell Cardiol* 48: 112–121, 2010.

220. Greenwood IA, Yeung SY, Tribe RM, Ohya S. Loss of functional K^+ channels encoded by ether-a-go-go-related genes in mouse myometrium prior to labour onset. *J Physiol* 587: 2313–2326, 2009.

221. Gronich N, Kumar A, Zhang Y, Efimov IR, Soldatov NM. Molecular remodeling of ion channels, exchangers and pumps in atrial and ventricular myocytes in ischemic cardiomyopathy. *Channels* 4: 101–107, 2010.

222. Grunnet M, Abbruzzese J, Sachse FB, Sanguinetti MC. Molecular determinants of human ether-a-go-go-related gene 1 (hERG1) K^+ channel activation by NS1643. *Mol Pharmacol* 79: 1–9, 2011.

223. Grunnet M, Hansen RS, Olesen SP. hERG1 channel activators: a new anti-arrhythmic principle. *Prog Biophys Mol Biol* 98: 347–362, 2008.

224. Guasti L, Cilia E, Crociani O, Hofmann G, Polvani S, Becchetti A, Wanke E, Tempia F, Arcangeli A. Expression pattern of the ether-a-go-go-related (ERG) family proteins in the adult mouse central nervous system: evidence for coassembly of different subunits. *J Comp Neurol* 491: 157–174, 2005.

225. Gullo F, Ales E, Rosati B, Lecchi M, Masi A, Guasti L, Cano-Abad MF, Arcangeli A, Lopez MG, Wanke E. ERG K^+ channel blockade enhances firing and epinephrine secretion in rat chromaffin cells: the missing link to LQT2-related sudden death? *FASEB J* 17: 330–332, 2003.

226. Guo J, Massaeli H, Li W, Xu J, Luo T, Shaw J, Kirshenbaum LA, Zhang S. Identification of IKr and its trafficking disruption induced by probucol in cultured neonatal rat cardiomyocytes. *J Pharmacol Exp Ther* 321: 911–920, 2007.

227. Guo J, Massaeli H, Xu J, Jia Z, Wigle JT, Mesaeli N, Zhang S. Extracellular K^+ concentration controls cell surface density of IKr in rabbit hearts and of the HERG channel in human cell lines. *J Clin Invest* 119: 2745–2757, 2009.

228. Guo J, Zhan S, Lees-Miller JP, Teng G, Duff HJ. Exaggerated block of hERG (KCNH2) and prolongation of action potential duration by erythromycin at temperatures between 37 degrees C and 42 degrees C. *Heart Rhythm* 2: 860–866, 2005.

229. Gurrola GB, Rosati B, Rocchetti M, Pimienta G, Zaza A, Arcangeli A, Olivotto M, Possani LD, Wanke E. A toxin to nervous, cardiac, and endocrine ERG K^+ channels isolated from *Centruroides noxius* scorpion venom. *FASEB J* 13: 953–962, 1999.

230. Gussak I, Brugada P, Brugada J, Wright RS, Kopecky SL, Chaitman BR, Bjerregaard P. Idiopathic short QT interval: a new clinical syndrome? *Cardiology* 94: 99–102, 2000.

231. Gustina AS, Trudeau MC. hERG potassium channel gating is mediated by N- and C-terminal region interactions. *J Gen Physiol* 137: 315–325, 2011.

232. Gustina AS, Trudeau MC. A recombinant N-terminal domain fully restores deactivation gating in N-truncated and long QT syndrome mutant hERG potassium channels. *Proc Natl Acad Sci USA* 106: 13082–13087, 2009.

233. Gutman GA, Chandy KG, Adelman JP, Aiyar J, Bayliss DA, Clapham DE, Covarriubias M, Desir GV, Furuichi K, Ganetzky B, Garcia ML, Grissmer S, Jan LY, Karschin A, Kim D, Kuperschmidt S, Kurachi Y, Lazdunski M, Lesage F, Lester HA, McKinnon D, Nichols CG, O'Kelly I, Robbins J, Robertson GA, Rudy B, Sanguinetti M, Seino S, Stuehmer W, Tamkun MM, Vandenberg CA, Wei A, Wulff H, Wymore RS. International Union of Pharmacology. XLI. Compendium of voltage-gated ion channels: potassium channels. *Pharmacol Rev* 55: 583–586, 2003.

234. Hackos DH, Chang TH, Swartz KJ. Scanning the intracellular S6 activation gate in the shaker K^+ channel. *J Gen Physiol* 119: 521–532, 2002.

235. Hagiwara S, Miyazaki S, Moody W, Patlak J. Blocking effects of barium and hydrogen ions on the potassium current during anomalous rectification in the starfish egg. *J Physiol* 279: 167–185, 1978.

236. Hagiwara S, Miyazaki S, Rosenthal NP. Potassium current and the effect of cesium on this current during anomalous rectification of the egg cell membrane of a starfish. *J Gen Physiol* 67: 621–638, 1976.

237. Hamill OP, Marty A, Neher E, Sakmann B, Sigworth FJ. Improved patch-clamp techniques for high-resolution current recording from cells and cell-free membrane patches. *Pflügers Arch* 391: 85–100, 1981.

238. Hancox JC, McPate MJ, El Harchi A, Zhang YH. The hERG potassium channel and hERG screening for drug-induced torsades de pointes. *Pharmacol Ther* 119: 118–132, 2008.

239. Hanrahan JP, Choo PW, Carlson W, Greineder D, Faich GA, Platt R. Terfenadine-associated ventricular arrhythmias and QT_c interval prolongation. A retrospective cohort comparison with other antihistamines among members of a health maintenance organization. *Ann Epidemiol* 5: 201–209, 1995.

240. Hansen RS, Diness TG, Christ T, Demnitz J, Ravens U, Olesen SP, Grunnet M. Activation of human ether-a-go-go-related gene potassium channels by the diphenylurea 1,3-bis-(2-hydroxy-5-trifluoromethyl-phenyl)-urea (NS1643). *Mol Pharmacol* 69: 266–277, 2006.

241. Hansen RS, Diness TG, Christ T, Wettwer E, Ravens U, Olesen SP, Grunnet M. Biophysical characterization of the new human ether-a-go-go-related gene channel opener NS3623 [*N*-(4-bromo-2-(1H-tetrazol-5-yl)-phenyl)-N'-(3'-trifluoromethyl-phenyl)urea]. *Mol Pharmacol* 70: 1319–1329, 2006.

242. Hansen RS, Olesen SP, Grunnet M. Pharmacological activation of rapid delayed rectifier potassium current suppresses bradycardia-induced triggered activity in the isolated guinea pig heart. *J Pharmacol Exp Ther* 321: 996–1002, 2007.

243. Hansen RS, Olesen SP, Ronn LC, Grunnet M. In vivo effects of the IKr agonist NS3623 on cardiac electrophysiology of the guinea pig. *J Cardiovasc Pharmacol* 52: 35–41, 2008.

244. Hansen SB, Tao X, MacKinnon R. Structural basis of PIP_2 activation of the classical inward rectifier K^+ channel Kir2.2. *Nature* 477: 495–498, 2011.

245. Hardman RM, Stansfeld PJ, Dalibalta S, Sutcliffe MJ, Mitcheson JS. Activation gating of hERG potassium channels: S6 glycines are not required as gating hinges. *J Biol Chem* 282: 31972–31981, 2007.

246. Harmati G, Banyasz T, Barandi L, Szentandrassy N, Horvath B, Szabo G, Szentmiklosi JA, Szenasi G, Nanasi PP, Magyar J. Effects of beta-adrenoceptor stimulation on delayed rectifier K^+ currents in canine ventricular cardiomyocytes. *Br J Pharmacol* 162: 890–896, 2011.

247. Harvey RD, Hume JR. Autonomic regulation of a chloride current in heart. *Science* 244: 983–985, 1989.

248. Hassel D, Scholz EP, Trano N, Friedrich O, Just S, Meder B, Weiss DL, Zitron E, Marquart S, Vogel B, Karle CA, Seemann G, Fishman MC, Katus HA, Rottbauer W. Deficient zebrafish ether-a-go-go-related gene channel gating causes short-QT syndrome in zebrafish reggae mutants. *Circulation* 117: 866–875, 2008.

249. Hayashi K, Fujino N, Ino H, Uchiyama K, Sakata K, Konno T, Masuta E, Funada A, Sakamoto Y, Tsubokawa T, Hodatsu A, Yasuda T, Kanaya H, Kim MY, Kupershmidt S, Higashida H, Yamagishi M. A KCR1 variant implicated in susceptibility to the long QT syndrome. *J Mol Cell Cardiol* 50: 50–57, 2011.

250. Hayashi K, Shuai W, Sakamoto Y, Higashida H, Yamagishi M, Kupershmidt S. Trafficking-competent KCNQ1 variably influences the function of HERG long QT alleles. *Heart Rhythm* 7: 973–980, 2010.

251. Heath BM, Terrar DA. Protein kinase C enhances the rapidly activating delayed rectifier potassium current, IKr, through a reduction in C-type inactivation in guinea-pig ventricular myocytes. *J Physiol* 522: 391–402, 2000.

252. Heginbotham L, MacKinnon R. The aromatic binding site for tetraethylammonium ion on potassium channels. *Neuron* 8: 483–491, 1992.

253. Hegle AP, Marble DD, Wilson GF. A voltage-driven switch for ion-independent signaling by ether-a-go-go K^+ channels. *Proc Natl Acad Sci USA* 103: 2886–2891, 2006.

254. Herzberg IM, Trudeau MC, Robertson GA. Transfer of rapid inactivation and sensitivity to the class III antiarrhythmic drug E-4031 from HERG to M-eag channels. *J Physiol* 511: 3–14, 1998.

255. Hill AP, Campbell TJ, Bansal PS, Kuchel PW, Vandenberg JI. The S631A mutation causes a mechanistic switch in the block of hERG channels by CnErg1. *Biophys J* 93: L32–34, 2007.

256. Hill AP, Sunde M, Campbell TJ, Vandenberg JI. Mechanism of block of the hERG K^+ channel by the scorpion toxin CnErg1. *Biophys J* 92: 3915–3929, 2007.

257. Hille B. *Ionic Channels of Excitable Membranes*. Sunderland, MA: Sinauer, 2001.

258. Hille B. Local anesthetics: hydrophilic and hydrophobic pathways for the drug-receptor reaction. *J Gen Physiol* 69: 497–515, 1977.

259. Hille B. The pH-dependent rate of action of local anesthetics on the node of Ranvier. *J Gen Physiol* 69: 475–496, 1977.

260. Hirdes W, Horowitz LF, Hille B. Muscarinic modulation of erg potassium current. *J Physiol* 559: 67–84, 2004.

261. Ho WK, Kim I, Lee CO, Earm YE. Voltage-dependent blockade of HERG channels expressed in *Xenopus* oocytes by external Ca^{2+} and Mg^{2+}. *J Physiol* 507: 631–638, 1998.

262. Ho WK, Kim I, Lee CO, Youm JB, Lee SH, Earm YE. Blockade of HERG channels expressed in *Xenopus laevis* oocytes by external divalent cations. *Biophys J* 76: 1959–1971, 1999.

263. Hodgkin AL, Huxley AF. A quantitative description of membrane current and its application to conduction and excitation in nerve. *J Physiol* 117: 500–544, 1952.

264. Hofmann G, Bernabei PA, Crociani O, Cherubini A, Guasti L, Pillozzi S, Lastraioli E, Polvani S, Bartolozzi B, Solazzo V, Gragnani L, Defilippi P, Rosati B, Wanke E, Olivotto M, Arcangeli A. HERG K^+ channels activation during beta(1) integrin-mediated adhesion to fibronectin induces an up-regulation of alpha(v)beta(3) integrin in the preosteoclastic leukemia cell line FLG 29.*1 J Biol Chem* 276: 4923–4931, 2001.

265. Hohnloser SH, Klingenheben T, Singh BN. Amiodarone-associated proarrhythmic effects. A review with special reference to torsade de pointes tachycardia. *Ann Intern Med* 121: 529–535, 1994.

266. Hondeghem LM, Carlsson L, Duker G. Instability and triangulation of the action potential predict serious proarrhythmia, but action potential duration prolongation is antiarrhythmic. *Circulation* 103: 2004–2013, 2001.

267. Hondeghem LM, Hoffmann P. Blinded test in isolated female rabbit heart reliably identifies action potential duration prolongation and proarrhythmic drugs: importance of triangulation, reverse use dependence, and instability. *J Cardiovasc Pharmacol* 41: 14–24, 2003.

268. Hondeghem LM, Katzung BG. Time- and voltage-dependent interactions of antiarrhythmic drugs with cardiac sodium channels. *Biochim Biophys Acta* 472: 373–398, 1977.

269. Hondeghem LM, Snyders DJ. Class III antiarrhythmic agents have a lot of potential but a long way to go. Reduced effectiveness and dangers of reverse use dependence. *Circulation* 81: 686–690, 1990.

270. Hool LC. Differential regulation of the slow and rapid components of guinea-pig cardiac delayed rectifier K^+ channels by hypoxia. *J Physiol* 554: 743–754, 2004.

271. Horie M, Hayashi S, Kawai C. Two types of delayed rectifying K^+ channels in atrial cells of guinea pig heart. *Jpn J Physiol* 40: 479–490, 1990.

272. Hosaka Y, Iwata M, Kamiya N, Yamada M, Kinoshita K, Fukunishi Y, Tsujimae K, Hibino H, Aizawa Y, Inanobe A, Nakamura H, Kurachi Y. Mutational analysis of block and facilitation of HERG current by a class III anti-arrhythmic agent, nifekalant. *Channels* 1: 198–208, 2007.

273. Hoshi N, Takahashi H, Shahidullah M, Yokoyama S, Higashida H. KCR1, a membrane protein that facilitates functional expression of non-inactivating K^+ currents associates with rat EAG voltage-dependent K^+ channels. *J Biol Chem* 273: 23080–23085, 1998.

274. Hoshi T, Zagotta WN, Aldrich RW. Biophysical and molecular mechanisms of Shaker potassium channel inactivation. *Science* 250: 533–538, 1990.

275. Hoshi T, Zagotta WN, Aldrich RW. Shaker potassium channel gating. I. Transitions near the open state. *J Gen Physiol* 103: 249–278, 1994.

276. Hoshi T, Zagotta WN, Aldrich RW. Two types of inactivation in *Shaker* K^+ channels: effects of alterations in the carboxy-terminal region. *Neuron* 7: 547–556, 1991.

277. Hu C, Yan C, Lin J, Liu S, Li Y. Down-regulation of the human ether-a-go-go-related gene in rat cardiac hypertrophy. *Am J Med Sci* 341: 119–125, 2011.

278. Huang XP, Mangano T, Hufeisen S, Setola V, Roth BL. Identification of human Ether-a-go-go related gene modulators by three screening platforms in an academic drug-discovery setting. *Assay Drug Dev Technol* 8: 727–742, 2010.

279. Huffaker SJ, Chen J, Nicodemus KK, Sambataro F, Yang F, Mattay V, Lipska BK, Hyde TM, Song J, Rujescu D, Giegling I, Mayilyan K, Proust MJ, Soghoyan A, Caforio G, Callicott JH, Bertolino A, Meyer-Lindenberg A, Chang J, Ji Y, Egan MF, Goldberg TE, Kleinman JE, Lu B, Weinberger DR. A primate-specific, brain isoform of KCNH2 affects cortical physiology, cognition, and neuronal repolarization and risk of schizophrenia. *Nat Med* 15: 509–518, 2009.

280. Iancu RV, Ramamurthy G, Warrier S, Nikolaev VO, Lohse MJ, Jones SW, Harvey RD. Cytoplasmic cAMP concentrations in intact cardiac myocytes. *Am J Physiol Cell Physiol* 295: C414–C422, 2008.

281. Imai T, Okamoto T, Yamamoto Y, Tanaka H, Koike K, Shigenobu K, Tanaka Y. Effects of different types of K^+ channel modulators on the spontaneous myogenic contraction of guinea-pig urinary bladder smooth muscle. *Acta Physiol Scand* 173: 323–333, 2001.

282. Imai YN, Ryu S, Oiki S. Docking model of drug binding to the human ether-a-go-go potassium channel guided by tandem dimer mutant patch-clamp data: a synergic approach. *J Med Chem* 52: 1630–1638, 2009.

283. Itoh H, Horie M, Ito M, Imoto K. Arrhythmogenesis in the short-QT syndrome associated with combined HERG channel gating defects: a simulation study. *Circ J* 70: 502–508, 2006.

284. Itoh H, Sakaguchi T, Ashihara T, Ding WG, Nagaoka I, Oka Y, Nakazawa Y, Yao T, Jo H, Ito M, Nakamura K, Ohe T, Matsuura H, Horie M. A novel KCNH2 mutation as a modifier for short QT interval. *Int J Cardiol* 137: 83–85, 2009.

285. Itoh T, Tanaka T, Nagai R, Kamiya T, Sawayama T, Nakayama T, Tomoike H, Sakurada H, Yazaki Y, Nakamura Y. Genomic organization and mutational analysis of HERG, a gene responsible for familial long QT syndrome. *Hum Genet* 102: 435–439, 1998.

286. Iyer V, Mazhari R, Winslow RL. A computational model of the human left-ventricular epicardial myocyte. *Biophys J* 87: 1507–1525, 2004.

287. Jackson RJ, Hellen CU, Pestova TV. The mechanism of eukaryotic translation initiation and principles of its regulation. *Nat Rev Mol Cell Biol* 11: 113–127, 2010.

288. James AF, Choisy SC, Hancox JC. Recent advances in understanding sex differences in cardiac repolarization. *Prog Biophys Mol Biol* 94: 265–319, 2007.

289. Jenke M, Sanchez A, Monje F, Stuhmer W, Weseloh RM, Pardo LA. C-terminal domains implicated in the functional surface expression of potassium channels. *EMBO J* 22: 395–403, 2003.

290. Jervell A, Lange-Nielsen F. Congenital deaf-mutism, functional heart disease with prolongation of the QT interval and sudden death. *Am Heart J* 54: 59–68, 1957.

291. Jia L, Sun H. Support vector machines classification of hERG liabilities based on atom types. *Bioorg Med Chem* 16: 6252–6260, 2008.

292. Jiang C, Atkinson D, Towbin J, Splawski I, Lehmann M, Li H, Timothy K, Taggart R, Schwartz P, Vincent G. Two long QT syndrome loci map to chromosomes 3 and 7 with evidence for further heterogeneity. *Nat Genet* 8: 141–147, 1994.

293. Jiang M, Dun W, Fan JS, Tseng GN. Use-dependent "agonist" effect of azimilide on the HERG channel. *J Pharmacol Exp Ther* 291: 1324–1336, 1999.

294. Jiang M, Dun W, Tseng GN. Mechanism for the effects of extracellular acidification on HERG-channel function. *Am J Physiol Heart Circ Physiol* 277: H1283–H1292, 1999.

295. Jiang M, Zhang M, Maslennikov IV, Liu J, Wu DM, Korolkova YV, Arseniev AS, Grishin EV, Tseng GN. Dynamic conformational changes of extracellular S5-P linkers in the hERG channel. *J Physiol* 569: 75–89, 2005.

296. Jiang Y, Lee A, Chen J, Cadene M, Chait BT, MacKinnon R. Crystal structure and mechanism of a calcium-gated potassium channel. *Nature* 417: 515–522, 2002.

297. Jiang Y, Lee A, Chen J, Ruta V, Cadene M, Chait BT, MacKinnon R. X-ray structure of a voltage-dependent K^+ channel. *Nature* 423: 33–41, 2003.

298. Johnson EA. The effects of quinidine, procaine amide and pyrilamine on the membrane resting and action potential of guinea pig ventricular muscle fibers. *J Pharmacol Exp Ther* 117: 237–244, 1956.

299. Johnson JN, Hofman N, Haglund CM, Cascino GD, Wilde AA, Ackerman MJ. Identification of a possible pathogenic link between congenital long QT syndrome and epilepsy. *Neurology* 72: 224–231, 2009.

300. Johnson JP Jr, Mullins FM, Bennett PB. Human ether-a-go-go-related gene K^+ channel gating probed with extracellular Ca^{2+}. Evidence for two distinct voltage sensors. *J Gen Physiol* 113: 565–580, 1999.

301. Jones EM, Roti Roti EC, Wang J, Delfosse SA, Robertson GA. Cardiac IKr channels minimally comprise hERG 1a and 1b subunits. *J Biol Chem* 279: 44690–44694, 2004.

302. Jost N, Virag L, Bitay M, Takacs J, Lengyel C, Biliczki P, Nagy Z, Bogats G, Lathrop DA, Papp JG, Varro A. Restricting excessive cardiac action potential and QT prolongation: a vital role for IKs in human ventricular muscle. *Circulation* 112: 1392–1399, 2005.

303. Jouven X, Lemaitre RN, Rea TD, Sotoodehnia N, Empana JP, Siscovick DS. Diabetes, glucose level, and risk of sudden cardiac death. *Eur Heart J* 26: 2142–2147, 2005.

304. Ju P, Pages G, Riek RP, Chen PC, Torres AM, Bansal PS, Kuyucak S, Kuchel PW, Vandenberg JI. The pore domain outer helix contributes to both activation and inactivation of the HERG K^+ channel. *J Biol Chem* 284: 1000–1008, 2009.

305. Ju YK, Saint DA, Gage PW. Hypoxia increases persistent sodium current in rat ventricular myocytes. *J Physiol* 497: 337–347, 1996.

306. Jurkiewicz NK, Sanguinetti MC. Rate-dependent prolongation of cardiac action potentials by a methanesulfonanilide class III antiarrhythmic agent. Specific block of IKr current by dofetilide. *Circ Res* 72: 75–83, 1993.

307. Kaab S, Dixon J, Duc J, Ashen D, Nabauer M, Beuckelmann DJ, Steinbeck G, McKinnon D, Tomaselli GF. Molecular basis of transient outward potassium current downregulation in human heart failure: a decrease in Kv4.3 mRNA correlates with a reduction in current density. *Circulation* 98: 1383–1393, 1998.

308. Kagan A, McDonald TV. Dynamic control of hERG/I(Kr) by PKA-mediated interactions with 14–3-3. *Novartis Found Symp* 266: 75–99, 2005.

309. Kagan A, Melman YF, Krumerman A, McDonald TV. 14–3-3 amplifies and prolongs adrenergic stimulation of HERG K^+ channel activity. *EMBO J* 21: 1889–1898, 2002.

310. Kagan A, Yu Z, Fishman GI, McDonald TV. The dominant negative LQT2 mutation A561V reduces wild-type HERG expression. *J Biol Chem* 275: 11241–11248, 2000.

311. Kamiya K, Niwa R, Mitcheson JS, Sanguinetti MC. Molecular determinants of HERG channel block. *Mol Pharmacol* 69: 1709–1716, 2006.

312. Kang J, Chen XL, Wang H, Ji J, Cheng H, Incardona J, Reynolds W, Viviani F, Tabart M, Rampe D. Discovery of a small molecule activator of the human ether-a-go-go-related gene (HERG) cardiac K^+ channel. *Mol Pharmacol* 67: 827–836, 2005.

313. Kannankeril P, Roden DM, Darbar D. Drug-induced long QT syndrome. *Pharmacol Rev* 62: 760–781, 2010.

314. Kaplan WD, Trout WE 3rd. The behavior of four neurological mutants of *Drosophila*. *Genetics* 61: 399–409, 1969.

315. Kapplinger JD, Tester DJ, Salisbury BA, Carr JL, Harris-Kerr C, Pollevick GD, Wilde AA, Ackerman MJ. Spectrum and prevalence of mutations from the first 2,500 consecutive unrelated patients referred for the FAMILION long QT syndrome genetic test. *Heart Rhythm* 6: 1297–1303, 2009.

316. Karle CA, Zitron E, Zhang W, Kathofer S, Schoels W, Kiehn J. Rapid component I(Kr) of the guinea-pig cardiac delayed rectifier K^+ current is inhibited by beta(1)-adrenoreceptor activation, via cAMP/protein kinase A-dependent pathways. *Cardiovasc Res* 53: 355–362, 2002.

317. Kaufman ES, Ficker E. Is restoration of intracellular trafficking clinically feasible in the long QT syndrome?: the example of HERG mutations. *J Cardiovasc Electrophysiol* 14: 320–322, 2003.

318. Keating M, Atkinson D, Dunn C, Timothy K, Vincent G, Leppert M. Linkage of a cardiac arrhythmia, the long QT syndrome, the Harvey ras-1 gene. *Science* 252: 704–706, 1991.

319. Keller SH, Platoshyn O, Yuan JX. Long QT syndrome-associated I593R mutation in HERG potassium channel activates ER stress pathways. *Cell Biochem Biophys* 43: 365–377, 2005.

320. Keseru GM. Prediction of hERG potassium channel affinity by traditional and hologram qSAR methods. *Bioorg Med Chem Lett* 13: 2773–2775, 2003.

321. Khodorov BI, Shishkova LD, Peganov EM. Effect of procaine and calcium ions on slow sodium inactivation in the frog Ranvier node membrane. *Bull Exp Biol Med* 77: 226–229, 1974.

322. Khositseth A, Tester DJ, Will ML, Bell CM, Ackerman MJ. Identification of a common genetic substrate underlying postpartum cardiac events in congenital long QT syndrome. *Heart Rhythm* 1: 60–64, 2004.

323. Kiehn J, Lacerda AE, Brown AM. Pathways of HERG inactivation. *Am J Physiol Heart Circ Physiol* 277: H199–H210, 1999.

324. Kiehn J, Lacerda AE, Wible B, Brown AM. Molecular physiology and pharmacology of HERG. Single-channel currents and block by dofetilide. *Circulation* 94: 2572–2579, 1996.

325. Kiehn J, Wible B, Lacerda AE, Brown AM. Mapping the block of a cloned human inward rectifier potassium channel by dofetilide. *Mol Pharmacol* 50: 380–387, 1996.

326. Kim I, Boyle KM, Carroll JL. Postnatal development of E-4031-sensitive potassium current in rat carotid chemoreceptor cells. *J Appl Physiol* 98: 1469–1477, 2005.

327. Kim JA, Lopes CM, Moss AJ, McNitt S, Barsheshet A, Robinson JL, Zareba W, Ackerman MJ, Kaufman ES, Towbin JA, Vincent M, Goldenberg I. Trigger-specific risk factors and response to therapy in long QT syndrome type 2. *Heart Rhythm* 7: 1797–1805, 2010.

328. Kirchberger NM, Wulfsen I, Schwarz JR, Bauer CK. Effects of TRH on heteromeric rat erg1a/1b K^+ channels are dominated by the rerg1b subunit. *J Physiol* 571: 27–42, 2006.

329. Kiyosue T, Arita M, Muramatsu H, Spindler AJ, Noble D. Ionic mechanisms of action potential prolongation at low temperature in guinea-pig ventricular myocytes. *J Physiol* 468: 85–106, 1993.

330. Kobayashi T, Cohen P. Activation of serum- and glucocorticoid-regulated protein kinase by agonists that activate phosphatidylinositide 3-kinase is mediated by 3-phosphoinositide-dependent protein kinase-1 (PDK1) and PDK2. *Biochem J* 339: 319–328, 1999.

331. Kolbe K, Schonherr R, Gessner G, Sahoo N, Hoshi T, Heinemann SH. Cysteine 723 in the C-linker segment confers oxidative inhibition of hERG1 potassium channels. *J Physiol* 588: 2999–3009, 2010.

332. Kopito RR. Biosynthesis and degradation of CFTR. *Physiol Rev* 79: 167–173, 1999.

333. Korolkova YV, Bocharov EV, Angelo K, Maslennikov IV, Grinenko OV, Lipkin AV, Nosyreva ED, Pluzhnikov KA, Olesen SP, Arseniev AS, Grishin EV. New binding site on common molecular scaffold provides HERG channel specificity of scorpion toxin BeKm-1. *J Biol Chem* 277: 43104–43109, 2002.

334. Korolkova YV, Kozlov SA, Lipkin AV, Pluzhnikov KA, Hadley JK, Filippov AK, Brown DA, Angelo K, Strobaek D, Jespersen T, Olesen SP, Jensen BS, Grishin EV. An ERG channel inhibitor from the scorpion *Buthus eupeus*. *J Biol Chem* 276: 9868–9876, 2001.

335. Korolkova YV, Tseng GN, Grishin EV. Unique interaction of scorpion toxins with the hERG channel. *J Mol Recognit* 17: 209–217, 2004.

336. Kramer C, Beck B, Kriegl JM, Clark T. A composite model for HERG blockade. *Chem Med Chem* 3: 254–265, 2008.

337. Kuo A, Gulbis JM, Antcliff JF, Rahman T, Lowe ED, Zimmer J, Cuthbertson J, Ashcroft FM, Ezaki T, Doyle DA. Crystal structure of the potassium channel KirBac1.1 in the closed state. *Science* 300: 1922–1926, 2003.

338. Kupershmidt S, Snyders DJ, Raes A, Roden DM. A K^+ channel splice variant common in human heart lacks a C-terminal domain required for expression of rapidly activating delayed rectifier current. *J Biol Chem* 273: 27231–27235, 1998.

339. Kupershmidt S, Yang IC, Hayashi K, Wei J, Chanthaphaychith S, Petersen CI, Johns DC, George AL Jr, Roden DM, Balser JR. The IKr drug response is modulated by KCR1 in transfected cardiac and noncardiac cell lines. *FASEB J* 17: 2263–2265, 2003.

340. Kupershmidt S, Yang T, Chanthaphaychith S, Wang Z, Towbin JA, Roden DM. Defective human Ether-a-go-go-related gene trafficking linked to an endoplasmic reticulum retention signal in the C terminus. *J Biol Chem* 277: 27442–27448, 2002.

341. Kurata Y, Hisatome I, Imanishi S, Shibamoto T. Roles of L-type Ca^{2+} and delayed-rectifier K^+ currents in sinoatrial node pacemaking: insights from stability and bifurcation analyses of a mathematical model. *Am J Physiol Heart Circ Physiol* 285: H2804–H2819, 2003.

342. Kuryshev YA, Ficker E, Wang L, Hawryluk P, Dennis AT, Wible BA, Brown AM, Kang J, Chen XL, Sawamura K, Reynolds W, Rampe D. Pentamidine-induced long QT syndrome and block of hERG trafficking. *J Pharmacol Exp Ther* 312: 316–323, 2005.

343. Kutteh R, Vandenberg JI, Kuyucak S. Molecular dynamics and continuum electrostatics studies of inactivation in the HERG potassium channel. *J Phys Chem B* 111: 1090–1098, 2007.

344. Kuzmiak H, Maquat L. Applying nonsense-mediated mRNA decay research to the clinic: progress and challenges. *Trends Mol Med* 12: 306–316, 2006.

345. Labro AJ, Grottesi A, Sansom MS, Raes AL, Snyders DJ. A Kv channel with an altered activation gate sequence displays both "fast" and "slow" activation kinetics. *Am J Physiol Cell Physiol* 294: C1476–C1484, 2008.

346. Labro AJ, Raes AL, Bellens I, Ottschytsch N, Snyders DJ. Gating of *Shaker*-type channels requires the flexibility of S6 caused by prolines. *J Biol Chem* 278: 50724–50731, 2003.

347. Lamarca V, Grasa L, Fagundes DS, Arruebo MP, Plaza MA, Murillo MD. K^+ channels involved in contractility of rabbit small intestine. *J Physiol Biochem* 62: 227–236, 2006.

348. Lamba S, Abraham WT. Alterations in adrenergic receptor signaling in heart failure. *Heart Fail Rev* 5: 7–16, 2000.

349. Langheinrich U, Vacun G, Wagner T. Zebrafish embryos express an orthologue of HERG and are sensitive toward a range of QT-prolonging drugs inducing severe arrhythmia. *Toxicol Appl Pharmacol* 193: 370–382, 2003.

350. Langsetmo K, Fuchs JA, Woodward C. The conserved, buried aspartic acid in oxidized *Escherichia coli* thioredoxin has a pKa of 7.5. Its titration produces a related shift in global stability. *Biochemistry* 30: 7603–7609, 1991.

351. Larsen AP, Bentzen BH, Grunnet M. Differential effects of Kv11.1 activators on Kv111a, Kv111b and Kv111a/Kv111b channels. *Br J Pharmacol* 161: 614–628, 2010.

352. Larsen AP, Olesen SP, Grunnet M, Poelzing S. Pharmacological activation of IKr impairs conduction in guinea pig hearts. *J Cardiovasc Electrophysiol* 21: 923–929, 2010.

353. Larsson HP, Baker OS, Dhillon DS, Isacoff EY. Transmembrane movement of the shaker K^+ channel S4. *Neuron* 16: 387–397, 1996.

354. Lastraioli E, Guasti L, Crociani O, Polvani S, Hofmann G, Witchel H, Bencini L, Calistri M, Messerini L, Scatizzi M, Moretti R, Wanke E, Olivotto M, Mugnai G, Arcangeli A.

herg1 gene and HERG1 protein are overexpressed in colorectal cancers and regulate cell invasion of tumor cells. *Cancer Res* 64: 606–611, 2004.

355. Lee IH, Dinudom A, Sanchez-Perez A, Kumar S, Cook DI. Akt mediates the effect of insulin on epithelial sodium channels by inhibiting Nedd4–2. *J Biol Chem* 282: 29866–29873, 2007.

356. Lees-Miller JP, Duan Y, Teng GQ, Duff HJ. Molecular determinant of high-affinity dofetilide binding to HERG1 expressed in Xenopus oocytes: involvement of S6 sites. *Mol Pharmacol* 57: 367–374, 2000.

357. Lees-Miller JP, Duan Y, Teng GQ, Thorstad K, Duff HJ. Novel gain-of-function mechanism in K^+ channel-related long-QT syndrome: altered gating and selectivity in the HERG1 N629D mutant. *Circ Res* 86: 507–513, 2000.

358. Lees-Miller JP, Kondo C, Wang L, Duff HJ. Electrophysiological characterization of an alternatively processed ERG K^+ channel in mouse and human hearts. *Circ Res* 81: 719–726, 1997.

359. Lees-Miller JP, Subbotina JO, Guo J, Yarov-Yarovoy V, Noskov SY, Duff HJ. Interactions of H562 in the S5 helix with T618 and S621 in the pore helix are important determinants of hERG1 potassium channel structure and function. *Biophys J* 96: 3600–3610, 2009.

360. Lehnart SE, Wehrens XH, Kushnir A, Marks AR. Cardiac ryanodine receptor function and regulation in heart disease. *Ann NY Acad Sci* 1015: 144–159, 2004.

361. Lei M, Brown HF. Two components of the delayed rectifier potassium current, IK, in rabbit sino-atrial node cells. *Exp Physiol* 81: 725–741, 1996.

362. Leier CV, Dei Cas L, Metra M. Clinical relevance and management of the major electrolyte abnormalities in congestive heart failure: hyponatremia, hypokalemia, and hypomagnesemia. *Am Heart J* 128: 564–574, 1994.

363. Leroy J, Abi-Gerges A, Nikolaev VO, Richter W, Lechêne P, Mazet JL, Conti M, Fischmeister R, Vandecasteele G. Spatiotemporal dynamics of beta-adrenergic cAMP signals and L-type Ca^{2+} channel regulation in adult rat ventricular myocytes: role of phosphodiesterases. *Circ Res* 102: 1091–1100, 2008.

364. Levy R. Clinical studies of quinidine. IV. The clinical toxicology of quinidine. *J Am Med Assoc* 79: 1108–1113, 1922.

365. Li M, Jan YN, Jan LY. Specification of subunit assembly by the hydrophilic amino-terminal domain of the Shaker potassium channel. *Science* 257: 1225–1230, 1992.

366. Li P, Ninomiya H, Kurata Y, Kato M, Miake J, Yamamoto Y, Igawa O, Nakai A, Higaki K, Toyoda F, Wu J, Horie M, Matsuura H, Yoshida A, Shirayoshi Y, Hiraoka M, Hisatome I. Reciprocal control of hERG stability by Hsp70 and Hsc70 with implication for restoration of LQT2 mutant stability. *Circ Res* 108: 458–468, 2011.

367. Li Q, Gayen S, Chen AS, Huang Q, Raida M, Kang C. NMR solution structure of the N-terminal domain of hERG and its interaction with the S4–S5 linker. *Biochem Biophys Res Commun* 403: 126–132, 2010.

368. Li Q, Jorgensen FS, Oprea T, Brunak S, Taboureau O. hERG classification model based on a combination of support vector machine method and GRIND descriptors. *Mol Pharm* 5: 117–127, 2008.

369. Li X, Xu J, Li M. The human delta1261 mutation of the HERG potassium channel results in a truncated protein that contains a subunit interaction domain and decreases the channel expression. *J Biol Chem* 272: 705–708, 1997.

370. Li Y, Sroubek J, Krishnan Y, McDonald TV. A-kinase anchoring protein targeting of protein kinase A and regulation of HERG channels. *J Membr Biol* 223: 107–116, 2008.

371. Lillich JD, Rakestraw PC, Roussel AJ, Finley MR, Ganta S, Freeman LC. Expression of the ether-a-go-go (ERG) potassium channel in smooth muscle of the equine gastrointestinal tract and influence on activity of jejunal smooth muscle. *Am J Vet Res* 64: 267–272, 2003.

372. Liman ER, Hess P, Weaver F, Koren G. Voltage-sensing residues in the S4 region of a mammalian K^+ channel. *Nature* 353: 752–756, 1991.

373. Lin H, Chen G, Li Z, Wang N, Bai Y, Luo X, Yang B, Wang Z. TG repeat length polymorphism in the promoter region of KCNH2 gene controls the transcription of hERG K^+ channel. *Canadian Cardiol Congr 2010* 41, 2010.

374. Linna EH, Perkiomaki JS, Karsikas M, Seppanen T, Savolainen M, Kesaniemi YA, Makikallio T, Huikuri HV. Functional significance of KCNH2 (HERG) K897T polymorphism for cardiac repolarization assessed by analysis of T-wave morphology. *Ann Noninvasive Electrocardiol* 11: 57–62, 2006.

375. Listed NA. *ICH (International Conference on Harmonization of Technical Requirement for Registration of Pharmaceuticals for Human Use) Guideline S7B: the Non-clinical Evaluation of the Potential for Delayed Ventricualr Repolarization (QT Interval Prolongation) by Human Pharmaceuticals*. 2002.

376. Liu GX, Choi BR, Ziv O, Li W, de Lange E, Qu Z, Koren G. Differential conditions for early afterdepolarizations and triggered activity in cardiomyocytes derived from transgenic LQT1 and LQT2 rabbits. *J Physiol* 2011.

377. Liu J, Zhang M, Jiang M, Tseng GN. Negative charges in the transmembrane domains of the HERG K channel are involved in the activation- and deactivation-gating processes. *J Gen Physiol* 121: 599–614, 2003.

378. Liu J, Zhang M, Jiang M, Tseng GN. Structural and functional role of the extracellular s5-p linker in the HERG potassium channel. *J Gen Physiol* 120: 723–737, 2002.

379. Liu M, Grigoriev A. Protein domains correlate strongly with exons in multiple eukaryotic genomes–evidence of exon shuffling? *Trends Genet* 20: 399–403, 2004.

380. Liu S, Rasmusson RL, Campbell DL, Wang S, Strauss HC. Activation and inactivation kinetics of an E-4031-sensitive current from single ferret atrial myocytes. *Biophys J* 70: 2704–2715, 1996.

381. Liu XK, Katchman A, Whitfield BH, Wan G, Janowski EM, Woosley RL, Ebert SN. In vivo androgen treatment shortens the QT interval and increases the densities of inward and delayed rectifier potassium currents in orchiectomized male rabbits. *Cardiovasc Res* 57: 28–36, 2003.

382. Liu Y, Holmgren M, Jurman ME, Yellen G. Gated access to the pore of a voltage-dependent K^+ channel. *Neuron* 19: 175–184, 1997.

383. London B, Trudeau MC, Newton KP, Beyer AK, Copeland NG, Gilbert DJ, Jenkins NA, Satler CA, Robertson GA. Two isoforms of the mouse ether-a-go-go-related gene coassemble to form channels with properties similar to the rapidly activating component of the cardiac delayed rectifier K^+ current. *Circ Res* 81: 870–878, 1997.

384. Long SB, Campbell EB, Mackinnon R. Crystal structure of a mammalian voltage-dependent Shaker family K^+ channel. *Science* 309: 897–903, 2005.

385. Long SB, Campbell EB, Mackinnon R. Voltage sensor of Kv1.2: structural basis of electromechanical coupling. *Science* 309: 903–908, 2005.

386. Long SB, Tao X, Campbell EB, Mackinnon R. Atomic structure of a voltage-dependent K^+ channel in a lipid membrane-like environment. *Nature* 450: 376–382, 2007.

387. Loots E, Isacoff EY. Protein rearrangements underlying slow inactivation of the Shaker K^+ channel. *J Gen Physiol* 112: 377–389, 1998.

388. Lopez-Barneo J, Hoshi T, Heinemann SH, Aldrich RW. Effects of external cations and mutations in the pore region on C-type inactivation of Shaker potassium channels. *Receptors Channels* 1: 61–71, 1993.

389. Lu HR, Vlaminckx E, Hermans AN, Rohrbacher J, Van Ammel K, Towart R, Pugsley M, Gallacher DJ. Predicting drug-induced changes in QT interval and arrhythmias: QT-shortening drugs point to gaps in the ICHS7B Guidelines. *Br J Pharmacol* 154: 1427–1438, 2008.

390. Lu Y, Mahaut-Smith MP, Varghese A, Huang CL, Kemp PR, Vandenberg JI. Effects of premature stimulation on HERG K^+ channels. *J Physiol* 537: 843–851, 2001.

391. Luo T, Luo A, Liu M, Liu X. Inhibition of the HERG channel by droperidol depends on channel gating and involves the S6 residue F656. *Anesth Analg* 106: 1161–1170, 2008.

392. Magidovich E, Yifrach O. Conserved gating hinge in ligand- and voltage-dependent K^+ channels. *Biochemistry* 43: 13242–13247, 2004.

393. Maier G, Palmada M, Rajamanickam J, Shumilina E, Bohmer C, Lang F. Upregulation of HERG channels by the serum and glucocorticoid inducible kinase isoform SGK3. *Cell Physiol Biochem* 18: 177–186, 2006.

394. Makkar RR, Fromm BS, Steinman RT, Meissner MD, Lehmann MH. Female gender as a risk factor for torsades de pointes associated with cardiovascular drugs. *JAMA* 270: 2590–2597, 1993.

395. Mannuzzu LM, Moronne MM, Isacoff EY. Direct physical measure of conformational rearrangement underlying potassium channel gating. *Science* 271: 213–216, 1996.

396. Marban E. Heart failure: the electrophysiologic connection. *J Cardiovasc Electrophysiol* 10: 1425–1428, 1999.

397. Marjamaa A, Newton-Cheh C, Porthan K, Reunanen A, Lahermo P, Vaananen H, Jula A, Karanko H, Swan H, Toivonen L, Nieminen MS, Viitasalo M, Peltonen L, Oikarinen L, Palotie A, Kontula K, Salomaa V. Common candidate gene variants are associated with QT interval duration in the general population. *J Intern Med* 265: 448–458, 2009.

398. Marx SO, Kurokawa J, Reiken S, Motoike H, D'Armiento J, Marks AR, Kass RS. Requirement of a macromolecular signaling complex for beta adrenergic receptor modulation of the KCNQ1-KCNE1 potassium channel. *Science* 295: 496–499, 2002.

399. Masetti M, Cavalli A, Recanatini M. Modeling the hERG potassium channel in a phospholipid bilayer: molecular dynamics and drug docking studies. *J Comput Chem* 29: 795–808, 2008.

400. Masi A, Becchetti A, Restano-Cassulini R, Polvani S, Hofmann G, Buccoliero AM, Paglierani M, Pollo B, Taddei GL, Gallina P, Di Lorenzo N, Franceschetti S, Wanke E, Arcangeli A. hERG1 channels are overexpressed in glioblastoma multiforme and modulate VEGF secretion in glioblastoma cell lines. *Br J Cancer* 93: 781–792, 2005.

401. Massaeli H, Guo J, Xu J, Zhang S. Extracellular K^+ is a prerequisite for the function and plasma membrane stability of HERG channels. *Circ Res* 106: 1072–1082, 2010.

402. Massaeli H, Sun T, Li X, Shallow H, Wu J, Xu J, Li W, Hanson C, Guo J, Zhang S. Involvement of caveolin in low K^+-induced endocytic degradation of cell-surface human ether-a-go-go-related gene (hERG) channels. *J Biol Chem* 285: 27259–27264, 2010.

403. Mazhari R, Greenstein JL, Winslow RL, Marban E, Nuss HB. Molecular interactions between two long-QT syndrome gene products, HERG and KCNE2, rationalized by in vitro and in silico analysis. *Circ Res* 89: 33–38, 2001.

404. McCrossan ZA, Roepke TK, Lewis A, Panaghie G, Abbott GW. Regulation of the Kv2.*1 potassium channel by MinK and MiRP1*. *J Membr Biol* 228: 1–14, 2009.

405. McDonald TV, Yu Z, Ming Z, Palma E, Meyers MB, Wang KW, Goldstein SA, Fishman GI. A minK-HERG complex regulates the cardiac potassium current I(Kr). *Nature* 388: 289–292, 1997.

406. McGrath MF, de Bold ML, de Bold AJ. The endocrine function of the heart. *Trends Endocrinol Metab* 16: 469–477, 2005.

407. McKay CM, Huizinga JD. Muscarinic regulation of ether-a-go-go-related gene K^+ currents in interstitial cells of Cajal. *J Pharmacol Exp Ther* 319: 1112–1123, 2006.

408. McPate MJ, Duncan RS, Hancox JC, Witchel HJ. Pharmacology of the short QT syndrome N588K-hERG K^+ channel mutation: differential impact on selected class I and class III antiarrhythmic drugs. *Br J Pharmacol* 155: 957–966, 2008.

409. McPate MJ, Zhang H, Cordeiro JM, Dempsey CE, Witchel HJ, Hancox JC. hERG1a/1b heteromeric currents exhibit amplified attenuation of inactivation in variant 1 short QT syndrome. *Biochem Biophys Res Commun* 386: 111–117, 2009.

410. Meißner FL. *Taubstummheit und Taubstummenbildung: nebst einer Geschichte der Leipziger Taubstummen-Anstalt.* Leipzig, Germany: Winter, 1856, p. VIII, 387.

411. Mewe M, Mauerhofer M, Wulfsen I, Szlachta K, Zhou XB, Schwarz JR, Bauer CK. Modulation of cardiac ERG1 K^+ channels by cGMP signaling. *J Mol Cell Cardiol* 49: 48–57, 2010.

412. Mewe M, Wulfsen I, Schuster AM, Middendorff R, Glassmeier G, Schwarz JR, Bauer CK. Erg K^+ channels modulate contractile activity in the bovine epididymal duct. *Am J Physiol Regul Integr Comp Physiol* 294: R895–R904, 2008.

413. Mikosch M, Homann U. How do ER export motifs work on ion channel trafficking? *Curr Opin Plant Biol* 12: 685–689, 2009.

414. Milan DJ, Jones IL, Ellinor PT, MacRae CA. In vivo recording of adult zebrafish electrocardiogram and assessment of drug-induced QT prolongation. *Am J Physiol Heart Circ Physiol* 291: H269–H273, 2006.

415. Milnes JT, Dempsey CE, Ridley JM, Crociani O, Arcangeli A, Hancox JC, Witchel HJ. Preferential closed channel blockade of HERG potassium currents by chemically synthesised BeKm-1 scorpion toxin. *FEBS Lett* 547: 20–26, 2003.

416. Mirams GR, Cui Y, Sher A, Fink M, Cooper J, Heath BM, McMahon NC, Gavaghan DJ, Noble D. Simulation of multiple ion channel block provides improved early prediction of compounds' clinical torsadogenic risk. *Cardiovasc Res* 2011.

417. Mitcheson J, Perry M, Stansfeld P, Sanguinetti MC, Witchel H, Hancox J. Structural determinants for high-affinity block of hERG potassium channels. *Novartis Found Symp* 266: 136–150, 2005.

418. Mitcheson JS. hERG potassium channels and the structural basis of drug-induced arrhythmias. *Chem Res Toxicol* 21: 1005–1010, 2008.

419. Mitcheson JS, Chen J, Lin M, Culberson C, Sanguinetti MC. A structural basis for drug-induced long QT syndrome. *Proc Natl Acad Sci USA* 97: 12329–12333, 2000.

420. Mitcheson JS, Chen J, Sanguinetti MC. Trapping of a methanesulfonanilide by closure of the HERG potassium channel activation gate. *J Gen Physiol* 115: 229–240, 2000.

421. Mitcheson JS, Hancox JC. An investigation of the role played by the E-4031-sensitive (rapid delayed rectifier) potassium current in isolated rabbit atrioventricular nodal and ventricular myocytes. *Pflügers Arch* 438: 843–850, 1999.

422. Mittelstadt SW, Hemenway CL, Craig MP, Hove JR. Evaluation of zebrafish embryos as a model for assessing inhibition of hERG. *J Pharmacol Toxicol Methods* 57: 100–105, 2008.

423. Mohammad S, Zhou Z, Gong Q, January CT. Blockage of the HERG human cardiac K^+ channel by the gastrointestinal prokinetic agent cisapride. *Am J Physiol Heart Circ Physiol* 273: H2534–H2538, 1997.

424. Monod J, Wyman J, Changeux JP. On the nature of allosteric transitions: a plausible model. *J Mol Biol* 12: 88–118, 1965.

425. Morais Cabral JH, Lee A, Cohen SL, Chait BT, Li M, Mackinnon R. Crystal structure and functional analysis of the HERG potassium channel N terminus: a eukaryotic PAS domain. *Cell* 95: 649–655, 1998.

426. Morgan TK Jr, Sullivan ME. An overview of class III electrophysiological agents: a new generation of antiarrhythmic therapy. *Prog Med Chem* 29: 65–108, 1992.

427. Moss A, Schwartz P, Crampton R, Locati E, Carleen E. The long QT syndrome: a prospective international study. *Circulation* 71: 17–21, 1985.

428. Moss A, Zareba W, Benhorin J, Locati E, Hall W, Robinson J, Schwartz P, Towbin J, Vincent G, Lehmann M. ECG T-wave patterns in genetically distinct forms of the hereditary long QT syndrome. *Circulation* 92: 2929–2934, 1995.

429. Motte G, Coumel P, Abitbol G, Dessertenne F, Slama R. The long QT syndrome and syncope caused by spike torsades. *Arch Mal Coeur Vaiss* 63: 831–853, 1970.

430. Murphy SM, Palmer M, Poole MF, Padegimas L, Hunady K, Danzig J, Gill S, Gill R, Ting A, Sherf B, Brunden K, Stricker-Krongrad A. Evaluation of functional and binding assays in cells expressing either recombinant or endogenous hERG channel. *J Pharmacol Toxicol Methods* 54: 42–55, 2006.

431. Muskett FW, Thouta S, Thomson SJ, Bowen A, Stansfeld PJ, Mitcheson JS. Mechanistic insight into human ether-a-go-go-related gene (hERG) K^+ channel deactivation gating from the solution structure of the EAG domain. *J Biol Chem* 286: 6184–6191, 2011.

432. Myokai T, Ryu S, Shimizu H, Oiki S. Topological mapping of the asymmetric drug binding to the human ether-a-go-go-related gene product (HERG) potassium channel by use of tandem dimers. *Mol Pharmacol* 73: 1643–1651, 2008.

433. Nakagawa M, Sekine Y, Ono M, Taniguchi Y, Takahashi N, Yonemochi H, Saikawa T. Gender differences in the effect of auditory stimuli on ventricular repolarization in healthy subjects. *J Cardiovasc Electrophysiol* 20: 653–657, 2009.

434. Nakajima T, Furukawa T, Hirano Y, Tanaka T, Sakurada H, Takahashi T, Nagai R, Itoh T, Katayama Y, Nakamura Y, Hiraoka M. Voltage-shift of the current activation in HERG S4 mutation (R534C) in LQT2. *Cardiovasc Res* 44: 283–293, 1999.

435. Nakajima T, Furukawa T, Tanaka T, Katayama Y, Nagai R, Nakamura Y, Hiraoka M. Novel mechanism of HERG current suppression in LQT2: shift in voltage dependence of HERG inactivation. *Circ Res* 83: 415–422, 1998.

436. Nakajima T, Hayashi K, Viswanathan PC, Kim MY, Anghelescu M, Barksdale KA, Shuai W, Balser JR, Kupershmidt S. HERG is protected from pharmacological block by alpha-1,2-glucosyltransferase function. *J Biol Chem* 282: 5506–5513, 2007.

437. Nakajima T, Kurabayashi M, Ohyama Y, Kaneko Y, Furukawa T, Itoh T, Taniguchi Y, Tanaka T, Nakamura Y, Hiraoka M, Nagai R. Characterization of S818L mutation in HERG C-terminus in LQT2. Modification of activation-deactivation gating properties. *FEBS Lett* 481: 197–203, 2000.

438. Nakamura H, Kurokawa J, Bai CX, Asada K, Xu J, Oren RV, Zhu ZI, Clancy CE, Isobe M, Furukawa T. Progesterone regulates cardiac repolarization through a nongenomic pathway: an in vitro patch-clamp and computational modeling study. *Circulation* 116: 2913–2922, 2007.

439. Nanduri J, Bergson P, Wang N, Ficker E, Prabhakar NR. Hypoxia inhibits maturation and trafficking of hERG K^+ channel protein: role of Hsp90 and ROS. *Biochem Biophys Res Commun* 388: 212–216, 2009.

440. Nanduri J, Wang N, Bergson P, Yuan G, Ficker E, Prabhakar NR. Mitochondrial reactive oxygen species mediate hypoxic down-regulation of hERG channel protein. *Biochem Biophys Res Commun* 373: 309–314, 2008.

441. Napolitano C, Priori SG, Schwartz PJ, Bloise R, Ronchetti E, Nastoli J, Bottelli G, Cerrone M, Leonardi S. Genetic testing in the long QT syndrome: development and validation of an efficient approach to genotyping in clinical practice. *JAMA* 294: 2975–2980, 2005.

442. Nattel S. Delayed-rectifier potassium currents and the control of cardiac repolarization: Noble and Tsien 40 years after. *J Physiol* 586: 5849–5852, 2008.

443. Nerbonne JM, Kass RS. Molecular physiology of cardiac repolarization. *Physiol Rev* 85: 1205–1253, 2005.

444. Newton-Cheh C, Guo CY, Larson MG, Musone SL, Surti A, Camargo AL, Drake JA, Benjamin EJ, Levy D, D'Agostino RB Sr, Hirschhorn JN, O'Donnell CJ. Common genetic variation in KCNH2 is associated with QT interval duration: the Framingham Heart Study. *Circulation* 116: 1128–1136, 2007.

445. Ng CA, Hunter MJ, Perry MD, Mobli M, Ke Y, Kuchel PW, King GF, Stock D, Vandenberg JI. The N-terminal tail of hERG contains an amphipathic alpha-helix that regulates channel deactivation. *PLoS One* 6: e16191, 2011.

446. Ng CA, Hunter MJ, Perry MD, Mobli M, Ke Y, Kuchel PW, King GF, Stock D, Vandenberg JI. The N-terminal tail of hERG contains an amphipathic α-helix that regulates channel deactivation. *PLoS One* 6: e16191, 2011.

447. Nisius B, Goller AH, Bajorath J. Combining cluster analysis, feature selection and multiple support vector machine models for the identification of human ether-a-go-go related gene channel blocking compounds. *Chem Biol Drug Des* 73: 17–25, 2009.

448. Noble D, Tsien RW. Outward membrane currents activated in the plateau range of potentials in cardiac Purkinje fibres. *J Physiol* 200: 205–231, 1969.

449. Noble D, Tsien RW. Reconstruction of the repolarization process in cardiac Purkinje fibres based on voltage clamp measurements of membrane current. *J Physiol* 200: 233–254, 1969.

450. Noma A, Irisawa H. A time- and voltage-dependent potassium current in the rabbit sinoatrial node cell. *Pflügers Arch* 366: 251–258, 1976.

451. Novotny T, Sisakova M, Kadlecova J, Florianova A, Semrad B, Gaillyova R, Vlasinova J, Chroust K, Toman O. Occurrence of notched T wave in healthy family members with the long QT interval syndrome. *Am J Cardiol* 94: 808–811, 2004.

452. Numaguchi H, Mullins FM, Johnson JP Jr, Johns DC, Po SS, Yang IC, Tomaselli GF, Balser JR. Probing the interaction between inactivation gating and Dd-sotalol block of HERG. *Circ Res* 87: 1012–1018, 2000.

453. O'Brien SE, de Groot MJ. Greater than the sum of its parts: combining models for useful ADMET prediction. *J Med Chem* 48: 1287–1291, 2005.

454. O'Hara T, Virag L, Varro A, Rudy Y. Simulation of the undiseased human cardiac ventricular action potential: model formulation and experimental validation. *PLoS Comput Biol* 7: e1002061, 2011.

455. Obiol-Pardo C, Gomis-Tena J, Sanz F, Saiz J, Pastor M. A multiscale simulation system for the prediction of drug-induced cardiotoxicity. *J Chem Inf Model* 51: 483–492, 2011.

456. Odening KE, Choi BR, Liu GX, Hartmann K, Ziv O, Chaves L, Schofield L, Centracchio J, Zehender M, Peng X, Brunner M, Koren G. Estradiol promotes sudden cardiac death in transgenic long QT type 2 rabbits while progesterone is protective. *Heart Rhythm* 2012.

457. Ohmoto M, Matsumoto I, Misaka T, Abe K. Taste receptor cells express voltage-dependent potassium channels in a cell age-specific manner. *Chem Senses* 31: 739–746, 2006.

458. Ohya S, Asakura K, Muraki K, Watanabe M, Imaizumi Y. Molecular and functional characterization of ERG, KCNQ, and KCNE subtypes in rat stomach smooth muscle. *Am J Physiol Gastrointest Liver Physiol* 282: G277–G287, 2002.

459. Ohya S, Horowitz B, Greenwood IA. Functional and molecular identification of ERG channels in murine portal vein myocytes. *Am J Physiol Cell Physiol* 283: C866–C877, 2002.

460. Ojeda C, Rougier O. Kinetic analysis of the delayed outward currents in frog atrium. Existence of two types of preparation. *J Phsyiol* 239: 51–73, 1974.

461. Omichi C, Momose Y, Kitahara S. Congenital long QT syndrome presenting with a history of epilepsy: misdiagnosis or relationship between channelopathies of the heart and brain? *Epilepsia* 51: 289–292, 2010.

462. Ono K, Ito H. Role of rapidly activating delayed rectifier K^+ current in sinoatrial node pacemaker activity. *Am J Physiol Heart Circ Physiol* 269: H453–H462, 1995.

463. Opthof T, Coronel R, Janse M. Is there a significant transmural gradient in repolarization time in the intact heart?: repolarization gradients in the intact heart. *Circ Arrhythm Electrophysiol* 2: 89–96, 2009.

464. Opthof T, Coronel R, Wilms-Schopman FJ, Plotnikov AN, Shlapakova IN, Danilo P Jr, Rosen MR, Janse MJ. Dispersion of repolarization in canine ventricle and the electrocardiographic T wave: Tp-e interval does not reflect transmural dispersion. *Heart Rhythm* 4: 341–348, 2007.

465. Overholt JL, Ficker E, Yang T, Shams H, Bright GR, Prabhakar NR. Chemosensing at the carotid body. Involvement of a HERG-like potassium current in glomus cells. *Adv Exp Med Biol* 475: 241–248, 2000.

466. Overholt JL, Ficker E, Yang T, Shams H, Bright GR, Prabhakar NR. HERG-like potassium current regulates the resting membrane potential in glomus cells of the rabbit carotid body. *J Neurophysiol* 83: 1150–1157, 2000.

467. Ozhan H, Akdemir R, Duran S, Yazici M, Arinc H, Gunduz H, Uyan C. Transient silent ischemia after percutaneous transluminal coronary angioplasty manifested with a bizarre electrocardiogram. *J Electrocardiol* 38: 206–209, 2005.

468. Paavonen KJ, Chapman H, Laitinen PJ, Fodstad H, Piippo K, Swan H, Toivonen L, Viitasalo M, Kontula K, Pasternack M. Functional characterization of the common amino acid 897 polymorphism of the cardiac potassium channel KCNH2 (HERG). *Cardiovasc Res* 59: 603–611, 2003.

469. Pannaccione A, Castaldo P, Ficker E, Annunziato L, Taglialatela M. Histidines 578 and 587 in the S5–S6 linker of the human Ether-a-gogo Related Gene-1 K^+ channels confer sensitivity to reactive oxygen species. *J Biol Chem* 277: 8912–8919, 2002.

470. Papa M, Boscia F, Canitano A, Castaldo P, Sellitti S, Annunziato L, Taglialatela M. Expression pattern of the ether-a-gogo-related (ERG) K^+ channel-encoding genes ERG1, ERG2, and ERG3 in the adult rat central nervous system. *J Comp Neurol* 466: 119–135, 2003.

471. Papazian DM, Timpe LC, Jan YN, Jan LY. Alteration of voltage-dependence of Shaker potassium channel by mutations in the S4 sequence. *Nature* 349: 305–310, 1991.

472. Pardo LA, del Camino D, Sanchez A, Alves F, Bruggemann A, Beckh S, Stuhmer W. Oncogenic potential of EAG K^+ channels. *EMBO J* 18: 5540–5547, 1999.

473. Pardo-Lopez L, Garcia-Valdes J, Gurrola GB, Robertson GA, Possani LD. Mapping the receptor site for ergtoxin, a specific blocker of ERG channels. *FEBS Lett* 510: 45–49, 2002.

474. Pardo-Lopez L, Zhang M, Liu J, Jiang M, Possani LD, Tseng GN. Mapping the binding site of a human ether-a-go-go-related gene-specific peptide toxin (ErgTx) to the channel's outer vestibule. *J Biol Chem* 277: 16403–16411, 2002.

475. Parr E, Pozo MJ, Horowitz B, Nelson MT, Mawe GM. ERG K^+ channels modulate the electrical and contractile activities of gallbladder smooth muscle. *Am J Physiol Gastrointest Liver Physiol* 284: G392–G398, 2003.

476. Patel C, Antzelevitch C. Cellular basis for arrhythmogenesis in an experimental model of the SQT1 form of the short QT syndrome. *Heart Rhythm* 5: 585–590, 2008.

477. Patel C, Yan GX, Antzelevitch C. Short QT syndrome: from bench to bedside. *Circ Arrhythm Electrophysiol* 3: 401–408, 2010.

478. Paulussen A, Raes A, Matthijs G, Snyders DJ, Cohen N, Aerssens J. A novel mutation (T65P) in the PAS domain of the human potassium channel HERG results in the long QT syndrome by trafficking deficiency. *J Biol Chem* 277: 48610–48616, 2002.

479. Payandeh J, Scheuer T, Zheng N, Catterall WA. The crystal structure of a voltage-gated sodium channel. *Nature* 475: 353–358, 2011.

480. Pearce LR, Komander D, Alessi DR. The nuts and bolts of AGC protein kinases. *Nat Rev Mol Cell Biol* 11: 9–22, 2010.

481. Pearlstein RA, Vaz RJ, Kang J, Chen XL, Preobrazhenskaya M, Shchekotikhin AE, Korolev AM, Lysenkova LN, Miroshnikova OV, Hendrix J, Rampe D. Characterization of HERG potassium channel inhibition using CoMSiA 3D QSAR and homology modeling approaches. *Bioorg Med Chem Lett* 13: 1829–1835, 2003.

482. Peitersen T, Grunnet M, Benson AP, Holden AV, Holstein-Rathlou NH, Olesen SP. Computational analysis of the effects of the hERG channel opener NS1643 in a human ventricular cell model. *Heart Rhythm* 5: 734–741, 2008.

483. Perozo E, Santacruz-Toloza L, Stefani E, Bezanilla F, Papazian DM. S4 mutations alter gating currents of Shaker K channels. *Biophys J* 66: 345–354, 1994.

484. Perrin MJ, Kuchel PW, Campbell TJ, Vandenberg JI. Drug binding to the inactivated state is necessary but not sufficient for high-affinity binding to human ether-a-go-go-related gene channels. *Mol Pharmacol* 74: 1443–1452, 2008.

485. Perry M, de Groot MJ, Helliwell R, Leishman D, Tristani-Firouzi M, Sanguinetti MC, Mitcheson J. Structural determinants of HERG channel block by clofilium and ibutilide. *Mol Pharmacol* 66: 240–249, 2004.

486. Perry M, Sachse FB, Abbruzzese J, Sanguinetti MC. PD-118057 contacts the pore helix of hERG1 channels to attenuate inactivation and enhance K^+ conductance. *Proc Natl Acad Sci USA* 106: 20075–20080, 2009.

487. Perry M, Sachse FB, Sanguinetti MC. Structural basis of action for a human ether-a-go-go-related gene 1 potassium channel activator. *Proc Natl Acad Sci USA* 104: 13827–13832, 2007.

488. Perry M, Sanguinetti M, Mitcheson J. Revealing the structural basis of action of hERG potassium channel activators and blockers. *J Physiol* 588: 3157–3167, 2010.

489. Perry M, Stansfeld PJ, Leaney J, Wood C, de Groot MJ, Leishman D, Sutcliffe MJ, Mitcheson JS. Drug binding interactions in the inner cavity of HERG channels: molecular insights from structure-activity relationships of clofilium and ibutilide analogs. *Mol Pharmacol* 69: 509–519, 2006.

490. Pessia M, Servettini I, Panichi R, Guasti L, Grassi S, Arcangeli A, Wanke E, Pettorossi VE. ERG voltage-gated K^+ channels regulate excitability and discharge dynamics of the medial vestibular nucleus neurones. *J Physiol* 586: 4877–4890, 2008.

491. Petersen CI, McFarland TR, Stepanovic SZ, Yang P, Reiner DJ, Hayashi K, George AL, Roden DM, Thomas JH, Balser JR. In vivo identification of genes that modify ether-a-go-go-related gene activity in *Caenorhabditis elegans* may also affect human cardiac arrhythmia. *Proc Natl Acad Sci USA* 101: 11773–11778, 2004.

492. Petrecca K, Atanasiu R, Akhavan A, Shrier A. *N*-linked glycosylation sites determine HERG channel surface membrane expression. *J Physiol* 515: 41–48, 1999.

493. Pfeufer A, Jalilzadeh S, Perz S, Mueller JC, Hinterseer M, Illig T, Akyol M, Huth C, Schopfer-Wendels A, Kuch B, Steinbeck G, Holle R, Nabauer M, Wichmann HE, Meitinger T, Kaab S. Common variants in myocardial ion channel genes modify the QT interval in the general population: results from the KORA study. *Circ Res* 96: 693–701, 2005.

494. Phartiyal P, Jones EM, Robertson GA. Heteromeric assembly of human ether-a-go-go-related gene (hERG) 1a/1b channels occurs cotranslationally via N-terminal interactions. *J Biol Chem* 282: 9874–9882, 2007.

495. Phartiyal P, Sale H, Jones EM, Robertson GA. Endoplasmic reticulum retention and rescue by heteromeric assembly regulate human ERG 1a/1b surface channel composition. *J Biol Chem* 283: 3702–3707, 2008.

496. Pietila E, Fodstad H, Niskasaari E, Laitinen PP, Swan H, Savolainen M, Kesaniemi YA, Kontula K, Huikuri HV. Association between HERG K897T polymorphism and QT interval in middle-aged Finnish women. *J Am Coll Cardiol* 40: 511–514, 2002.

497. Pillozzi S, Brizzi MF, Balzi M, Crociani O, Cherubini A, Guasti L, Bartolozzi B, Becchetti A, Wanke E, Bernabei PA, Olivotto M, Pegoraro L, Arcangeli A. HERG potassium channels are constitutively expressed in primary human acute myeloid leukemias and regulate cell proliferation of normal and leukemic hemopoietic progenitors. *Leukemia* 16: 1791–1798, 2002.

498. Pillozzi S, Brizzi MF, Bernabei PA, Bartolozzi B, Caporale R, Basile V, Boddi V, Pegoraro L, Becchetti A, Arcangeli A. VEGFR-1 (FLT-1), beta1 integrin, and hERG K^+ channel for a macromolecular signaling complex in acute myeloid leukemia: role in cell migration and clinical outcome. *Blood* 110: 1238–1250, 2007.

499. Piper DR, Duff SR, Eliason HC, Frazee WJ, Frey EA, Fuerstenau-Sharp M, Jachec C, Marks BD, Pollok BA, Shekhani MS, Thompson DV, Whitney P, Vogel KW, Hess SD. Development of the predictor HERG fluorescence polarization assay using a membrane protein enrichment approach. *Assay Drug Dev Technol* 6: 213–223, 2008.

500. Piper DR, Hinz WA, Tallurri CK, Sanguinetti MC, Tristani-Firouzi M. Regional specificity of human ether-a'-go-go-related gene channel activation and inactivation gating. *J Biol Chem* 280: 7206–7217, 2005.

501. Piper DR, Rupp J, Sachse FB, Sanguinetti MC, Tristani-Firouzi M. Cooperative interactions between R531 and acidic residues in the voltage sensing module of hERG1 channels. *Cell Physiol Biochem* 21: 37–46, 2008.

502. Piper DR, Varghese A, Sanguinetti MC, Tristani-Firouzi M. Gating currents associated with intramembrane charge displacement in HERG potassium channels. *Proc Natl Acad Sci USA* 100: 10534–10539, 2003.

503. Po SS, Wang DW, Yang IC, Johnson JP Jr, Nie L, Bennett PB. Modulation of HERG potassium channels by extracellular magnesium and quinidine. *J Cardiovasc Pharmacol* 33: 181–185, 1999.

504. Pond AL, Scheve BK, Benedict AT, Petrecca K, Van Wagoner DR, Shrier A, Nerbonne JM. Expression of distinct ERG proteins in rat, mouse, human heart. Relation to functional I(Kr) channels. *J Biol Chem* 275: 5997–6006, 2000.

505. Potet F, Petersen CI, Boutaud O, Shuai W, Stepanovic SZ, Balser JR, Kupershmidt S. Genetic screening in *C. elegans* identifies rho-GTPase activating protein 6 as novel HERG regulator. *J Mol Cell Cardiol* 46: 257–267, 2009.

506. Priebe L, Beuckelmann DJ. Simulation study of cellular electric properties in heart failure. *Circ Res* 82: 1206–1223, 1998.

507. Priori SG, Chen SR. Inherited dysfunction of sarcoplasmic reticulum Ca^{2+} handling and arrhythmogenesis. *Circ Res* 108: 871–883, 2011.

508. Priori SG, Schwartz PJ, Napolitano C, Bloise R, Ronchetti E, Grillo M, Vicentini A, Spazzolini C, Nastoli J, Bottelli G, Folli R, Cappelletti D. Risk stratification in the long-QT syndrome. *N Engl J Med* 348: 1866–1874, 2003.

509. Raab CE, Butcher JW, Connolly TM, Karczewski J, Yu NX, Staskiewicz SJ, Liverton N, Dean DC, Melillo DG. Synthesis of the first sulfur-35-labeled hERG radioligand. *Bioorg Med Chem Lett* 16: 1692–1695, 2006.

510. Raitakari OT, Blom-Nyholm J, Koskinen TA, Kahonen M, Viikari JS, Lehtimaki T. Common variation in NOS1AP and KCNH2 genes and QT interval duration in young adults. The Cardiovascular Risk in Young Finns. *Study Ann Med* 41: 144–151, 2009.

511. Rajamani S, Anderson CL, Anson BD, January CT. Pharmacological rescue of human K^+ channel long-QT2 mutations: human ether-a-go-go-related gene rescue without block. *Circulation* 105: 2830–2835, 2002.

512. Rajamani S, Eckhardt LL, Valdivia CR, Klemens CA, Gillman BM, Anderson CL, Holzem KM, Delisle BP, Anson BD, Makielski JC, January CT. Drug-induced long QT syndrome: hERG K^+ channel block and disruption of protein trafficking by fluoxetine and norfluoxetine. *Br J Pharmacol* 149: 481–489, 2006.

513. Ramstrom C, Chapman H, Viitanen T, Afrasiabi E, Fox H, Kivela J, Soini S, Korhonen L, Lindholm D, Pasternack M, Tornquist K. Regulation of HERG (KCNH2) potassium channel surface expression by diacylglycerol. *Cell Mol Life Sci* 67: 157–169, 2010.

514. Rautaharju PM, Zhou SH, Wong S, Calhoun HP, Berenson GS, Prineas R, Davignon A. Sex differences in the evolution of the electrocardiographic QT interval with age. *Can J Cardiol* 8: 690–695, 1992.

515. Ray WA, Chung CP, Murray KT, Hall K, Stein CM. Atypical antipsychotic drugs and the risk of sudden cardiac death. *N Engl J Med* 360: 225–235, 2009.

516. Ren XQ, Liu GX, Organ-Darling LE, Zheng R, Roder K, Jindal HK, Centracchio J, McDonald TV, Koren G. Pore mutants of HERG and KvLQT1 downregulate the reciprocal currents in stable cell lines. *Am J Physiol Heart Circ Physiol* 299: H1525–H1534, 2010.

517. Restano-Cassulini R, Korolkova YV, Diochot S, Gurrola G, Guasti L, Possani LD, Lazdunski M, Grishin EV, Arcangeli A, Wanke E. Species diversity and peptide toxins blocking selectivity of ether-a-go-go-related gene subfamily K^+ channels in the central nervous system. *Mol Pharmacol* 69: 1673–1683, 2006.

518. Rezazadeh S, Hesketh JC, Fedida D. Rb^+ flux through hERG channels affects the potency of channel blocking drugs: correlation with data obtained using a high-throughput Rb^+ efflux assay. *J Biomol Screen* 9: 588–597, 2004.

519. Ridley JM, Shuba YM, James AF, Hancox JC. Modulation by testosterone of an endogenous hERG potassium channel current. *J Physiol Pharmacol* 59: 395–407, 2008.

520. Riordan JR. Assembly of functional CFTR chloride channels. *Annu Rev Physiol* 67: 701–718, 2005.

521. Robertson GA. LQT2: amplitude reduction and loss of selectivity in the tail that wags the HERG channel. *Circ Res* 86: 492–493, 2000.

522. Robertson GA, January CT. HERG trafficking and pharmacological rescue of LQTS-2 mutant channels. *Handb Exp Pharmacol* 349–355, 2006.

523. Roche O, Trube G, Zuegge J, Pflimlin P, Alanine A, Schneider G. A virtual screening method for prediction of the HERG potassium channel liability of compound libraries. *Chembiochem* 3: 455–459, 2002.

524. Rockman HA, Koch WJ, Lefkowitz RJ. Seven-transmembrane-spanning receptors and heart function. *Nature* 415: 206–212, 2002.

525. Roden DM. Drug-induced prolongation of the QT interval. *N Engl J Med* 350: 1013–1022, 2004.

526. Roden DM. Taking the "idio" out of "idiosyncratic": predicting torsades de pointes. *Pacing Clin Electrophysiol* 21: 1029–1034, 1998.

527. Roden DM, Hoffman BF. Action potential prolongation and induction of abnormal automaticity by low quinidine concentrations in canine Purkinje fibers. Relationship to potassium and cycle length. *Circ Res* 56: 857–867, 1985.

528. Rodriguez de la Vega RC, Possani LD. Current views on scorpion toxins specific for K^+-channels. *Toxicon* 43: 865–875, 2004.

529. Romano C, Gemme G, Pongiglione R. Rare cardiac arrythmias of the pediatric age. II. Syncopal attacks due to paroxysmal ventricular fibrillation (presentation of 1st case in italian pediatric literature). *Clin Pediatr* 45: 656–683, 1963.

530. Rosati B, Marchetti P, Crociani O, Lecchi M, Lupi R, Arcangeli A, Olivotto M, Wanke E. Glucose- and arginine-induced insulin secretion by human pancreatic beta-cells: the role of HERG K^+ channels in firing and release. *FASEB J* 14: 2601–2610, 2000.

531. Rossenbacker T, Mubagwa K, Jongbloed RJ, Vereecke J, Devriendt K, Gewillig M, Carmeliet E, Collen D, Heidbuchel H, Carmeliet P. Novel mutation in the Per-Arnt-Sim domain of KCNH2 causes a malignant form of long-QT syndrome. *Circulation* 111: 961–968, 2005.

532. Roti EC, Myers CD, Ayers RA, Boatman DE, Delfosse SA, Chan EK, Ackerman MJ, January CT, Robertson GA. Interaction with GM130 during HERG ion channel trafficking. Disruption by type 2 congenital long QT syndrome mutations Human Ether-a-go-go-Related Gene. *J Biol Chem* 277: 47779–47785, 2002.

533. Rotin D, Staub O. Role of the ubiquitin system in regulating ion transport. *Pflügers Arch* 461: 1–21, 2011.

534. Rouet R, Picard S, Libersa C, Ghadanfar M, Alabaster C, Gerard JL. Electrophysiological effects of dofetilide in an in vitro model of "border zone" between normal and ischemic/reperfused myocardium. *Circulation* 101: 86–93, 2000.

535. Rougier JS, van Bemmelen MX, Bruce MC, Jespersen T, Gavillet B, Apotheloz F, Cordonier S, Staub O, Rotin D, Abriel H. Molecular determinants of voltage-gated sodium channel regulation by the Nedd4/Nedd4-like proteins. *Am J Physiol Cell Physiol* 288: C692–C701, 2005.

536. Sacco T, Bruno A, Wanke E, Tempia F. Functional roles of an ERG current isolated in cerebellar Purkinje neurons. *J Neurophysiol* 90: 1817–1828, 2003.

537. Sadlish H, Skach WR. Biogenesis of CFTR and other polytopic membrane proteins: new roles for the ribosome-translocon complex. *J Membr Biol* 202: 115–126, 2004.

538. Saenen JB, Labro AJ, Raes A, Snyders DJ. Modulation of HERG gating by a charge cluster in the N-terminal proximal domain. *Biophys J* 91: 4381–4391, 2006.

539. Saganich MJ, Machado E, Rudy B. Differential expression of genes encoding subthreshold-operating voltage-gated K^+ channels in brain. *J Neurosci* 21: 4609–4624, 2001.

540. Sager PT, Uppal P, Follmer C, Antimisiaris M, Pruitt C, Singh BN. Frequency-dependent electrophysiologic effects of amiodarone in humans. *Circulation* 88: 1063–1071, 1993.

541. Saint DA. The role of the persistent Na^+ current during cardiac ischemia and hypoxia. *J Cardiovasc Electrophysiol* 17 *Suppl* 1: S96–S103, 2006.

542. Sale H, Wang J, O'Hara TJ, Tester DJ, Phartiyal P, He JQ, Rudy Y, Ackerman MJ, Robertson GA. Physiological properties of hERG 1a/1b heteromeric currents and a hERG 1b-specific mutation associated with Long-QT syndrome. *Circ Res* 103: e81–95, 2008.

543. Sanchez-Chapula JA, Sanguinetti MC. Altered gating of HERG potassium channels by cobalt and lanthanum. *Pflügers Arch* 440: 264–274, 2000.

544. Sanders CR, Myers JK. Disease-related misassembly of membrane proteins. *Annu Rev Biophys Biomol Struct* 33: 25–51, 2004.

545. Sanguinetti MC, Curran ME, Spector PS, Keating MT. Spectrum of HERG K^+-channel dysfunction in an inherited cardiac arrhythmia. *Proc Natl Acad Sci USA* 93: 2208–2212, 1996.

546. Sanguinetti MC, Curran ME, Zou A, Shen J, Spector PS, Atkinson DL, Keating MT. Coassembly of K(V)LQT1 and minK (IsK) proteins to form cardiac I(Ks) potassium channel. *Nature* 384: 80–83, 1996.

547. Sanguinetti MC, Jiang C, Curran ME, Keating MT. A mechanistic link between an inherited and an acquired cardiac arrhythmia: HERG encodes the IKr potassium channel. *Cell* 81: 299–307, 1995.

548. Sanguinetti MC, Jurkiewicz NK. Two components of cardiac delayed rectifier K^+ current. Differential sensitivity to block by class III antiarrhythmic agents. *J Gen Physiol* 96: 195–215, 1990.

549. Sanguinetti MC, Jurkiewicz NK, Scott A, Siegl PK. Isoproterenol antagonizes prolongation of refractory period by the class III antiarrhythmic agent E-4031 in guinea pig myocytes. Mechanism of action. *Circ Res* 68: 77–84, 1991.

550. Sanguinetti MC, Tristani-Firouzi M. hERG potassium channels and cardiac arrhythmia. *Nature* 440: 463–469, 2006.

551. Sanguinetti MC, Xu QP. Mutations of the S4–S5 linker alter activation properties of HERG potassium channels expressed in *Xenopus* oocytes. *J Physiol* 514: 667–675, 1999.

552. Sasano T, Ueda K, Orikabe M, Hirano Y, Kawano S, Yasunami M, Isobe M, Kimura A, Hiraoka M. Novel C-terminus frameshift mutation, 1122fs/147, of HERG in LQT2: additional amino acids generated by frameshift cause accelerated inactivation. *J Mol Cell Cardiol* 37: 1205–1211, 2004.

553. Sato S, Ward CL, Krouse ME, Wine JJ, Kopito RR. Glycerol reverses the misfolding phenotype of the most common cystic fibrosis mutation. *J Biol Chem* 271: 635–638, 1996.

554. Schafer R, Wulfsen I, Behrens S, Weinsberg F, Bauer CK, Schwarz JR. The erg-like potassium current in rat lactotrophs. *J Physiol* 518: 401–416, 1999.

555. Schaub MC, Hefti MA, Zaugg M. Integration of calcium with the signaling network in cardiac myocytes. *J Mol Cell Cardiol* 41: 183–214, 2006.

556. Schimpf R, Veltmann C, Papavassiliu T, Rudic B, Goksu T, Kuschyk J, Wolpert C, Antzelevitch C, Ebner A, Borggrefe M, Brandt C. Drug-induced QT-interval shortening following antiepileptic treatment with oral rufinamide. *Heart Rhythm* 2012.

557. Schmalhofer WA, Swensen AM, Thomas BS, Felix JP, Haedo RJ, Solly K, Kiss L, Kaczorowski GJ, Garcia ML. A pharmacologically validated, high-capacity, functional thallium flux assay for the human Ether-a-go-go related gene potassium channel. *Assay Drug Dev Technol* 8: 714–726, 2010.

558. Schonherr R, Heinemann SH. Molecular determinants for activation and inactivation of HERG, a human inward rectifier potassium channel. *J Physiol* 493: 635–642, 1996.

559. Schoonmaker FW, Osteen RT, Greenfield JC Jr. Thioridazine (mellaril)-induced ventricular tachycardia controlled with an artificial pacemaker. *Ann Intern Med* 65: 1076–1078, 1966.

560. Schwartz PJ, Priori SG, Spazzolini C, Moss AJ, Vincent GM, Napolitano C, Denjoy I, Guicheney P, Breithardt G, Keating MT, Towbin JA, Beggs AH, Brink P, Wilde AA, Toivonen L, Zareba W, Robinson JL, Timothy KW, Corfield V, Wattanasirichaigoon D, Corbett C, Haverkamp W, Schulze-Bahr E, Lehmann MH, Schwartz K, Coumel P,

Bloise R. Genotype-phenotype correlation in the long-QT syndrome: gene-specific triggers for life-threatening arrhythmias. *Circulation* 103: 89–95, 2001.

561. Schwarz W, Palade PT, Hille B. Local anesthetics. Effect of pH on use-dependent block of sodium channels in frog muscle. *Biophys J* 20: 343–368, 1977.

562. Seierstad M, Agrafiotis DK. A QSAR model of HERG binding using a large, diverse, internally consistent training set. *Chem Biol Drug Des* 67: 284–296, 2006.

563. Selzer A, Wray HW. Quinidine syncope: aroxysmal Ventricular fibrillation occurring during treatment of chronic atrial arrhythmias. *Circulation* 30: 17–26, 1964.

564. Seoh SA, Sigg D, Papazian DM, Bezanilla F. Voltage-sensing residues in the S2 and S4 segments of the Shaker K^+ channel. *Neuron* 16: 1159–1167, 1996.

565. Sesti F, Abbott GW, Wei J, Murray KT, Saksena S, Schwartz PJ, Priori SG, Roden DM, George AL Jr, Goldstein SA. A common polymorphism associated with antibiotic-induced cardiac arrhythmia. *Proc Natl Acad Sci USA* 97: 10613–10618, 2000.

566. Seth R, Moss AJ, McNitt S, Zareba W, Andrews ML, Qi M, Robinson JL, Goldenberg I, Ackerman MJ, Benhorin J, Kaufman ES, Locati EH, Napolitano C, Priori SG, Schwartz PJ, Towbin JA, Vincent GM, Zhang L. Long QT syndrome and pregnancy. *J Am Coll Cardiol* 49: 1092–1098, 2007.

567. Shah RR, Hondeghem LM. Refining detection of drug-induced proarrhythmia: QT interval and TRIaD. *Heart Rhythm* 2: 758–772, 2005.

568. Shealy RT, Murphy AD, Ramarathnam R, Jakobsson E, Subramaniam S. Sequence-function analysis of the K^+-selective family of ion channels using a comprehensive alignment and the KcsA channel structure. *Biophys J* 84: 2929–2942, 2003.

569. Shen MY, Su BH, Esposito EX, Hopfinger AJ, Tseng YJ. A comprehensive support vector machine binary hERG classification model based on extensive but biased end point hERG data sets. *Chem Res Toxicol* 2011.

570. Shen NV, Chen X, Boyer MM, Pfaffinger PJ. Deletion analysis of K^+ channel assembly. *Neuron* 11: 67–76, 1993.

571. Shi W, Wymore RS, Wang HS, Pan Z, Cohen IS, McKinnon D, Dixon JE. Identification of two nervous system-specific members of the erg potassium channel gene family. *J Neurosci* 17: 9423–9432, 1997.

572. Shibasaki T. Conductance and kinetics of delayed rectifier potassium channels in nodal cells of the rabbit heart. *J Physiol* 387: 227–250, 1987.

573. Shimizu H, Toyoshima C, Oiki S. Interaction between tetraethylammonium and permeant cations at the inactivation gate of the HERG potassium channel. *Jpn J Physiol* 53: 25–34, 2003.

574. Shimizu W, Antzelevitch C. Differential effects of beta-adrenergic agonists and antagonists in LQT1, LQT2 and LQT3 models of the long QT syndrome. *J Am Coll Cardiol* 35: 778–786, 2000.

575. Shoeb F, Malykhina AP, Akbarali HI. Cloning and functional characterization of the smooth muscle ether-a-go-go-related gene K^+ channel. Potential role of a conserved amino acid substitution in the S4 region. *J Biol Chem* 278: 2503–2514, 2003.

576. Shuba YM, Degtiar VE, Osipenko VN, Naidenov VG, Woosley RL. Testosterone-mediated modulation of HERG blockade by proarrhythmic agents. *Biochem Pharmacol* 62: 41–49, 2001.

577. Sigworth FJ. Voltage gating of ion channels. *Q Rev Biophys* 27: 1–40, 1994.

578. Silva J, Rudy Y. Subunit interaction determines IKs participation in cardiac repolarization and repolarization reserve. *Circulation* 112: 1384–1391, 2005.

579. Singh BN, Vaughan Williams EM. The effect of amiodarone, a new anti-anginal drug, on cardiac muscle. *Br J Pharmacol* 39: 657–667, 1970.

580. Singh BN, Vaughan Williams EM. A third class of anti-arrhythmic action Effects on atrial and ventricular intracellular potentials, other pharmacological actions on cardiac muscle, of MJ 1999 and AH 3474. *Br J Pharmacol* 39: 675–687, 1970.

581. Smale ST, Kadonaga JT. The RNA polymerase II core promoter. *Annu Rev Biochem* 72: 449–479, 2003.

582. Smith GA, Tsui HW, Newell EW, Jiang X, Zhu XP, Tsui FW, Schlichter LC. Functional up-regulation of HERG K^+ channels in neoplastic hematopoietic cells. *J Biol Chem* 277: 18528–18534, 2002.

583. Smith PL, Baukrowitz T, Yellen G. The inward rectification mechanism of the HERG cardiac potassium channel. *Nature* 379: 833–836, 1996.

584. Smith PL, Yellen G. Fast and slow voltage sensor movements in HERG potassium channels. *J Gen Physiol* 119: 275–293, 2002.

585. Snyder PM, Olson DR, Thomas BC. Serum and glucocorticoid-regulated kinase modulates Nedd4–2-mediated inhibition of the epithelial Na^+ channel. *J Biol Chem* 277: 5–8, 2002.

586. Snyders DJ, Chaudhary A. High affinity open channel block by dofetilide of HERG expressed in a human cell line. *Mol Pharmacol* 49: 949–955, 1996.

587. Spector PS, Curran ME, Keating MT, Sanguinetti MC. Class III antiarrhythmic drugs block HERG, a human cardiac delayed rectifier K^+ channel. Open-channel block by methanesulfonanilides. *Circ Res* 78: 499–503, 1996.

588. Spector PS, Curran ME, Zou A, Keating MT, Sanguinetti MC. Fast inactivation causes rectification of the IKr channel. *J Gen Physiol* 107: 611–619, 1996.

589. Splawski I, Shen J, Timothy KW, Lehmann MH, Priori S, Robinson JL, Moss AJ, Schwartz PJ, Towbin JA, Vincent GM, Keating MT. Spectrum of mutations in long-QT syndrome genes. KVLQT1, HERG, SCN5A, KCNE1, and KCNE2. *Circulation* 102: 1178–1185, 2000.

590. Sroubek J, McDonald TV. PKA activity at the ER surface is responsible for augmentation of human ether-a-go-go-related gene product (HERG). *J Biol Chem* 2011.

591. Stansfeld PJ, Gedeck P, Gosling M, Cox B, Mitcheson JS, Sutcliffe MJ. Drug block of the hERG potassium channel: insight from modeling. *Proteins* 68: 568–580, 2007.

592. Stansfeld PJ, Grottesi A, Sands ZA, Sansom MS, Gedeck P, Gosling M, Cox B, Stanfield PR, Mitcheson JS, Sutcliffe MJ. Insight into the mechanism of inactivation and pH sensitivity in potassium channels from molecular dynamics simulations. *Biochemistry* 47: 7414–7422, 2008.

593. Starkus JG, Kuschel L, Rayner MD, Heinemann SH. Ion conduction through C-type inactivated Shaker channels. *J Gen Physiol* 110: 539–550, 1997.

594. Starkus JG, Kuschel L, Rayner MD, Heinemann SH. Macroscopic Na^+ currents in the "Nonconducting" Shaker potassium channel mutant W434F. *J Gen Physiol* 112: 85–93, 1998.

595. Stary A, Wacker SJ, Boukharta L, Zachariae U, Karimi-Nejad Y, Aqvist J, Vriend G, de Groot BL. Toward a consensus model of the HERG potassium channel. *Chem Med Chem* 5: 455–467, 2010.

596. Stork D, Timin EN, Berjukow S, Huber C, Hohaus A, Auer M, Hering S. State dependent dissociation of HERG channel inhibitors. *Br J Pharmacol* 151: 1368–1376, 2007.

597. Strichartz GR. The inhibition of sodium currents in myelinated nerve by quaternary derivatives of lidocaine. *J Gen Physiol* 62: 37–57, 1973.

598. Stump MR, Gong Q, Zhou Z. Multiple splicing defects caused by hERG splice site mutation 2592+1G>A associated with long QT syndrome. *Am J Physiol Heart Circ Physiol* 300: H312–H318, 2011.

599. Su BH, Shen MY, Esposito EX, Hopfinger AJ, Tseng YJ. In silico binary classification QSAR models based on 4D-fingerprints and MOE descriptors for prediction of hERG blockage. *J Chem Inf Model* 50: 1304–1318, 2010.

600. Su Z, Limberis J, Souers A, Kym P, Mikhail A, Houseman K, Diaz G, Liu X, Martin RL, Cox BF, Gintant GA. Electrophysiologic characterization of a novel hERG channel activator. *Biochem Pharmacol* 77: 1383–1390, 2009.

601. Subbiah RN, Clarke CE, Smith DJ, Zhao J, Campbell TJ, Vandenberg JI. Molecular basis of slow activation of the human ether-a-go-go related gene potassium channel. *J Physiol* 558: 417–431, 2004.

602. Subbiah RN, Kondo M, Campbell TJ, Vandenberg JI. Tryptophan scanning mutagenesis of the HERG K^+ channel: the S4 domain is loosely packed and likely to be lipid exposed. *J Physiol* 569: 367–379, 2005.

603. Subbotina J, Yarov-Yarovoy V, Lees-Miller J, Durdagi S, Guo J, Duff HJ, Noskov SY. Structural refinement of the hERG1 pore and voltage-sensing domains with ROSETTA-membrane and molecular dynamics simulations. *Proteins* 78: 2922–2934, 2010.

604. Suessbrich H, Schonherr R, Heinemann SH, Lang F, Busch AE. Specific block of cloned Herg channels by clofilium and its tertiary analog LY97241. *FEBS Lett* 414: 435–438, 1997.

605. Suh BC, Hille B. PIP_2 is a necessary cofactor for ion channel function: how and why? *Annu Rev Biophys* 37: 175–195, 2008.

606. Sun H. An accurate and interpretable bayesian classification model for prediction of HERG liability. *Chem Med Chem* 1: 315–322, 2006.

607. Sun T, Guo J, Shallow H, Yang T, Xu J, Li W, Hanson C, Wu JG, Li X, Massaeli H, Zhang S. The role of monoubiquitination in endocytic degradation of human ether-a-go-go-related gene (hERG) channels under low K^+ conditions. *J Biol Chem* 286: 6751–6759, 2011.

608. Sun Y, Quan XQ, Fromme S, Cox RH, Zhang P, Zhang L, Guo D, Guo J, Patel C, Kowey PR, Yan GX. A novel mutation in the KCNH2 gene associated with short QT syndrome. *J Mol Cell Cardiol* 50: 433–441, 2011.

609. Sun Y, Zhang P, Li X, Zhang H, Li J, Liu G, Guo J. A novel nonsense mutation Y652X in the S6/pore region of human ether-go-go gene found in a long QT syndrome family. *Scand Cardiovasc J* 43: 181–186, 2009.

610. Swartz KJ. Tarantula toxins interacting with voltage sensors in potassium channels. *Toxicon* 49: 213–230, 2007.

611. Swartz KJ, MacKinnon R. Hanatoxin modifies the gating of a voltage-dependent K^+ channel through multiple binding sites. *Neuron* 18: 665–673, 1997.

612. Taglialatela M, Castaldo P, Iossa S, Pannaccione A, Fresi A, Ficker E, Annunziato L. Regulation of the human ether-a-gogo related gene (HERG) K^+ channels by reactive oxygen species. *Proc Natl Acad Sci USA* 94: 11698–11703, 1997.

613. Taglialatela M, Castaldo P, Pannaccione A, Giorgio G, Genovese A, Marone G, Annunziato L. Cardiac ion channels and antihistamines: possible mechanisms of cardiotoxicity. *Clin Exp Allergy* 29 Suppl 3: 182–189, 1999.

614. Takemasa H, Nagatomo T, Abe H, Kawakami K, Igarashi T, Tsurugi T, Kabashima N, Tamura M, Okazaki M, Delisle BP, January CT, Otsuji Y. Coexistence of hERG current block and disruption of protein trafficking in ketoconazole-induced long QT syndrome. *Br J Pharmacol* 153: 439–447, 2008.

615. Takenaka K, Ai T, Shimizu W, Kobori A, Ninomiya T, Otani H, Kubota T, Takaki H, Kamakura S, Horie M. Exercise stress test amplifies genotype-phenotype correlation in the LQT1 and LQT2 forms of the long-QT syndrome. *Circulation* 107: 838–844, 2003.

616. Tamarappoo BK, Verkman AS. Defective aquaporin-2 trafficking in nephrogenic diabetes insipidus and correction by chemical chaperones. *J Clin Invest* 101: 2257–2267, 1998.

617. Tan Y, Chen Y, You Q, Sun H, Li M. Predicting the potency of hERG K^+ channel inhibition by combining 3D-QSAR pharmacophore and 2D-QSAR models. *J Mol Model* 2011.

618. Tang W, Kang J, Wu X, Rampe D, Wang L, Shen H, Li Z, Dunnington D, Garyantes T. Development and evaluation of high throughput functional assay methods for HERG potassium channel. *J Biomol Screen* 6: 325–331, 2001.

619. Tao X, Avalos JL, Chen J, MacKinnon R. Crystal structure of the eukaryotic strong inward-rectifier K^+ channel Kir2.2 at 31 A resolution. *Science* 326: 1668–1674, 2009.

620. ten Tusscher KH, Noble D, Noble PJ, Panfilov AV. A model for human ventricular tissue. *Am J Physiol Heart Circ Physiol* 286: H1573–H1589, 2004.

621. Ten Tusscher KH, Panfilov AV. Cell model for efficient simulation of wave propagation in human ventricular tissue under normal and pathological conditions. *Phys Med Biol* 51: 6141–6156, 2006.

622. Teng GQ, Zhao X, Lees-Miller JP, Quinn FR, Li P, Rancourt DE, London B, Cross JC, Duff HJ. Homozygous missense N629D hERG (KCNH2) potassium channel mutation causes developmental defects in the right ventricle and its outflow tract and embryonic lethality. *Circ Res* 103: 1483–1491, 2008.

623. Terai T, Furukawa T, Katayama Y, Hiraoka M. Effects of external acidosis on HERG current expressed in Xenopus oocytes. *J Mol Cell Cardiol* 32: 11–21, 2000.

624. Terrenoire C, Clancy CE, Cormier JW, Sampson KJ, Kass RS. Autonomic control of cardiac action potentials: role of potassium channel kinetics in response to sympathetic stimulation. *Circ Res* 96: e25–34, 2005.

625. Terrenoire C, Houslay MD, Baillie GS, Kass RS. The cardiac IKs potassium channel macromolecular complex includes the phosphodiesterase PDE4D3. *J Biol Chem* 284: 9140–9146, 2009.

626. Tester DJ, Cronk LB, Carr JL, Schulz V, Salisbury BA, Judson RS, Ackerman MJ. Allelic dropout in long QT syndrome genetic testing: a possible mechanism underlying false-negative results. *Heart Rhythm* 3: 815–821, 2006.

627. Thai KM, Ecker GF. Similarity-based SIBAR descriptors for classification of chemically diverse hERG blockers. *Mol Divers* 13: 321–336, 2009.

628. Thai KM, Windisch A, Stork D, Weinzinger A, Schiesaro A, Guy RH, Timin EN, Hering S, Ecker GF. The hERG potassium channel and drug trapping: insight from docking studies with propafenone derivatives. *Chem Med Chem* 5: 436–442, 2010.

629. Thermann R, Neu-Yilik G, Deters A, Frede U, Wehr K, Hagemeier C, Hentze MW, Kulozik AE. Binary specification of nonsense codons by splicing and cytoplasmic translation. *EMBO J* 17: 3484–3494, 1998.

630. Thomas D, Hammerling BC, Wimmer AB, Wu K, Ficker E, Kuryshev YA, Scherer D, Kiehn J, Katus HA, Schoels W, Karle CA. Direct block of hERG potassium channels by the protein kinase C inhibitor bisindolylmaleimide I (GF109203X). *Cardiovasc Res* 64: 467–476, 2004.

631. Thomas D, Wu K, Wimmer AB, Zitron E, Hammerling BC, Kathofer S, Lueck S, Bloehs R, Kreye VA, Kiehn J, Katus HA, Schoels W, Karle CA. Activation of cardiac human ether-a-go-go related gene potassium currents is regulated by alpha(1A)-adrenoceptors. *J Mol Med* 82: 826–837, 2004.

632. Thomas D, Zhang W, Karle CA, Kathofer S, Schols W, Kubler W, Kiehn J. Deletion of protein kinase A phosphorylation sites in the HERG potassium channel inhibits activation shift by protein kinase A. *J Biol Chem* 274: 27457–27462, 1999.

633. Thomas D, Zhang W, Wu K, Wimmer AB, Gut B, Wendt-Nordahl G, Kathofer S, Kreye VA, Katus HA, Schoels W, Kiehn J, Karle CA. Regulation of HERG potassium channel activation by protein kinase C independent of direct phosphorylation of the channel protein. *Cardiovasc Res* 59: 14–26, 2003.

634. Tian Q, Oberhofer M, Ruppenthal S, Scholz A, Buschmann V, Tsutsui H, Miyawaki A, Zeug A, Lipp P, Kaestner L. Optical action potential screening on adult ventricular myocytes as an alternative QT-screen. *Cell Physiol Biochem* 27: 281–290, 2011.

635. Titus SA, Beacham D, Shahane SA, Southall N, Xia M, Huang R, Hooten E, Zhao Y, Shou L, Austin CP, Zheng W. A new homogeneous high-throughput screening assay for profiling compound activity on the human ether-a-go-go-related gene channel. *Anal Biochem* 394: 30–38, 2009.

636. Titus SA, Warmke JW, Ganetzky B. The Drosophila erg K^+ channel polypeptide is encoded by the seizure locus. *J Neurosci* 17: 875–881, 1997.

637. Tiwari-Woodruff SK, Lin MA, Schulteis CT, Papazian DM. Voltage-dependent structural interactions in the Shaker K^+ channel. *J Gen Physiol* 115: 123–138, 2000.

638. Tobita M, Nishikawa T, Nagashima R. A discriminant model constructed by the support vector machine method for HERG potassium channel inhibitors. *Bioorg Med Chem Lett* 15: 2886–2890, 2005.

639. Tomas M, Napolitano C, De Giuli L, Bloise R, Subirana I, Malovini A, Bellazzi R, Arking D, Marban E, Chakravarti A, Spooner P, Priori S. Polymorphisms in the NOS1AP gene modulate QT interval duration and risk of arrhythmias in the long QT syndrome. *J Am Coll Cardiol* 55: 2745–2752, 2010.

640. Tombola F, Pathak MM, Isacoff EY. How does voltage open an ion channel? *Annu Rev Cell Dev Biol* 22: 23–52, 2006.

641. Torres AM, Bansal PS, Sunde M, Clarke CE, Bursill JA, Smith DJ, Bauskin A, Breit SN, Campbell TJ, Alewood PF, Kuchel PW, Vandenberg JI. Structure of the HERG K^+ channel S5P extracellular linker: role of an amphipathic alpha-helix in C-type inactivation. *J Biol Chem* 278: 42136–42148, 2003.

642. Tristani-Firouzi M, Chen J, Sanguinetti MC. Interactions between S4–S5 linker and S6 transmembrane domain modulate gating of HERG K^+ channels. *J Biol Chem* 277: 18994–19000, 2002.

643. Trudeau MC, Warmke JW, Ganetzky B, Robertson GA. HERG, a human inward rectifier in the voltage-gated potassium channel family. *Science* 269: 92–95, 1995.

644. Tseng GN. Linkage between "disruption of inactivation" and "reduction of K^+ selectivity" among hERG mutants in the S5-P linker region. *J Physiol* 577: 459–460, 2006.

645. Tseng GN, Guy HR. Structure-function studies of the outer mouth and voltage sensor domain of hERG. *Novartis Found Symp* 266: 19–45, 2005.

646. Tseng GN, Sonawane KD, Korolkova YV, Zhang M, Liu J, Grishin EV, Guy HR. Probing the outer mouth structure of the HERG channel with peptide toxin footprinting and molecular modeling. *Biophys J* 92: 3524–3540, 2007.

647. Tzivoni D, Banai S, Schuger C, Benhorin J, Keren A, Gottlieb S, Stern S. Treatment of torsade de pointes with magnesium sulfate. *Circulation* 77: 392–397, 1988.

648. Van Slyke AC, Rezazadeh S, Snopkowski M, Shi P, Allard CR, Claydon TW. Mutations within the S4–S5 linker alter voltage sensor constraints in hERG K^+ channels. *Biophys J* 99: 2841–2852, 2010.

649. Vandenberg JI, Varghese A, Lu Y, Bursill JA, Mahaut-Smith MP, Huang CL. Temperature dependence of human Ether-a-go-go Related Gene (hERG) K^+ currents. *Am J Physiol Cell Physiol* 2006.

650. Velu CS, Niture SK, Doneanu CE, Pattabiraman N, Srivenugopal KS. Human p53 is inhibited by glutathionylation of cysteines present in the proximal DNA-binding domain during oxidative stress. *Biochemistry* 46: 7765–7780, 2007.

651. Vembar SS, Brodsky JL. One step at a time: endoplasmic reticulum-associated degradation. *Nat Rev Mol Cell Biol* 9: 944–957, 2008.

652. Verheijck EE, Wilders R, Bouman LN. Atrio-sinus interaction demonstrated by blockade of the rapid delayed rectifier current. *Circulation* 105: 880–885, 2002.

653. Viskin S, Postema PG, Bhuiyan ZA, Rosso R, Kalman JM, Vohra JK, Guevara-Valdivia ME, Marquez MF, Kogan E, Belhassen B, Glikson M, Strasberg B, Antzelevitch C, Wilde AA. The response of the QT interval to the brief tachycardia provoked by standing: a bedside test for diagnosing long QT syndrome. *J Am Coll Cardiol* 55: 1955–1961, 2010.

654. Vrtovec B, Okrajsek R, Golicnik A, Ferjan M, Starc V, Radovancevic B. Atorvastatin therapy increases heart rate variability, decreases QT variability, and shortens QT_c interval duration in patients with advanced chronic heart failure. *J Card Fail* 11: 684–690, 2005.

655. Walker VE, Atanasiu R, Lam H, Shrier A. Co-chaperone FKBP38 promotes HERG trafficking. *J Biol Chem* 282: 23509–23516, 2007.

656. Walker VE, Wong MJ, Atanasiu R, Hantouche C, Young JC, Shrier A. Hsp40 chaperones promote degradation of the HERG potassium channel. *J Biol Chem* 285: 3319–3329, 2010.

657. Walsh KB, Kass RS. Regulation of a heart potassium channel by protein kinase A and C. *Science* 242: 67–69, 1988.

658. Wang DT, Hill AP, Mann SA, Tan PS, Vandenberg JI. Mapping the sequence of conformational changes underlying selectivity filter gating in the K(v)11.1 potassium channel. *Nat Struct Mol Biol* 18: 35–41, 2011.

659. Wang J, Myers CD, Robertson GA. Dynamic control of deactivation gating by a soluble amino-terminal domain in HERG K^+ channels. *J Gen Physiol* 115: 749–758, 2000.

660. Wang J, Salata JJ, Bennett PB. Saxitoxin is a gating modifier of HERG K^+ channels. *J Gen Physiol* 121: 583–598, 2003.

661. Wang J, Trudeau MC, Zappia AM, Robertson GA. Regulation of deactivation by an amino terminal domain in human ether-a-go-go-related gene potassium channels. *J Gen Physiol* 112: 637–647, 1998.

662. Wang J, Wang H, Zhang Y, Gao H, Nattel S, Wang Z. Impairment of HERG K^+ channel function by tumor necrosis factor-alpha: role of reactive oxygen species as a mediator. *J Biol Chem* 279: 13289–13292, 2004.

663. Wang L, Dennis AT, Trieu P, Charron F, Ethier N, Hebert TE, Wan X, Ficker E. Intracellular potassium stabilizes human ether-a-go-go-related gene channels for export from endoplasmic reticulum. *Mol Pharmacol* 75: 927–937, 2009.

664. Wang L, Duff HJ. Identification and characteristics of delayed rectifier K^+ current in fetal mouse ventricular myocytes. *Am J Physiol Heart Circ Physiol* 270: H2088–H2093, 1996.

665. Wang L, Feng ZP, Kondo CS, Sheldon RS, Duff HJ. Developmental changes in the delayed rectifier K^+ channels in mouse heart. *Circ Res* 79: 79–85, 1996.

666. Wang Q, Curran M, Splawski I, Burn T, Millholland J, VanRaay T, Shen J, Timothy K, Vincent G, de Jager T, Schwartz P, Toubin J, Moss A, Atkinson D, Landes G, Connors T, Keating M. Positional cloning of a novel potassium channel gene: KVLQT1 mutations cause cardiac arrhythmias. *Nat Genet* 12: 17–23, 1996.

667. Wang Q, Shen J, Splawski I, Atkinson D, Li Z, Robinson JL, Moss AJ, Towbin JA, Keating MT. SCN5A mutations associated with an inherited cardiac arrhythmia, long QT syndrome. *Cell* 80: 805–811, 1995.

668. Wang S, Liu S, Morales MJ, Strauss HC, Rasmusson RL. A quantitative analysis of the activation and inactivation kinetics of HERG expressed in *Xenopus* oocytes. *J Physiol* 502: 45–60, 1997.

669. Wang S, Morales MJ, Liu S, Strauss HC, Rasmusson RL. Modulation of HERG affinity for E-4031 by $[K^+]_o$ and C-type inactivation. *FEBS Lett* 417: 43–47, 1997.

670. Wang S, Morales MJ, Liu S, Strauss HC, Rasmusson RL. Time, voltage and ionic concentration dependence of rectification of h-erg expressed in *Xenopus* oocytes. *FEBS Lett* 389: 167–173, 1996.

671. Wang S, Xu DJ, Cai JB, Huang YZ, Zou JG, Cao KJ. Rapid component I(Kr) of cardiac delayed rectifier potassium currents in guinea-pig is inhibited by alpha(1)-adrenoreceptor activation via protein kinase A and protein kinase C-dependent pathways. *Eur J Pharmacol* 608: 1–6, 2009.

672. Wang X, Xu R, Abernathey G, Taylor J, Alzghoul MB, Hannon K, Hockerman GH, Pond AL. Kv11.1 channel subunit composition includes MinK and varies developmentally in mouse cardiac muscle. *Dev Dyn* 237: 2430–2437, 2008.

673. Wang XJ, Reynolds ER, Deak P, Hall LM. The seizure locus encodes the *Drosophila* homolog of the HERG potassium channel. *J Neurosci* 17: 882–890, 1997.

674. Wang Y, Huang X, Zhou J, Yang X, Li D, Mao H, Sun HH, Liu N, Lian J. Trafficking-deficient G572R-hERG and E637K-hERG activate stress and clearance pathways in endoplasmic reticulum. *PLoS One* 7: e29885, 2012.

675. Wang Y, Zhang Y, Yang L, Cai B, Li J, Zhou Y, Yin L, Yang L, Yang BF, Lu YJ. Arsenic trioxide induces the apoptosis of human breast cancer MCF-7 cells through activation of caspase-3 and inhibition of HERG channels. *Exp Ther Med* 2: 481–486, 2011.

676. Wang YH, Shi CX, Dong F, Sheng JW, Xu YF. Inhibition of the rapid component of the delayed rectifier potassium current in ventricular myocytes by angiotensin II via the AT1 receptor. *Br J Pharmacol* 154: 429–439, 2008.

677. Ward OC. A new familial cardiac syndrome in children. *J Ir Med Assoc* 54: 103–106, 1964.

678. Warmke JW, Ganetzky B. A family of potassium channel genes related to eag in *Drosophila* and mammals. *Proc Natl Acad Sci USA* 91: 3438–3442, 1994.

679. Weerapura M, Nattel S, Chartier D, Caballero R, Hebert TE. A comparison of currents carried by HERG, with and without coexpression of MiRP1, the native rapid delayed rectifier current. Is MiRP1 the missing link? *J Physiol* 540: 15–27, 2002.

680. Weidmann S. Effects of calcium ions and local anesthetics on electrical properties of Purkinje fibres. *J Physiol* 129: 568–582, 1955.

681. Weiss DL, Seemann G, Sachse FB, Dossel O. Modelling of short QT syndrome in a heterogeneous model of the human ventricular wall. *Europace: European pacing, arrhythmias, cardiac electrophysiology: journal of the working groups on cardiac pacing, arrhythmias, cardiac cellular electrophysiology of the European Society of Cardiology* 7 *Suppl* 2: 105–117, 2005.

682. Whorton MR, MacKinnon R. Crystal structure of the mammalian GIRK2 K^+ channel and gating regulation by G proteins, PIP_2, sodium. *Cell* 147: 199–208, 2011.

683. Wible BA, Hawryluk P, Ficker E, Kuryshev YA, Kirsch G, Brown AM. HERG-Lite: a novel comprehensive high-throughput screen for drug-induced hERG risk. *J Pharmacol Toxicol Methods* 52: 136–145, 2005.

684. Wilde AA, Jongbloed RJ, Doevendans PA, Duren DR, Hauer RN, van Langen IM, van Tintelen JP, Smeets HJ, Meyer H, Geelen JL. Auditory stimuli as a trigger for arrhythmic events differentiate HERG-related (LQTS2) patients from KVLQT1-related patients (LQTS1). *J Am Coll Cardiol* 33: 327–332, 1999.

685. Winston NJ, Johnson MH, McConnell JM, Cook DI, Day ML. Expression and role of the ether-a-go-go-related (MERG1A) potassium-channel protein during preimplantation mouse development. *Biol Reprod* 70: 1070–1079, 2004.

686. Wong JA, Gula LJ, Klein GJ, Yee R, Skanes AC, Krahn AD. Utility of treadmill testing in identification and genotype prediction in long-QT syndrome. *Circ Arrhythm Electrophysiol* 3: 120–125, 2010.

687. Wu L, Ma J, Li H, Wang C, Grandi E, Zhang P, Luo A, Bers DM, Shryock JC, Belardinelli L. Late sodium current contributes to the reverse rate-dependent effect of IKr inhibition on ventricular repolarization. *Circulation* 123: 1713–1720, 2011.

688. Wu ZY, Chen K, Haendler B, McDonald TV, Bian JS. Stimulation of N-terminal truncated isoform of androgen receptor stabilizes human ether-a-go-go-related gene-encoded potassium channel protein via activation of extracellular signal regulated kinase 1/2. *Endocrinology* 149: 5061–5069, 2008.

689. Wynia-Smith SL, Gillian-Daniel AL, Satyshur KA, Robertson GA. hERG gating microdomains defined by S6 mutagenesis and molecular modeling. *J Gen Physiol* 132: 507–520, 2008.

690. Xia Y, Liang Y, Kongstad O, Holm M, Olsson B, Yuan S. Tpeak-Tend interval as an index of global dispersion of ventricular repolarization: evaluations using monophasic action potential mapping of the epi- and endocardium in swine. *J Interv Card Electrophysiol* 14: 79–87, 2005.

691. Yamaguchi M, Shimizu M, Ino H, Terai H, Uchiyama K, Oe K, Mabuchi T, Konno T, Kaneda T, Mabuchi H. T wave peak-to-end interval and QT dispersion in acquired long QT syndrome: a new index for arrhythmogenicity. *Clin Sci* 105: 671–676, 2003.

692. Yamazaki K, Furukawa Y, Kasama M, Imamura H, Chiba S. Negative chronotropic and dromotropic effects of E-4031, an IKr blocker, on the atrioventricular node in anesthetized dog hearts. *Eur J Pharmacol* 297: 233–239, 1996.

693. Yan GX, Antzelevitch C. Cellular basis for the electrocardiographic J wave. *Circulation* 93: 372–379, 1996.

694. Yang BF, Xu DH, Xu CQ, Li Z, Du ZM, Wang HZ, Dong DL. Inactivation gating determines drug potency: a common mechanism for drug blockade of HERG channels. *Acta Pharmacol Sin* 25: 554–560, 2004.

695. Yang T, Kupershmidt S, Roden DM. Anti-minK antisense decreases the amplitude of the rapidly activating cardiac delayed rectifier K^+ current. *Circ Res* 77: 1246–1253, 1995.

696. Yang T, Roden DM. Extracellular potassium modulation of drug block of IKr. Implications for torsade de pointes and reverse use-dependence. *Circulation* 93: 407–411, 1996.

697. Yang T, Snyders D, Roden DM. Drug block of I(kr): model systems and relevance to human arrhythmias. *J Cardiovasc Pharmacol* 38: 737–744, 2001.

698. Yang T, Snyders DJ, Roden DM. Ibutilide, a methanesulfonanilide antiarrhythmic, is a potent blocker of the rapidly activating delayed rectifier K^+ current (IKr) in AT-1 cells. Concentration-, time-, voltage-, and use-dependent effects. *Circulation* 91: 1799–1806, 1995.

699. Yeh JZ, Armstrong CM. Immobilisation of gating charge by a substance that simulates inactivation. *Nature* 273: 387–389, 1978.

700. Yellen G, Sodickson D, Chen TY, Jurman ME. An engineered cysteine in the external mouth of a K^+ channel allows inactivation to be modulated by metal binding. *Biophys J* 66: 1068–1075, 1994.

701. Yi H, Cao Z, Yin S, Dai C, Wu Y, Li W. Interaction simulation of hERG K^+ channel with its specific BeKm-1 peptide: insights into the selectivity of molecular recognition. *J Proteome Res* 6: 611–620, 2007.

702. Yifrach O, MacKinnon R. Energetics of pore opening in a voltage-gated K^+ channel. *Cell* 111: 231–239, 2002.

703. Yoshida K, Niwa T. Quantitative structure-activity relationship studies on inhibition of HERG potassium channels. *J Chem Inf Model* 46: 1371–1378, 2006.

704. Yu H, Wu J, Potapova I, Wymore RT, Holmes B, Zuckerman J, Pan Z, Wang H, Shi W, Robinson RB, El-Maghrabi MR, Benjamin W, Dixon J, McKinnon D, Cohen IS, Wymore R. MinK-related peptide 1: a beta subunit for the HCN ion channel subunit family enhances expression and speeds activation. *Circ Res* 88: E84–87, 2001.

705. Zachariae U, Giordanetto F, Leach AG. Side chain flexibilities in the human ether-a-go-go related gene potassium channel (hERG) together with matched-pair binding studies suggest a new binding mode for channel blockers. *J Med Chem* 52: 4266–4276, 2009.

706. Zagotta WN, Hoshi T, Aldrich RW. Restoration of inactivation in mutants of Shaker potassium channels by a peptide derived from ShB. *Science* 250: 568–571, 1990.

707. Zagotta WN, Olivier NB, Black KD, Young EC, Olson R, Gouaux E. Structural basis for modulation and agonist specificity of HCN pacemaker channels. *Nature* 425: 200–205, 2003.

708. Zarraga IG, Zhang L, Stump MR, Gong Q, Vincent GM, Zhou Z. Nonsense-mediated mRNA decay caused by a frameshift mutation in a large kindred of type 2 long QT syndrome. *Heart Rhythm* 2011.

709. Zeng H, Lozinskaya IM, Lin Z, Willette RN, Brooks DP, Xu X. Mallotoxin is a novel human ether-a-go-go-related gene (hERG) potassium channel activator. *J Pharmacol Exp Ther* 319: 957–962, 2006.

710. Zerangue N, Schwappach B, Jan YN, Jan LY. A new ER trafficking signal regulates the subunit stoichiometry of plasma membrane K(ATP) channels. *Neuron* 22: 537–548, 1999.

711. Zhang DY, Wang Y, Lau CP, Tse HF, Li GR. Both EGFR kinase and Src-related tyrosine kinases regulate human ether-a-go-go-related gene potassium channels. *Cell Signal* 20: 1815–1821, 2008.

712. Zhang H, Hancox JC. In silico study of action potential and QT interval shortening due to loss of inactivation of the cardiac rapid delayed rectifier potassium current. *Biochem Biophys Res Commun* 322: 693–699, 2004.

713. Zhang J, Sun X, Qian Y, LaDuca JP, Maquat LE. At least one intron is required for the nonsense-mediated decay of triosephosphate isomerase mRNA: a possible link between nuclear splicing and cytoplasmic translation. *Mol Cell Biol* 18: 5272–5283, 1998.

714. Zhang J, Sun X, Qian Y, Maquat LE. Intron function in the nonsense-mediated decay of beta-globin mRNA: indications that pre-mRNA splicing in the nucleus can influence mRNA translation in the cytoplasm. *RNA* 4: 801–815, 1998.

715. Zhang L, Timothy KW, Vincent GM, Lehmann MH, Fox J, Giuli LC, Shen J, Splawski I, Priori SG, Compton SJ, Yanowitz F, Benhorin J, Moss AJ, Schwartz PJ, Robinson JL, Wang Q, Zareba W, Keating MT, Towbin JA, Napolitano C, Medina A. Spectrum of ST-T-wave patterns and repolarization parameters in congenital long-QT syndrome: ECG findings identify genotypes. *Circulation* 102: 2849–2855, 2000.

716. Zhang L, Vincent GM, Baralle M, Baralle FE, Anson BD, Benson DW, Whiting B, Timothy KW, Carlquist J, January CT, Keating MT, Splawski I. An intronic mutation causes long QT syndrome. *J Am Coll Cardiol* 44: 1283–1291, 2004.

717. Zhang M, Jiang M, Tseng GN. minK-related peptide 1 associates with Kv4.2 and modulates its gating function: potential role as beta subunit of cardiac transient outward channel? *Circ Res* 88: 1012–1019, 2001.

718. Zhang M, Korolkova YV, Liu J, Jiang M, Grishin EV, Tseng GN. BeKm-1 is a HERG-specific toxin that shares the structure with ChTx but the mechanism of action with ErgTx1. *Biophys J* 84: 3022–3036, 2003.

719. Zhang M, Liu J, Jiang M, Wu DM, Sonawane K, Guy HR, Tseng GN. Interactions between charged residues in the transmembrane segments of the voltage-sensing domain in the hERG channel. *J Membr Biol* 207: 169–181, 2005.

720. Zhang M, Liu J, Tseng GN. Gating charges in the activation and inactivation processes of the HERG channel. *J Gen Physiol* 124: 703–718, 2004.

721. Zhang M, Liu XS, Diochot S, Lazdunski M, Tseng GN. APETx1 from sea anemone *Anthopleura elegantissima* is a gating modifier peptide toxin of the human ether-a-go-go-related potassium channel. *Mol Pharmacol* 72: 259–268, 2007.

722. Zhang M, Wang Y, Jiang M, Zankov DP, Chowdhury S, Kasirajan V, Tseng GN. KCNE2 protein is more abundant in ventricles than in atria and can accelerate hERG protein degradation in a phosphorylation-dependent manner. *Am J Physiol Heart Circ Physiol* 2011.

723. Zhang Y, Han H, Wang J, Wang H, Yang B, Wang Z. Impairment of human ether-a-go-go-related gene (HERG) K^+ channel function by hypoglycemia and hyperglycemia. Similar phenotypes but different mechanisms. *J Biol Chem* 278: 10417–10426, 2003.

724. Zhang Y, Ouyang P, Post WS, Dalal D, Vaidya D, Blasco-Colmenares E, Soliman EZ, Tomaselli GF, Guallar E. Sex-steroid hormones and electrocardiographic QT-interval duration: findings from the Third National Health and Nutrition Examination Survey and the Multi-Ethnic Study of Atherosclerosis. *Am J Epidemiol* 174: 403–411, 2011.

725. Zhang Y, Wang H, Wang J, Han H, Nattel S, Wang Z. Normal function of HERG K^+ channels expressed in HEK293 cells requires basal protein kinase B activity. *FEBS Lett* 534: 125–132, 2003.

726. Zhang Y, Xiao J, Wang H, Luo X, Wang J, Villeneuve LR, Zhang H, Bai Y, Yang B, Wang Z. Restoring depressed HERG K^+ channel function as a mechanism for insulin treatment of abnormal QT prolongation and associated arrhythmias in diabetic rabbits. *Am J Physiol Heart Circ Physiol* 291: H1446–H1455, 2006.

727. Zhang YH, Colenso CK, Sessions RB, Dempsey CE, Hancox JC. The hERG K^+ channel S4 domain L532P mutation: characterization at 37 degrees C. *Biochim Biophys Acta* 1808: 2477–2487, 2011.

728. Zhao JT, Hill AP, Varghese A, Cooper AA, Swan H, Laitinen-Forsblom PJ, Rees MI, Skinner JR, Campbell TJ, Vandenberg JI. Not All hERG pore domain mutations have a severe phenotype: G584S has an inactivation gating defect with mild phenotype compared with G572S, which has a dominant negative trafficking defect and a severe phenotype. *J Cardiovasc Electrophysiol* 20: 923–930, 2009.

729. Zhou J, Augelli-Szafran CE, Bradley JA, Chen X, Koci BJ, Volberg WA, Sun Z, Cordes JS. Novel potent human ether-a-go-go-related gene (hERG) potassium channel enhancers and their in vitro antiarrhythmic activity. *Mol Pharmacol* 68: 876–884, 2005.

730. Zhou Q, Bett GC. Regulation of the voltage-insensitive step of HERG activation by extracellular pH. *Am J Physiol Heart Circ Physiol* 298: H1710–H1718, 2010.

731. Zhou S, Yung Chan S, Cher Goh B, Chan E, Duan W, Huang M, McLeod HL. Mechanism-based inhibition of cytochrome P450 3A4 by therapeutic drugs. *Clin Pharmacokinet* 44: 279–304, 2005.

732. Zhou W, Cayabyab FS, Pennefather PS, Schlichter LC, DeCoursey TE. HERG-like K^+ channels in microglia. *J Gen Physiol* 111: 781–794, 1998.

733. Zhou Z, Gong Q, Epstein ML, January CT. HERG channel dysfunction in human long QT syndrome. *Intracellular transport and functional defects. J Biol Chem* 273: 21061–21066, 1998.

734. Zhou Z, Gong Q, January CT. Correction of defective protein trafficking of a mutant HERG potassium channel in human long QT syndrome. Pharmacological and temperature effects. *J Biol Chem* 274: 31123–31126, 1999.

735. Zhou Z, Gong Q, Ye B, Fan Z, Makielski JC, Robertson GA, January CT. Properties of HERG channels stably expressed in HEK 293 cells studied at physiological temperature. *Biophys J* 74: 230–241, 1998.

736. Zhu Y, Golden CM, Ye J, Wang XY, Akbarali HI, Huizinga JD. ERG K^+ currents regulate pacemaker activity in ICC. *Am J Physiol Gastrointest Liver Physiol* 285: G1249–G1258, 2003.

737. Zipes DP. The long QT interval syndrome. A Rosetta stone for sympathetic related ventricular tachyarrhythmias. *Circulation* 84: 1414–1419, 1991.

738. Zou A, Curran ME, Keating MT, Sanguinetti MC. Single HERG delayed rectifier K^+ channels expressed in *Xenopus* oocytes. *Am J Physiol Heart Circ Physiol* 272: H1309–H1314, 1997.

739. Zou A, Xu QP, Sanguinetti MC. A mutation in the pore region of HERG K^+ channels expressed in *Xenopus* oocytes reduces rectification by shifting the voltage dependence of inactivation. *J Physiol* 509: 129–137, 1998.